Reactivity Ratio Estimation in Multicomponent Polymerizations Using the Error-in-Variables-Model (EVM) Framework

by

Niousha Kazemi

A thesis
presented to the University of Waterloo
in fulfillment of the
thesis requirement for the degree of
Doctor of Philosophy
in
Chemical Engineering

Waterloo, Ontario, Canada, 2014

Author's Declaration

I hereby declare that I am the sole author of this thesis. This is a true copy of the thesis, including any required final revisions, as accepted by my examiners.

I understand that my thesis may be made electronically available to the public.

Abstract

Studying multicomponent polymerizations is an active area of research and one of the most important aspects of such studies is to understand the underlying reaction kinetics. For multicomponent polymerization systems, such as copolymerizations and terpolymerizations, one cannot explain their characteristics only based on information for each individual monomer. In fact, characteristics of such systems depend strongly on the interaction between the various monomers (and their radicals), which is also the key factor in creating diverse polymeric products with versatile properties. One of the basic characteristics of a polymer for specific polymer applications is its polymer composition, influenced by the relative reactivities of the monomers present in the reaction medium. The relative reactivities of monomers are expressed as monomers reactivity ratios. Predicting and controlling polymer composition from the knowledge of monomer concentrations and their reactivity ratios is crucial to research in this field and the polymerization industry due to the clear impact of polymer chain composition on chemical, physical and mechanical properties.

There are several discrepancies and ambiguities in the copolymerization literature regarding the true values of monomer reactivity ratios. This situation is due to the fact that most studies on the kinetics of copolymerization systems have been using statistically incorrect parameter estimation techniques, experimental trials conducted to collect the required data are only at low conversion, and more disturbingly, experimental trials are chosen completely randomly and away from any kind of optimal design of experiments for the purpose of estimating reactivity ratios. For terpolymerizations, despite the importance of the kinetics of terpolymerization reactions, limited research has been conducted to study and estimate ternary reactivity ratios, and mainly reactivity ratios from copolymerization pairs have been used as approximate values for ternary reactivity ratios. For larger multicomponent systems, there are no studies for estimating reactivity ratios whatsoever.

This brings us to a currently observed paradox in the overall picture. There are numerous published experimental studies, with a wealth of experimental information for estimating reactivity ratios; however, almost all existing approaches in this field suffer from oversimplifications and/or violation of certain basic assumptions. The objective is to go through the details of this repeatedly

misinterpreted research problem and set the record straight with the use of appropriate choices of data/information and rigorous statistical/numerical techniques.

The parameter estimation technique used in this work is the error-in-variables-model (EVM), since this technique is one of the most general and advanced parameter estimation methods that takes into account the error in all variables involved (i.e., it does not distinguish between dependent and independent variables). This property matches the characteristics of the reactivity ratio estimation problem perfectly. In order to provide a general and complete procedure for estimating reliable reactivity ratios, we have put together the EVM framework that combines parameter estimation and optimal design of experiments, along with full conversion experimentation. The combination of these steps maximizes the amount of information in the experimental data and minimizes the amount of experimental workload. This framework is iterative and sequential and continues until satisfactory results for reactivity ratio estimates are obtained.

With respect to copolymerization reactivity ratios, the EVM framework provides a concrete, superior approach after almost 70 years of fragmented attempts in this area. We have established the utilization of high conversion data for estimating reactivity ratios using a direct numerical integration approach that is not limited to any assumptions, and more importantly, the combination of the design of experiments and parameter estimation steps within the correct EVM context with a sequential scheme that can continue to improve the results for reactivity ratio estimates. All these features provide a solution that has never been implemented before in the literature for this problem, a solution that has a significant effect on the reliability of reactivity ratio estimation results.

Compared to copolymerization systems, our knowledge about the behavior of ternary system with respect to the reactivity ratios of three monomers is at an extremely introductory level, and there are several questions that should be considered about the kinetics of ternary polymerization and the interaction between the three monomers. We have established the correct procedure for estimating ternary reactivity ratios using terpolymerization experimental data directly. Then, the design of experiments step from the EVM framework was implemented on terpolymerization systems, for the first time in the literature. Finally, the performance of the EVM framework on ternary reactivity ratio studies has been illustrated in detail and confirmed experimentally with a novel terpolymerization system of 2-Acrylamido-2-methyl-1-propanesulfonic acid (AMPS)/Acrylamide (AAm)/Acrylic acid

(AAc) (a water-soluble terpolymer with applications in enhanced oil recovery and flocculation). Therefore, all the framework steps developed in this thesis for copolymerizations and terpolymerizations have been verified with both extensive simulation studies and experimental data (from the literature and our own).

Acknowledgements

First and foremost, I would like to express my sincere gratitude to my supervisor Professor Alexander Penlidis for providing me with excellent guidance, mentorship, and great atmosphere for doing research. I am truly thankful for his supportive, understanding, and encouraging presence, and his selfless dedication to both my personal and academic development.

I wish to thank Professor Thomas A. Duever, for his support of my research and helping me to develop my background in statistics. I would like to express my appreciation to the members of my dissertation committee for taking the time to read my thesis and attend my defense session.

I would like to acknowledge the rewarding collaboration with Dr. Benoit Lessard, University of Toronto, and Professor Milan Maric, McGill University. A special mention for Marzieh Riahinezhad, for her cooperation in our joint projects; for Alison Scott, for her dedicated help in the experimental work; and for many others in the Department of Chemical Engineering, University of Waterloo.

I also thank everyone in my research group for all the nice memories we have from the last four years, and also, to all my friends in Waterloo, as it was a blast sharing countless wonderful moments with them.

Words cannot express how grateful I am to everyone in my family. For life, I am in debt of my mother, for her enormous heart, unconditional love and support; my father, for being my role model and taking my hand and helping in every single step of life; my sister, for being the joy of my life; and last but not least, my husband for his support, encouragement, and love. This accomplishment would have not been possible without them.

Dedication

This thesis is dedicated to my parents who have been my constant source of inspiration in life.

Table of Contents

List of Figures

List of Tables

Chapter 1

Introduction, Objectives, and Thesis Outline

1.1 Introduction

In modern life, synthetic polymers are indispensable materials as plastics, fibers, paints, coatings, etc. with a wealth of applications ranging from every day uses to construction materials and all the way to specialty materials for nanotechnology. Most of these polymers are mainly obtained by polymerizing a number of monomers in a multicomponent system. Such multicomponent polymerization systems can deliver specific properties that cannot be achieved with one or even two monomers only, and so they can facilitate the production of polymeric materials with new and improved properties. The simplest case of a multicomponent polymerization is a binary system (a.k.a., copolymerization), which is the starting point for more complex systems. Terpolymerization systems with three monomers and even more complex polymers are being utilized to generate polymeric materials with tailor-made properties.

Studying multicomponent polymerizations is an active area of research and one of the important aspects of such studies is the effort to understand the underlying kinetics. For such products, one needs to describe the micro- and macro-structures of polymers that determine the physical properties of polymeric products and, in turn, their final utilization. The micro- and macro-structures of a polymer are also linked to the kinetics of polymerization, which can be studied by the use of powerful mathematical models. Due to the practical impact and versatility of the properties of multicomponent polymers, understanding the underlying kinetics of such systems is not only advantageous for exploring strategies for advanced technologies but also necessary for producing materials with desirable physico-chemical properties in pilot-plant and/or industrial scales.

For multicomponent polymerization systems, one cannot explain their characteristics only based on information of each monomer. In fact, the interaction between the various monomers is the key in creating diverse polymeric products with versatile properties. One of the basic characteristics of a polymer for specific polymer applications is its composition, controlled by the polymerization rate

and influenced by the relative reactivities of the monomers present in the reaction medium. These relative reactivities of monomers are the original source of the definition of important parameters referred to as reactivity ratios. Reactivity ratios describe the rate of incorporation of each monomer in the polymer chain, compared to the other (co)monomers. The knowledge of these reactivity ratio parameters enables us to predict copolymer composition from any starting feed composition. The impact of copolymer chain composition on chemical, physical, and mechanical properties clearly indicates how important it is to be able to predict and, furthermore, control polymer chain composition from the knowledge of (feed) monomer concentrations and the reactivity ratios.

There are numerous publications in the literature for determining reactivity ratios for different monomers in multicomponent systems (mostly copolymers). One of the main purposes of these studies is to explore polymerization kinetics in order to optimize the polymerization conditions for specific polymer properties and particular applications. The values of reactivity ratios enable us to use models for predicting the polymer composition beyond the studied experimental region, and perhaps more importantly, they enable us to learn more about monomers and their different characteristics. There are several studies where reactivity ratios of a monomer with a series of other monomers are being investigated to explore the behavior and interactions of that monomer in multicomponent systems. In addition, there are modeling studies where the reactivity ratios are related to other characteristics of polymer products such as azeotropic composition or glass transition temperature (Tg), that again relate polymer properties to monomers interactions. Reactivity ratios have also been studied to explain the effect of different factors in the reaction medium, such as temperature, solvent, and pH, on the monomers' characteristics to the extent possible (see, for example, representative papers by Dube and Penlidis (1995a,b), McManus and Penlidis (1996), Odian (2004), O`Driscoll and Reilly (1990), Tidwell and Mortimer (1965), and Wittmer (1967)). Overall, these parameters are more than just essential components of composition models, as they can be used to explain the properties of polymers and monomers, and also to explore new and unstudied systems.

Looking at the general picture of previous efforts in this area, it can be seen that starting from 1944, basic theories for multicomponent polymerization kinetics were developed, mainly for co- and ter-polymerizations and in general for N-component systems (Mayo and Lewis (1944), Alfrey and Goldfinger (1944), and Wallings and Briggs (1954)). Following this pioneering work, studies of copolymerization reactions and kinetics dominated the publications in this area, trying to understand reactions and kinetics of different systems for various applications. Also, a lot of studies tried to

verify the composition models for copolymers, mainly the so-called Mayo-Lewis model, and use them with monomer reactivity ratios to predict the behavior of the system. These types of work, that have continued to emerge in the literature up to date, offer one part of the overall picture, and contribute greatly with extensive experimental work and bench-marking (verification) steps for these composition models.

The other side of this picture is not that great. It is concerned with publications that have appeared in the literature along with the above mentioned pioneering work in the modeling of multicomponent systems, with an effort to provide solutions for determining monomer reactivity ratios. Fineman and Ross (1950) and Kelen and Tudos (1975) were amongst the first groups that published techniques for calculating reactivity ratios using the Mayo-Lewis model. Their approaches were based on using linear regression for the linearized version of the Mayo-Lewis model. Several other groups, later on, proposed other linearized techniques for estimating/calculating reactivity ratios as well, and in general, these types of approaches became the most widely-used techniques for this matter. Behnken (1964) and Tidwell and Mortimer (1965) were the first to propose nonlinear parameter estimation techniques for estimating reactivity ratios, while pointing out the composition models are, in fact, nonlinear and using linearized approaches is statistically incorrect. Their work was followed by other groups, showing the application of nonlinear parameter estimation methods for determining reactivity ratios (O'Driscoll and Rielly (1987), Hagiopol et al. (1989), van Herk and Dorge (1997), van der Brink et al. (1999), etc.). As the most recent approach, Dubé et al. (1991), Reilly et al. (1993), and Polic et al. (1998) showed the application of the error-in-variables-model (EVM) method for this problem, which is believed to be the most appropriate technique for this problem, as studied rigorously throughout this thesis.

Unfortunately, more than 90-95% of the experimental studies on the kinetics of different copolymerization systems have been employing Fineman-Ross, Kelen-Tudos, and other linearized techniques to calculate monomers reactivity ratios. Since these techniques have an incorrect basis, as a result contradictory reactivity ratio values have been obtained over the years by different groups, even for the same systems. Hence, there are several discrepancies and ambiguities in the literature for the true values of reactivity ratios of the majority of monomers. The root of several arguments in the literature on the behavior of different monomers has no actual foundation but the use of incorrect techniques and therefore the resulting bias in the obtained reactivity ratios. Unfortunately, the nonlinear techniques that were proposed later on in the literature have not caught the attention of most

practitioners/experimental researchers in the field. For example, even very recently, in the first few months of 2014, there are several publications that report extensive experimental work for kinetic studies of certain copolymerization systems by estimating reactivity ratios through statistically incorrect linearized methods that were proposed 50 years ago (Sioleck and Matlengiewicz (2014), Kazantsev et al. (2014), Mielancyk et al. (2014), Benbayer et al. (2014), just to name a few)!

For terpolymerizations, unlike the story for copolymerizations and despite the importance of the kinetics of terpolymerization reactions, not a lot of research has been conducted to study and estimate reactivity ratios in terpolymerization modeling. This is partly due to the complexity of the terpolymer composition model, the Alfrey-Goldfinger model, and more importantly related to an analogy between copolymerization and terpolymerization mechanisms that allowed researcher to use reactivity ratios obtained for binary pairs from copolymerization experiments in models dealing with terpolymerizations. The inaccuracies in binary reactivity ratios can simply propagate into the terpolymerization composition model, thus becoming a much more serious (than in copolymerization) source of error in parameter estimation and prediction variance. Using binary reactivity ratios in terpolymerization studies also treats a ternary system as one of three completely independent and non-interacting binary copolymerizations, and therefore the interactions between the three monomers (and their respective radicals) are essentially ignored. This past approach is, therefore, an unjustified simplification that could have been acceptable at the time because of limited computation power, but not nowadays.

As a result, the state of the art for estimating ternary reactivity ratio has only seen random efforts with little or no intention for estimating reliable reactivity ratios (for example, binary reactivity ratios, almost randomly selected from the literature, have been used for studying polypeptides for medical/pharmaceutical applications (Zelzer and Heise (2014))! Using binary reactivity ratios in place of ternary ones has been a source for profound ambiguities and contradictory results for terpolymerization studies to the extent that researchers in this field never invested sufficient effort to relate the kinetics of terpolymerizations to different applications. Hence, compared to copolymerization systems, our knowledge about the behavior of ternary systems with respect to the reactivity ratios of three monomers is at an extremely introductory level, and there are several questions that should be considered about the kinetics of ternary reactions and the interaction between the three monomers based on the reactivity ratios of three monomers. In addition to this research potential, there are countless applications for terpolymerization systems in industry with very scarce

information as to how we can optimize the synthesis process for those applications. Having reactivity ratios and learning more about the terpolymerization reactions can open the doors to a significant source of improvements in this industry as well.

Therefore, promoting a correct and comprehensive approach can be a solution for dealing with inconsistencies in the reactivity ratio database in the literature, at the same time enabling practitioners to estimate reactivity ratios for their systems with efficient and reasonable workload. Given that there is no such thing as “all purpose” reactivity ratio set for a system, the ability to find these values with an efficient procedure and in a reliable fashion can be significantly useful. This option can also be a great asset in other relevant studies based on reactivity ratios, since by having accurate and reliable reactivity ratio estimates, differences in reaction conditions can actually be studied (and process observations explained) through differences in reactivity ratio values.

1.2 Objectives

Looking in depth at the overall picture of the attempts by polymer researchers and chemists for determining reactivity ratios shows that not only are the majority of these techniques incorrect, but also the experimental trials conducted to collect the required data are only at low conversion. This is due to the fact that instantaneous composition models (the Mayo-Lewis and the Alfrey-Goldfinger models) are being used (again, often combined incorrectly with cumulative composition data)! So, this approach is only acceptable at low conversion levels, owing to the assumption that composition drifts in monomer feed (and, hence, in copolymer chain composition) are negligible at low conversion levels. However, most polymerization reactions will inevitably show compositional drift as the degree of conversion increases, and composition versus conversion data at higher conversion levels are a valuable source of information for reactivity ratio estimation. Therefore, it is reasonable to utilize cumulative composition models, i.e., the integrated form of instantaneous models, that can be applied over the whole conversion trajectory, and therefore to medium/high conversion levels.

Another missing component in this picture is the lack of the optimal design of experiments for estimating reactivity ratios. Polymer chemists traditionally started by performing experiments covering a broad range of feed compositions (the so-called empirical approach), believing that such an approach would provide a large number of experimental points (trials) and hence the best results

for estimating reactivity ratios. Even though design of experiments approaches for obtaining improved reactivity ratios were proposed since the mid-60s (notably by Tidwell and Mortimer (1965)), empirical approaches dominated among chemists and were readily used by almost all researchers, often slightly modified, but mainly far from any optimality consideration. This issue is further compounded by the fact that the experiments conducted are not replicated, and therefore, they do not yield the necessary estimate of the underlying experimental error. Combining design of experiments techniques with any parameter estimation problem is highly recommended as a problem-solving approach but rarely practised!

This brings us to a currently observed paradox in the overall picture. There are numerous published experimental papers, and hence a wealth of experimental information for estimating reactivity ratios; however, almost all existing approaches in this field suffer from oversimplifications and/or violation of certain basic assumptions (both experimental and statistical). It is thus imperative to go through the details of this repeatedly misinterpreted research problem and set the record straight with the use of appropriate choices of data/information and rigorous statistical/numerical techniques. To offer a general framework, resulting in reliable and consistent reactivity ratio estimates, we need to have a clear idea, in advance, of the steps and condition needed to be considered and satisfied. Such framework brings together all key components, as depicted in Figure 1-1. As shown in this figure, steps of “parameter estimation”, “design of experiments”, and “experimentation” should be combined in the framework. All of these steps are defined according to the statistical nature of the reactivity ratio estimation problem, while keeping in mind polymerization reaction details as well as the practicality of the whole framework.

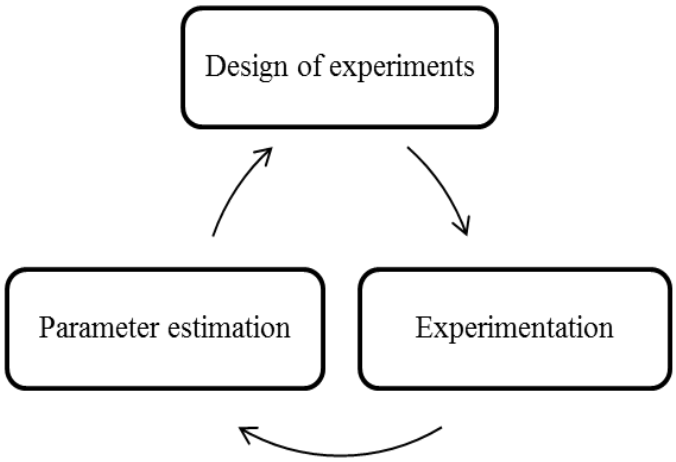

Figure 1-1. The overall procedure for estimating reliable reactivity ratios

The parameter estimation technique used in this work is the error-in-variables-model (EVM), since this technique is one of the most general and advanced parameter estimation methods that takes into account the error in all variables involved (i.e., it does not distinguish between dependent and independent variables). This property matches the characteristics of the reactivity ratio estimation problem perfectly, as in this problem, all of the variables are subject to error, and the use of traditional regression analysis where some of the variables are considered to be perfectly known results in biased reactivity ratio estimates. Although the basic EVM equations and parts of the EVM algorithm applied to several nonlinear parameter estimation problems have appeared before in such papers as Reilly and Patino-Leal (1981), Duever et al. (1983) , Keeler and Reilly (1991, 1992), Reilly et al. (1993), Polic et al. (1998), Sutton and MacGregor (1977), Jitjareonchai et al. (2006) and Biglari et al. (2006), they appeared in a rather fragmented way and certainly not all of them in one source traversing the full spectrum from the design of experiments all the way to parameter estimation and diagnostic checks.

The objectives of this research are to develop a comprehensive EVM framework with the components shown in Figure 1-1. The parameter estimation step in this framework should be able to handle not only low conversion but also medium/high conversion composition data, so that all available information can be included for estimating reactivity ratios. The design of experiments step ensures that the experiments are run at optimal feed compositions so that they contain the most amount of information with respect to the reactivity ratio parameters (while at the same time minimizing the experimental effort). Finally, the experimental data should contain composition values up to high

conversion levels, from all responses, and with independent replication to ensure reproducibility in the data (another issue that is almost always neglected).

The implementation of this framework for copolymerization and terpolymerization examples in this thesis can clearly show how efficiently reliable reactivity ratios can be achieved. In addition to solving the reactivity ratio estimation problem throughout this thesis, another important contribution of the current work is presenting the full EVM framework, from the design of experiments to parameter estimation, so that the user/reader can have a full overview of the equations and implementation steps, along with specific examples. In the verification examples, the general EVM equations are translated and applied on interesting aspects, both academically and industrially, of the important reactivity ratio estimation problem, expressed both as a single-response (copolymer composition data) and a multi-response (terpolymer composition data) scenario.

1.3 Thesis Outline

The work in this thesis is presented in 9 chapters. Brief descriptions for the thesis chapters are given below:

Chapter 2 offers general background information about three main topics discussed throughout this thesis. First, the free-radical copolymerization and terpolymerization mechanistic models and the definition of reactivity ratios are explained. Then, the concepts of parameter estimation and design of experiments for nonlinear models are explained; and finally, detailed statistical and numerical explanations about the EVM concept and its algorithm are mentioned.

Chapter 3 presents the method for estimating reactivity ratios of copolymerization systems based on high conversion data and the EVM parameter estimation approach. The choice of the cumulative composition model, to be used in this problem, is discussed and the corresponding aspects of the implementation of the EVM method are explained. The performance of our approach in comparison with conventional methods is shown with representative examples.

With the goal of completing the EVM framework, **Chapter 4** implements the design of experiments approach using the EVM design criterion to locate optimal feed compositions for estimating reactivity ratios in copolymerization systems. This problem is studied in great details for existing

copolymerization systems from the literature as well as hypothetical (simulated) ones in order to have a comprehensive view of the potential and applicability of the EVM design criterion.

Chapter 5 concludes our investigations for copolymerization reactivity ratios by putting together all the components and presenting the complete EVM framework, as a set of recommended steps. This framework is then applied to an experimental system and its performance confirmed.

In the next part of this research, **Chapter 6** looks at the problem of estimating reactivity ratios of terpolymerization systems. This problem is at a much earlier stage than the copolymerization case. The choice of the mechanistic model for estimating reactivity ratios, the implementation of the EVM method, and the performance of this approach with alternative schemes for the number of responses as well as using low and high conversion data are illustrated. Finally, the correct method for estimating ternary reactivity ratios is established.

Chapter 7 looks at the problem of designing experiments for estimating ternary reactivity ratios for the first time in the literature. The EVM design criterion is implemented for this purpose and several important details with respect to this design of experiments problem are discussed. The relation between the optimal ternary experiments and reactivity ratios is investigated to arrive at a practical heuristic that gives us the optimal ternary experiments without the need to carry out complex mathematical derivations.

Chapter 8 presents the culmination of the use of the EVM framework for the terpolymerization reactivity ratio estimation problem. To illustrate the performance of this framework, an experimental verification project is conducted. Experiments are conducted for the water-soluble and unstudied terpolymerization system of 2-Acrylamido-2-methyl-1-propanesulfonic acid (AMPS)/Acrylamide (AAm)/Acrylic acid (AAc), and monomer reactivity ratios are determined using optimal experiments at high conversion. The results confirm that implementing the EVM framework for estimating ternary reactivity ratios is a significant improvement for the research in this area.

Chapter 9 presents the main thesis conclusions (for the overall thesis, as more specific concluding remarks are made at the end of each chapter), the main contributions of our work, and recommendations for future steps (immediate and longer-term).

Finally, ten **appendices** at the end of the thesis complement the different thesis chapters.

Chapter 2

Background Literature

Basic background information for the three main topics that are discussed throughout this thesis is included in this chapter. Since each of the following chapters touches upon one of the important components of this work, the specific (and more detailed) literature review and related references for each problem will be presented at the beginning of each relevant chapter. In this chapter, we begin by an overview of multicomponent polymerization kinetics, and more specifically copolymerization and terpolymerization reactions, and the important equations that are used in the following chapters. Also, the definition and implication of reactivity ratios in this context are reviewed. Next, the statistical background information for solving nonlinear parameter estimation problems and the design of experiments for this purpose is discussed in general terms. The error-in-variables-model (EVM) algorithm is then discussed in detail. Details about the EVM algorithm with special attention to its requirements, mathematical implementation, numerical steps, and other related information, are provided.

2.1 Multicomponent Polymerizations Kinetics and Modeling

2.1.1 Copolymerization systems

2.1.1.1 The instantaneous copolymer composition model

The most widely used model for copolymerization composition is the so-called Mayo-Lewis model (Mayo and Lewis (1944)), as shown in equation (2.1). This equation describes the instantaneous copolymer composition based on the reactions happening in the propagation step of a copolymerization reaction. In this equation, the instantaneous copolymer composition, F_1, is related to the unreacted monomer feed composition, f_1, and two reactivity ratio parameters for monomer 1 and 2, r_1 and r_2. Equation (2.2) shows expressions of f_1 and F_1, with $[M_1]$ and $[M_2]$ as the concentrations of monomer 1 (M_1) and monomer 2 (M_2) in the polymerizing mixture. Reactivity

ratios, as described in Chapter 1, are the ratios of rate constants of homo-propagation (e.g., k_{11}) over cross-propagation (e.g., k_{12}) of each reactive species (M_1 or M_2), and are given by equation (2.3).

$$F_1 = \frac{r_1 f_1^2 + f_1(1-f_1)}{r_1 f_1^2 + 2f_1(1-f_1) + r_2(1-f_1)^2} \tag{2.1}$$

$$F_1 = \frac{d[M_1]}{d[M_1]+d[M_2]} \text{ and } f_1 = \frac{[M_1]}{[M_1]+[M_2]} \tag{2.2}$$

$$r_1 = \frac{k_{11}}{k_{12}},\ r_2 = \frac{k_{22}}{k_{21}} \tag{2.3}$$

The derivation of the Mayo-Lewis model is shown in Appendix A. This model is based on the assumptions that the copolymerization composition is determined based on the reaction at the propagation step and the identity of the monomer unit at the growing radical end. The latter assumption is also known as the terminal model for copolymerization which states that the propagation reaction is independent of the chain composition preceding the last monomer unit. A limitation with the Mayo-Lewis model is that it assumes that all variables are measured instantaneously, which is rarely the case. However, the model can be used if one can analyze the copolymer over very short time intervals from time zero, in which case the cumulative composition (from H-NMR or other techniques) should equal the instantaneous copolymer composition. Another alternative would be to have very frequent cumulative composition data points, discretize them over very short intervals, and take successive differences in order to obtain instantaneous data (i.e., take derivatives of the cumulative distribution). However, one has the latter luxury only rarely. Therefore, the instantaneous model requires the polymerization process to be run at low conversion levels, often less than 5-10%.

Most commercial copolymerizations go to high conversion; therefore, the effect of conversion on copolymer composition is of considerable interest. It is also important to know the polymer compositions at any time during the polymerization. With the exception of azeotropic copolymerizations, one cannot in general assume that composition would remain constant at higher conversion levels (due to composition drift resulting from unequal reactivities between radicals and monomers); therefore, a model is required that would account for the feed composition at the end of (or any other point in) the reaction. There are two commonly used model forms that give the

copolymer composition at high conversion levels (or over the entire conversion trajectory), and these are discussed in the next two sections.

2.1.1.2 Cumulative copolymer composition model: Numerical integration

Skeist (1946) developed a useful approach to analyze mole fraction of unreacted monomer, f_1, and cumulative copolymer composition, $\bar{F}_1$, as a function of conversion, X_n. To obtain f_1, assuming that there is a total of M moles of two monomers and dM moles of polymerized monomers, a material balance for monomer 1 (at any instant) results in equation (2.4), which can be integrated to calculate f_1 at any conversion level. X_n is molar conversion, defined by equation (2.5), assuming that the polymerizing mixture has a constant volume. F_1 in this equation is evaluated using the Mayo-Lewis model, which means that the right-hand side of the equation (2.4) is only a function of X_n, f_1, r_1, and r_2. In order to solve (i.e., numerically integrate) the ordinary differential equation (2.4), the initial condition $f_1=f_{10}$ when $X_n=0$ is required.

$$\frac{df_1}{dX_n} = \frac{f_1 - F_1}{1 - X_n} \tag{2.4}$$

$$X_n = 1 - \frac{M_1 + M_2}{M_{10} + M_{20}} \tag{2.5}$$

To obtain the cumulative mole fraction of monomer 1 incorporated in the copolymer, $\bar{F}_1$, a mole balance for monomer 1 after reaching to a certain conversion level, X_n, gives the famous Skeist equation, as shown in equation (2.6). In this equation, f_{10} is the initial feed composition, and as the reaction proceeds with time, X_n changes and f_1 is evaluated by the numerical solution of equation (2.4). The definition of $\bar{F}_1$ and f_{10} are also given by equations (2.7) and (2.8), respectively. Equation (2.6) can be used to calculate the cumulative copolymer composition directly from numerical integration of the copolymer composition equation. The derivation procedure for equations (2.4) and (2.6) are shown in Appendix B.

$$\bar{F}_1 = \frac{f_{10} - f_1(1 - X_n)}{X_n} \tag{2.6}$$

$$f_{10} = \frac{[M_{10}]}{[M_{10}] + [M_{20}]} \tag{2.7}$$

$$\bar{F}_1 = \frac{[M_{10}] - [M_1]}{[M_{10}] + [M_{20}] - [M_1] + [M_2]} \tag{2.8}$$

Compared with the numerical integration approach, there is an analytical integrated form of the cumulative copolymer composition model that has been used in several literatures. This analytical approach in introduced in the next section.

2.1.1.3 Cumulative copolymer composition model: Analytical integration

The so-called Meyer-Lowry model (1965) is the result of the analytical integration of the Mayo-Lewis equation, equation (2.1). The general form of the Meyer-Lowry model is given by equation (2.9):

$$X_n = 1 - [\frac{f_1}{f_{10}}]^{\alpha}[\frac{f_2}{f_{20}}]^{\beta}[\frac{f_{10}-\delta}{f_1-\delta}]^{\gamma} \tag{2.9}$$

where $\alpha = \frac{r_2}{(1-r_2)}$; $\beta = \frac{r_1}{(1-r_1)}$; $\gamma = \frac{1-r_1 r_2}{(1-r_1)(1-r_2)}$; $\delta = \frac{(1-r_2)}{(2-r_1-r_2)}$

f_1 and f_2 are the free (unreacted, unbound) monomer mole fractions at time, t, whereas f_{10} and f_{20} are the initial monomer (feed) mole fractions. One must note that typical measurements in an experiment are the initial monomer mole fractions and final copolymer mole fractions. Therefore, the molar conversion cannot be obtained as described in equation (2.5). To avoid this problem, and using the Skeist expression, equation (2.6), the molar conversion can be obtained by equation (2.10). Subsequently, the Meyer-Lowry model can be rewritten as equation (2.11).

$$X_n = \frac{f_1-f_{10}}{f_1-\bar{F}_1} \tag{2.10}$$

$$\frac{f_1-f_{10}}{f_1-\bar{F}_1} = 1 - [\frac{f_1}{f_{10}}]^{\alpha}[\frac{f_2}{f_{20}}]^{\beta}[\frac{f_{10}-\delta}{f_1-\delta}]^{\gamma} \tag{2.11}$$

Equation (2.11) is referred to as the molar conversion form of the Meyer-Lowry model. An alternative form could also be developed to yield a relationship between the initial monomer (feed) mole fraction, f_{10}, final copolymer mole fraction, $\bar{F}_1$, and conversion on a weight basis, X_w. This relation is shown in equation (2.12), in which X_n can be replaced by mass conversion using equation (2.13), with Mw_1 and Mw_2 as the molecular weights of monomer 1 and 2. Equation (2.12) is usually referred to as the mass conversion form of the Meyer-Lowry model and this is the form that will be used in this research, for parameter estimation purposes.

$$X_n = 1 - [\frac{f_{10}-\bar{F}_1 X_n}{f_{10}(1-X_n)}]^{\alpha}[\frac{1-X_n-f_{10}-\bar{F}_1 X_n}{(1-f_{10})(1-X_n)}]^{\beta}[\frac{(\delta-f_{10})(1-X_n)}{\delta-\delta X_n-f_{10}+\bar{F}_1 X_n}]^{\gamma} \tag{2.12}$$

$$X_n = X_w \frac{Mw_1 f_{10} + (1-f_{10}) Mw_2}{Mw_1 \bar{F}_1 + (1-\bar{F}_1) Mw_2} \tag{2.13}$$

The Meyer-Lowry model can predict the copolymer composition for reactions at low to moderate levels of conversion (i.e., say, up to 30%-50% conversion, with the range of up to 25-30% conversion being safer). These approximate conversion ranges have been defined due to certain simplifying and restrictive assumptions involved in the derivation of this model. For instance, the polymerization should be isothermal, hence no temperature-varying scenarios can be accommodated. This assumption could be considered a minor problem, since reactivity ratios are weak functions of temperature (for many systems but not all), unless of course temperature levels change by more than 30 degrees Celsius (see section 2.1.4). Another (relatively minor) assumption is that the volume of the polymerizing mixture does not shrink considerably. This would again be true at low to moderate conversion levels, but not throughout the entire reaction. Since it is likely that these assumptions might be violated during a typical copolymerization, utilizing this model for kinetic investigations (especially above a conversion level of 25-40%, always depending on the specific copolymer system) can be a source of error.

2.1.2 Terpolymerization

2.1.2.1 Instantaneous terpolymer composition model

For terpolymerization reactions, the instantaneous composition model was first proposed by Alfrey and Goldfinger (1944). This model is based on the same assumptions as the Mayo-Lewis model. That is, the propagation step determines the terpolymer composition and the terminal model describes the reaction of each reactive monomer with polymer chains. The Alfrey-Goldfinger model is given in equations (2.14) to (2.16), where f_i is the mole fraction of unbound monomer i in the polymerizing mixture (as shown in equation (2.2)) and df_i is the mole fraction of monomer i incorporated (bound) into the polymer chains. The derivation of the Alfrey-Goldfinger model is included in Appendix C.

$$\frac{df_1}{df_2} = \frac{f_1\left(\frac{f_1}{r_{21}r_{31}} + \frac{f_2}{r_{21}r_{32}} + \frac{f_3}{r_{31}r_{23}}\right)\left(f_1 + \frac{f_2}{r_{12}} + \frac{f_3}{r_{13}}\right)}{f_2\left(\frac{f_1}{r_{12}r_{31}} + \frac{f_2}{r_{21}r_{32}} + \frac{f_3}{r_{13}r_{32}}\right)\left(f_2 + \frac{f_1}{r_{21}} + \frac{f_3}{r_{23}}\right)} \tag{2.14}$$

$$\frac{df_1}{df_3} = \frac{f_1\left(\frac{f_1}{r_{21}r_{31}}+\frac{f_2}{r_{21}r_{32}}+\frac{f_3}{r_{31}r_{23}}\right)\left(f_1+\frac{f_2}{r_{12}}+\frac{f_3}{r_{13}}\right)}{f_3\left(\frac{f_1}{r_{13}r_{21}}+\frac{f_2}{r_{23}r_{12}}+\frac{f_3}{r_{13}r_{23}}\right)\left(f_3+\frac{f_1}{r_{31}}+\frac{f_2}{r_{32}}\right)} \tag{2.15}$$

$$\frac{df_2}{df_3} = \frac{f_2\left(\frac{f_1}{r_{12}r_{31}}+\frac{f_2}{r_{21}r_{32}}+\frac{f_3}{r_{13}r_{32}}\right)\left(f_2+\frac{f_1}{r_{21}}+\frac{f_3}{r_{23}}\right)}{f_3\left(\frac{f_1}{r_{13}r_{21}}+\frac{f_2}{r_{23}r_{12}}+\frac{f_3}{r_{13}r_{23}}\right)\left(f_3+\frac{f_1}{r_{31}}+\frac{f_2}{r_{32}}\right)} \tag{2.16}$$

Reactivity ratios in the Alfrey-Goldfinger equation are defined analogous to the copolymerization composition model, as these two models are derived based on the same assumption (mainly the terminal model). The six reactivity ratios in the Alfrey-Golfinder model are given in equation (2.17).

$$r_{12} = \frac{k_{11}}{k_{12}},\ \ r_{13} = \frac{k_{11}}{k_{13}},\ \ r_{21} = \frac{k_{22}}{k_{21}},\ \ r_{23} = \frac{k_{22}}{k_{23}},\ \ r_{31} = \frac{k_{33}}{k_{31}},\ \ r_{32} = \frac{k_{33}}{k_{32}} \tag{2.17}$$

In order to find the composition of a terpolymer by using the terpolymerization composition model, knowledge of six reactivity ratios is required. Also, the equations are of the differential type; assuming polymerization does not proceed to high conversions and stays in the low conversion region, df_i can be replaced by F_i, which is the instantaneous mole fraction of monomer *i* in the resulting polymer. Use of the Alfrey-Goldfinger model has shown to give good agreement between calculated terpolymer composition and experimental results. However, similar to the Mayo-Lewis model, the Alfrey-Goldfinger model is only applicable to low conversion experiment, and an integrated form of this model is required for predicting terpolymer compositions at higher conversion. The integrated form is shown in the next section.

2.1.2.2 Cumulative terpolymer composition model

Similar to the copolymerization models, mole balances for each monomer in a terpolymerization system can provide equations for the mole fraction of unreacted monomer, f_i, and cumulative copolymer composition, $\overline{F_i}$, as a function of conversion, X_n. A set of differential equations, as shown in equation (2.18), should be simultaneously integrated to obtain f_i. F_i in these equations should be evaluated using the Alfrey-Goldfinger model, equations (2.14) to (2.16). Then, the Skeist equation for each monomer, as shown in equations (2.19) to (2.21) can be used to calculate the cumulative mole fraction of monomer *i* incorporated in the copolymer, $\overline{F_i}$. Conversion, $X_{n,}$ is given by equation (2.22) and the rest of the compositions for terpolymerization feed and terpolymer chains can be determined

in a fashion similar to copolymerizations, considering three components instead of two for the binary copolymerization.

$$\begin{cases} \frac{df_1}{dX_n} = \frac{f_1 - F_1}{1 - X_n} \\ \frac{df_2}{dX_n} = \frac{f_2 - F_2}{1 - X_n} \\ \frac{df_3}{dX_n} = \frac{f_3 - F_3}{1 - X_n} \end{cases} \tag{2.18}$$

$$\overline{F_1} = \frac{f_{10} - f_1(1 - X_n)}{X_n} \tag{2.19}$$

$$\overline{F_2} = \frac{f_{20} - f_2(1 - X_n)}{X_n} \tag{2.20}$$

$$\overline{F_3} = \frac{f_{30} - f_3(1 - X_n)}{X_n} \tag{2.21}$$

$$X_n = 1 - \frac{M_1 + M_2 + M_3}{M_{10} + M_{20} + M_{30}} \tag{2.22}$$

2.1.3 Different types of behavior of multicomponent polymerizations

In basic books describing polymerization principles, the behavior of multicomponent polymerizations can be categorized based on their reactivity ratio values into classes of ideal and alternating systems, and occasionally block and graft systems (see, for example, Odian (2004)).

The ideal behavior belongs to a system where the product of all reactivity ratios equals one. For example, for copolymerizations, $r_1 \times r_2 = 1$. In the particular case of all reactivity ratios equal to one, we have a random multicomponent polymer where the composition of the polymer is the same as the feed. In this system, each monomer has equal tendencies to homo-propagation and cross-propagation, and as a result, there will be completely random placement of the monomer units along the polymer chain. The alternating behavior belongs to a system where the monomers have no tendency for homo-propagation, and therefore, they alternate along the chain. The extreme case of this class, for copolymerization, is defined when $r_1 \times r_2 = 0$ (or a very small value for all practical purposes). Most of multicomponent systems are between the two extremes of ideal and alternating types, if the reactivity ratios are acceptable.

A unique behavior of multicomponent polymers happens at the azeotropic composition, i.e., the point at which the compositions of the polymer and the (unreacted) monomer (feed) mixture are the same. For copolymerizations, azeotropic composition can be found when both reactivity ratios are less than one. The composition of the azeotrope can be calculated directly from the values of monomer reactivity ratios, as shown in equation (2.23). Wittmer et al. (1967) cited an extensive table with reactivity ratios for various binary systems along with their azeotropic compositions, which is a good source of information for many copolymerization systems.

$$F_1 = f_1 = \frac{1-r_2}{2-r_1-r_2} \tag{2.23}$$

For terpolymerization systems, the relation between the behavior of the multicomponent polymer and reactivity ratios is not as straight-forward as for copolymerization systems. The ideal behavior of copolymerizations can be extended to terpolymerizations directly; however, the alternating behavior has been expressed in different ways by different publications (for example, see, Ham and Lipman (1967)). Likewise, calculation of the azeotropic composition is more complicated compared to copolymerization systems, and there has been much controversy around this issue as it goes back to the uncertainties in ternary reactivity ratios in the literature. Kazemi et al. (2010) provided a review of the literature in this regard and proposed a novel approach based on the Alfrey-Goldfinger equation for calculating the composition of azeotropic composition in terpolymerization systems.

2.1.4 Effect of reaction conditions on reactivity ratios

"Monomer reactivity ratios are generally but not always independent of the reaction medium in radical multicomponent polymerizations" (Odian (2004)). It has been observed that reactivity ratios are different for experiments that occur in non-homogeneous media (e.g., emulsion and suspension polymerization) from those in bulk or solution polymerization. In bulk polymerization, it is well known that at moderate to high conversion levels, the gel effect happens and reactions become diffusion-controlled, which may change reactivity ratio values. For very acidic or basic monomers, the pH of the medium is very important as monomers exhibit different characteristics (as if they are different species) in different pH levels (Odian (2004)).

Among other reaction conditions, reaction temperature influences reactivity ratio values as well. Since reactivity ratios are ratios of rate constants and rate constants are functions of temperature

(Arrhenius equation), the relation between a reactivity ratio and temperature is given by equation (2.24) (Odian (2004)), where E_{11} and A_{11} are the activation energy and frequency factor of the propagation rate constant describing the reaction between M_1 and M_1^*, and E_{12} and A_{12} for the propagation rate constant between M_2 and M_1^*. The effect of temperature is not significant (at least over typical terpolymerization temperature ranges), as the activation energies for the different propagation reactions are relatively similar.

$$r_1 = \frac{k_{11}}{k_{12}} = \frac{A_{11}}{A_{12}} exp\left(\frac{E_{12}-E_{11}}{RT}\right) \tag{2.24}$$

2.2 Nonlinear Regression Analysis

2.2.1 Nonlinear least squares (NLLS) parameter estimation

The problem of estimating parameters in nonlinear models from experimental data can be found in almost every field of science and engineering, and the nonlinear least squares (NLLS) method is a widely accepted method for this purpose. The method is based on the principle of minimizing the sum of squares of residuals. In this section, the basic equations of this method are briefly presented and more information can be found in classical references, such as Bard (1974) and Draper and Smith (1981). A general form of a model can be written as in equation (2.25), where the vector of dependent variables, $\underline{y_i}$, is related to the vector of independent variables, $\underline{x_i}$, and vector of parameters, $\underline{\theta}$, though a function, $g(\underline{x_i}, \underline{\theta})$, and an error term, $\underline{\varepsilon_i}$. "Underline" characters denote vectors or matrices. The function in NLLS is nonlinear in the parameters and has a single equation (single-response).

$$\underline{y_i} = g(\underline{x_i}, \underline{\theta}) + \underline{\varepsilon_i} \qquad i=1, 2, ..., n \tag{2.25}$$

The assumptions of NLLS are that (1) the model perfectly describes the system, (2) the error in the independent variables is negligible, and (3) the error is assumed to be independent and identically normally distributed with mean zero and variance σ^2. That is, the error covariance matrix is $I\sigma^2$.

In NLLS, the objective function is given by equation (2.26). Note that this equation is for problems with a single response model and constant error variances. If the problem is a multiresponse case, the determinant criterion, derived in Box and Draper (1965), can be used. Also, if different responses

have different error variances, a weighted least squares procedure should be used instead of equation (2.26) (see, for example, Box (1970)). The parameter estimates, $\underline{\hat{\theta}}$, can be found using equation (2.27), given the initial parameter estimates values, $\underline{\theta}_0$. Vectors $\underline{Y}$ and $\underline{X}$ represent the values of dependent and independent variables for all the measurements, and $\underline{Z}$ is the Jacobian matrix for the derivatives of the model with respect to the parameters. The converged values of parameters, $\underline{\hat{\theta}}$, correspond to the least squares estimates (Bard (1974)). The variance-covariance matrix of $\underline{\hat{\theta}}$ is given by equation (2.28), where $\underline{Z}'\underline{Z}$ is the information matrix.

$$S(\underline{\theta}) = \sum_{i=1}^{n} (y_i - g(\underline{x}_i, \underline{\theta}))' (y_i - g(\underline{x}_i, \underline{\theta})) \tag{2.26}$$

$$\underline{\theta}^{(k+1)} = \underline{\theta}^{(k)} + (\underline{Z}'\underline{Z})^{-1} \underline{Z}' (\underline{Y} - g(\underline{X}, \underline{\theta}^{(k)})) \tag{2.27}$$

$$Var(\underline{\hat{\theta}}) = (\underline{Z}'\underline{Z})^{-1} \sigma^2 \tag{2.28}$$

2.2.2 Joint confidence regions for parameter estimates

The evaluation of the parameter estimation results is a crucial task in any parameter estimation procedure, almost as important as estimating the parameters themselves. There are some indicators that quantitatively define the uncertainty of the results, allowing us to decide whether the results are reliable or not. Confidence intervals are common indicators for this objective. However, for cases where there are more than one parameter, being simultaneously estimated, a joint confidence region (JCR) should be presented that quantifies and visualizes the measure of uncertainty in the estimated parameters by presenting a contour/JCR. Values of the parameters inside or on the contour represent plausible values of the parameters at the specified confidence level, and the smaller the JCR the higher the precision of the results. A JCR is in fact a hyper-ellipse with dimensions equal to the number of parameters. Normally, if there are more than two parameters, a conditional joint confidence region is calculated for every two parameters, by fixing the remaining parameters at their point estimate values.

For linear regression analysis, parameters' JCR has an elliptical shape (an ellipse with the center of parameter estimates) with exact shape and probability. For nonlinear models, however, the simplest

way to calculate JCR is using the idea of elliptical JCR, knowing that the shape and the size of such JCR is approximate to the extent of nonlinearity of the model. For NLLS problem with known measurement error variance of σ^2, the formula of JCR is given in equation (2.29), where χ^2 represents the value of the chi-squared distribution, p is the number of parameters, and (1-α) is the chosen confidence level.

$$\left(\underline{\theta} - \underline{\hat{\theta}}\right)' \underline{Z}' \underline{Z} \left(\underline{\theta} - \underline{\hat{\theta}}\right) \leq \sigma^2 \chi^2_{(p,1-\alpha)} \tag{2.29}$$

The elliptical shape of JCR from equation (2.29) can be close to the exact shape of this contour, provided that the extent of nonlinearity of model is not significant. If the model is very nonlinear, a JCR from equation (2.29) would be a very poor approximation to the true shape of that contour. An alternative approach is to calculate JCR with exact shape and approximate probability. For NLLS problem with known variance, this JCR can be calculated by equation (2.30) (Bates and Watts (1988)).

$$S\left(\underline{\theta}\right) \leq S\left(\underline{\hat{\theta}}\right) + \sigma^2 \chi^2_{(p,1-\alpha)} \tag{2.30}$$

2.2.3 Design of experiments

Model-based design of experiments is a methodology that can be used to increase the precision of parameter estimates through utilizing optimally designed experiments. It is therefore desirable to combine this technique with the parameter estimation procedure in order to improve the quality of the parameter estimation results. The model-based design of experiments approaches aim at providing the most informative data for this matter. Increasing parameters' precision is equivalent in mathematical terms to decreasing the size of the inference regions of the parameters of any given model; that is, reducing the elements of the variance-covariance matrix of the parameters. Geometrically speaking, in nonlinear regression analysis, if we consider the model shown in equation (2.25), with the error following a normal distribution, the parameter estimates are normally distributed as well.

The volume of the confidence region of the parameters is proportional to the square root of the determinant of the variance-covariance matrix, $\underline{V}_\theta$ matrix (i.e., $|\underline{V}_\theta|^{1/2}$) (Bard (1974)). For linear models, the inverse of the $\underline{V}_\theta$ matrix is called the information matrix, which possesses similar

properties as $\underline{V}_\theta$ (i.e., it holds only approximately for nonlinear models, as well, and is dependent on the values of the parameters). For nonlinear models, the size of the joint confidence region is approximately inversely proportional to the square root of the determinant of the information matrix (Box (1969) and Britt and Luecke (1973)). The information matrix is given by equation (2.31) for single-response problems and equation (2.32) for multi-response problems, where $\underline{Z}_i$ is the Jacobian matrix of the i^{th} response, given by equation (2.33), where p is the number of parameters, n is the number of experiments, m is the number of responses, and σ^{ij} is an element of the inverse variance-covariance matrix of the measurements.

$$I = \frac{1}{\sigma^2}\underline{Z}'\underline{Z} \tag{2.31}$$

$$I = \sum_{i=1}^{m}\sum_{j=1}^{m}\sigma^{ij}Z_i'Z_j \tag{2.32}$$

$$\underline{Z}_j = \begin{bmatrix} \frac{\partial \underline{g}_i{}^{(1)}}{\partial\theta_1} & \cdots & \frac{\partial \underline{g}_i{}^{(1)}}{\partial\theta_p} \\ \vdots & \ddots & \vdots \\ \frac{\partial \underline{g}_i{}^{(n)}}{\partial\theta_1} & \cdots & \frac{\partial \underline{g}_i{}^{(n)}}{\partial\theta_p} \end{bmatrix} \qquad \textit{for the } i^{th} \textit{ response} \tag{2.33}$$

Different criteria chosen for optimal design aim at minimizing certain aspects of the variance-covariance matrix, which in turn aim at reducing the variability in the parameters. Table 2-1 cites some of the popular criteria used for this purpose. The D-optimal criterion is the most common criterion used in the literature for obtaining improved parameter estimates, which aims at minimization of the determinant of the variance-covariance matrix of the parameters ($|\underline{V}_\theta|$). Therefore, minimizing the variance (hence, uncertainty) in the estimated parameters can be done by minimizing $|\underline{V}_\theta|$. Minimizing $|\underline{V}_\theta|$ is also equivalent to maximizing the determinant of the information matrix. D-optimality requires the determinant of the information matrix, as given in equations (2.31) and (2.32) to be maximized. This criterion, by concentrating on the determinant of the information matrix, not only affects the variances of the parameters but also involves their covariances (Draper and Hunter, 1966).

In order to use the D-optimal criterion, the values of the model parameters and the number of optimal points should be specified. The question of how many points in the variables' space should be chosen for this purpose does not have a clear answer; yet, the majority of the publications have stated that in

a problem with "*p*" parameters, the number of optimal points can be chosen as "p" (e.g., Draper and Hunter (1966)).

Table 2-1. List of optimal design criteria used in literature

Criterion	Objective function to be minimized	Reference
A-optinal	trace $[(\underline{Z}'\underline{Z})^{-1}]$	Atkinson and Donev (1992)
D-optimal	det$[(\underline{Z}'\underline{Z})^{-1}]$	Box and Lucas (1959)
E-optimal	maximum eigenvalue of $[(\underline{Z}'\underline{Z})]$	Atkinson and Donev (1992)
G-optimal	Variance of predicted responses	Atkinson and Donev (1992)
V-optimal	Variance of selected predicted responses	Atkinson and Donev (1992)

2.3 Error-in-Variables-Model (EVM) Methodology

Nonlinear parameter estimation problems where all variables (both dependent and independent) contain error are encountered frequently in science and engineering, including process engineering studies, medical applications, polymerization reactors, thermodynamic models, and so on. For such cases, results from basic nonlinear regression, where only dependent variables contain considerable amounts of error, would yield imprecise and biased parameter estimates. From the time this fact has been acknowledged in the literature, modified nonlinear regression techniques have been proposed to accommodate error present in all variables. These include weighted least squares, error propagation methods, and generalized least squares (e.g., see Deming (1947), Britt and Luecke (1973), Bard (1974), Sutton and MacGregor (1977), and Seber and Wild (1989) for an overview of the earliest publications).

A relatively recent approach is the error-in-variables-model (EVM) that is probably the most complete approach for situations where the dependent and independent variables cannot be distinguished. In general, EVM is capable of handling linear and nonlinear, single- and multi-response problems, and amongst its several advantages, it treats each measurement as an unknown

true value plus an error term; thus, one is compelled to consider errors involved in all the data. Also, it can handle implicit models for which the dependent variable cannot be isolated on one side of the equation.

There are several approaches proposed in the literature to implement EVM. Our work is based on the nested-iterative EVM algorithm proposed by Reilly and Patino-Leal (1981), which, in comparison with other proposed approaches, can manage the computational complexity of the problem more efficiently while providing reliable estimates of both true values of variables and parameters (Kim et al. (1990)). Nonetheless, the capabilities and potential of this technique have often been overlooked due to technical/numerical limitations that were present at the time. Nowadays, with current advances in computational facilities, such excuses are no longer justified, and thus, EVM should be readily employed to relevant parameter estimation problems.

2.3.1 Interpretation of EVM

Essentially, the EVM method treats all the measurements as if they come from an unknown true value with the addition of an error term. This relation is given by equation (2.34), in which $\underline{x_i}$ is the vector of obtained measurements, $\underline{\xi_i}$ is the vector of unknown true values, and $\underline{\varepsilon_i}$ is the error for the ith trial; n is the number of trials (Reilly and Patino-Leal (1981)).

$$\underline{x_i} = \underline{\xi_i} + \underline{\varepsilon_i} \qquad where\ i = 1,\ 2, \dots,\ n \tag{2.34}$$

The error vector is assumed to be normally distributed with mean of 0, and a non-singular variance-covariance matrix of $\underline{V}$, which may be known or unknown (Keeler and Reilly (1991)). $\underline{V}$ is a v by v square matrix where v is the number of variables in the problem. The relation between true values of the variables and estimated parameters can be shown in general by a model that is given by equation (2.35), where $\underline{\theta}^*$ is the vector of the true (yet unknown) parameter values to be estimated. The vector function $\underline{g}(\ )$ in equation (2.35) may be linear or nonlinear in the elements of $\underline{\xi_i}$ and $\underline{\theta}^*$.

$$\underline{g}\left(\underline{\xi_i}, \underline{\theta}^*\right) = 0 \qquad where\ i = 1,\ 2, \dots,\ n \tag{2.35}$$

In nonlinear least squares, parameter estimation is carried out by minimizing the sum of squared vertical distances between observed values and model predicted values. In contrast, and as shown in Figure 2-1, for a two dimensional case in EVM, the error associated with each measurement can be visualized as an ellipse with its center being the observed value. The ellipse is tangent to the predicted model with the direction determined by the $\underline{V}$ matrix. Therefore, EVM minimizes the sum of the sizes of ellipses surrounding the observed values in order to estimate the parameters. The objective function of the EVM algorithm is given by equation (2.36). This expression should be minimized so that the posterior density function of the parameters is maximized and $\underline{\hat{\theta}}$, the vector of the estimated parameters, would be obtained. This derivation of equation (2.36) is included in Appendix D, as well as in the original reference paper of Reilly and Patino-Leal (1981), in detail.

$$\phi = \frac{1}{2}\sum_{i=1}^{n} r_i \left(\underline{\overline{x}}_i - \underline{\hat{\xi}}_i\right)' \underline{V}^{-1} \left(\underline{\overline{x}}_i - \underline{\hat{\xi}}_i\right) \tag{2.36}$$

In equation (2.36), r_i is the number of replicates at the i[th] trial (out of n trials again), $\underline{\overline{x}}_i$ is the average of the r_i measurements, $\underline{x}_i$, and $\underline{\hat{\xi}}_i$ denotes the estimates of the true values of the variables (the tangent points of the EVM ellipses and the predicted model, as shown in Figure 2-1). Now, it is important to define the variance-covariance matrix $\underline{V}$, related to the underlying error structure.

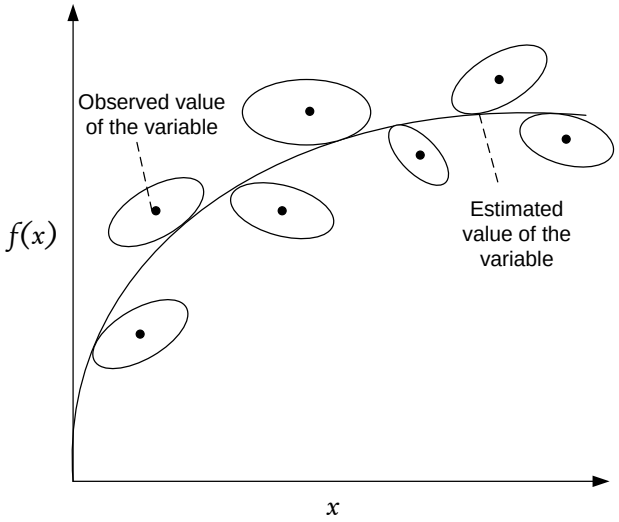

Figure 2-1. Visual interpretation of EVM

2.3.2 Error structure and variance-covariance matrix

The measurement variance-covariance matrix, $\underline{V}$, in EVM can be defined according to the error structure of the measurements. In this regard, error structure refers to (1) the magnitude of the error, (2) the error distribution, (3) the relation between variables and errors, and (4) for multi-response problems, whether measurements are correlated (Rossignolli and Duever (1995)). These key factors can be studied through analyzing experimental data from independent replication that eventually enable us to determine the elements of the variance-covariance matrix. In the absence of replicated experiments, researchers should use all information available for quantifying variability in the data from either present experimental work or related prior information or even a reasonable guess. If there is not sufficient knowledge whatsoever, the elements of the $\underline{V}$ matrix can be estimated. In fact, the EVM method allows us to work with cases where the variance-covariance matrix is known, partially known, and even completely unknown (Keeler and Reilly (1991)).

The magnitude of the error is quantified by the variance of the measurements that is determined through independent replication. The distribution of the error is generally unknown, but it is commonly assumed to be normal. Regarding the relation between a variable and its error, we are looking at two possible options: error being either absolute (additive) or relative (multiplicative) as shown with equations (2.37) and (2.38), respectively. And finally, for multi-response problems, if measurements have interrelated dependencies, correlation terms should be considered in the error structure as well.

$$x = \xi + k\varepsilon \tag{2.37}$$

$$x = \xi(1 + k\varepsilon) \tag{2.38}$$

$$\ln(x) = \ln(\xi) + k\varepsilon \tag{2.39}$$

ξ is the true value of the measured quantity and k is a constant that reflects the uncertainty in the variables and could be different for different variables. Error, ε, is a random variable, which, in the simplest case, has a uniform distribution in the interval from -1 to 1. For the case of the multiplicative error model, a log transformation on the variables is also necessary so that the error term becomes additive again. Taking logarithms of both sides of equation (2.38) gives equation (2.39), in which $ln\ (1+k\varepsilon)$ can be replaced by $k\varepsilon$, provided that the magnitude of the error does not exceed 10% ($k < 0.1$).

Moreover, equations (2.40) and (2.41) calculate the variance of *x* and *ln(x)* and show that regardless of the choice of error structure, the variance of measured variable is expressed as in equation (2.43). Equation (2.42) shows the variance of a uniformly distributed error in the interval of -1 to 1.

$$V(\ln(x)) = V(\ln(\xi) + k\varepsilon) = k^2 V(\varepsilon) \tag{2.40}$$

$$V(x) = V(\xi + k\varepsilon) = k^2\, V(\varepsilon) \tag{2.41}$$

$$V(\varepsilon) = E(\varepsilon^2) - [E(\varepsilon)]^2 = \int_{-1}^{1} \frac{\varepsilon^2}{2} d\varepsilon = 1/3 \tag{2.42}$$

$$V(\ln(x)) = V(x) = k^{\,2}/3 \tag{2.43}$$

Using equation (2.43), one can construct the covariance matrix $\underline{V}$ with equation (2.44), which is used in the remaining of the parameter estimation procedure. The diagonal elements of $\underline{V}$ are $\sigma_{x_i}^2$, the variances of the measurements, whereas the off-diagonal elements, $\sigma_{x_i x_j}^2$, represent the covariances between measurements.

$$\underline{V} = \begin{bmatrix} \sigma_{x_1}^2 & \sigma_{x_1 x_2}^2 & \cdots & \sigma_{x_1 x_v}^2 \\ \sigma_{x_2 x_1}^2 & \sigma_{x_2}^2 & \cdots & \sigma_{x_2 x_v}^2 \\ \vdots & \vdots & \cdots & \vdots \\ \sigma_{x_v x_1}^2 & \sigma_{x_v x_2}^2 & \cdots & \sigma_{x_v}^2 \end{bmatrix} \tag{2.44}$$

Finally, the additive versus multiplicative error question can be clarified based on extensive replicated experiments, from which statistical inference (e.g., residual plots) can be used to confirm the error structure. For the reactivity ratio estimation problem, however, since the number of experiments is usually limited, residual plots cannot be used as a reliable source of information. Hence, we are bound to make assumptions and choose a certain type of error structure. The common way we express error associated with experimental data in our field is usually in the form of a certain percentage of the measured observation; hence, most of the practitioners "believe" that the error is multiplicative in nature. In order to appreciate the type of error effect, results from both types of error are included in our analysis in Chapters 4 and 7, as their contrast will be quite informative.

2.3.3 EVM Algorithm

The nested-iterative EVM algorithm, as explained in Reilly and Patino-Leal (1981) and Reilly et al. (1993), has two iteration loops, namely the inner and outer iteration. In simple terms, at each iteration step for parameter estimates, the outer loop searches for the estimates of the parameters, after the inner loop finds the true values of the variables. In the following, the equations used in each step as well as numerical explanations of how these steps can be carried out are discussed. To further guide researchers with respect to implementing this algorithm, Chapter 3 discusses the "implementation" of this algorithm for a specific application, and provides a flowchart illustrating the recommended set of steps.

Given the function $\underline{g}\left(\underline{\xi}_i, \underline{\theta}^*\right)$ and the known and non-singular variance-covariance matrix $\underline{V}$, the goal is to minimize the EVM objective function, shown in equation (2.36), to find parameter estimates. The optimization procedure starts by choosing the initial parameter estimates, $\underline{\theta}^{(o)}$, and the initial variable values, $\underline{\xi}_i{}^{(o)}$, which are being set equal to the measured variables $\underline{x}_i$. Then, the inner iteration uses equation (2.45) to update the estimates of $\underline{\xi}_i{}^{(k)}$, with *k* as the iteration step and $\underline{B}_i$ as the vector of partial derivatives of the function, $\underline{g}\left(\underline{\xi}_i, \underline{\theta}^*\right)$, with respect to the variables, shown in equation (2.46). Numerically, $\underline{\xi}_i{}^{(k+1)}$ can be found using equation (2.48), in which $\underline{t}_i$ is the solution of $\underline{S}\,\underline{t}_i = \underline{h}_i$, and $\underline{S}$ and $\underline{h}_i$ are calculated from equation (2.47), using Cholesky decomposition.

$$\underline{\xi}_i{}^{(k+1)} = \bar{\underline{x}}_i - \underline{V}\underline{B}_i'\left(\underline{B}_i\underline{V}\underline{B}_i'\right)^{-1}\left[\underline{g}\left(\underline{\xi}^{(k)}, \underline{\theta}\right) + \underline{B}_i\left(\bar{\underline{x}}_i - \underline{\xi}^{(k)}\right)\right] \tag{2.45}$$

$$\underline{B}_i = \left[\frac{\partial g\left(\underline{\xi}_i, \underline{\theta}\right)}{\partial\left(\underline{\xi}_i\right)_t}\right]_{\underline{\xi}_i = \underline{\xi}_i{}^{(k)}} \quad for\ the\ t^{th}\ element \tag{2.46}$$

$$\underline{S}'\left[\underline{S} \vdots \underline{h}_i\right] = \left[\underline{B}_i\,\underline{V}\,\underline{B}_i' \vdots \underline{g}\left(\hat{\underline{\xi}}_i^{(k)}, \underline{\theta}\right) + \underline{B}_i\left(\bar{\underline{x}}_i - \hat{\underline{\xi}}_i^{(k)}\right)\right] \tag{2.47}$$

$$\underline{\xi}_i{}^{(k+1)} = \bar{\underline{x}}_i - \underline{V}\,\underline{B}_i'\,\underline{t}_i \tag{2.48}$$

Subsequently, the outer iteration loop utilizes Newton's method of optimization, in which the minimum of the objective function (ϕ) is obtained through updating the parameter estimates using

equation (2.49) until $\underline{\theta}^{(u+1)}$ is calculated as the converged estimated parameters. u denotes the iteration step, $\underline{q}$ is a gradient vector (equation (2.50)) and $\underline{G}$ is the expected information matrix (equation (2.52)). The $\underline{q}$ vector and $\underline{G}$ matrix are in fact the first and the second derivatives of ϕ with respect to parameters that can be computed by equations (2.51) and (2.53), respectively, and $\underline{Z_j}$ is the vector of partial derivatives of the function with respect to the parameters, given by equation (2.54).

$$\underline{\theta}^{(u+1)} = \underline{\theta}^{(u)} - \underline{G}^{-1}\underline{q} \tag{2.49}$$

$$\underline{q} = \left[\frac{d\phi}{d\theta_m}\right] \qquad m^{th}\ element \tag{2.50}$$

$$\underline{q} = \sum_{i=1}^{n} r_i \underline{Z_i}' \left(\underline{B_i} \underline{V} \underline{B_i}'\right)^{-1} \underline{B_i} \left(\underline{\bar{x}_i} - \underline{\hat{\xi}_i}\right) \tag{2.51}$$

$$\underline{G} = E\left[\frac{d^2\phi}{d\theta_i d\theta_j}\right] \qquad i,j\ elements \tag{2.52}$$

$$\underline{G} = \sum_{i=1}^{n} r_i \underline{Z_i}' (\underline{B_i} \underline{V} \underline{B_i}')^{-1} \underline{Z_i} \tag{2.53}$$

$$\underline{Z_j} = \left[\frac{\partial g(\underline{\xi_i}, \underline{\theta})}{\partial \theta_m}\right] \qquad m^{th}\ element \tag{2.54}$$

Numerically, after inner loop convergence, ϕ, $\underline{G}$, and $\underline{q}$ are calculated by the use of equations (2.55), (2.56), and (2.57), in which $\underline{P_i}$ is calculated by solving $\underline{S}'\underline{P_i} = \underline{Z_i}$.

$$\phi = \frac{1}{2} \sum_{i=1}^{n} \underline{\hat{h}_i}' \underline{\hat{h}_i} \tag{2.55}$$

$$\underline{G} = \sum_{i=1}^{n} \underline{P_i}' \underline{P_i} \tag{2.56}$$

$$\underline{q} = \sum_{i=1}^{n} \underline{P_i}' \underline{\hat{h}_i} \tag{2.57}$$

It must be noted that the results of using Newton's method for optimization can only offer convergence to local minima, and therefore, choosing appropriate initial guesses for the parameters is important. When working with optimization problem with many local minima, this problem can be potentially solved by choosing different initial guesses and examining the optimization solution to

make sure the results are, in fact, global. Different optimization methods, used in our work, are explained in section 2.3.5.

2.3.4 Evaluation of Results

Following the same principles explained earlier in section 2.2.2, the joint confidence regions can be constructed using the formula for an elliptical JCR, as shown for equation (2.29). Also, from the EVM algorithm, the inverse of the $\underline{G}$ matrix provides an approximation of the variance-covariance matrix for the parameters and thus, based on the assumption that error is normally distributed, the estimated parameters will have a normal distribution as $\underline{\hat{\theta}}$: $N(0, \underline{G}^{-1})$. Therefore, JCRs can be constructed using equation (2.58) (Keeler (1989)).

$$(\underline{\theta} - \underline{\hat{\theta}})' \underline{G} (\underline{\theta} - \underline{\hat{\theta}}) \leq \chi^2_{(p,1-\alpha)} \tag{2.58}$$

Meanwhile, depending on the nonlinearity of the problem under study, it could be more informative to construct JCRs with true shape (as explained earlier for equation (2.30)). The formula for a true (exact) shape JCR is given by equation (2.59), where $\phi(\underline{\hat{\theta}})$ is defined by equation (2.36) after convergence is reached and the values of $\underline{\hat{\theta}}$ are determined from equation (2.49) (a brief explanation about the derivation is given in Appendix E and the original derivation is given in Keeler (1989)).

$$\phi(\underline{\theta}) = \phi(\underline{\hat{\theta}}) + \frac{1}{2}\chi^2_{(p,1-\alpha)} \tag{2.59}$$

Also, as mentioned earlier, a major advantage of EVM is that it provides not only parameter estimates but also true values of the variables. This allows the investigation of residual plots, which are very well known to be great assets in analyzing the reliability of the parameter estimation results, especially in cases where the number of experiments are large enough that residual plots represent possible trends and/or dependencies amongst variables. It should also be noted that this feature of the EVM algorithm can be a good starting point for investigations on the effect of the error structure of the measurements.

2.3.5 Optimization Techniques

2.3.5.1 Newton's method

This technique is one of the most famous gradient-based optimization routine that can very effectively reach the nearest minimum from a given initial guess. This method uses the gradient to search for the minimum point of an objective function. Such gradient-based optimization methods are supposed to reach a point where the gradient is zero. Newton's method approximates the objective function using a Taylor series expansion and then tries to find the zero of the gradient function. Its implementation would result in an iterative procedure (shown in equation (2.49)) that can converge to local minima (Fletcher (1987)). In this work, Newton's method is used in the original algorithm of the EVM method, as derived by Reilly and Patino-Leal. (1981).

2.3.5.2 Shuffled Complex Evolutionary (SCE) method

The Shuffled Complex Evolutionary (SCE) method was proposed originally by Duan et al. (1993). The idea behind the SCE algorithm is to treat the global search as a process of natural evolution. This algorithm starts from a population of samples within the feasible range. Then this population is divided into several complexes (simplexes) and each one of these simplexes gets evolved towards the optimum point. These simplexes are then re-shuffled and again divided into new complexes. This procedure is repeated for as many times as required until the global optimum point(s) is found. In our research we have employed the SCE method via the SCE library in Matlab (Donckels (2012)). This SCE library can handle nonlinear constrained optimization problems subject to inequality (bounds) constraints.

2.3.5.3 Sequential Quadratic Programming (SQP) method

This technique is a gradient-based optimization routine that can effectively reach the nearest minimum from given initial guesses. This procedure substitutes the nonlinear problem with quadratic functions and has a satisfactory rate of convergence. The method is most simply explained as being Newton's method applied to find the stationary point of the Lagrangian function, and hence might be referred to as the Lagrange-Newton method (Fletcher (1987)). In our research, we have used the built-in Matlab function of "fmincon" that is suitable for nonlinear constrained optimization problems, with the SQP algorithm. One issue with this method is that it is a local optimization algorithm that depends

on the initial points. Also, this method is well suited for problems where computation of gradient functions is cheap and the objective functions and nonlinear constraints are not too complex.

2.3.5.4 Generalized Pattern Search (GPS) method

The Generalized Pattern Search (GPS) is a generalized version of the well-known direct search optimization method, the Pattern Search (PS) method, proposed originally by Hooke and Jeeves (1961). A distinguishing characteristics of the PS method is that, starting from the initial points, it evaluates the function over a predefined pattern of points (i.e., the polling step), by accepting any point with a simple decrease on the value of the objective function at the current iteration. The idea behind the GPS algorithm is to implement polling methods that explore more points around the current point at each iteration, as well as a random search in a sufficient number of directions from the current iterate to guarantee that a potential direction of descent is not overlooked. In our work, we used the GPS method via the built-in function of “patternsearch.m” function in Matlab. This optimizer function can handle nonlinear constrained optimization problems subject to equality, inequality, and nonlinear constraints. In our program, we used the “GPS positive basis 2N” as the polling method and the “Nelder-Mead search” as the searching method.

Chapter 3

Reactivity Ratios in Copolymerization Systems: Parameter Estimation

As shown in Chapter 2, there are alternative models that can be used in the reactivity ratio estimation problem for copolymerization systems. The most common one is the Mayo-Lewis model that is the instantaneous composition model, limited by assumptions that makes it applicable only to low conversion data. The alternative approache would be to use the cumulative copolymer composition model for estimating reactivity ratios by using the EVM method and medium to high conversion data points through the direct numerical integration of the differential copolymer composition equation. This chapter demonstrates the step by step implementation along with evaluation techniques of the EVM technique, followed by illustrative examples of reactivity ratio estimation for copolymerization systems using the different forms of composition models, discussed in Chapter 2. This chapter also presents several case studies, touching upon many related issues, while the successful performance of the direct numerical approach (relatively easy to implement) is demonstrated. The work presented in this chapter is published in Kazemi et al. (2011) and Kazemi et al. (2013a).

3.1 Introduction and Literature Review

Looking at the literature regarding copolymerization studies, it becomes evident that among the copolymerization models introduced in Chapter 2, section 2.1.1, the Mayo-Lewis model has been, by far, the most commonly used model for determining reactivity ratios. This model is strictly applicable to low conversion data only, owing to the assumption that the composition drift in the monomer feed is negligible at low conversion levels. The initial approaches for reactivity ratio estimation appeared in the literature based on the Mayo-Lewis model as early as in the late 1940s. All those initial attempts were through outdated and statistically incorrect methods such as curve fitting, intersection, and linearizations, which are all in conflict with the nonlinear nature of the Mayo-Lewis model. As a result, even though numerous studies were published in the literature reporting reactivity ratios of

different copolymerization systems, their parameter estimation results were highly unreliable and have led to a very inconsistent database for copolymerization reactivity ratios.

Amongst the first to publish about the problems of the reactivity ratio database were Behnken (1964) and Tidwell and Mortimer (1965). These works presented brief reviews of previous biased approaches along with the solutions for the reactivity ratio estimation problem using nonlinear estimation techniques. Since these works, there have been a number of key publications that investigated and proposed important approaches for dealing with this problem. German and Heikens (1971), Van der Meer et al. (1978), Patino-Leal et al. (1980), McFarlane et. al. (1980), O' Driscoll and Reilly (1987), and Plaumann and Branston (1989) were the early groups that explored the application of nonlinear least squares for parameter estimation with the Mayo-Lewis and the integrated copolymer composition model (the Meyer-Lowry model) for estimating reactivity ratios.

Dubé et al. (1991) and Van der Brink et al. (1999) illustrated the application of an approximate EVM methodology on the Mayo-Lewis model with low conversion data and on the Meyer-Lowry model with high conversion data, while indicating that using high conversion experimental data for reactivity ratio estimation can potentially result in more accurate reactivity ratios. This point comes from the fact that many copolymerization reactions will inevitably show compositional drift as the degree of conversion increases (the exception being certain specific, not frequently encountered, cases). Also, the requirement of stopping a reaction at low conversion results often in experimental difficulties which could be considered as significant sources of error in most of the cases. On top of that, most of the polymerization reactions are carried out to high conversion levels and by determining reactivity ratios based on low conversion data only, a great amount of useful experimental information is being neglected. Utilizing medium to high conversion range experimental data with cumulative copolymer composition models has received little attention in the literature with respect to reactivity ratio estimation. From all the publications reviewed in this work (about 60 to 70 copolymerization systems), 15 publications used high conversion data and cumulative composition models for estimating reactivity ratios (see, for instance, Fernandez-Garcia et al. (2008), Preusser and Hutchinson (2013), Touchal et al. (2004), Yilmaz and Kucukyavuz (1993), and Erbil et al. (2009)).

As explained in Chapter 2, section 2.1.1.3, high conversion copolymer composition data can be handled by the Meyer-Lowry model, which is based on the analytical integration of the instantaneous copolymer composition equation. Using this model, high conversion data can be included in the

parameter estimation procedure; however, due to difficulties arising from the use of the Meyer-Lowry model, researchers had to restrict the conversion levels of the data sets from low to moderate levels of conversion (i.e., say, up to 30%-50% conversion, with the range of up to 25-30% conversion being safer). Because of the way this model has been formulated, there have been several numerical problems that have extensively been discussed by Hautus et al. (1985). Their conclusion, on one hand, pointed out mathematical and numerical deficiencies and issues with this model. On the other hand, some of their qualitative and/or rather speculative remarks about problematic feed composition regions could not be verified.

Another approach for including high conversion data for reactivity ratio estimation is to use the cumulative copolymer composition model that is based on direct integration of the copolymer composition equation. Details for this scheme have been explained in Chapter 2, section 2.1.12. Shawki and Hamielec (1979) proposed using this approach to estimate reactivity ratios through nonlinear regression and concluded that this alternative process avoids the difficulties of the Meyer-Lowry model. Amongst all the work that has been done on estimating reactivity ratios in copolymer systems, utilizing the cumulative copolymer composition model through direct integration can be seen as the most sound and correct approach. That is, the whole conversion trajectory, and therefore high conversion level data, can be used for estimation of the reactivity ratios. Compared with the analytical form of the Meyer-Lowry model, numerically solving a differential equation with simultaneous parameter estimation may be computationally more intensive but it has the great advantages of employing a direct approach and avoiding transformations that tend to distort the error structure (in addition to avoiding simplifying or other restrictive assumptions).

Our goal is to obtain reactivity ratios for copolymerization systems with the best possible precision. Amongst estimation techniques mentioned in the literature, nonlinear regression (e.g., nonlinear least squares) can be considered as an appropriate method for handling the nonlinear copolymer composition models. However, as also discussed in Chapter 2, section 2.3, more recent developments in nonlinear estimation suggest that the EVM technique (based on Reilly and Patino-Leal (1981), Seber and Wild (1989), and Reilly et al. (1993)) is the best choice for this problem. Due to the fact that determining monomer reactivity ratios with the highest possible precision is vital, our goal is to offer comparisons and indicate some of the limitations of existing approaches, while presenting a novel method of estimation of monomer reactivity ratios at moderate/high conversion levels. More specifically, the objectives of this chapter are to: (1) employ integrated models in order to estimate

monomer reactivity ratios from high conversion data, and (2) determine which one of the available models can provide better estimates of the reactivity ratios, and offer comparative comments.

3.2 Reactivity Ratios Estimation

3.2.1 The instantaneous copolymer composition model

The instantaneous copolymer composition model is given by the Mayo-Lewis model, as shown earlier in Chapter 2 and here again with equation (3.1). This model relates the instantaneous copolymer composition, F_1, to the unreacted monomer feed composition, f_1, (as variables) and the reactivity ratios. r_1 and r_2, as parameters

$$F_1 = \frac{r_1 f_1^2 + f_1(1-f_1)}{r_1 f_1^2 + 2f_1(1-f_1) + r_2(1-f_1)^2} \tag{3.1}$$

To implement the EVM method to estimate r_1 and r_2 based on equation (3.1), the first statement of EVM, as shown in Chapter 2, equation (2.34), is used to relate the measurement values to their true values. For composition data, this relation is assumed to be multiplicative, shown in equations (3.2) and (3.3) for the feed composition, f_1, and instantaneous copolymer composition, F_1, where an asterisk denotes true values and ε is the error term. Via a logarithmic transformation (equations (3.4) and (3.5)), the relation of observed variable with its true value can be simplified, provided that the error term is less than 10% and ln(1+ε) can be approximated with ε. Subsequently, ln(f_1) and ln(F_1) become the EVM variable for the Mayo-Lewis model. The EVM model is given by equation (3.6).

$$f_1 = f_1^*\left(1 + \varepsilon_{f_1}\right) \tag{3.2}$$

$$F_1 = F_1^*(1 + \varepsilon_{F_1}) \tag{3.3}$$

$$\ln(f_1) = \ln(f_1^*) + \varepsilon_{f_1} \tag{3.4}$$

$$\ln(F_1) = \ln(F_1^*) + \varepsilon_{F_1} \tag{3.5}$$

$$\underline{g}\left(\underline{\xi}, \underline{\theta}^*\right) = {F_1}^* - \frac{{r_1}^* {f_1^*}^2 + {f_1}^*(1-{f_1}^*)}{{r_1}^* {f_1^*}^2 + 2{f_1}^*(1-{f_1}^*) + {r_2}^*(1-{f_1}^*)^2} \tag{3.6}$$

The EVM algorithm needs derivatives of the $\underline{g}\left(\underline{\xi},\underline{\theta}^*\right)$ function with respect to the parameters for the $\underline{Z}$ matrix (Chapter 2, equation (2.54)), which is a ($r\times p$) matrix with r the number of responses (elements of $\underline{g}\left(\underline{\xi},\underline{\theta}^*\right)$) and p the number of parameters. For the Mayo-Lewis model, $\underline{Z}$ is a 1×2 matrix (1 equation and 2 parameters), and the two elements of this matrix are given by equations (3.7) and (3.8). The EVM algorithm also requires the derivative of the function with respect to the variables for the $\underline{B}$ matrix (Chapter 2, equation (2.46)), which is in general a ($r\times v$) matrix, with v the number of EVM variables (in this case, $\underline{B}$ is a 1×2 matrix). With multiplicative error, the derivatives of $\underline{B}$ matrix are actually with respect to the logarithm of the measured variable, $\ln(\underline{\xi})$, and not $\underline{\xi}$. This transformation is given by equation (3.9). Hence, for the Mayo-Lewis model, we have the derivative shown in equations (3.10) and (3.11).

$$\frac{\partial \underline{g}\left(\underline{\xi},\underline{\theta}\right)}{\partial r_1} = \frac{-f_1^2\left(f_1(1-f_1)+r_1(1-f_1)^2\right)}{\left(r_1^2f_1^2+2r_1f_1(1-f_1)+(1-f_1)^2\right)^2} \tag{3.7}$$

$$\frac{\partial \underline{g}\left(\underline{\xi},\underline{\theta}\right)}{\partial r_2} = \frac{-(1-f_1)^2\left(r_1f_1^2+f_1(1-f_1)\right)}{\left(r_1^2f_1^2+2r_1f_1(1-f_1)+(1-f_1)^2\right)^2} \tag{3.8}$$

$$\frac{\partial g(\xi_i,\theta)}{\partial \ln(\xi_i)} = \frac{\partial g(\xi_i,\theta)}{\partial \xi_i}.\frac{\partial \xi_i}{\partial \ln(\xi_i)} = \xi_i.\frac{\partial g(\xi_i,\theta)}{\partial \xi_i} \tag{3.9}$$

$$\frac{\partial \underline{g}\left(\underline{\xi},\underline{\theta}\right)}{\partial \ln(f_1)} = f_1.\frac{\left((2f_1(r_1-1)+1)\left(r_1f_1^2+2r_1f_1(1-f_1)+(1-f_1)^2\right)-(2f_1(r_1+r_2-2)+2-r_2)(f_1^2(r_1-1)+f_1)\right)}{\left(r_1f_1^2+2r_1f_1(1-f_1)+(1-f_1)^2\right)^2} \tag{3.10}$$

$$\frac{\partial \underline{g}\left(\underline{\xi},\underline{\theta}\right)}{\partial \ln(F_1)} = F_1.1 \tag{3.11}$$

Finally, the variance-covariance matrix for the measurements needs to be defined for the EVM algorithm, as shown in equation (3.12). The diagonal elements of this matrix are the variances of the measurements that can be estimates based on independently replicated experiments. For the problem of reactivity ratio estimation, however, the number of data points in typical data sets is limited and there are rarely replicated experimental points in the literature (this problem can be partly attributed to the fact that polymerization reactions could be complicated, time-consuming, and costly). Commonly, the variability in a polymerization measurement is specified as a percentage of the measured value, which can be interpreted as a uniformly distributed error within the range of ±*k%* of the measured variable.

For the feed composition, *k* could be ±1%, while for the copolymer composition, *k* could be one of three error levels of ±2%, ±5%, and ±10%, representing experimental data with good, normal and poor precision, respectively. These error levels were mainly based on previous replicated experimental work in the literature (e.g., Dubé and Penlidis (1996)). Evidently, based on the information accompanying the experimental data, one can decide which error level best reflects the corresponding experimental situation. Based on the properties of the uniform error distribution, the variance-covariance matrix for the feed and copolymer composition is given by equation (3.12), where the errors of the mole fraction of monomer *i* in the feed and copolymer are $\pm k_{f_i}$ and $\pm k_{F_i}$ units, respectively. To see the details of the calculations for this equation, see Chapter 2, section 2.3.2.

$$\underline{V} = \begin{bmatrix} \frac{k_{f_1}^2}{3} & 0 \\ 0 & \frac{k_{F_1}^2}{3} \end{bmatrix} \tag{3.12}$$

3.2.2 The integrated copolymer composition model

The integrated form of the copolymer composition equation, the so-called Meyer-Lowry model, is also mentioned in Chapter 2 and given here again with equation (3.13). This model yields a relationship between the initial monomer (feed) mole fraction, f_{10}, final copolymer mole fraction, $\overline{F}_1$, and conversion on a weight basis, X_w.

$$g(\underline{\xi}, \underline{\theta}^*) = X_n^* - 1 + \left[\frac{f_{10}^* - \overline{F}_1^* X_n^*}{f_{10}^*(1-X_n^*)}\right]^{\alpha} \left[\frac{1-X_n^*-f_{10}^*-\overline{F}_1^* X_n^*}{(1-f_{10}^*)(1-X_n^*)}\right]^{\beta} \left[\frac{(\delta-f_{10}^*)(1-X_n^*)}{\delta-\delta X_n^*-f_{10}^*+\overline{F}_1^* X_n^*}\right]^{\gamma} \tag{3.13}$$

where $\alpha = \frac{r_2^*}{(1-r_2^*)}$; $\beta = \frac{r_1^*}{(1-r_1^*)}$; $\gamma = \frac{1-r_1^* r_2^*}{(1-r_1^*)(1-r_2^*)}$; $\delta = \frac{(1-r_2^*)}{(2-r_1^*-r_2^*)}$.

X_n in equation (3.13) should be replaced by mass conversion using equation (3.14) where Mw_1 and Mw_2 are the molecular weights of monomer 1 and 2. Equation (3.13) is usually referred to as the mass conversion form of the Meyer-Lowry model and this is the form that is used in this thesis for parameter estimation purposes.

$$X_n = X_w \frac{Mw_1 f_{10} + (1-f_{10}) Mw_2}{Mw_1 \bar{F}_1 + (1-\bar{F}_1) Mw_2} \tag{3.14}$$

In the EVM formulation for this model, initial feed composition, f_{10}, conversion, X_n (X_w), and the cumulative copolymer composition, $\overline{F}_1$, are the variables. The true values of these variables are related to their measured values according to the multiplicative error structure. Moreover, the EVM algorithm requires the $\underline{Z}_{(1\times2)}$ and $\underline{B}_{(1\times3)}$ matrices, which can be calculated in the same fashion as shown earlier for equations (3.7) to (3.11). Likewise to equation (3.12), the variance-covariance matrix of the measurements should be expressed in terms of the EVM variables, resulting in 3×3 matrix. For the initial feed composition and conversion (f_{10} and X_w), k could be ±1%, and for the cumulative copolymer composition, $\bar{F}_1$, k could be one of three error levels of ±2%, ±5%, and ±10%, as explained earlier.

3.2.3 The Direct Numerical Integration (DNI) approach

The numerical integration approach consists of a model that relates cumulative copolymer composition, $\bar{F}_1$, to the mole fraction of unreacted monomer, f_1, in the polymerizing mixture and molar conversion, X_n. The EVM model for this problem is given by the so-called Skeist equation, given here again by equation (3.15), where f_{10} and f_1 are mole fractions of monomer 1 in initial and remaining feed mixtures, and F_1 and $\bar{F}_1$ are instantaneous and cumulative copolymer compositions. As the reaction proceeds with time, X_n changes, and f_1 is evaluated by the numerical solution of the differential copolymer composition equation, given by equation (3.16), given the initial conditions of $f_1=f_{10}$ when $X_n=0$. The Runge-Kutta method of order 4 and 5 was used to carry out the integrations. F_1 is given by the Mayo-Lewis model in equation (3.1). Equation (3.14) allows us to replace the molar conversion (X_n) in the differential equation with mass conversion (X_w), which is a typical measurement for a polymerization reaction.

$$\underline{g}\left(\underline{\xi}, \underline{\theta}^*\right) = \bar{F}_1^* - \frac{f_{10} - f_1(1-X_n)}{X_n} \tag{3.15}$$

$$\frac{df_1}{dX_n} = \frac{f_1 - F_1}{1-X_n} \tag{3.16}$$

The EVM variable for this model is $\overline{F}_{1j}$, and since f_{10} and X_n (or X_w) are used during the numerical solution of equation (3.16) to calculate $\overline{F}_1$, they are not considered as the EVM variables. The $\underline{Z}_{(1\times2)}$ matrix for the EVM algorithm with this model cannot be calculated explicitly. Therefore, the elements of the $\underline{Z}$ matrix are worked out using equations (3.17) and (3.18) below, in which the values of Δr_i are chosen to be reasonably small. $\underline{B}_{(1\times1)}$ matrix has one element that is calculated as shown in equation (3.19).

$$\frac{\partial \underline{g}\left(\underline{\xi},\underline{\theta}\right)}{\partial r_1} = \frac{\underline{g}\left(\underline{\xi},\, r_1 + \Delta r_1,\, r_2\right)}{\Delta r_1} \tag{3.17}$$

$$\frac{\partial \underline{g}\left(\underline{\xi},\underline{\theta}\right)}{\partial r_2} = \frac{\underline{g}\left(\underline{\xi},\, r_1,\, r_2 + \Delta r_2\right)}{\Delta r_2} \tag{3.18}$$

$$\frac{\partial \underline{g}\left(\underline{\xi},\underline{\theta}\right)}{\partial \ln(\overline{F}_1)} = \overline{F}_1 \tag{3.19}$$

The variance-covariance matrix for this problem can be obtained similar to equation (3.12). The variance-covariance matrix is a 1×1 matrix, reflecting the error in the cumulative copolymer composition, $\overline{F}_1$. Value of *k*, as mentioned for the other two models, is usually ±5%, and in case of dealing with unreliable data can be increased to ±10% or even higher.

3.2.4 EVM implementation

Figure 3-1 is a detailed flowchart of the EVM algorithm, demonstrating the sequence of its steps. Essentially, this estimation procedure requires the user to provide the variance-covariance matrix of measurements, the experimental data, the convergence criterion/tolerance level, and the initial guesses for reactivity ratios. The procedure starts, similar to any other iterative procedure, with those particular values of initial parameter estimates that will be changed in each iteration step until the convergence criterion is met. Then, the obtained results will be assessed in several ways for validation. The following points are supplementary explanations regarding some of the steps for further clarification. References are made to key equations explained in Chapter 2, section 2.3.3.

- Step 4: The inner iteration loop is executed using equation (2.48) that is the numerical expression of equation (2.48). In our work, starting from $\underline{\xi}^{(o)} = \underline{x_i}$, the convergence to a tolerance level of 10^{-6}, which is the difference between two consecutive values of the variables ($\underline{\xi}^{(k+1)} - \underline{\xi}^{(k)}$), is ordinarily reached with less than 10 iterations on an Intel® Core™2 CPU, T7200 @ 2.00 GHz computer.
- Step 5: The values of ϕ, $\underline{G}$, and $\underline{q}$ are calculated using equations (2.55), (2.56), and (2.57), respectively.
- Step 6: The outer iteration loop is implemented by equation (2.49). Convergence of the outer loop for obtaining the best estimates of the parameters ($\underline{\hat{\theta}}$) depends on the initial guesses. The convergence criterion (tolerance level) is usually 10^{-6}, again the difference between two consecutive estimates of the parameters ($\underline{\theta}^{(k+1)}$ and $\underline{\theta}^{(k)}$). This is met within 6-10 iterations, provided that the initial guesses are reasonable.
- Step 9: In our program, the true values of the variables are used for preparing residual plots (step 9-1); the parameter estimates and the information matrix are important pieces of info for plotting JCRs (step 9-2).

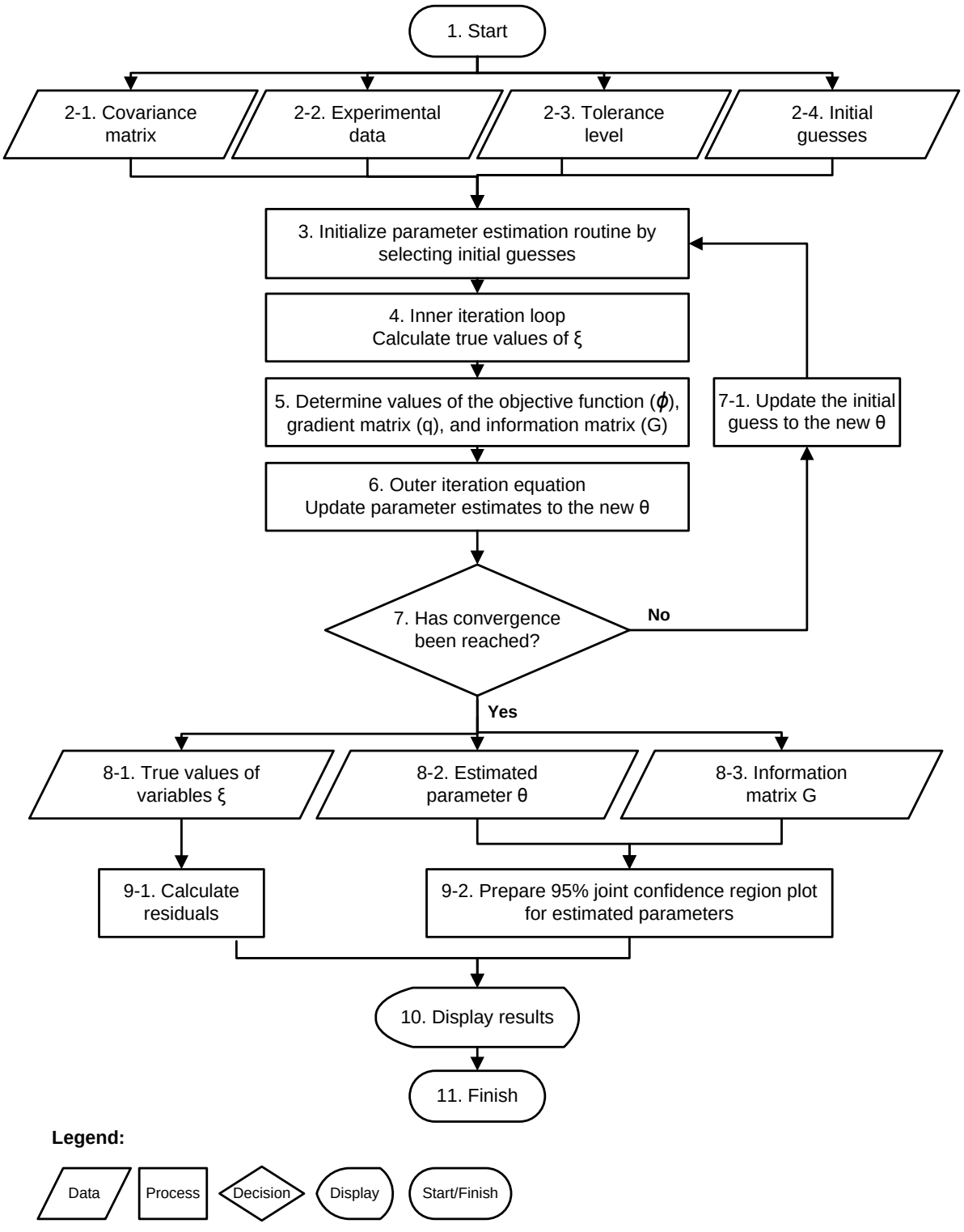

Figure 3-1. The flowchart of EVM algorithm

3.3 Results and Discussion

In this section, a number of copolymerization systems were studied using cumulative composition data to estimate reactivity ratios via the EVM method. In general, it was intended to (a) demonstrate the agreement between the point estimates obtained from cumulative model forms and those obtained from the instantaneous model using low conversion data, and (b) emphasize the advantages of using cumulative copolymerization composition model for moderate to high conversion levels, where compositional drift may be significant.

3.3.1 Styrene/Ethyl acrylate copolymerization

An experimental study of the bulk free radical copolymerization of styrene (Sty, M_1) and ethyl acrylate (EA, M_2) was conducted by McManus and Penlidis (1996). Copolymerization reactions at 50°C were carried out for reactivity ratio determination at low conversion levels (conversion below 2%). In addition, full conversion range copolymerizations were conducted at three different initial feed compositions (including the azeotropic feed composition for this system) and cumulative copolymer compositions were obtained. Experimental data for the low and full conversion levels are shown in Tables 3-1 and 3-2. It is important to note that the first initial feed composition is the Sty/EA copolymerization azeotropic point, $(f_o)_{Sty}$=0.762, the third point is the composition with the largest compositional drift, $(f_o)_{Sty}$=0.152, and the second feed mole fraction corresponds to somewhere in between the two extremes, $(f_o)_{Sty}$=0.458.

Table 3-1. Low conversion range experimental data for Sty/EA copolymerization (McManus and Penlidis (1996))

$(f_o)_{Sty}$	X_w	F_{Sty}
0.079	0.012	0.296
0.079	0.013	0.308
0.079	0.012	0.303
0.079	0.010	0.286
0.719	0.015	0.716
0.719	0.015	0.736
0.719	0.014	0.736
0.719	0.015	0.732

Table 3-2. Full conversion range experimental data for Sty/EA copolymerization (McManus and Penlidis (1996))

$(f_o)_{Sty}$	X_w	$\bar{F}_{Sty}$	$(f_o)_{Sty}$	X_w	$\bar{F}_{Sty}$	$(f_o)_{Sty}$	X_w	$\bar{F}_{Sty}$
0.762	0.059	0.757	0.458	0.058	0.606	0.152	0.042	0.355
0.762	0.110	0.798	0.458	0.118	0.627	0.152	0.080	0.382
0.762	0.166	0.763	0.458	0.163	0.605	0.152	0.122	0.368
0.762	0.216	0.736	0.458	0.210	0.621	0.152	0.160	0.362
0.762	0.265	0.768	0.458	0.265	0.632	0.152	0.196	0.380
0.762	0.370	0.758	0.458	0.310	0.619	0.152	0.225	0.351
0.762	0.382	0.747	0.458	0.368	0.587	0.152	0.271	0.329
0.762	0.395	0.753	0.458	0.447	0.586	0.152	0.300	0.360
0.762	0.468	0.807	0.458	0.528	0.599	0.152	0.344	0.338
0.762	0.552	0.776	0.458	0.630	0.585	0.152	0.387	0.325
0.762	0.619	0.781	0.458	0.704	0.566	0.152	0.457	0.310
0.762	0.693	0.784	0.458	0.783	0.555	0.152	0.627	0.285
0.762	0.782	0.795	0.458	0.917	0.486	0.152	0.738	0.272
0.762	0.982	0.753	0.458	0.986	0.537	0.152	0.962	0.174

McManus and Penlidis (1996) estimated reactivity ratios based on the Mayo-Lewis model with the low conversion range data (Table 3-1) and the EVM method, and their point estimates are presented in Table 3-3. In this work, the reactivity ratios are estimated using the EVM method, based on both low and full conversion data using the cumulative model forms (the Meyer-Lowery and the direct numerical integration). This procedure requires starting points (initial guesses) which are set as the reported reactivity ratios in the reference paper. Our point estimates are presented in Table 3-3, as well. At low conversion level, both the Mayo-Lewis model and cumulative models resulted in nearly identical point estimates and these values are in complete agreement with the published reactivity ratios in the reference paper. Also, the point estimates obtained from the Meyer-Lowry model and the direct numerical integration approach are very close.

As pointed out in the introduction, there are several problems reported in the literature regarding convergence issues with the Meyer-Lowery model. Potential reasons are related to the assumptions involved in the derivation of this model which are most likely violated during a typical copolymerization reaction. Therefore, it is necessary to compare the performance of this model with

the direct numerical integration approach. For this study, the composition points corresponding to certain conversion levels (e.g., conversions greater than 85%) were eliminated from the data set, step by step, and subsequently, the new data sets were analyzed by both cumulative model forms and reactivity ratios were re-estimated using the Meyer-Lowry model and the direct numerical integration approach. The point estimates from all these different data sets with both cumulative models are cited in Table 3-3.

As can be seen in this table, the point estimates obtained with full conversion and moderate conversion range data ($X_w \leq 60\%$) have shifted, indicating again that considering higher conversion level data (often ignored) does affect the reactivity ratio estimation results. In addition, for the data sets from full conversion, and from conversion less than 85% or 70%, the Meyer-Lowry model failed to converge, while the direct numerical approach had no problem in estimating the reactivity ratios. For the data set with conversion values of 60% and less, both cumulative model forms resulted in acceptable reactivity ratio estimates. Based on these results, it seems reasonable to suggest that the Meyer-Lowry model cannot perform well with high conversion range data sets. This observation can be partly due to the conflicts of the associated assumptions in the Meyer-Lowry model derivation, but it is also related to the information in the data and their associated error levels, which is something that cannot be handled with the Meyer-Lowery model, while the direct numerical integration handles all kinds of data perfectly fine.

Table 3-3.Reactivity ratio estimates for Sty (M_1)/EA (M_2) copolymerization (low and high conversion) with different models and data ranges for parameter estimation

	Copolymerization model	Conversion level	r_1	r_2
McManus and Penlidis (1996)	Mayo-Lewis	Low	0.72	0.13
Current work	Mayo-Lewis	Low	0.72	0.13
Current work	Meyer-Lowry	Low	0.72	0.13
Current work	Direct Numerical Integration	Low	0.71	0.13
Current work	Meyer-Lowry	$X_w \leq 50\%$	0.91	0.14
Current work	Direct Numerical Integration	$X_w \leq 50\%$	0.91	0.14
Current work	Meyer-Lowry	$X_w \leq 60\%$	0.92	0.14
Current work	Direct Numerical Integration	$X_w \leq 60\%$	0.92	0.14
Current work	Meyer-Lowry	$X_w \leq 70\%$	---	---
Current work	Direct Numerical Integration	$X_w \leq 70\%$	0.93	0.14
Current work	Meyer-Lowry	$X_w \leq 85\%$	---	---
Current work	Direct Numerical Integration	$X_w \leq 85\%$	0.93	0.14
Current work	Meyer-Lowry	High	---	---
Current work	Direct Numerical Integration	High	0.93	0.14
Current work	Mayo-Lewis	Combined data set (low and high conversion at azeotropic point)	0.76	0.13

In order to further explore the performance of different models used for reactivity ratio estimation, the corresponding JCRs were plotted, as well. Firstly, the JCRs for low conversion data (Table 3-1) by using the Mayo-Lewis model, the Meyer-Lowry model, and the direct numerical integration were plotted together in Figure 3-2. In this figure, the point estimates obtained from the Mayo-Lewis

model, the Meyer-Lowry model, and the direct numerical integration are shown by o, Δ, and □, respectively, and the star denotes the published reactivity ratios. It can be seen that the point estimates are in very good agreement, observed in Table 3-3 as well, and the sizes of JCRs for all three models are almost the same. It was expected that the cumulative models would provide higher quality parameter estimates (smaller JCRs) due to the fact that they incorporate more information in the parameter estimation procedure (values of conversion that are not considered when working with the Mayo-Lewis model).

The fact that all JCRs in Figure 3-2 are effectively the same can be explained based on the nature of the collected experimental data, shown in Table 3-1: the (low) conversion data points are almost the same. Since changes in the values of conversion and copolymer composition are minimal, these data points do not offer any additional information to the cumulative models, i.e., they do not increase the information content of the cumulative models more than what the instantaneous model knows. Hence, it makes sense that all models give almost the same JCRs. If for some points the conversion level X_w had been allowed to go to slightly higher levels, say, 2-4 % (still below 5 %), then the cumulative models would have yielded higher precision reactivity ratio point estimates (i.e., smaller JCRs) compared with the Mayo-Lewis model.

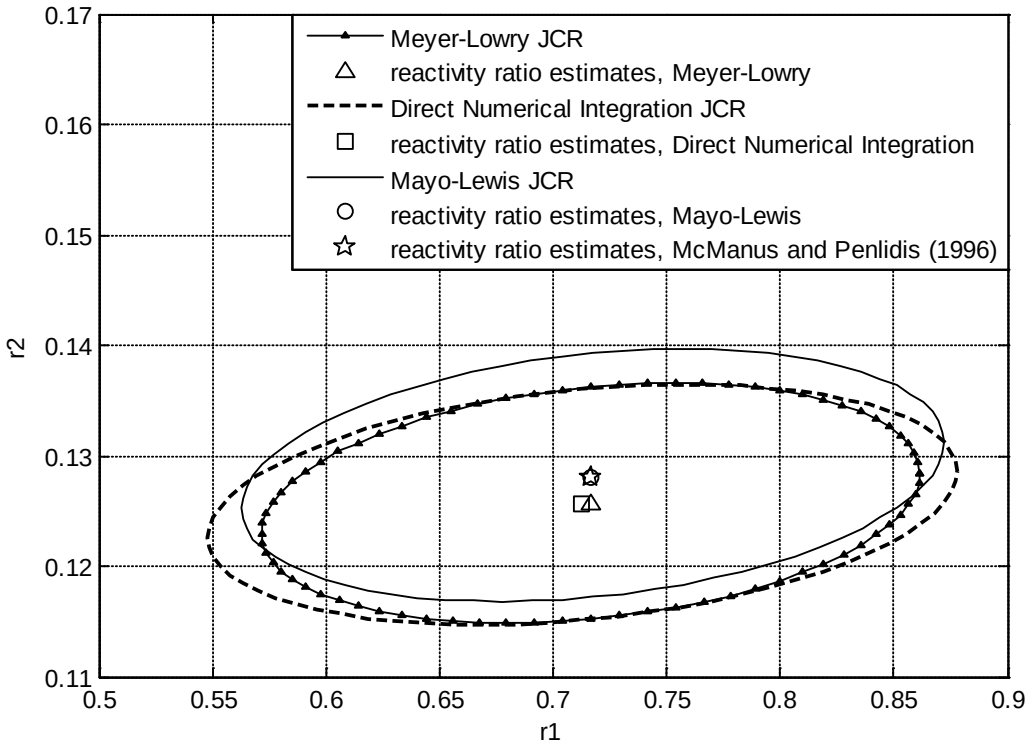

Figure 3-2. JCRs for the Mayo-Lewis model, Meyer-Lowry model, and direct numerical integration with low conversion data for Sty (M_1)/EA (M_2) copolymerization

Figure 3-3 shows the cumulative model JCRs based on moderate level conversion data ($X_w \leq 60\%$) along with the Mayo-Lewis JCR obtained from low conversion data. It can clearly be seen from this figure that the point estimates have shifted for the cumulative model results and their corresponding JCRs are only partly overlapping with the instantaneous model, the Mayo-Lewis model. Also, it can be seen that the Meyer-Lowry model and the direct numerical integration results are in excellent agreement (JCR contours overlap significantly and of course the point estimates are very close). The final observation from this figure is that the point estimates published in McManus and Penlidis (1996) do not fall inside neither of the cumulative model JCRs, as expected, since they had been obtained based on low conversion experimental data.

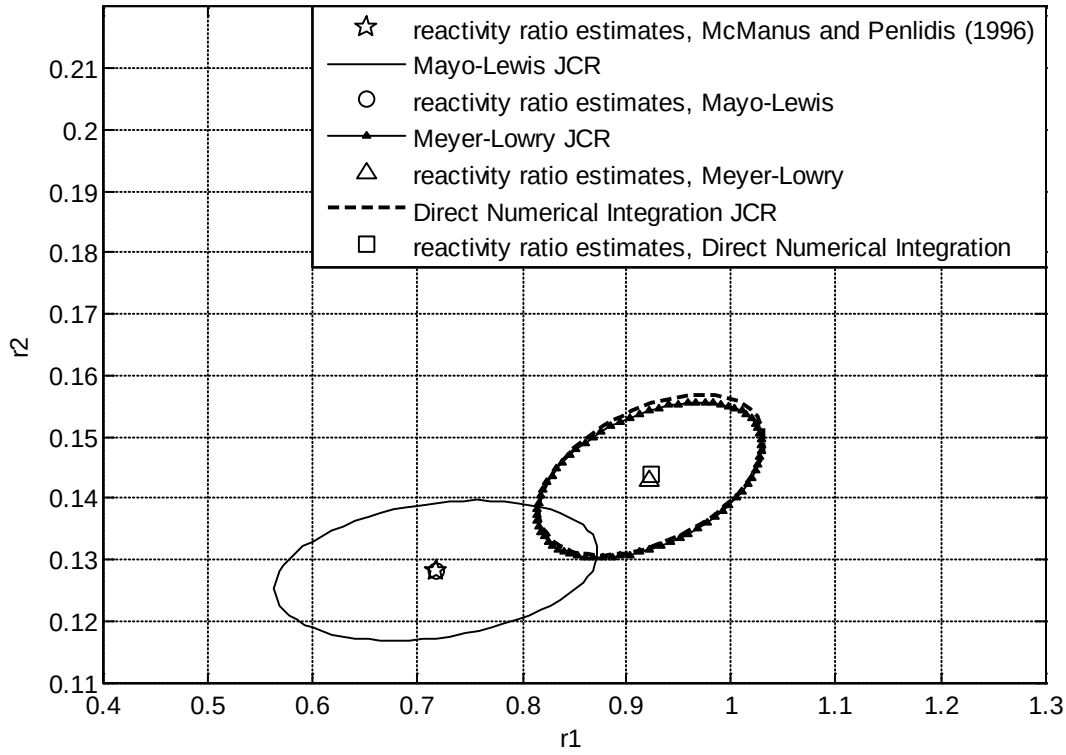

Figure 3-3. JCRs for the Mayo-Lewis model with low conversion data and the Meyer-Lowry model and direct numerical integration with moderate conversion data for Sty (M_1)/EA (M_2) copolymerization

In the full conversion range experiments conducted by McManus and Penlidis (1996) for Sty/EA copolymerization, the azeotropic composition ((f_o)$_{Sty}$=0.762) was one of the initial feed points. According to the definition of the azeotropic point, the cumulative copolymer composition remains constant and equal to the feed composition during the course of polymerization. In other words, since the cumulative copolymer composition remains constant with conversion, then the cumulative copolymer composition is equal to the instantaneous copolymer composition at any point throughout the reaction. This would then mean that the Mayo-Lewis equation (instantaneous composition equation) could be applicable over the full conversion range data that were obtained with initial feed composition of (f_o)$_{Sty}$=0.762 at the azeotropic condition. Table 3-4 presents a combined data set from azeotropic high conversion data points from Table 3-2 and low conversion data points from Table 3-1.

Table 3-4. Combined data set from low and high conversion ranges at the azeotropic point for Sty (M_1)/EA (M_2) copolymerization (McManus and Penlidis (1996))

$(f_o)_{Sty}$	$\bar{F}_{Sty}$	X_w	$(f_o)_{Sty}$	$\bar{F}_{Sty}$	X_w
0.079	0.296	0.012	0.762	0.757	0.059
0.079	0.308	0.013	0.762	0.798	0.110
0.079	0.303	0.012	0.762	0.763	0.166
0.079	0.286	0.010	0.762	0.736	0.216
0.719	0.716	0.015	0.762	0.768	0.265
0.719	0.736	0.015	0.762	0.758	0.370
0.719	0.736	0.014	0.762	0.747	0.382
0.719	0.732	0.015	0.762	0.753	0.395
			0.762	0.807	0.468
			0.762	0.776	0.552
			0.762	0.781	0.619
			0.762	0.784	0.693
			0.762	0.795	0.782
			0.762	0.753	0.982

The point estimates obtained from this analysis are shown in the last row of Table 3-3. Also, Figure 3-4 shows the Mayo-Lewis JCR based on the combined data set, along with the Mayo-Lewis JCR from the low conversion data. It can be seen in this figure that the point estimates from the combined data set are in good agreement with point estimates from low conversion data and also the reported values in McManus and Penlidis (1996). The most important observation from this figure is that the JCR from the combined data set is greatly overlapping with (in fact, completely included within) the JCR based on low conversion data. In addition, the JCR from the combined set is much smaller than the low conversion one. This first-ever observation is a greatly convincing demonstration of the fact that combining high conversion information at azeotropic conditions with low conversion data is much preferable, as it will increase the reliability/quality of the reactivity ratio estimates. Needless to say, the results of Figure 3-4 confirm once more that combined and enhanced information content will improve the parameter estimates, as long as the combination of different pieces of information is the appropriate one.

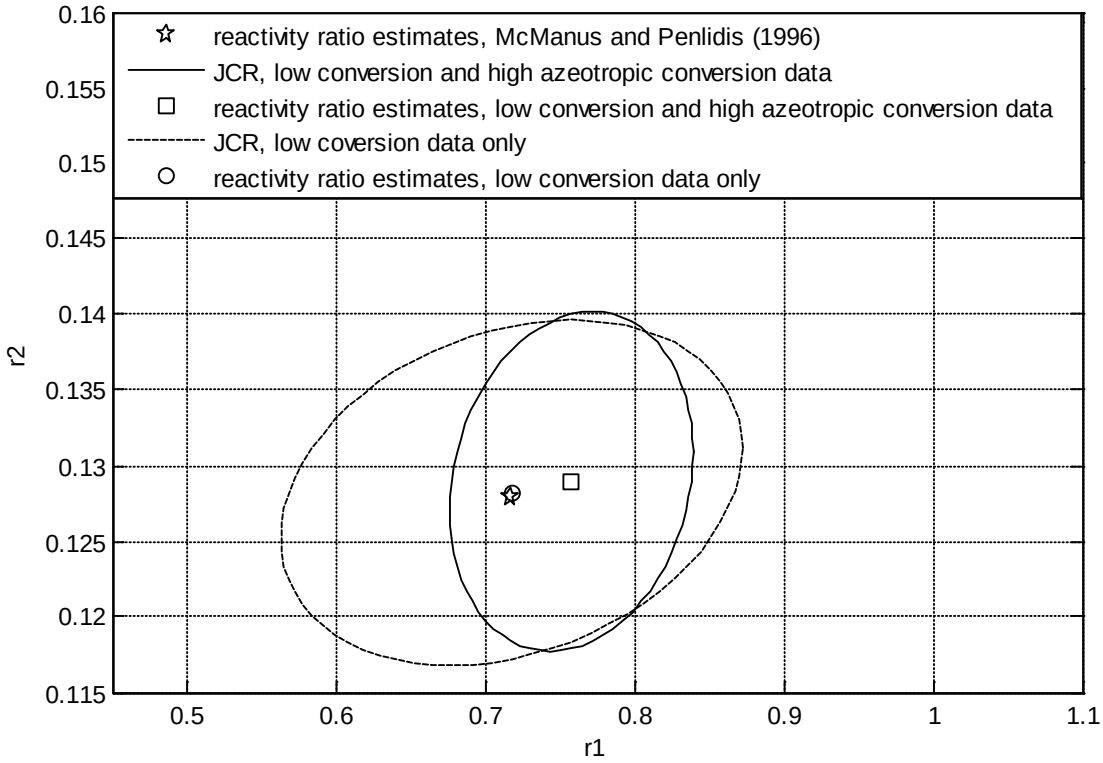

Figure 3-4. JCRs for the Mayo-Lewis model with low conversion data and combined data set from low conversion and azeotropic high conversion data for Sty (M_1)/EA (M_2) copolymerization

Finally, in order to check once more the validity of simulation results obtained from the estimation procedures, a practical diagnostic check is presented to study the behavior of the azeotropic point for the Sty/EA copolymerization system. The binary azeotropic feed composition, as shown in Chapter 2, equation (2.23), is only a function of r_1 and r_2. Based on our point estimates and the reported ones, two azeotropic compositions are 0.926 and 0.765, respectively. These two compositions are not very close and hence, the question arises: which one is the true azeotropic feed composition? To answer this question, the cumulative copolymer compositions versus conversion were calculated from both sets of reactivity ratios. The results of this comparison can be seen in Figure 3-5, where the dashed line shows the cumulative composition versus conversion based on reported reactivity ratios and the solid line is obtained based on our reactivity ratios. The experimental data from the azeotropic feed composition, from Table 3-4, are also included in this figure as black dots. As it was expected, feed composition of 0.926 shows the characteristics of a true binary azeotropic composition since it

remains constant throughout the whole conversion range, whereas the experimental data and their predicted line show compositional drift for higher conversion levels.

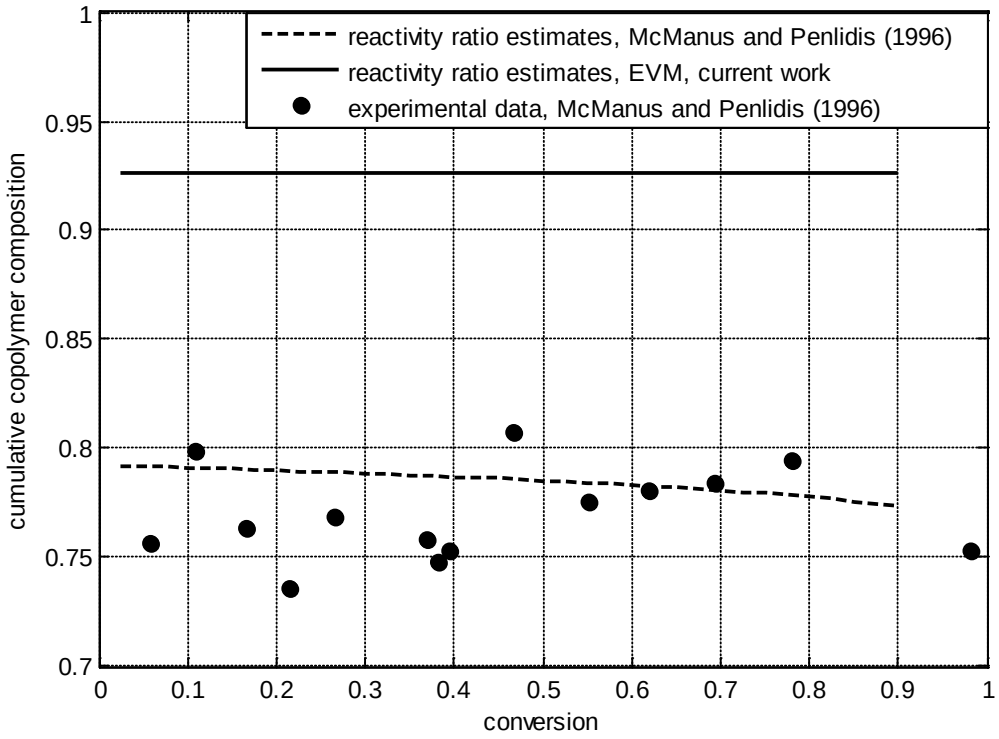

Figure 3-5. Predicted and simulated cumulative copolymer composition versus conversion based on the Mayo-Lewis reactivity ratios and cumulative model reactivity ratios of Sty (M_1)/EA (M_2) copolymerization

3.3.2 Butyl Acrylate/Methyl Methacrylate

As another case study, the free radical copolymerization of butyl acrylate (BA, M_1) and methyl methacrylate (MMA, M_2), experimentally conducted by Dubé and Penlidis (1995a) is studied. The polymerizations were carried out in bulk at 60°C to different conversion levels (low, mid-range, and high). These experimental data sets are presented in Tables 3-5 and 3-6. Table 3-5 shows low conversion composition data, with the maximum of conversion of 1.2%, whereas Table 3-6 shows the composition data up to the full conversion level (99%). The authors estimated the reactivity ratios

from low conversion composition data using the Mayo-Lewis model and the EVM parameter estimation technique. Table 3-7 shows the composition data from Table 3-6 that correspond to moderate (mid-range) conversion levels, which will be discussed shortly. The results of parameter estimation analysis are presented in Table 3-8.

In this case study our objectives were to estimate reactivity ratios with data at different conversion levels using the direct numerical integration model in order to study the effect of considering available experimental data at different conversion levels (from very low to moderate and up to full conversion) on the reactivity ratio estimates. First, the reactivity ratios were estimated by the EVM program for the low conversion data set (Table 3-5) using the Mayo-Lewis model. In order to contrast the results of the cumulative model versus the instantaneous model, the EVM program was implemented on the direct numerical integration based on the low conversion data set. Also, since it is interesting to observe the effect of using full conversion range data versus moderate level (mid-range) conversion data, the data points with conversion values, $X_{w,}$ less than 70% were selected from the high conversion data set (Table 3-6) and were used in the subsequent analysis as the moderate conversion range data (shown in Table 3-7). The point estimates obtained from all these data sets are presented in Table 3-8.

Table 3-5. Low conversion experimental data for BA (M_1)/MMA (M_2) copolymerization (Dubé and Penlidis (1995a))

$(f_o)_{BA}$	X_w	$\bar{F}_{BA}$
0.798	0.011	0.598
0.798	0.011	0.606
0.798	0.009	0.594
0.798	0.012	0.599
0.543	0.004	0.385
0.543	0.004	0.343
0.543	0.004	0.335
0.543	0.003	0.341

Table 3-6. High conversion experimental data for BA (M_1)/MMA (M_2) copolymerization (Dubé and Penlidis (1995a))

$(f_o)_{BA}$	X_w	$\bar{F}_{BA}$
0.439	0.220	0.281
0.439	0.292	0.305
0.439	0.336	0.288
0.439	0.670	0.354
0.439	0.791	0.349
0.439	0.941	0.426
0.439	0.966	0.411
0.439	0.193	0.258
0.439	0.365	0.317
0.439	0.603	0.295
0.439	0.652	0.326
0.439	0.843	0.374
0.439	0.959	0.407
0.439	0.987	0.426
0.163	0.212	0.087
0.163	0.244	0.065
0.163	0.292	0.097
0.163	0.365	0.0920
0.163	0.441	0.110
0.163	0.830	0.096
0.163	0.999	0.115
0.163	0.999	0.160
0.163	0.999	0.146

Table 3-7. Mid-range conversion experimental data for BA (M_1)/MMA (M_2) copolymerization (Dubé and Penlidis (1995a))

$(f_o)_{BA}$	X_w	$\bar{F}_{BA}$
0.439	0.193	0.258
0.439	0.220	0.281
0.439	0.292	0.305
0.439	0.336	0.288
0.439	0.365	0.317
0.439	0.603	0.295
0.439	0.652	0.326
0.439	0.670	0.354
0.163	0.212	0.087
0.163	0.244	0.065
0.163	0.292	0.097
0.163	0.365	0.092
0.163	0.441	0.110

Table 3-8. Reactivity ratio estimates for BA (M_1)/MMA (M_2) copolymerization (low and high conversion) based on different copolymerization models

	Copolymerization model	Conversion level	r_1	r_2
Dubé and Penlidis (1995a)	Mayo-Lewis	Low	0.30	1.79
Current work	Mayo-Lewis	Low	0.30	1.80
Current work	Direct Numerical Integration	Low	0.29	1.73
Current work	Direct Numerical Integration	Mid-range	0.60	2.48
Current work	Direct Numerical Integration	high	0.55	2.47

It can be seen in Table 3-8 that our point estimates based on low conversion level data are in agreement with the reported values in Dubé and Penlidis (1995a). In order to further investigate the reliability of these point estimates, JCRs of the Mayo-Lewis model and the direct numerical integration were plotted together in Figure 3-6. The reported point estimates in the reference paper are

also presented in this figure. It can be seen that our point estimates obtained from the Mayo-Lewis model and reported ones based on low conversion data are very close (shown by "□" and "▲" in Figure 3, respectively); also, our point estimates from the direct numerical integration based on low conversion data are in good agreement with the published ones (shown by "○"); in addition, the Mayo-Lewis JCR is almost the same size as the cumulative model JCR. This example again confirms that since changes in the values of conversion and copolymer composition are minimal at this low conversion region, the reactivity ratio estimates from the cumulative model are of the same precision as those from the instantaneous model.

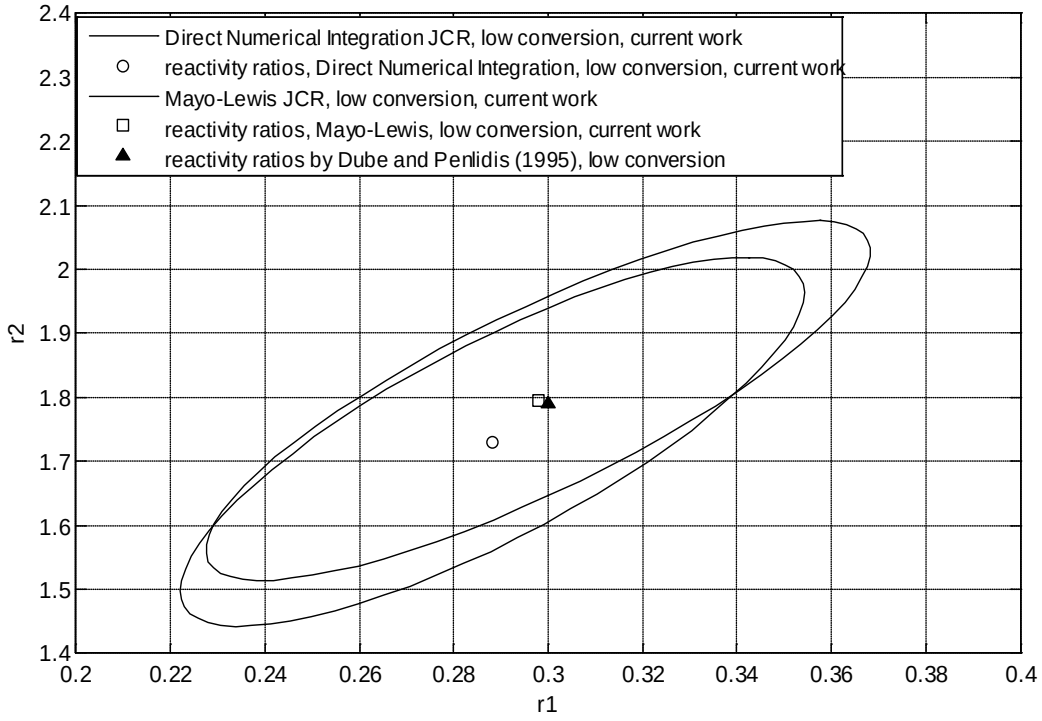

Figure 3-6. JCRs for the Mayo-Lewis model (low conversion data) and the direct numerical integration (low conversion data) for BA (M_1)/MMA (M_2) copolymerization

As the next step, in order to study the effect of using composition data of higher conversion, the direct numerical integration were applied on the high conversion data (Table 3-7) and the moderate (mid-range) conversion level data (Table 3-8), and the reactivity ratios were re-estimated. That way, an extra comparison could also be made between moderate and full (high) conversion data. It can be seen in Table 3-8 that the point estimates of low conversion data and moderate conversion data are

noticeably different, while the point estimates of moderate conversion data and full (high) conversion data are close. These results further emphasize the effect high conversion data can have on the output of parameter estimation analysis.

The corresponding JCRs for the direct numerical integration, obtained from moderate conversion data, are shown in Figure 3-7 along with the direct numerical integration JCR, obtained from full (high) conversion data. It can be clearly seen from this figure that the sizes of the JCRs from the moderate conversion data and the full conversion data are very similar, indicating that these two data sets provide almost the same amount of information for the point estimates. This is despite the fact that the full conversion data set contains more data points at higher conversion levels. This observation is not surprising due to the fact that, in general, the conversion versus time trajectory for free-radical polymerizations reaches a plateau after a certain high conversion level, and therefore do not have more useful information with respect to the reactivity ratio estimation. This limit can also coincide with onset of the gel effect in the polymerization reaction.

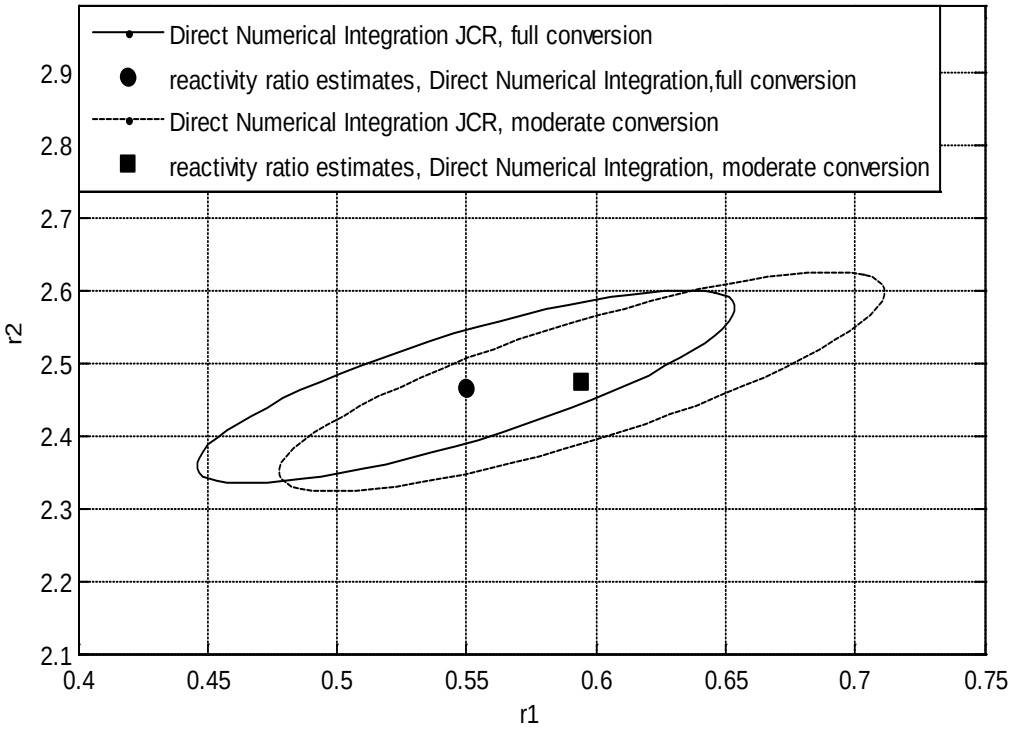

Figure 3-7. JCRs for the direct numerical integration, moderate conversion data and full conversion data, for BA (M_1)/MMA (M_2) copolymerization

Finally, we can conclude that the trend observed for the reactivity ratio estimates obtained from different conversion levels can be explained essentially by the effect of including additional (more) information accompanying higher conversion data. It must also be emphasized here that very high conversion data points do not contribute considerably in this regard and it is even more likely that data collected after the onset of the gel effect contain some level of noise, which is should be avoided for the reactivity ratio estimation.

3.4 Concluding Remarks

Due to outlined practical and theoretical deficiencies in using instantaneous models for copolymerization reactivity ratio estimation, this chapter has shown that monomer reactivity ratios could equally well be estimated based on cumulative copolymer composition model forms. The parameter estimation technique used in this work is the EVM method, which has been shown to be the most appropriate one for parameter estimation. Two cumulative model forms were discussed in particular, namely, the analytical integration of the differential composition equation or Meyer-Lowry model, and the one resulting from the direct numerical integration of the differential composition equation. Our objective was to show that the latter approach is a reliable and more direct method of estimating reactivity ratios through a step-by-step integration of the copolymerization composition ordinary differential equations. In addition, we presented the implementation of the EVM algorithm for the nonlinear copolymerization composition models along with details on the various steps involved. Some of the possible evaluation methods based on the output data from EVM were also discussed. The following general overall conclusions can be drawn based on the results of the case studies:

- Reactivity ratio point estimates based on low conversion data only can significantly deviate from more improved point estimates, obtained from cumulative copolymer composition data taking into account the conversion level (moderate to high conversions) as well. In essence, reactivity ratio estimates from cumulative data represent a much more balanced compromise among low, moderate and high conversion levels, thus taking into account richer information from both copolymer

composition and conversion data (and hence offering a more balanced prediction of polymerization variables over the whole trajectory).

- At higher conversion levels (i.e., moderate range, say, between 10-50%), it has been shown that both the Meyer-Lowry model and the direct numerical integration approach are capable of providing consistent reactivity ratio estimates that are comparable and in acceptable agreement with literature values. Moreover, the performances of the Meyer-Lowry model (analytical approach) and the direct numerical approach were shown to be indistinguishable.
- In general, if one considers the full conversion range, the reactivity ratio estimation results illustrate that at both low and high conversion levels, the direct numerical integration is straightforward, easy, and a more reliable approach, since it avoids convergence issues associated with the Meyer-Lowry model.
- In the case of inadequate experimental data or experimental data with large amount of associated error, the final results are affected to an unacceptable degree. Such deviations coincide with higher than moderate conversion levels (diffusional limitations) and increase with increasing conversion. A statistical technique, no matter how novel or sophisticated it might be, cannot compensate for low (or complete lack of) information content in the data. The estimation results and analysis are not to be trusted and no valid conclusions can be drawn based on an ill-conditioned data set (which may arise either from badly designed experiments or from experimental analysis with significant error).
- The same trends and observations were also confirmed with many other copolymerization systems, including data sets from low, moderate and high conversion levels from acrylamide/acrylic acid (Bourdais (1955), Shawki and Hamielec (1979)), styrene/methyl methacrylate (Burke et al. (1994), O'Driscoll and Huang (1990)), glycidyl methacrylate/styrene (Wang and Hutchinson (2008)), and several systems from Gao and Penlidis (1998). The similar results from these additional systems (not cited here for the sake of brevity) corroborated the validity of the trends described in the two case studies of the current chapter.

Chapter 4

Reactivity Ratios in Copolymerization Systems: Design of Experiments

With the goal of creating a general approach for determining reactivity ratios in copolymerization systems, the parameter estimation approach that was discussed in Chapter 3 should be combined with the design of experiments step in order to ensure reliable reactivity ratio estimation. This chapter considers the issue of model-based design of experiments in the error-in-variables-model (EVM) context. The fundamental differences between the design of experiments in the traditional nonlinear regression versus the EVM context are discussed, and it is pointed out that for cases where there are errors in all variables, using the EVM design criterion is the only appropriate approach. In addition, the implementation of the EVM design criterion and its characteristics for both initial and sequential design schemes are discussed. The main application is the implementation of the EVM criterion to design optimal trials for reliable estimation of reactivity ratios for typical copolymerization systems, along with prescriptions for the practitioner.

The 'Results and Discussion' section (mentioned in section 4.3) illustrates, firstly, a case study of a typical copolymerization system. Then, based on the most extensive to date simulated table of reactivity ratios, representing almost all possible pairs of comonomers (both well studied and largely unstudied systems), several practical scenarios are highlighted in order to demonstrate results with the EVM design criterion Finally, this chapter ends with important prescriptions for the recommended approach for interested experimenters/researchers in using the EVM design criterion, and possible future steps in this research field. Our work in this chapter is published in Kazemi et al. (2013b).

4.1 Introduction and literature review

The purpose of any experiment is to provide information. The "best" experiment is therefore the most informative one. In the research field of copolymerization reactivity ratio estimation, polymer chemists started by performing experiments covering a broad range of feed compositions (the so-called empirical approach), believing that such an approach would provide a large number of

experimental points (trials) and hence the best results for estimating reactivity ratios. Even though design of experiments (DOE) approaches for obtaining improved reactivity ratios were proposed since the mid-60s (notably by Tidwell and Mortimer (1965)) empirical approaches dominated among chemists and were readily used by almost all researchers, often slightly modified, but mainly far from any optimality consideration, and largely unreplicated. Looking at the literature for design of experiments in copolymerization systems, there have been only a couple of publications in the literature that are mostly based on classical nonlinear regression analysis (Tidwell and Mortimer (1965), McFarlane et al. (1980), Keeler and Reilly (1992), Burke et al. (1993), and Rossignolli and Duever (1995)).

The problem of design of experiments for copolymerization models is a nonlinear design of experiments problem. As explained in Chapter 2, section 2.2.3, there are a number of approaches/criteria aiming at minimizing the "size" of the confidence region of the parameters, such as a set of alphabetical optimal design criteria (e.g., A-, E-, G-, and D-optimal design criteria) that have been used in the literature for several years (see, for instance, Draper and Hunter (1966), Box and Locus (1959), Atkinson and Donev (1992), and Atkinson and Bogacka (1997)). Each one of these optimal design techniques focuses on minimizing some aspects of the variance-covariance matrix of the parameters ($\underline{V}_\theta$) matrix, which are advantageous in several cases and with drawbacks for some other cases.

The most popular and widely used design criterion even for nonlinear models is D-optimality which aims at minimizing the volume of the corresponding parameter JCR. It is implemented by maximizing the determinant of the information matrix (as shown in Chapter 2, equations (2.31) and (2.32)) which is equivalent to minimizing the determinant of $\underline{V}_\theta$ matrix. This criterion, by concentrating on the determinant of the information matrix, not only affects the variances of the parameters but also involves their covariances (Draper and Hunter (1966)). The D-optimal design criterion handles cases with explicit models (i.e., distinguishable dependent and independent variables), and independent variables are obvious candidates as design variables. Due to the basic assumption in traditional nonlinear regression analysis, values of the independent variables are errorless and thus can be fixed at the optimum points in a designed experiment. They can be changed independently and the experiments can be performed at their exact optimum values.

The D-optimal design criterion assumptions, however, might be violated if there is error in all variables (i.e., EVM structure). For EVM problems, the variables are related to each other with single or multiple equations in an implicit form, and these variables cannot be distinguished as dependent or independent variables anymore. Instead, they are divided into two groups of responses; the first contains the measured outcomes of the experiments, whereas the second group contains the design variables that determine the conditions under which the experiments will be (or have been) conducted. In addition, due to the presence of inherent experimental error, it is not possible to fix the values of the variables to their exact optimum values.

Thus, it is imperative to use a DOE technique in the EVM context that can actually take into account this error (unlike the traditional nonlinear regressions approaches where these variables are assumed to be errorless). The difference between the EVM context and the traditional nonlinear regression analysis is how they treat errors in the variables involved. Hence, if a parameter estimation problem, and hence the related design of experiments procedure, should be studied by the EVM method, using traditional nonlinear regression design of experiments techniques (like classical D-optimality) will lead to unreliable results.

While several applications of EVM for parameter estimation exist in the literature (for instance, see Duever et al. (1987), Kazemi et al. (2011), Keeler and Reilly (1991), and Dubé et al. (1991)), sources on the design question are extremely limited. The fact that using nonlinear regression DOE techniques is not suitable for implicit models with error in all variables was mentioned in passing in some literature (i.e., see Dovi et al. (1993) and ad-hoc design of experiments techniques were proposed to remedy the problem (Sutton and MacGregor (1977)). To our knowledge, Keeler and Reilly (1992) were the first to publish on the subject and certain improvements were suggested later by Zwanzig (2000) who investigated the consistency of the EVM design criterion.

In this chapter, the main topic of the design of experiments for copolymerization reactivity ratio estimation is investigated in two parts. The first part (section 4.2) introduces the EVM design criterion as a general design criterion that can be potentially implemented on various problems. Herein, we start with basic background on the EVM design criterion (i.e., the basic equations), followed by discussions about the main strengths of this powerful design criterion, the question of how to treat error (additive vs. multiplicative), and subsequently the question of how to implement the optimization algorithms (gradient-based vs. random search). The second part of this chapter (section

4.3) is more specifically about the design of experiments for the copolymerization reactivity ratio estimation problem, studied in the EVM context. Our results are illustrated, firstly, as a case study for a typical copolymerization system. Subsequently, based on an extensive simulated table of reactivity ratios, several practical scenarios are identified in order to highlight the results with the EVM design criterion: (1) compared to classical optimal design procedures, (2) with different error structures/levels, (3) with different feed constraints, and (4) with different optimization methodologies.

4.2 EVM Design Criterion

4.2.1 Design criterion for parameter estimation

In order to design experiments in the EVM context, we should extend the ideas from classical nonlinear regression analysis to EVM by maximizing the determinant of the information matrix, which will result in locating optimal settings. This task can be accomplished by maximizing the (analogous to that information matrix) $\underline{G}$ matrix, as introduced in Chapter 2, section 2.3.3. In this section, a number of key equations are repeated for the sake of clarity. $\underline{G}$ matrix is shown by equations (4.1) and (4.2). Under the assumption of normal distribution of errors, the inverse of the $\underline{G}$ matrix is an approximation for the variance-covariance matrix of the parameter estimates. Therefore, the optimal design can be found by maximizing the det ($\underline{G}$) or minimizing the det ($\underline{G}^{-1}$).

$$\underline{G} = E\left[\frac{d^2\phi}{d\theta_i d\theta_j}\right] \qquad i,j\ element \tag{4.1}$$

$$\underline{G} = \sum_{i=1}^{n} r_i \underline{Z}_i' (\underline{B}_i \underline{V} \underline{B}_i')^{-1} \underline{Z}_i \tag{4.2}$$

$\underline{B}_i$ and $\underline{Z}_i$ are the matrices for partial derivatives with respect to the variables and parameters, as shown by equation (4.3) and (4.4), respectively.

$$\underline{B}_i = \left[\frac{\partial \underline{g}(\underline{\xi}_i, \underline{\theta})}{\partial (\underline{\xi}_i)_u}\right] \qquad u^{th}\ element \tag{4.3}$$

$$\underline{Z_j} = \left[\frac{\partial \underline{g}(\underline{\xi_i}, \underline{\theta})}{\partial \theta_v}\right] \qquad v^{th}\ element \tag{4.4}$$

In order to show how D-optimality is extended to the EVM design criterion, a comparison can be made between the information matrix of the D-optimal design criterion ($I_{D\text{-}opt}$) and the one obtained from the EVM design criterion (G_{EVM}) for an explicit model of the form of $y_i = \underline{g}\left(\underline{\xi_i}, \underline{\theta}\right)$, given by equations (4.5) and (4.6).

$$I_{D-opt} = \sum_{i=1}^{n} \frac{1}{\sigma_{1i}^2} Z_i' Z_i \tag{4.5}$$

$$G_{EVM} = \sum_{i=1}^{n} \frac{1}{\sigma_{1i}^2 + \sigma_{2i}^2 (B_i(\underline{\xi_i}, \underline{\theta}))^2} Z_i\left(\underline{\xi_i}, \underline{\theta}\right) Z_i{}'\left(\underline{\xi_i}, \underline{\theta}\right) \tag{4.6}$$

In these equations, $\sigma^2{}_1$ denotes the variance of the dependent variables and $\sigma^2{}_2$ the variance of the independent variable(s). Obviously, if experimental errors in the independent variables are negligible ($\sigma^2{}_2 \rightarrow 0$), G_{EVM} reduces to the expression for $I_{D\text{-}opt}$.

4.2.2 Comparing different design criteria

One of the main discussions in almost every publication in the field of model-based DOE is about the problem of determining a criterion of optimality or efficiency by which designs can be ranked. The determinant of the information matrix can be one comparison metric that can quantitatively determine which one of the DOE methods is the superior one, due to the relation of this determinant with the volume of the confidence region. So, a ratio between the corresponding volumes obtained from different DOE techniques is one metric that is frequently used in the literature (for example, see Vila and Gauchi (2007)) to compare two design criteria, Design I and II, as shown in equation (4.7).

$$\frac{Volume_{Design\ I}}{Volume_{Design\ II}} \propto \left(\frac{|G_{Design\ II}|}{|I_{Design\ I}|}\right)^{1/2} \tag{4.7}$$

This ratio compares results directly based on the size of the confidence regions of the parameters. The interpretation of this ratio is that a better design, with a larger criterion magnitude, results in a smaller volume of the parameter estimation inference. Thus, more precise parameter estimates (smaller

confidence region) is a trait for a better and more efficient design. For instance, if the ratio (as in equation (4.7)) of the volumes of the parameters confidence regions for Design I over Design II is 0.75, this means that Design I is more efficient, and hence Design II needs more observations (information) to perform as well as Design I and reduce the volume of the parameters confidence region.

When comparing the EVM design and D-optimal design criteria, if measurements are all contaminated with some level of error, one should keep in mind that for such cases, using the EVM design criterion is the only correct approach. This is due to the fact that neglecting the effect of uncertainties in the independent variables under the nonlinear regression-based approach is invalid. In addition, for implicit models in which the variables cannot be separated, the EVM design criterion (the formulation of the $\underline{G}$ matrix in equation (4.2)) provides the proper design. Another advantage is that single- or multi-response problems do not need different mathematical formulations with the EVM information matrix.

4.2.3 Initial and sequential design schemes

Generally, there are two approaches for model-based DOE, namely, initial and sequential design. The initial design refers to the problem where no prior information is available and the objective is to design the first data set to permit parameter estimation. The sequential design problem, on the other hand, applies to the case where some data, be they from a DOE or not, are available, but the parameters have not yet been estimated with sufficient precision. Such a procedure consists of a series of alternating steps between designing experiments, using the experimental data for parameter estimation and designing further experiments, which continues until the parameter estimates achieve satisfactory levels of precision.

The EVM design criterion can be applied in both situations. Most of the works in optimal design in nonlinear regression and even the limited attempts with EVM design have focused on using the initial design criterion only (Keeler and Reilly (1992) and Rossignolli and Duever (1995)). For the initial design, no previous experimental information is considered. It is desired to determine what set of experiments to perform so as to provide the most information about the unknown parameters (hence, initial design). An important decision that should be made is about the number of optimal

experimental trials. As discussed in Chapter 2, section 2.2.3, if *n* experiments are designed non-sequentially to estimate *p* model parameters, with $p < n$, then an optimal design is obtained if *p* experiments are each replicated *n/p* times. The design criterion for maximization is given by equation (4.8) (Keeler (1989)).

$$Max_{\underline{\xi}^d} \left| \sum_{i=1}^{n} \underline{Z_i}' \left(\underline{B_i} \underline{V} \underline{B_i}' \right)^{-1} \underline{Z_i} \right| \quad (4.8)$$

$$\text{subject to } \begin{cases} \underline{g}(\underline{\xi_i}, \underline{\theta}) = 0 \\ L \leq \underline{\xi_i}^d \leq U \end{cases}$$

The choice of which variables are the subjects of the design problem (i.e., the design variables, $\underline{\xi_i}^d$) is related to the nature of the system under study. In general, the design variables involved in the optimization are those that determine the experimental conditions. Nonetheless, the model expression, $\underline{g}(\underline{\xi_i}, \underline{\theta}) = 0$, must hold between all the variables in the design, which means that the maximization/minimization procedures are all subject to a constraint given by $\underline{g}(\underline{\xi_i}, \underline{\theta}) = 0$. This constraint ensures that the variables chosen for the designed experiments fall on the function's surface (i.e., they satisfy the model). This criterion is also subject to inequality constraints of the feasible ranges (with L and U being the lower and upper bound of the feasible range, respectively) for the magnitudes of the variables involved, governed by the physic-chemical limitations of the variables.

In the sequential design of experiments, and after having conducted a set of *n* experiments, it is desired to find the optimal location of the next experiment(s) which can increase the precision of the results. Such a procedure consists of a series of alternating steps between designing experiments and using the optimally obtained experimental data for parameter estimation, which continues until the parameter estimates achieve satisfactory levels of precision. The objective function is given by equation (4.9) (Keeler (1989)) and the constraints are similar to those discussed for equation (4.8).

$$Max_{\underline{\xi}_{n+1}} \left| \left[\sum_{i=1}^{n} \underline{\hat{Z}_i}' \left(\underline{\hat{B}_i} \underline{V} \underline{\hat{B}_i}' \right)^{-1} \underline{\hat{Z}_i} \right] + \underline{\hat{Z}}'_{n+1} \left(\underline{\hat{B}}_{n+1} \underline{V} \underline{\hat{B}}'_{n+1} \right)^{-1} \underline{\hat{Z}}_{n+1} \right| \quad (4.9)$$

$$\text{subject to } \begin{cases} \underline{g}(\underline{\xi}_{n+1}, \underline{\theta}) = 0 \\ L \leq \underline{\xi}_{n+1}{}^d \leq U \end{cases}$$

In equation (4.9), the hat sign (ˆ) denotes that the converged parameter estimates from the first set of *n* experiments are being used to compute $\underline{B_i}$ and $\underline{Z_i}$ (as per equations (4.3) and (4.4)). The only term

that is not known in equation (4.9) is the second term, involving $\underline{\xi}_{n+1}{}^{d}$. A search is then performed to find the maximum of this equation. Once this optimal point has been chosen, the experiment is performed and the new point is added to the first set of *n* points. Using *n+1* data points, the parameters are now re-estimated. The new experiments are then used to choose the next experimental location and so on.

Even though using any optimal design compared to an empirical design (arbitrary design, e.g., equally spread points covering the variable range), enhances the amount of information for the subsequent analysis (i.e., parameter estimation), the sequential design scheme has the potential of improving the results even further. Utilizing prior information into the sequential design increases the information content considerably, and thus the reliability of the results. Finally, it must be noted that how far the procedure of sequential design should be pursued and the question of "when to stop" have to be answered with the desired magnitude of error in the final results in mind (e.g., the level of tolerance dictated from by target application).

4.2.4 Error structure

As mentioned in Chapter 2, section 2.3.2, discussion of measurement errors is an imperative part of any parameter estimation and design of experiments procedure, especially in the EVM context. The relation between a variable and its error can be either additive or multiplicative, as shown with equations (2.37) and (2.38), respectively. The additive error is the most common type of error, in which error is usually handled as an additive term to the true value of the corresponding variable. This is potentially the main reason that regression analysis is mostly based on an additive error structure. Multiplicative error, although less commonly encountered, is very important to be recognized, as it has been frequently observed in experimental publications that the error term is given in terms of a fraction of the measured response. That is, the error has a relative value with respect to the measured response. It is important to note that the choice of additive versus multiplicative error changes the mathematical structure of the objective function in both parameter estimation and design of experiments procedures. The effect of using either types of these error structures are shown in the following sections.

4.2.5 Optimization algorithms

The optimization problem of optimal design for the traditional nonlinear regression models has been extensively discussed in the literature. The focus is on steady-state optimization problems. Based on the size of the variable space and the number of parameters in the problem, the number of optimal points to be determined can vary. As the magnitude of this search problem increases, several difficulties can arise in the process of locating optimal points. The surface of a criterion (on which we are searching for the minimum/maximum) can have multiple local optima. In addition, in many physical operations, the optimal points are located on the extremes of feasible regions which could become a potential difficulty for the experimenter and of course a source of error in measurements. The minimization of the EVM design criterion is a nonlinear constrained optimization problem, in which the objective function minimization is subject to constraints consisting of a nonlinear model that relates the variables (nonlinear equality constraints), and lower and upper bounds on the magnitudes of the variables (inequality constraints).

Chapter 2 provided explanations about different optimization techniques that we used throughout this thesis for different problems. For the problem of design of experiments for copolymerization systems, we have concentrated on two approaches/algorithms from the literature: the Shuffled Complex Evolutionary (SCE) algorithm (see Chapter 2, section 2.3.5.2), which belongs to the evolutionary class of optimization algorithms, and the Sequential Quadratic Programming (SQP) algorithm (see Chapter 2, section 2.3.5.3) for nonlinear constrained optimization problems. The details of these methods are not mentioned here again, however, their applications on the EVM design of experiments problem for copolymerizations are explained as part of the design efficiency in section 4.3.2.

4.3 Results and Discussion: Design of Experiments for Reactivity Ratio Estimation in Copolymerization

As mentioned in the introduction, the question of estimating reactivity ratios for multicomponent polymerizations needs to be combined with the design of experiments step that aims at improving the results of parameter estimation. For this problem, the Mayo-Lewis model, as shown in equation (2.1), is the equivalent of the model equation, $\underline{g}(\underline{\xi_i}, \underline{\theta}) = 0$. The reactivity ratio estimation problem contains

variables (compositions) that are all subject to error. This situation could be the case for many other problems/systems in which the underlying assumptions regarding nonlinear regression are no longer valid.

Tidwell and Mortimer (1965) criterion is the first and the most cited criterion used for calculating optimal copolymerization feed compositions in the literature. This criterion is based on an approximate D-optimal approach and provides equations for the choice of two initial feed compositions. These equations were obtained based on a table of different values of r_1 and r_2, plausible for typical experimental systems, and formulated as equation (4.10). f_{11} and f_{12} in equation (4.10) denote the two optimal feed compositions with respect to the mole fraction of monomer 1.

$$f_{11} \cong \frac{r_2}{2+r_2} \qquad f_{12} \cong \frac{2}{2+r_1} \tag{4.10}$$

Due to the EVM nature of the reactivity ratio estimation problem, the basic assumptions of D-optimal design are violated and thus the Tidwell and Mortimer approach can no longer be trusted. As mentioned earlier, the EVM design criterion is an extension to the idea of the D-optimal design within the EVM context. To show the details of this criterion used for the problem of locating optimal feed compositions for a copolymerization system, firstly, a case study for a copolymerization system is discussed in which we present numerical results obtained from the implementation of the different design criteria. Design criteria surfaces and joint confidence plots are used to illustrate the numerical results. Next, practical insights are offered in a summary table based on trends from several copolymerization systems (real and hypothetical) with different reactivity ratio values. These tips can be particularly useful in troubleshooting the design of experiments for copolymerization systems. Finally, a set of recommended steps for implementing the EVM design criterion to locate optimal copolymer feed compositions is presented in form of a flowchart.

4.3.1 EVM design: A case study

As an illustrative example, the well-established system of Sty (M_1) / MMA (M_2) was chosen. The procedure herein is divided into five main steps, in which the performance of our approach and several important considerations are discussed.

Step 1: Finding initial values of reactivity ratios

As mentioned earlier, DOE methods for nonlinear models need initial guesses for the parameters, and so initial guesses for the reactivity ratios were obtained from a recent study by Kazemi et al. (2011) as r_1=0.4402 and r_2=0.4385. These reactivity ratios were estimated based on moderate and high conversion copolymerization experimental data, obtained from O'Driscoll et al. (1984).

Step 2: Locating optimal feed compositions

Regarding existing DOE approaches for copolymer reactivity ratio estimation, two approaches were used and compared with our work: the Tidwell and Mortimer (TM) criterion, for which two approximate expressions for optimal initial feed compositions are shown in equation (4.10); and the D-optimal criterion (without any approximation), which is implemented by maximizing the determinant of the information matrix (the information matrix is given by equation (4.5)). The optimal feed compositions are also obtained from our EVM design criterion. Based on the initial reactivity ratio values, mentioned in step 1, initial optimal feed compositions (for further experimentation) are shown in Table 4-1.

The design criteria for the initial and sequential design schemes are based on equations (4.8) and (4.9), respectively. For the initial design procedure, two optimal feed compositions are obtained, using equation (4.8), presented in Table 4-1. For the sequential design, the (next) optimal feed composition (titled as f_{1next}) is calculated based on equation (4.9) and is included in Table 4-1. The comparison of these different criteria is mentioned in step 3 of the analysis (where the "volume ratio" and "Information matrix determinant" column entries will be explained). Moreover, to have a comprehensive study with the EVM design criterion, two possible cases for error type in the copolymerization experimental data, additive and multiplicative error, are considered for all these criteria and are compared in step 4. Finally, the effect of including the sequentially designed experiment in the process of (re)estimating reactivity ratios is discussed in step 5.

Table 4-1 also includes the magnitudes of the different design criteria. The magnitudes of the criteria are in fact the information matrix determinants, which are subject to maximization; their magnitudes relative to each other can be interpreted as the efficiency of these designs. This type of comparison can also be made by looking at the volume ratios of different designs; so, the ratio of the volumes of their confidence regions (as shown in equation (4.7)) is also included in Table 4-1. The volume of the

confidence region obtained from the EVM initial design criterion is chosen as the basis, hence the other ratios are the ratio of a certain volume to this basis. Therefore, a ratio smaller than one indicates a more efficient (better) design with respect to the EVM initial design criterion, as the parameter confidence region volume is smaller for that specific design and so is the uncertainty of the parameter estimates.

Table 4-1. Optimal feed compositions for Sty (M_1)/MMA (M_2) with r_1=0.4402 and r_2=0.4385

	Initial Design				Sequential design		
	f_{11}	f_{12}	Information matrix determinant	Volume ratio	f_{1next}	Information matrix determinant	Volume ratio
Tidwell and Mortimer	0.179	0.819	*N/A*	*N/A*	*N/A*	*N/A*	*N/A*
D-optimal criterion	0.178	0.820	12062	0.950	0.800	4769116	1.067
EVM- Additive error	0.183	0.816	10887	1.000	0.799	5445923	1.000
EVM- Multiplicative error	0.100	0.736	591418	0.136	0.687	10171154	0.732

To implement the EVM design criterion, the inverse of the design objective function can be subject to minimization with either the SCE or SQP algorithm. Both of these algorithms are capable of finding the global or near global optimum feed composition(s). For copolymerization systems, the dimension of the problem allows us to use the SCE algorithm readily, which guarantees that we obtain the global optimum and thus could be the preferred route (more discussion about the performance of SCE versus SQP algorithm can be found at the end of the discussion in the section 4.3.2).

Step 3: EVM versus TM and D-optimal design criteria

This step is about the comparison between conventional approaches (TM and D-optimal criteria) and the EVM design criterion. The optimal feed compositions of the initial design scheme from TM and D-optimal criteria are very close to the optimal feed compositions from the EVM design criterion

with additive error. The magnitude of the determinant of the information matrix of the D-optimal design in Table 4-1 is slightly greater than that of the EVM design. The reason why is evident from the mathematical formulations for both information matrices (see equation (4.5) and (4.6)). The criterion of the D-optimal design for the copolymerization model would always be greater than that of the EVM design, as the D-optimal design criterion does not include the variance of the independent variables. This fundamental difference between these two design criteria is also reflected in the ratio of the volumes of the confidence regions of the D-optimal design over EVM (the volume ratio of 0.95), indicating that the confidence region of the D-optimal design is slightly smaller. However, on closer inspection, it can be realized that the fact that the D-optimal design considers only error on the dependent variables artificially deflates the confidence region for the parameter estimates (i.e., it artificially yields a smaller region). This is an artefact due to the nature of the D-optimal criterion and should not be interpreted as if the D-optimal design were more efficient.

In addition, as clearly shown in Table 4-1, the EVM design criterion with multiplicative error is superior in terms of efficiency to all other criteria. To further examine the impact of using the EVM design criterion compared to the TM approach, the optimal points from both techniques were used to simulate data and re-estimate the reactivity ratios. The results, as shown in Figure 4-1, illustrate that, even for a system with similar reactivity ratios, the EVM-estimated reactivity ratios have a smaller joint confidence region (JCR) and thus are clearly more reliable than the TM-estimated reactivity ratios.

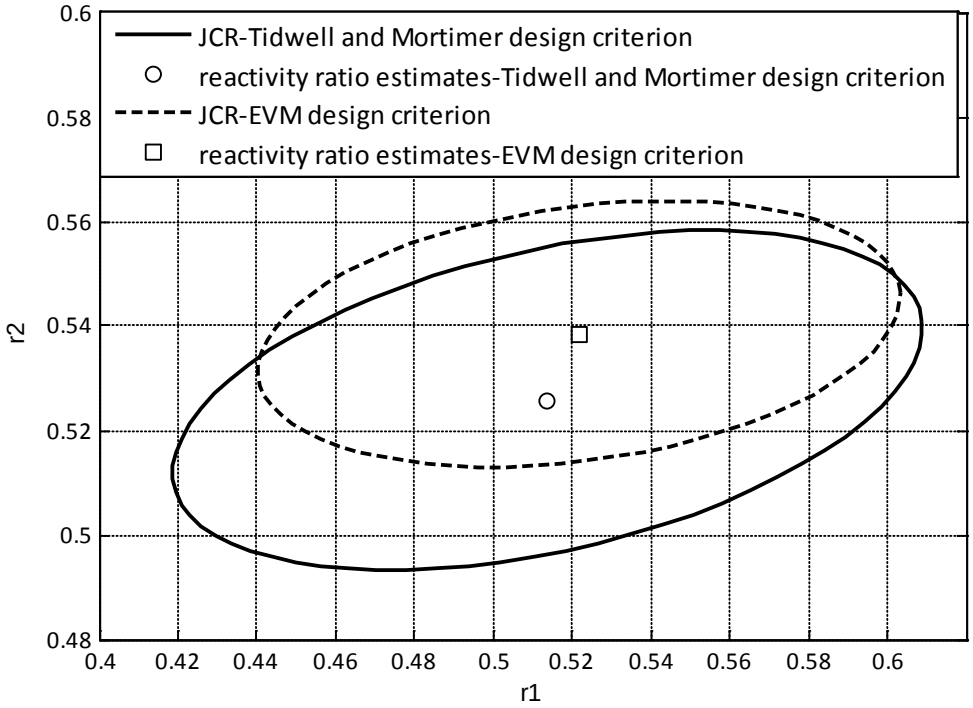

Figure 4-1. JCRs reactivity ratio estimates from EVM initial design-multiplicative error and Tidwell-Mortimer optimal experiments for Sty (M_1)/MMA (M_2)

Step 4: Additive versus multiplicative error structure

Another important point is about the difference between the results for additive versus multiplicative error. The choice of the error relation with the true (yet, unknown) values of the variables lies in the physical nature of the experimental procedures, analytical instruments, etc. For the problem of estimating reactivity ratios, it has been shown that this choice does not changes the point estimates, yet the multiplicative error model provides more precise results (Rossignolli and Duever (1995) and Hauch (2005)). As mentioned earlier in Chapter 2, for the additive versus multiplicative error issue, we are bound to make assumptions and choose a certain type of error structure. Since the error associated with experimental data in our field is usually in the form of a certain percentage of the measured observation; hence, most of the practitioners "believe" that the error is multiplicative in nature. In order to appreciate the type of error effect on the designed experiments, results from both types of error are included, since their contrast will be quite informative.

For the design of experiments problem, this selection affects the optimization procedures, as the mathematical expression of the objective functions and feasible ranges of variables are all influenced by this selection. Hence, results of DOE with the EVM design criterion, as shown in Table 4-1, are different for these two error models in terms of both the optimal points and the magnitude of the information matrix. Figures 4-2 and 4-3 are the plots showing the EVM design criterion surface along the two axes of feed compositions f_{11} and f_{12}, for the two types of error. As shown in these figures, there are two peaks for these surfaces that appear as maxima of this criterion and therefore yield the desired optimal points. Comparing these figures, the contrast between additive and multiplicative error is evident.

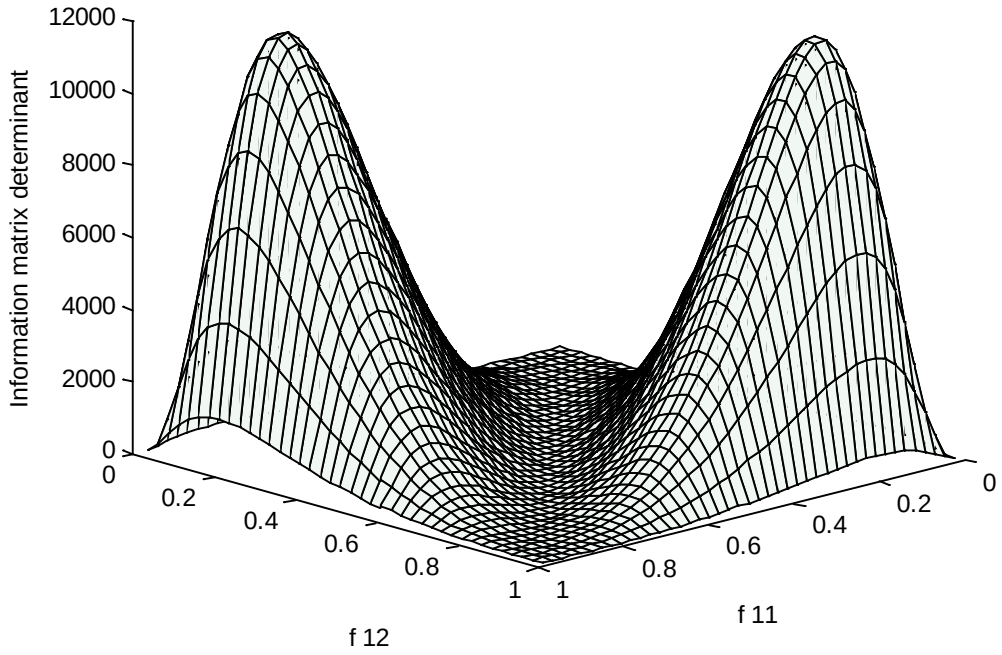

Figure 4-2. EVM initial design criterion for Sty (M_1)/MMA (M_2) - Additive error

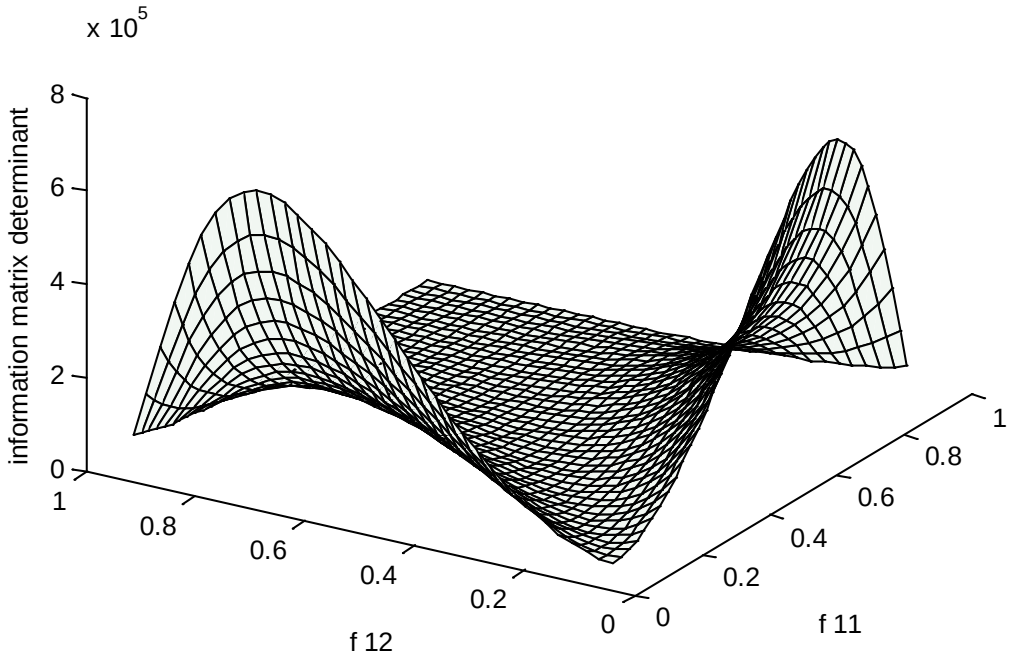

Figure 4-3. EVM initial design criterion for Sty (M_1)/MMA (M_2) - Multiplicative error

For additive error, the design criterion surface in Figure 4-2 has two very distinct maxima which define two unique optimal feed compositions. On the contrary, the EVM design criterion surface for multiplicative error in Figure 4-3 does not have two unique maxima within the range of 0 to 1 for optimal feed compositions. One of the maxima is at the very initial part of the feed composition range ($f_{11} \rightarrow 0$), whereas the other is located somewhere in between the range ($0 < f_{12} < 1$). The fact that the optimum point for the multiplicative error falls on the boundary of the feasible region is a phenomenon that is frequently observed in DOE problems. Basically, for a copolymerization system, f_1 can range from 0 to 1 and for the multiplicative error, with $ln\ (f_1)$ as the variable, this is converted to the range from ln (0) to ln (1), or from $-\infty$ to 0. So, at the vicinity of $f_1=0$, $ln\ (f_1)$ goes to negative infinity which maximizes the criterion. However, the design with $f_1=0$ does not make practical sense because at this point the system would become a homopolymerization which gives no information about the comonomers involved.

If we consider a sufficiently small value of f_1 as the lower limit of the feasible region for the optimization, then that very small value would be chosen as the first optimal feed composition. It

must be noted that even though this arbitrary choice may make the design less efficient, it makes it practical. Our choice, as can be seen in Table 4-1, is $f_1=0.1$ for the lowest bound of the feasible region; this choice is consistent for all of the analyses in this case study, yet the effect of considering other values of f_1 as the lower bound of the feasible region is investigated at the end of the discussion in the section 4.3.2.

Another striking point about additive versus multiplicative error structure is their design criteria efficiencies. As shown in Table 4-1, the volume of the parameter confidence region for multiplicative error is 0.136 of this volume for additive error. Hence based on these numerical results, the multiplicative error choice seems more efficient than the additive one. However, as the choice of additive versus multiplicative goes back to the nature of the error and experimental procedures, such numerical comparison cannot be used as a supporting fact for choosing either one of these error models. Meanwhile, if the volume ratio of 0.136 can be translated into an efficiency term, then for the sake of the argument, this would mean that the design criterion with the multiplicative error works 86.4% more efficiently than with the additive error. It is instructive to note that this efficiency value indicates the portion of replication needed to achieve the same precision for the parameter estimates as for the multiplicative model, and thus the relative time, effort, and cost of assuming the incorrect error structure.

Step 5: Initial versus sequential design schemes

The final point is about the initial and sequential design schemes. These two designs, as discussed earlier, provide great improvements for parameter estimation results, if used consecutively. In order to find the optimal feed compositions of the sequential design scheme, we need to, first, carry out the initial design procedure by using equation (4.8), find the optimal points and conduct copolymerization experiments at these optimal feed compositions. Here, in order to demonstrate the approach, we will simulate data with these optimal feed compositions and follow as realistic a scenario as possible (by adding realistic levels of noise). The new data set is then used for reactivity ratio estimation, using our EVM program. Then the updated point estimates along with the information matrix, $\underline{G}$ of equation (4.2), are fed to the sequential optimization routine to locate the next optimal feed composition, using equation (4.9). Figures 4-4 and 4-5 show the inverse of the design criterion (to be minimized) along the initial feed composition range for both additive and multiplicative error structures.

In Figure 4-4, it can be seen that the minimum is located at a distinct point, also shown in Table 4-1. In Figure 4-5, it can be seen that, similar to the initial design scheme for multiplicative error, the true minimum is located at $f_1=0$. However, if the lowest feasible limit of the initial feed composition is fixed at a larger feed composition, for example 0.1, then the minimum would be located around 0.7, which is also shown in Table 4-1. Therefore, it can be concluded that for the sequential design scheme, we have to impose the same restriction for the lower bound of the feasible region as we do for the initial design scheme.

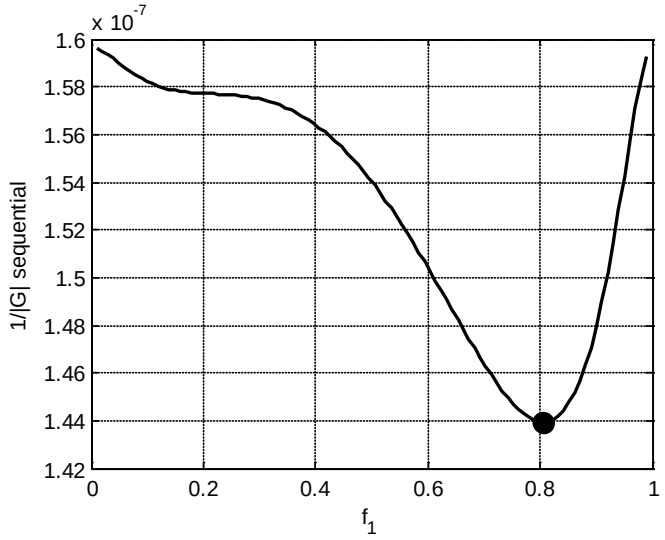

Figure 4-4. EVM sequential design criterion for Sty (M_1)/MMA (M_2) - Additive error

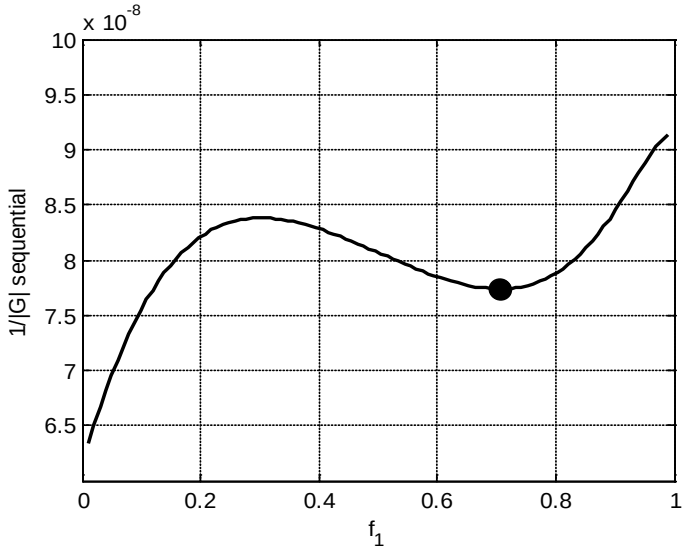

Figure 4-5. EVM sequential design criterion for Sty (M_1)/MMA (M_2) - Multiplicative error

In terms of comparing the initial and sequential designs with our results, it can be seen in Table 4-1 that even performing a single ("one-step ahead") sequential experiment shows promising results, as the magnitudes of the information matrix determinants all increase considerably from the initial to the sequential design. With respect to the volume of the parameter confidence regions, this volume shrinks considerably after the sequential design for D-optimal, additive-EVM, and multiplicative-EVM design criteria by 95%, 96%, and 76%, respectively.

Finally, Figure 4-6 shows the joint confidence regions (JCR) for the results of parameter estimation (for multiplicative error) based on these optimal points (initial versus sequential). The JCR of the reactivity ratio estimates based on the sequentially designed experiments is smaller (and hence more reliable) than the JCR of the initially designed experiments. This point emphasizes the importance of performing sequentially designed experiments (rarely conducted in the literature) in order to reach the desired precision in the parameters.

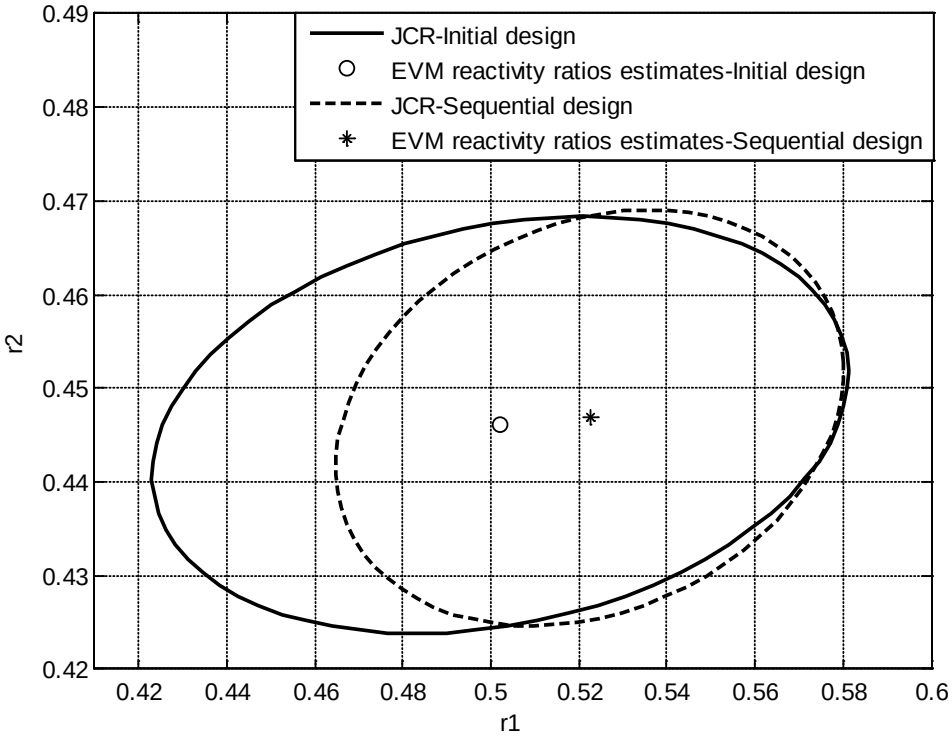

Figure 4-6. JCR for EVM reactivity ratio estimates from designed experiments (initial vs. sequential) for Sty (M_1)/MMA (M_2)

4.3.2 EVM design efficiency

Since model-based design of experiments for the problem of reactivity ratio estimation is directly dependent on the value of reactivity ratios of copolymerization systems, it is reasonable to wonder whether the performance of the aforementioned design criteria would show similar trends when applied on different systems with various reactivity ratio values. To investigate this issue, we extended our studies by examining many sets of reactivity ratios, with reactivity ratio values from $0.01 \leq r_1 \leq 1.5$ and $0.01 \leq r_2 \leq 20$. Many existing/studied copolymerization systems have reactivity ratios within the range of 0 to 1, and there are several cases where one reactivity ratio is still within the range of 0 to 1 while the other one has a relatively larger value in the range of 1 to 20. Cases where both reactivity ratios are greater than 1 have not been observed, yet their possibility was also included.

Overall, there were 153 systems that were studied for this purpose. The observed trends based on our extensive simulation studies with respect to the following characteristics are shown in Table 4-2. The extensive tables, showing all the detailed analysis are included in Appendix F. Among several critical factors that can affect the results of DOE with the EVM design criterion, we focused on the following characteristics:

1) "Goodness of the design", which tries to determine what the most appropriate design criterion is for many copolymer system.
2) "Error levels", which involve the experimental error in the calculations.
3) "Feasible region", which plays a crucial role in locating optimal, yet practical, feed compositions for any copolymerization system.
4) "Computational load", related to the numerical execution of the design criteria.

Table 4-2. Important characteristics of the performance of the EVM design criterion

Source of variation	Comments
"Goodness" of the design	• EVM design with multiplicative error is the most suitable criterion for finding optimal feed compositions. • The EVM design criterion provides more reliable results than the conventional D-optimal design (a.k.a., Tidwell-Mortimer design criterion); on the average, an 83% increase in the precision of the results. • For the ranges of ($0.1 \leq r_1 \leq 10$ & $0.05 \leq r_2 \leq 0.3$), the improvement is approximately 70% on the average, whereas for the ranges of ($0.1 \leq r_1 \leq 10$ & $0.4 \leq r_2 \leq 1$), the improvement in the precision of the results can rise to more than 85% on average. • Comparing the EVM-multiplicative error with the initial and sequential design schemes shows that using the sequential design improves parameter reliability in all cases (an average of 84% increase in the precision of the results).
Error levels	• For higher error levels, the differences between the performance of the Tidwell-Mortimer and the EVM design criteria become more significant. • If the error in the design variables (i.e., feed composition) increases from 1% to 5%, choosing Tidwell-Mortimer over the EVM design criterion can 'cost' up to a 56% loss in the precision of the results. • For the ranges of ($0.5 \leq r_1 \leq 0.9$ & $0.5 \leq r_2 \leq 0.7$), the difference between the performance of the EVM design criterion over Tidwell-Mortimer increases by almost 40%; for the ranges of ($0.1 \leq r_1 \leq 5$ & $0.01 \leq r_2 \leq 1$) and ($4 \leq r_1 \leq 20$ & $0.01 \leq r_2 \leq 1$), this difference goes up to 60% and 75%. • It is imperative to work with the EVM over the Tidwell-Mortimer design criterion when the error in the design variables is large and/or r_1 and r_2 are outside of the range 0.5 ± 0.1.
Feasible region	• With a lower bound, the volume ratio is considerably smaller, meaning that we could end up with less uncertainty in parameters with this initial optimal feed composition (39% increase in the precision of the results). • With a greater lower bound, we obtain a significantly larger volume for the parameter confidence region (86% decrease in the precision of the results).
Computational load	• The SQP algorithm (quasi-Newton descent direction) shows a lower number of function evaluations, whereas the nature of the SCE algorithm calls for several function evaluations, which means longer computational times. • Number of function evaluations of SCE/SQP ~ 11.

	• The SQP method performs about 6 times more iterations to reach convergence, compared to SCE method. • The SCE algorithm may give more flexibility since it is not dependent on reasonable initial guesses (an advantage when studying new systems). Also, it does not need the gradients of objective functions, which can be very beneficial for complicated/large models. • The SQP technique can handle larger systems with several optimal points, provided that reasonable initial guesses are provided.

4.3.3 Recommended approach

Based on the results from sections 4.2 and 4.3, so far, we can now outline a recommended approach for the problem of the design of experiments for the reactivity ratio estimation problem in copolymerization systems, summarized in the following steps and shown in Figure 4-7.

1. Choose your copolymerization system.
2. Search related literature for reasonable preliminary reactivity ratio estimates from similar experimental conditions.
   2.1. If initial guesses for reactivity ratios are available, go to step 5.
3. In no information is available, perform preliminary experiments and collect data.
4. Use EVM to estimate reactivity ratios.
5. Determine the following:
   5.1. The number of optimal points, which can be selected equal to the number of parameters. Working with the Mayo-Lewis model, there are two parameter to be estimated (r_1 and r_2) and thus, there are two optimal feed compositions to be calculated.
   5.2. The design variables.
   5.3. The feasible region for the design variables with their lower and upper bounds. The feasible range of the optimal points can be chosen within a relatively small range; close to 0 for the first feed composition and closer 1 for the other feed composition.
   5.4. The error structure, which can be assumed to be multiplicative.

6. Choose an optimization algorithm (SCE or SQP). The SCE algorithm can be used to find the global optima, independent of the initial guesses, but requires good computation power; whereas, for the SQP, reasonable initial guesses are required but the convergence is very fast.
7. Use the EVM design criterion (equation (4.8)) to locate the optimal feed composition.
8. Make sure that the optimal points are practical experimentally; if not, return to step 5 and adjust the feasible region accordingly. For the multiplicative error model, the lower bound of the feasible region is always chosen as one of the optimal points. So, set/adjust this value at the lowest possible practical feed composition.
9. Present the optimal feed compositions, f_{11} and f_{12}.
10. Finish.

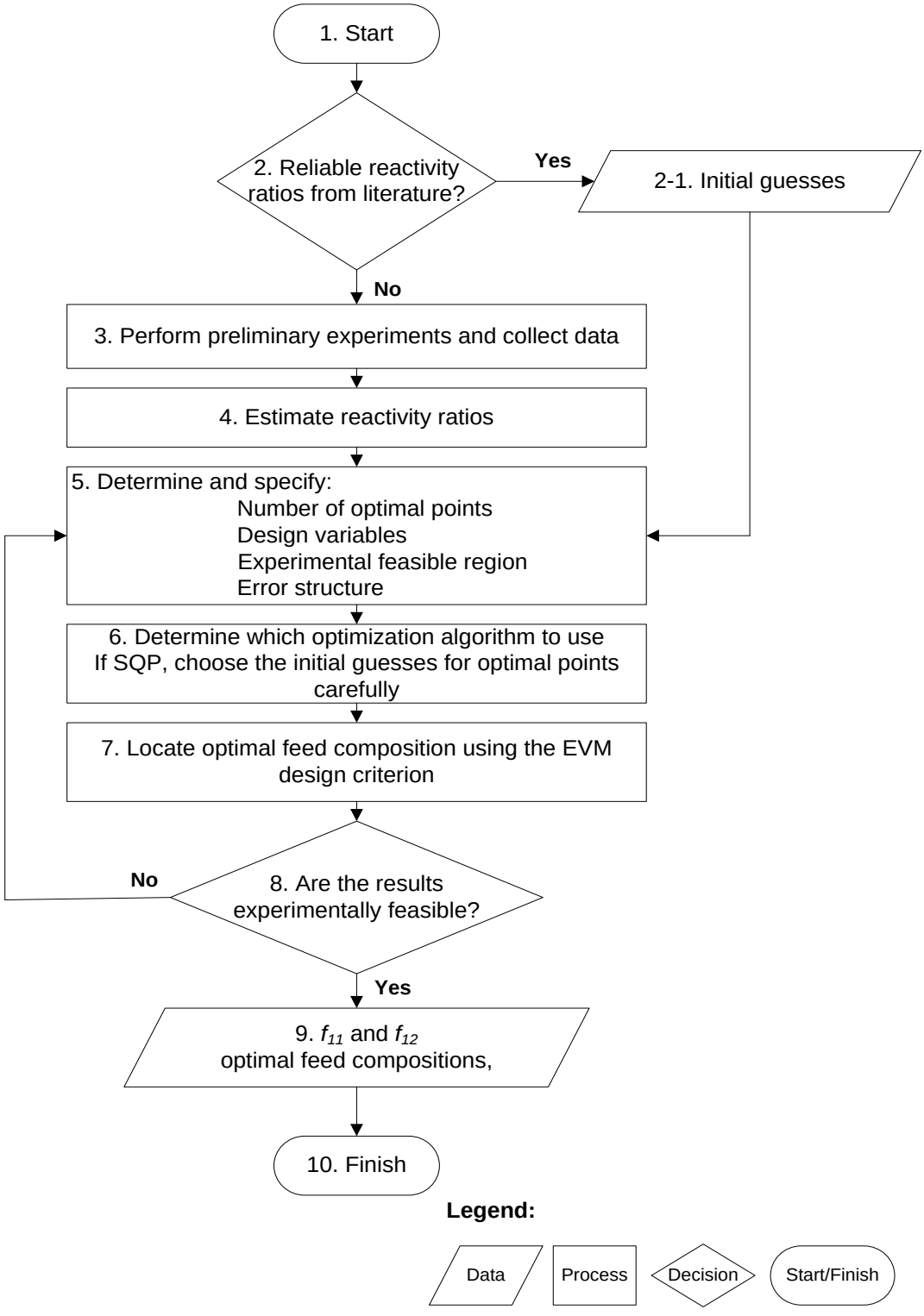

Figure 4-7. Design of experiments (DOE) flowchart for reactivity ratio estimation

4.4 Concluding Remarks

The focus of this chapter is on the issue of model-based design of experiments for problems with EVM statistical characteristics. The EVM design criterion is studied in great detail in terms of efficiency, error structure of the process data, effect of constraints on the design variables, and the optimization algorithm. Comparisons are made between the classical nonlinear approaches for design of experiments (e.g., the D-optimal design criterion) and the EVM design criterion in terms of optimal settings and design efficiency.

It is pointed out that since the main assumptions of D-optimality are violated for problems in the EVM context, the D-optimal prescriptions may be biased and, subsequently, unreliable parameter estimates are obtained. In fact, the difference between the D-optimal and EVM design criteria becomes more considerable as the error in the independent variables (the error that is completely ignored in the classical nonlinear regression approaches) turns out to be more significant; thus, it is critical to use the EVM design criterion in such situations.

The main application of our work is the problem of reactivity ratio estimation in copolymerization systems. This problem has the EVM characteristics, and yet has never been thoroughly dealt with in this context. It was also clearly illustrated in terms of design efficiency (see Table 4-2) and/or size of the parameter estimates inference that the sequential design scheme can improve the quality of the reactivity ratio estimates.

Similar to the reactivity ratio estimation problem, EVM has many applications in science and engineering and it is hoped that the powerful EVM design criterion will replace other, more traditionally used, yet more approximate, design criteria.

Chapter 5

Implementation of the Complete EVM Framework for Copolymerization Systems

The problem of estimating reactivity ratios for copolymerization systems has been revisited in great detail in Chapter 3 and a novel approach that leads to reliable reactivity ratio estimation for copolymerizations was established. Chapter 4 takes the estimation problem a step further (literally, a step before the estimation stage) by looking at different optimal design (of experimental trials) criteria that can lead to more reliable reactivity ratio estimates, highly superior to those from other currently implemented techniques. In the current chapter, we give the full story with respect to how one can go from preliminary reactivity ratio estimates to optimal estimates, i.e., we give an overview of the (statistically) correct design of experiments followed by the (statistically) correct parameter estimation. The steps are iterative, sequential and optimal, and deal with nonlinear mathematical models and estimation procedures. The overall procedure is experimentally demonstrated and verified with data from a largely unstudied and novel copolymerization system, the nitroxide-mediated controlled radical copolymerization between 9-(4-vinylbenzyl)-9H-carbazole (VBK) and methyl methacrylate (MMA) (Lessard et al. (2011)). Our work in this chapter is published in Kazemi et al. (2014a).

5.1 Introduction

There is no doubt about the importance of reactivity ratios in copolymerization (simplest case) and other multicomponent polymerizations, for describing chain microstructure and hence determining polymer chain composition and sequence length. At the same time, there is also no doubt that these important copolymerization parameters have been estimated incorrectly for several decades and are still being handled incorrectly (from a statistical estimation perspective) in the scientific literature. This has resulted in a database of relatively biased and unreliable reactivity ratios. Looking at the literature, it can be seen that even though efforts for correct parameter estimation techniques and the design of experiments have been made to rectify related issues, there still is a weak point in this

general picture. That is, we are facing a large, split literature that can be more confusing than helpful to the practitioner who tries to determine reactivity ratios of a system.

Our previous attempts were with respect to establishing the most appropriate reactivity ratio estimation procedure in Chapter 3, and with respect to improving the quality of the information used for this reactivity ratio estimation by implementing the design of experiments approach in Chapter 4. Those steps along with our evaluations of other existing approaches throughout all these steps brings us to a critical mass of research findings and experience that can be used to develop a systematic approach, a general framework, to solve this problem. Following a framework can organize the actions for a specific goal and guide practitioners to critical decision points. A framework-driven approach (1) promotes clear thinking and purpose, (2) helps to gather required information, (3) provides comments, explanations, and comparisons, (4) provides accessible descriptions of the required sources and methodologies, and (5) provides reliable information about the strengths and limitations of the procedures in use.

As mentioned earlier, as opposed to classical regression analysis, the EVM method is the perfect method for estimating reactivity ratios in multicomponent polymerizations (Kazemi et al. (2011)). The EVM framework aims at the optimal estimation of reactivity ratios in copolymerization systems. This complete framework is based on a combination of using the EVM algorithm, the proper copolymerization model and data for estimating reactivity ratios, and implementation of the design of experiments approach within the EVM context.

This framework consists of several sequential steps and practical prescriptions that can yield reliable and statistically correct reactivity ratio values. These steps include: (a) screening experiments for estimating preliminary reactivity ratios, (b) optimal design of experiments, (c) full conversion range experiments and estimation of optimal reactivity ratios, and if necessary, (d) design of sequentially optimal experiments, re-estimation of reactivity ratios and diagnostic checks. This complete methodology should become common practice for determining reactivity ratios with the highest possible level of confidence.

In addition to examples of applications of different steps of the EVM framework, herein we present a collaborative work with the authors of Lessard et al. (2011) verifying the performance of the EVM framework experimentally with data from the controlled nitroxide-mediated copolymerization of 9-

(4-vinylbenzyl)-9H-carbazole (VBK) and methyl methacrylate (MMA), a novel and largely unstudied copolymer system.

5.2 Reactivity Ratio Determination: The Complete EVM Framework

In this section a complete framework for the reactivity ratio estimation problem is presented and the individual steps are described. This complete framework is based on the error-in-variables-model (EVM) method that is probably the most complete approach for situations where the dependent and independent variables do not need to be distinguished. This feature makes EVM the perfect method for estimating reactivity ratios in multicomponent polymerizations. Since collecting experimental data that result in precise parameter estimates is a resource-intensive task, there is always a need for designing experiments in an optimal fashion, thus minimizing the overall effort and maximizing the information from the process in question. Such a procedure consists of a series of alternating steps between designing experiments and using the optimally obtained experimental data for parameter estimation, which continues until the parameter estimates achieve satisfactory levels of precision.

It is therefore desirable to combine the design of experiments technique with the EVM procedure in one multifaceted framework in order to improve the quality of the parameter estimation results. This structure consists of certain key components, (1) Parameter estimation and design of experiments, (2) Full conversion range experiments, (3) Recommended steps, which are briefly explained here. Each component is described in detail in the previous chapters.

5.2.1 Parameter estimation and design of experiments

In order to have a complete picture of the EVM framework, the key equations of different steps are mentioned in this section again. At first, the vector of measurements $\underline{x_i}$ is equated to the vector of true (yet unknown) values $\underline{\xi_i}$, plus a multiplicative error term, $k\underline{\varepsilon_i}$, as shown in equation (5.1), The error structure is chosen to be multiplicative (relative) due to the nature of the actual (physical) measurements in the reactivity ratio estimation problem. In addition to equation (5.1), there is a

statement that relates the true (yet unknown) values of the parameters, $\underline{\theta}^*$, and variables, $\underline{\xi}_i$, via the mathematical model, represented by equation (5.2).

$$\underline{x}_i = \underline{\xi}_i(1 + k\underline{\varepsilon}_i) \qquad where\ i = 1, 2, \dots, n \tag{5.1}$$

$$\underline{g}\left(\underline{\xi}_i, \underline{\theta}^*\right) = 0 \qquad where\ i = 1, 2, \dots, n \tag{5.2}$$

where *i* refers to the trial number, *k* is a constant, and $\underline{\varepsilon}_i$ is a random variable, which, in the simplest case, has a uniform distribution in the interval from -1 to 1. The explanations about the value of the constant *k* and how it is used for constructing the variance-covariance matrix of the measurements, $\underline{V}$, are given in Chapter 2, section 2.3.2. For the feed composition, *k* could be ±1%; while for the copolymer composition, *k* could be one of three error levels of ±2%, ±5%, and ±10%, representing experimental data with good, normal and poor precision, respectively.

The objective function for minimization in order to find the point estimates, $\underline{\hat{\theta}}$, is given by equation (5.3), where r_i is the number of replicates at the i^{th} trial, $\underline{\overline{x}}_i$ is the average of the r_i measurements $\underline{x}_i$, and $\underline{\hat{\xi}}_i$ denotes estimates of the true values of the variables $\underline{\xi}_i$. The procedure for parameter estimation is a nested iterative one. There is a main iterative loop that searches for the parameter values (minimizing equation (5.3)), while an inner loop finds the true values of the variables. This procedure results in both parameter estimates and estimates of the true values of the variables. Finally, point estimates should be accompanied by joint confidence regions that reflect their level of uncertainty (for more details on these steps, see Chapter 2).

$$\phi = \frac{1}{2}\sum_{i=1}^{n} r_i \left(\underline{\overline{x}}_i - \underline{\hat{\xi}}_i\right)' \underline{V}^{-1} \left(\underline{\overline{x}}_i - \underline{\hat{\xi}}_i\right) \tag{5.3}$$

The variance-covariance matrix of the parameters is given by the inverse of the information matrix, given by matrix $\underline{G}$ (Chapter 2, equation (2.3.3)). To design experiments for parameter estimation in the EVM context, as explained in Chapter 4, we should aim at maximizing the determinant of the information matrix (which aims at reducing the elements of the variance-covariance matrix of the parameters) (Keeler (1989)). This forms the basis for locating optimal experiments. The EVM design criterion is given in equation (5.4), $\underline{B}_i$ and $\underline{Z}_i$ can be calculated based on equations (2.46) and (2.54), respectively.

$$Max_{\underline{\xi}^d} \left| \sum_{i=1}^{n} \underline{Z}_i' \left(\underline{B}_i \underline{V} \underline{B}_i' \right)^{-1} \underline{Z}_i \right| \qquad (5.4)$$

$$\text{subject to} \begin{cases} \underline{g}(\underline{\xi}_i, \underline{\theta}) = 0 \\ L \leq \underline{\xi}_i{}^d \leq U \end{cases}$$

Generally, equation (5.4) is the inital EVM design criterion, where no prior information is available and the objective is to design initial trials in order to collect the first data set and commence the parameter estimation process. The constraints for this problem are the function (model) itself as well as lower (L) and upper (U) bounds of the experimentally feasible region. An additional step can be taken, after having conducted a set of *n* prior experiments, to find the optimal location of the next experiment(s) which can increase the precision of the results. This step involves the sequential design criterion, as shown in equation (5.5). Such a procedure consists of a series of alternating steps between designing experiments, using the experimental data for parameter estimation, and designing further experiments. This continues until the parameter estimates achieve a satisfactory level of precision. In equation (5.5), the hat sign (^) denotes that the converged parameter estimates from the first set of *n* experiments are being used to compute $\underline{B}_i$ and $\underline{Z}_i$.

$$Max_{\underline{\xi}_{n+1}{}^d} \left| \left[\sum_{i=1}^{n} \hat{\underline{Z}}_i' \left(\hat{\underline{B}}_i \underline{V} \hat{\underline{B}}_i' \right)^{-1} \hat{\underline{Z}}_i \right] + \hat{\underline{Z}}_{n+1}' \left(\hat{\underline{B}}_{n+1} \underline{V} \hat{\underline{B}}_{n+1}' \right)^{-1} \hat{\underline{Z}}_{n+1} \right| \qquad (5.5)$$

$$\text{subject to} \begin{cases} \underline{g}(\underline{\xi}_{n+1}, \underline{\theta}) = 0 \\ L \leq \underline{\xi}_{n+1}{}^d \leq U \end{cases}$$

For designing experiments for the purpose of estimating reactivity ratios, perhaps the most cited work is by Tidwell and Mortimer (1965). The very useful (and often ignored) Tidwell-Mortimer criterion is, however, based on the assumptions of classical nonlinear regression. The criterion results in two optimal initial feed compositions, f_{11} and f_{12}, with respect to the mole fraction of monomer 1, shown in equation (5.6). These two optimal compositions are solely functions of (initially available) reactivity ratios.

$$f_{11} \cong \frac{r_2}{2+r_2} \qquad f_{12} \cong \frac{2}{2+r_1} \qquad (5.6)$$

But, as mentioned above, the nature of the reactivity ratio estimation problem is different from traditional nonlinear regression analysis, in that there are errors in all the variables. Because of this difference, the assumptions behind the Tidwell-Mortimer criterion do not hold for this problem and

thus using equation (5.6) to choose optimal experiments is not appropriate within the EVM context. Implementation of the EVM design criterion, both with initial and sequential design schemes (as shown in equations (5.4) and (5.5), respectively), has been described Chapter 4, with extensive details about the method, the equations, and the overall algorithm.

5.2.2 Full conversion range experiments

For the purpose of reactivity ratio estimation in copolymerization systems, there have been numerous publications in the literature over the past 50 years, during which two main approaches have established themselves. The first and main practice is to use low conversion experimental data with the instantaneous copolymer composition model (the so-called Mayo-Lewis model), as discussed in details in Chapter 3. The second approach, as already mentioned previously, is to use the Tidwell-Mortimer equations to identify feed mole fractions for the design of experiments for reactivity ratio estimation. Both of these methodologies have drawbacks, with the former having much more severe defects than the latter. In our EVM framework, these two techniques have been modified in order to avoid their underlying problems. Similar to the explanations regarding the design of experiments problem (discussed in the previous section), the other modification is about including higher conversion data, or in fact, data from the whole experimental conversion trajectory for estimating reactivity ratios.

In this method, the differential equation for the unreacted monomer fraction f_1 with respect to conversion, X_n, is being integrated over the course of conversion, as shown in equation (5.7). The unreacted monomer mixture composition, f_1, is then used in equation (5.8) to evaluate the cumulative copolymer composition, $\overline{F_1}$. The instantaneous copolymer composition, F_1, in this model is given by the Mayo-Lewis model, as shown in equation (5.9).

$$\frac{df_1}{dX_n} = \frac{f_1 - F_1}{1 - X_n} \tag{5.7}$$

$$\overline{F_1} = \frac{f_{10} - f_1(1 - X_n)}{X_n} \tag{5.8}$$

$$F_1 = \frac{r_1 f_1^2 + f_1(1-f_1)}{r_1 f_1^2 + 2f_1(1-f_1) + r_2(1-f_1)^2} \quad (5.9)$$

The performance of this approach, which is referred to as direct numerical integration (DNI), without resorting to any analytical integration, was evaluated and discussed in detail in Chapter 3, with comparisons to the Mayo-Lewis model or the Meyer-Lowry analytically integrated model (See Chapter 3, section 3.2.3). It was shown that using the DNI approach and using medium and high conversion data for estimating reactivity ratios can significantly improve the quality of the results by (simply) including more information in the analysis as well as avoiding (practical) limitations of collecting low conversion data (with their inherent sources of errors). Therefore, our EVM framework based on the DNI approach can handle experimental data at any conversion level.

Given the discussion on sections 5.2.1 and 5.2.2, the following section summarizes presents the recommended set of steps in the EVM framework that can be considered as the prescriptions for obtaining reactivity ratios both efficiently and consistently.

5.2.3 Recommended steps

The flowchart of Figure 5-1 gives an overview and summary of the recommended steps of the complete methodology. Following the steps on this flowchart will increase the reliability of the reactivity ratio estimates for any copolymerization system (an example from a novel experimental system is shown in the results and discussion section). Also, these steps can be implemented during investigations of any larger multicomponent polymerization. The recommended approach is summarized in the following steps:

1. Start with the given copolymerization system.
2. Check the related literature for reasonable preliminary guesses (e.g., reactivity ratio estimates that have been estimated in similar experimental settings).
    2.1. If initial guesses for reactivity ratios are available, go to step 5.
3. If no information is available, perform preliminary experiments and collect data.
    3.1. Experiments can be performed up to medium conversion levels (say, up to 20-40%).

3.2. Cover low, medium and high feed compositions and note any limitations in the feasible experimental region (constraints).

3.3. Collect data on feed composition, copolymer composition, and conversion.

3.4. Perform independent replicates (this important step is rarely done).

4. Use EVM to estimate reactivity ratios ***(Estimation*)**.

4.1. Work with the DNI approach, since it is more general.

4.2. If measurement error levels are known, specify k (as per equation (1)) and populate the variance-covariance matrix of the measurements. If not enough replicates are available to calculate k, typical values which are based on the usual amount of error in common polymerization measurements can be used (i.e., k as 1% for gravimetric analysis and 5% for NMR analysis).

4.3. Run the EVM parameter estimation algorithm (see Chapter 3, section 3.2.4).

4.4. Construct joint confidence regions for reactivity ratios (see Chapter 2, section 2.3.4).

5. Locate optimal feed compositions ***(Design).***

5.1. With copolymerizations, there are two parameters to be estimated (r_1 and r_2) and thus at least two optimal feed compositions to be calculated (see Chapter 4, section 4.2.3).

5.2. Note infeasible and feasible experimental regions. The feasible range for the optimal experiments can be chosen from a relatively small mole fraction (below 0.1) up to 1. Using the EVM design criterion, the first feed composition is always at the lowest limit of the feasible region, while the second one is a feed composition within the range of 0 to 1, depending on the reactivity ratio values. This rule of thumb also applies for the sequential design scheme.

5.3. Use the EVM design criterion as shown in equation (5.4) for the initial design scheme and equation (5.5) for the sequential design scheme. Refer to Chapter 4 for more information.

5.4. It is preferable to use a global optimization technique (see Chapter 4, section 4.2.5).

6. Make sure that the optimal points are experimentally feasible (i.e., they do not violate any process constraints). If not feasible, return to step 5 and adjust accordingly. For copolymerizations, the lower bound of the feasible region is always chosen as one of the optimal points. So, set/adjust this value at the lowest possible practical feed composition.

7. Perform the optimal experiments ***(Experimentation)***.

7.1. Initial feed compositions (f_{10}) are at the optimal points.

7.2. Run experiments up to "moderate/high" conversion. That is, for each designed initial feed composition, experimental data on copolymer composition can be collected at conversion levels of 5%, 10%, 20%, 30% and 40%, even up to approximately 60% (i.e., the EVM approach does not have any low conversion restrictions, as common practice stipulated before).

7.3. Perform replicated experiments; collecting independent replicates for each run increases the accuracy of the results significantly and it is therefore highly recommended.

8. Using EVM, re-estimate reactivity ratios, as per step 4 ***(Estimation*)**.

9. If results are satisfactory, proceed with step 10. If not, use the new point estimates and the information matrix from step 7 to carry out the next sequentially designed experiment(s).

9.1. Find the next optimal trial, using equation (5.5) and go to step 7.

- Repeat steps 7 to 9 until the outcome is satisfactory.

10. Check/plot the r_1/r_2 joint confidence region.

11. Finish.

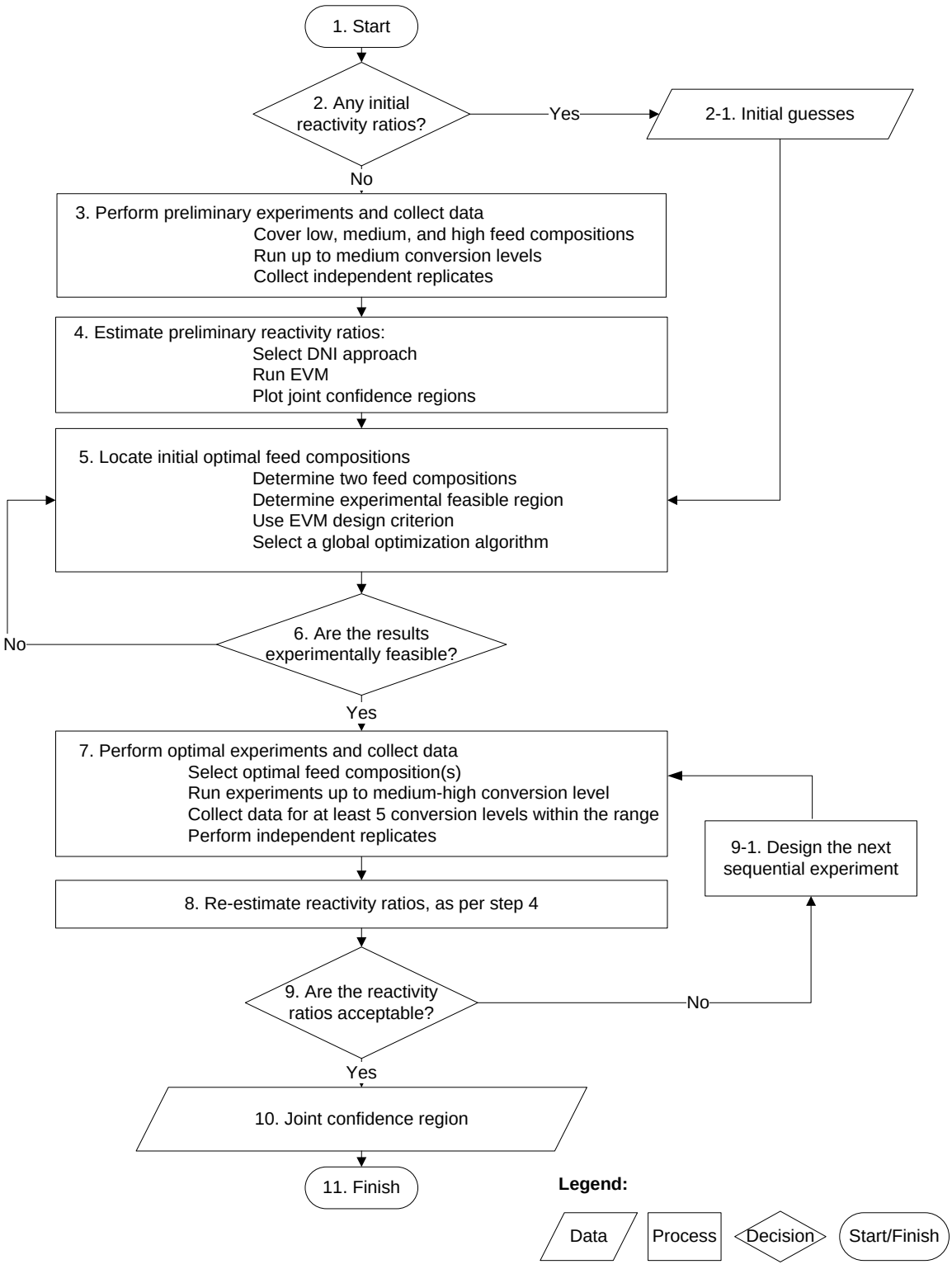

Figure 5-1. EVM framework flowchart for reactivity ratio estimation

5.3 Experimental

The synthesis of VBK monomer and the VBK/MMA copolymerizations were carried out under similar conditions to those reported by Lessard et al. (2011, 2012a). 2-({tert-butyl[1-(diethoxyphosphoryl)-2,2-dimethylpropyl]amino}oxy)-2-methylpropionic acid (BlocBuilder, 99%) was obtained from Arkema, while {tert-butyl[1-(diethoxyphosphoryl)-2,2-dimethylpropyl]amino} nitroxide (SG1, >85%) was donated by Noah Macy of Arkema. In a typical copolymerization, a mixture of BlocBuilder, SG1, DMF, VBK and MMA was polymerized. The ratio of BlocBuilder to monomer was determined to give a target molecular weight at complete conversion of 20-25 $kg.mol^{-1}$ while using an initial molar ratio of $[SG1]_0/[BlocBuilder] \approx 0.1$. In all cases, DMF added to the mixture gave a ≈20wt% solution. The polymerization reaction was at 80 °C. The polymerization was allowed to proceed for 8-24 hours depending on the experiment and the final polymer was precipitated in methanol. Copolymer composition was determined by 1H NMR spectroscopy, as explained in Lessard et al. (2011, 2012a).

5.4 Results and Discussion: Experimental Verification of Complete EVM Framework

The following subsections illustrate the complete procedure with the EVM framework, for estimating the reactivity ratios of the 9-(4-vinylbenzyl)-9H-carbazole (VBK) and methyl methacrylate (MMA) copolymerization system. This is a novel and largely unstudied controlled radical copolymerization (due to the electron-donating properties of VBK), and hence fertile ground to illustrate the procedure with it. VBK has been identified as a controlling comonomer for a variety of methacrylates, such as oligo (ethylene glycol) methylether methacrylate (OEGMA) (Lessard et al. (2012a), 2-N-morpholinoethyl methacrylate (MEMA) (Lessard et al. (2012b)), and methacrylic acid (MAA) (Lessard et al. (2013a)). The VBK reactivity ratios with the corresponding methacrylates have been identified as a contributing factor to this control (Lessard et al. (2013b)). A preliminary investigation concerning the reactivity ratios of VBK/MMA was described in Lessard et al. (2011). In summary, preliminary experimental data from Lessard et al. (2011) were analyzed first to obtain preliminary reactivity ratio values, which were subsequently used for the optimal design of experiments. In the second step, experiments were performed based on these optimal feed compositions. In the third step,

reactivity ratios were re-estimated based on the designed data. Finally, these updated reactivity ratios were used once more in order to design the next optimal experiment but now in a sequential fashion. After performing sequential experiments, the reactivity ratios were re-estimated. The results showed a clear improvement in the quality and precision of the reactivity ratios obtained.

5.4.1 Preliminary experimentation (Steps 1-4, Figure 5-1)

Preliminary attempts at determining the reactivity ratios for this system involved low conversion experiments and a nonlinear fitting procedure for estimating reactivity ratios (Lessard et al. (2011)). The preliminary low conversion data are shown in Table 5-1, where the X_w, $f_{o,VBK}$, and $\overline{F}_{VBK}$ columns show the mass conversion, initial feed composition, and cumulative copolymer composition, respectively. The reference reactivity ratios from Lessard et al. (2011) with their confidence intervals are shown in Table 5-2.

Table 5-1. Low conversion data for VBK/MMA copolymerization, Lessard et al. (2011)

X_w,	$f_{o,VBK}$	$\overline{F}_{VBK}$
0.170	0.010	0.030
0.130	0.030	0.060
0.160	0.050	0.140
0.100	0.100	0.370
0.100	0.100	0.290
0.080	0.300	0.710
0.080	0.300	0.550
0.040	0.400	0.790
0.040	0.400	0.590
0.070	0.500	0.740
0.070	0.500	0.620
0.040	0.800	0.910
0.040	0.800	0.890

Note that the data of Table 5-1 are the preliminary data of our scheme (step 3 of Figure 5-1). It contains low conversion data for this “experimentally difficult” system. It is easy to observe that the data points are noisy, i.e., significant error is present in the measurements. The presence of error is a

fact of life. The error is more significant in our case due to the nature of the experimental system, and this makes use of EVM even more relevant and imperative in order to handle such a data set.

To obtain reactivity ratios for the subsequent design of experiments, low conversion data points, as in Table 5-1, were analyzed with the DNI approach (as explained in Chapters 2 and 3) and new reactivity ratios were obtained, as shown in the second row of Table 5-2. The Mayo-Lewis model was not employed in the current work, as the conversion levels of the data points (shown in Table 5-1) went higher than 5-10%; hence, this is a perfect application of the DNI approach. Figure 5-2 shows joint confidence regions (JCR) for the reactivity ratios in Table 5-2. The reference reactivity ratios are not contained in the JCR (dashed line). The JCR, reflecting the level of uncertainty in the estimates, is quite large (especially with respect to the uncertainty in the r_{VBK} (r_1) value). Note that for the EVM implementation of the DNI approach and calculation of the JCR, the k values (see equation (5.1)) for feed mole fraction and conversion measurements were 0.005, corresponding to a typical error level of 0.5% (coming from gravimetry). The k value for copolymer composition measured via NMR was 0.10 (i.e., error level of 10%).

Table 5-2. Reactivity ratio estimates for VBK (M_1)/MMA (M_2) copolymerization

	Copolymerization model	Data set/Conversion level	r_1	r_2
Lessard et al. (2011)	Mayo-Lewis	Lessard et al. (2011)	2.7 ± 1.5	0.24 ± 0.14
Current work	DNI	Lessard et al. (2011)	4.13	0.29
Current work	DNI	EVM initial optimal data	2.42	0.45
Current work	DNI	EVM initial and sequential optimal data	2.08	0.44
Current work	DNI	Tidwell-Mortimer initial optimal data	2.66	0.48

The next step was to calculate initial optimal feed compositions. As mentioned earlier, since there are two parameters under study, two optimal feed compositions (mole fractions), f_{11} and f_{12}, should be located (f_{11} refers to the mole fraction of M_1 (VBK) for the first trial and f_{12} is the mole fraction of VBK for the second trial). The values of these points depend on the prior values of reactivity ratios, and in this case, we used the reactivity ratios estimated from the low conversion data (second row of

Table 5-2). The EVM design criterion (equation (5.4)) resulted in two feed compositions, with $f_{11} \rightarrow 0$ and $0 < f_{12} < 1$. In order to keep the design procedure optimal and practical, a (practically) small value of f_{11} should be the lower limit of the feasible region that is determined for each system based on operating conditions and experimental settings. Therefore, in this case, feed compositions of f_{11}=0.04 and f_{12}=0.30 were suggested by the optimal design criterion for the initial optimal trials.

5.4.2 Optimal design of experiments (Steps 5-11, Figure 5-1)

New optimal experiments were performed at the specified feed compositions in 20% DMF (by weight). The early stages of copolymerization are dominated by VBK incorporation, since r_{VBK} is larger than r_{MMA}. As conversion increases, the amount of VBK in the copolymer decreases. To capture this information, experiments should be run up to relatively medium-high conversion (otherwise, this information is completely lost at low conversion level trials with copolymer chains rich in VBK). The maximum achievable conversion for the new trials was 40% and six samples per experiment were collected at different conversion values. Table 5-3 shows the new optimal data set. Independent replicates were also conducted and are included in the table as well.

Note again that the data points of Table 5-3 are quite noisy, again due to the nature of the experimental system. Once more, the use of EVM becomes imperative. Observe also that the lower conversion level data exhibit more error, as expected, and this makes the use of DNI equally relevant and imperative. In essence, this is like a worst case scenario testing of our EVM scheme.

Using the inital optimal data set, the reactivity ratios were re-estimated and the results are shown in Table 5-2 (third row), as well as in Figure 5-2. The JCR of the new reactivity ratios (solid line) is considerably smaller. The optimally designed experiments are expected to provide the best set of observations for the purpose of parameter estimation and, therefore, the point estimates would show a lower amount of uncertainty (smaller JCR). This part of the analysis clearly proves our point that implementing the EVM framework increases the certainty of the results and in turn our understanding about the true (yet unknown) values of these reactvity ratios.

Table 5-3. Optimally designed data (initial design scheme)

X_w,	$f_{o,VBK}$	$\overline{F}_{VBK}$	X_w,	$f_{o,VBK}$	$\overline{F}_{VBK}$
0.056	0.040	0.029	0.029	0.290	0.550
0.172	0.040	0.148	0.148	0.290	0.420
0.225	0.040	0.154	0.154	0.290	0.510
0.380	0.040	0.161	0.161	0.290	0.490
0.326	0.040	0.190	0.190	0.290	0.500
0.365	0.040	0.289	0.289	0.290	0.520
0.069	0.040	0.043	0.043	0.300	0.610
0.079	0.040	0.156	0.156	0.300	0.360
0.113	0.040	0.183	0.183	0.300	0.410
0.147	0.040	0.203	0.203	0.300	0.410
			0.235	0.300	0.420
			0.268	0.300	0.420

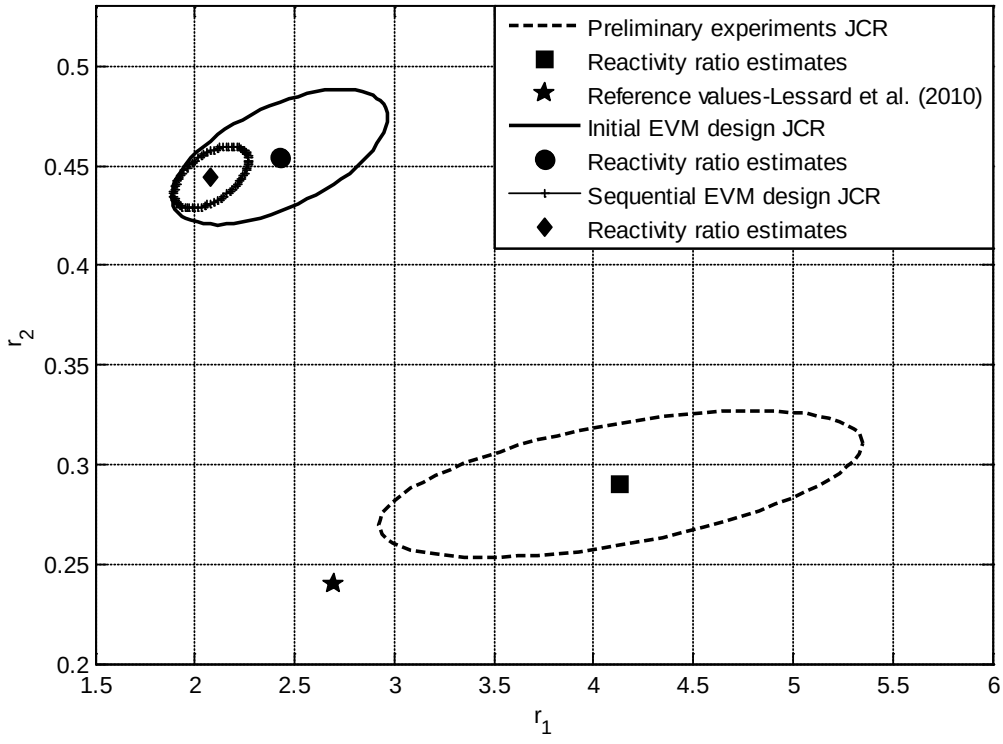

Figure 5-2. Preliminary, initial, and sequential optimal reactivity ratio estimates (VBK (M_1)/MMA (M_2))

To complete the analysis, the next step was taken in order to study the effect of including the next sequentially optimal experiment as well. The next sequentially optimal trial, given by the EVM design criterion in equation (5.5), was at the feed composition of f_1 =0.45. Very similar to the initial set of optimal experiments, six samples per experiment at different conversion levels were run. Table 5-4 shows these data points. These data points were added to those of initial optimal experiments and the combined data set (Tables 5-3 and 5-4) was re-analyzed by the DNI approach for updating the reactivity ratios.

Table 5-4. Optimally designed data (sequential design scheme)

X_w,	$f_{o,VBK}$	$\overline{F}_{VBK}$
0.037	0.450	0.420
0.054	0.450	0.610
0.102	0.450	0.610
0.077	0.450	0.600
0.065	0.450	0.760
0.078	0.450	0.670

The final set of estimated reactivity ratios is included in Table 5-2 (fourth row) and also in Figure 5-2 along with the corresponding JCR. Based on the results in Figure 5-2, it can be clearly seen that using f_1=0.45, as the next sequential experiment, resulted in the smallest JCR (i.e., the most reliable reactivity ratio estimates among all analyzed cases). This was also in complete agreement with the previously obtained reactivity ratios. For all these cases, the sizes of JCRs are considerably smaller than JCRs obtained from initially designed (or non-designed) experiments, thus validating our premise that performing sequentially optimal experiments improves the quality of reactivity ratios, thus making it a very useful step in the process of determining reliable reactivity ratios.

5.4.3 An important aside: comparison between the EVM and Tidwell-Mortimer design criteria

As the last part of the analysis for this case study, we decided to compare the performance of the relatively new EVM design criterion with the Tidwell-Mortimer design criterion, experimentally. For

this purpose, the Tidwell-Mortimer optimal feed compositions were calculated using equation (5.6) and then experiments were performed with those feed compositions at f_{11} =0.13 and f_{12}=0.33 (again, f_{11} refers to the mole fraction of VBK for the first trial, whereas f_{12} refers to the mole fraction of VBK for the second trial). The data points from this stage of experimentation are shown in Table 4-5 (the same comments apply to the data entries of Table 4-5 as previously made for Tables 5-1 and 5-3).

Using these data points, the reactivity ratios were re-estimated and the results are shown in Table 5-2 (last row) as well as in Figure 5-3, along with their JCR (dashed line). This figure also shows the previously obtained reactivity ratios from the initial EVM optimal experiments with their JCR (solid line). As can clearly be seen in this figure, the Tidwell-Mortimer design reactivity ratios have a larger JCR than the EVM design reactivity ratios, indicating that these point estimates are not as precise as the EVM design reactivity ratios. This first-ever comparison perfectly supports our claims about the superiority of the EVM design criterion for the purpose of estimating reactivity ratios, which is related to the fact that the EVM statistical framework is the most appropriate methodology for the problem of reactivity ratio estimation.

Table 5-5. Designed data using Tidwell-Mortimer criterion (initial design scheme)

X_w,	$f_{o,VBK}$	$\overline{F}_{VBK}$	X_w,	$f_{o,VBK}$	$\overline{F}_{VBK}$
0.054	0.13	0.29	0.024	0.33	0.74
0.120	0.13	0.23	0.042	0.33	0.59
0.194	0.13	0.19	0.062	0.33	0.57
0.202	0.13	0.21	0.2924	0.33	0.26
0.448	0.13	0.18	0.091	0.33	0.48
0.063	0.13	0.31	0.246	0.33	0.33
0.087	0.13	0.25	0.036	0.33	0.72
0.093	0.13	0.24	0.057	0.33	0.46
0.232	0.13	0.17	0.037	0.33	0.57
0.158	0.13	0.25	0.036	0.33	0.63
0.195	0.13	0.27	0.056	0.33	0.57
			0.339	0.33	0.30

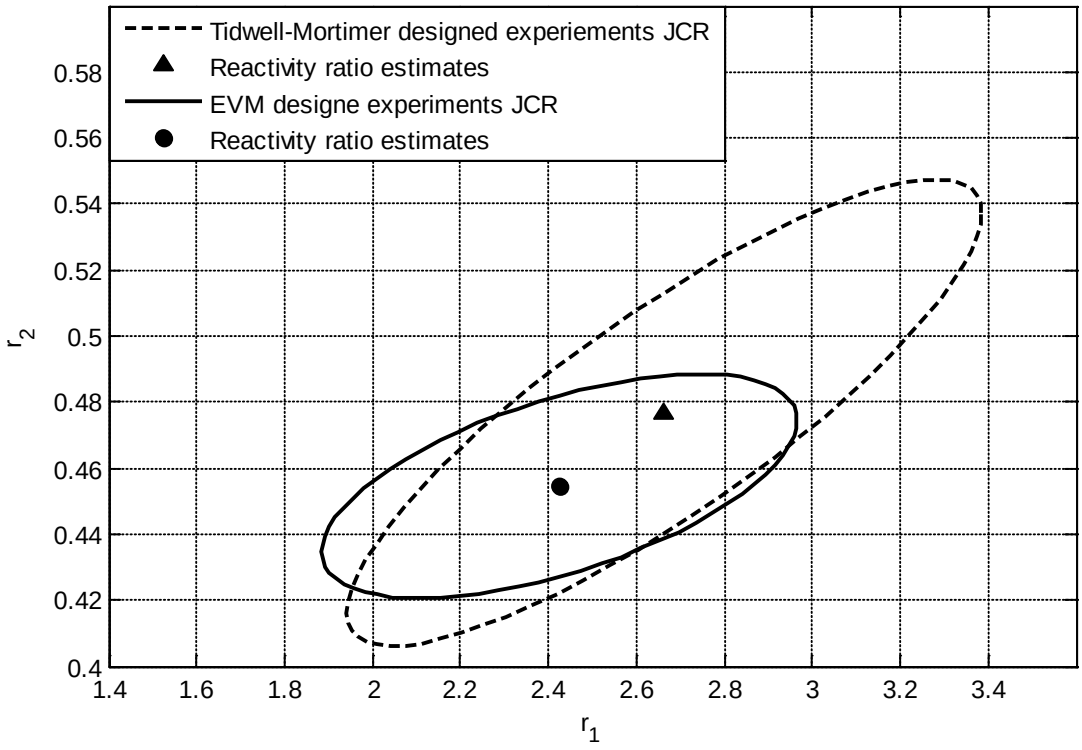

Figure 5-3. EVM vs. Tidwell-Mortimer reactivity ratio estimates (VBK (M_1)/MMA (M_2))

5.5 Concluding Remarks

We have discussed statistically correct EVM estimation procedures and extended them to include optimal design of experiments for reactivity ratio estimation in copolymerization. For a comprehensive approach to yield reliable reactivity ratio values, several sequential steps and practical prescriptions have been suggested: (a) reactivity ratio estimation from screening experiments (typically but not necessarily at low conversion levels), (b) optimal design of experiments, (c) reactivity ratio estimation from full conversion range experiments, and (d) sequential design of experiments and re-estimation of reactivity ratios and diagnostic checks. This complete methodology, which should become the norm, especially in copolymerization or terpolymerization kinetic studies, has subsequently been experimentally demonstrated and verified with the new, largely unstudied, and experimentally difficult VBK/MMA nitroxide-mediated copolymerization system. The estimated optimal reactivity ratios are $r_{VBK} = 2.08$ and $r_{MMA} = 0.44$, whereas the 95% joint confidence region for these values is shown in Figure 5-2.

Chapter 6

Reactivity Ratios in Terpolymerization Systems: Parameter Estimation

A thorough study for estimating ternary reactivity ratios is presented in this chapter. In typical practice for terpolymerizations so far, binary reactivity ratios have been used directly in the instantaneous Alfrey-Goldfinger composition model, effectively ignoring the presence of the third monomer. It is intended in this chapter to point out the problems of conventional approaches while applying the EVM algorithm, as explained in Chapters 2 and 3, with terpolymerization data directly based both on instantaneous (low conversion) and cumulative composition data (medium and high conversions). Several examples and counter-examples highlight such important issues as the choice of the correct number of responses, accounting for the appropriate error structure, and incorporating the right information content, all with diagnostic checks whose target is the eventual reliability of the reactivity ratio estimates. The work of this chapter is published in Kazemi et al. (2014b).

6.1 Introduction

Polymeric materials with new and optimized properties are being produced with an ever increasing frequency by the use of multicomponent polymerization techniques. Terpolymerization systems with three monomers are being utilized to generate polymeric materials with tailor-made properties. For such products, one needs to describe (among other characteristics) the composition of the terpolymer, which is directly linked to its physical properties. This composition is also linked to the kinetics of the polymerization, which can be studied by the use of powerful mathematical models that have been developed. Due to the practical impact and versatility of the properties of terpolymers, understanding the kinetics of ternary systems is not only advantageous for exploring strategies for advanced technologies but also necessary for producing terpolymers with desirable physico-chemical properties in pilot-plant and/or industrial scales.

The relative reactivities of the monomers present in the reaction medium govern monomer reactivity ratios, which play a very important role in polymerization kinetics, as they describe the rate of

incorporation of each monomer in the polymer chain. The impact of polymer chain composition for terpolymerizations on their chemical, physical and mechanical properties clearly indicates how important it is to be able to predict and, furthermore control terpolymer composition from the knowledge of three monomer concentrations and their reactivity ratios. Despite the importance of these terpolymerization reactivity ratios, not a lot of research has been conducted to estimate and study these parameters in terpolymerization modeling. This is partly due to the complexity of the developed mathematical models and their poor performance in predicting real data. It is more importantly related to the fact that, based on an analogy between copolymerization and terpolymerization mechanisms, reactivity ratios obtained for binary pairs from copolymerization experiments have commonly (albeit misleadingly) been used in models dealing with terpolymerizations.

As it has been mentioned repeatedly throughout this thesis, with even a quick screening of the literature regarding binary reactivity ratios, it can be realized that there are many ambiguities and inconsistencies around these reactivity ratios (even for the same copolymerization system). The inaccuracies in these reactivity ratios can simply propagate into the terpolymerization composition model (consisting of more than one equations, unlike the simpler and single-equation Mayo-Lewis model for copolymerization), thus becoming a much more serious (than in copolymerization) source of error in parameter estimation and prediction variance. Using binary reactivity ratios in terpolymerization studies also treats the ternary system as separate and unrelated binary pairs and the interactions between three monomers are ignored. This past approach is therefore an unjustified simplification that could have been acceptable at a time when computation power was very limited, but not nowadays.

The correct approach for determining ternary reactivity ratios is to use the experimental data directly from terpolymerization and estimate reactivity ratios for each system. Such studies based on ternary experimental data are very limited and quite unclear with respect to experimental descriptions, which have led to very little use of their data in estimation schemes in ternary investigations (see, for example, Duever et al. (1983) and Hagiopol (1999)). Therefore, our goal is to conduct a thorough study of this problem, from the terpolymerization composition equations to the statistical approaches that have been implemented in this regard.

The work in this chapter is presented in four parts. Firstly, the related literature is reviewed and information about existing techniques and their potential problems are discussed. Secondly, our approach and the most appropriate statistical procedure for this problem are explained. This involves re-casting of the traditional terpolymerization composition equations and implementing the error-in-variables-model (EVM) algorithm (as described in previous chapters) for parameter estimation. In the third part, we highlight important details about our findings and observations, along with more detailed explanations about the implementation of our approach, with examples and counter-examples. This section also contains a summary table that presents several studied systems with their reactivity ratios. Finally, the last part discusses how the results of reactivity ratio estimation from different sources can be evaluated in order to "weigh" the reliability of these reactivity ratios for terpolymerization systems.

6.2 Related literature

6.2.1 Terpolymer composition equations

As mentioned in Chapter 2, a typical terpolymerization in which three monomers are polymerized simultaneously was mathematically described originally by Alfrey and Goldfinger (1944), AG model, shown herein with a set of three differential equations (equations (6.1) to (6.3)), where f_i is the mole fraction of unbound monomer i in the polymerizing mixture and df_i is the mole fraction of monomer i incorporated (bound) into the terpolymer chains.

$$\frac{df_1}{df_2} = \frac{F_1}{F_2} = \frac{f_1\left(\frac{f_1}{r_{21}r_{31}}+\frac{f_2}{r_{21}r_{32}}+\frac{f_3}{r_{31}r_{23}}\right)\left(f_1+\frac{f_2}{r_{12}}+\frac{f_3}{r_{13}}\right)}{f_2\left(\frac{f_1}{r_{12}r_{31}}+\frac{f_2}{r_{21}r_{32}}+\frac{f_3}{r_{13}r_{32}}\right)\left(f_2+\frac{f_1}{r_{21}}+\frac{f_3}{r_{23}}\right)} \tag{6.1}$$

$$\frac{df_1}{df_3} = \frac{F_1}{F_3} = \frac{f_1\left(\frac{f_1}{r_{21}r_{31}}+\frac{f_2}{r_{21}r_{32}}+\frac{f_3}{r_{31}r_{23}}\right)\left(f_1+\frac{f_2}{r_{12}}+\frac{f_3}{r_{13}}\right)}{f_3\left(\frac{f_1}{r_{13}r_{21}}+\frac{f_2}{r_{23}r_{12}}+\frac{f_3}{r_{13}r_{23}}\right)\left(f_3+\frac{f_1}{r_{31}}+\frac{f_2}{r_{32}}\right)} \tag{6.2}$$

$$\frac{df_2}{df_3} = \frac{F_2}{F_3} = \frac{f_2\left(\frac{f_1}{r_{12}r_{31}}+\frac{f_2}{r_{21}r_{32}}+\frac{f_3}{r_{13}r_{32}}\right)\left(f_2+\frac{f_1}{r_{21}}+\frac{f_3}{r_{23}}\right)}{f_3\left(\frac{f_1}{r_{13}r_{21}}+\frac{f_2}{r_{23}r_{12}}+\frac{f_3}{r_{13}r_{23}}\right)\left(f_3+\frac{f_1}{r_{31}}+\frac{f_2}{r_{32}}\right)} \tag{6.3}$$

The instantaneous form of the AG model (equations (6.1) to (6.3)) applies to low conversion data, where df_i is substituted by F_i, the instantaneous mole fraction of monomer *i* incorporated (bound) in the terpolymer, owing to the assumption that compositional drift at that very early stage of the polymerization is negligible. The composition of a terpolymer can thus be calculated by using any two equations of the three combinations shown above for the AG model. In order to find the terpolymer composition, knowledge of six reactivity ratios is required and none of these values can be infinite or equal to zero. These important monomer reactivity ratios are defined as:

$$r_{12} = \frac{k_{11}}{k_{12}},\ \ r_{13} = \frac{k_{11}}{k_{13}},\ \ r_{21} = \frac{k_{22}}{k_{21}},\ \ r_{23} = \frac{k_{22}}{k_{23}},\ \ r_{31} = \frac{k_{33}}{k_{31}},\ \ r_{32} = \frac{k_{33}}{k_{32}} \tag{6.4}$$

The visualization of the composition of a terpolymerization system has been done by the use of a triangular plot, proposed first by Slocombe (1957). The sides of a triangle represent the mole fraction of the monomer assigned to those sides, the corners of the triangle represent 100% concentration of each monomer, and the sides describe the corresponding binary mixtures. Experimental compositions of the polymer chains can be represented as points inside the triangle and the drift in the terpolymer composition mixture can be illustrated by arrows (the head of the arrow indicates the instantaneous composition of the resulting polymer and its tail the composition of the monomer mixture). An example of such a triangular plot is shown in the results and discussion section.

The calculations with the AG model and therefore its usage are quite simple nowadays. However, at the time that these equations were proposed, computational tasks were not as simple and this motivated researchers to devise even simpler forms of these composition equations. A probabilistic approach was developed by Fordyce and Ham (1951) that still involved six reactivity ratios but with simpler mathematical expressions. Valvassori and Sartori (1967) also proposed the same simpler forms by extending the steady state assumption of binary copolymerizations to ternary systems. Later on, Hocking and Climchuck (1996) presented yet another form of the terpolymer composition equations which was based on the Valvassori and Sartori model, but with symmetrical characteristics. Also, Kahn and Horowitz (1961) were the first to develop the integrated form of the AG model for prediction of higher conversion level data, given the values of the six reactivity ratios, confirming that the model is capable of predicting terpolymer compositions at full conversion as well.

Despite all these attempts to predict terpolymer composition, it has often been observed that the prediction results do not have an acceptable agreement with experimental data. To resolve such

issues, some have suggested that for systems where one of the monomers is unreactive towards itself or other monomers, modified forms of the AG model should be used (Hagiopol (1999)). These types of adjustments are rather arbitrary and, while eliminating some of the reactivity ratios, introduce other parameters as ratios of remaining rate constants. These new parameters, however, have unclear physical meaning and so these modified equations do not have the extensive usage nor the applicability of the original AG model.

In addition to the special forms of the AG model, other attempts have been made by considering different mechanisms for developing the terpolymerization composition equation. While the AG model (or its simplified forms) is based on the terminal mechanism in the propagation steps, the penultimate mechanism can also be used to derive the terpolymerization composition equations. This approach has been rarely used or even studied mainly due to the cumbersome calculations and even larger number of unknown parameters in the model (Ham (1964)). Another suggested mechanism for some ternary systems is the charge-transfer complex participation mechanism, which can be valid for systems where complexes are formed between two out of three monomers (Iwatsuki et al. (1967)). That is, the system can be treated as a binary case between two complexes. Discussions about whether the penultimate model versus the terminal model or the free-radical propagation versus the complex participation model can perform better with ternary data belong to ongoing research which is out of the scope of this chapter.

6.2.2 Conventional approaches for reactivity ratio estimation

The assumptions involved in the development of the AG model are similar to those used for describing copolymerization systems. Therefore, studies about the ternary composition equations were initially based on the reactivity ratios extracted from binary systems. Based on this analogy, a ternary system is treated as a “mixture” of three binary copolymerizations, instead of one specific ternary system, and the effect of the interactions between all three monomers on their reactivity towards each other is overlooked. This approach, even though established as common practice, is neither reliable nor precise for predicting ternary compositions. In fact, several issues with prediction results of the terpolymer composition equations are simply due to the usage of binary reactivity ratios instead of reactivity ratios based directly on terpolymerization experimental data.

It is also worth considering that even if the analogy between binary and ternary mechanisms allows the utilization of binary reactivity ratios, the database of binary reactivity ratios in the literature is very dubious and inconsistent, suffering over many years from the implementation of several incorrect binary reactivity ratio estimation techniques and/or poorly designed experimental data sets. These inaccuracies propagate in the ternary composition model, and result in serious deviations between predictions of terpolymerization composition and experimental data. A simple example of this problem is that there are several differing (often widely) reactivity ratio values for the same copolymerization system in the literature, and so the question becomes which set of values should be used (averaging and any random selection between the existing sets of reactivity ratios would definitely increase the uncertainty level of the calculations).

In one of the early applications of estimation techniques with terpolymerization models, Duever et al. (1983) pointed out some problems in earlier methodologies, while illustrating the application of the EVM parameter estimation method with the AG model for estimation of ternary reactivity ratios. Some efforts tried to handle terpolymerization data directly (see, for example, Luft et al. (1993) and Iglesias et al. (1996)), but given the paucity of actual terpolymerization data and studies, these efforts were overall just too few and vague to get the attention of people studying ternary systems. As a result, using binary reactivity ratios became the de facto procedure in ternary kinetic studies. Our premise in the current chapter is that using binary reactivity ratios is an oversimplification, not only with respect to the reliability of the values themselves, but also with respect to not including measures (and, hence, the effect) of their uncertainty.

In addition to the inaccurate conventional estimation approach, the AG model itself can be a source of error for the problem of reactivity ratio estimation. In preliminary studies, we looked at several ternary case studies where reactivity ratios were estimated using the AG model and pointed out that the results were not reliable for all cases, which can be directly attributed to either the lack of information in the existing data sets (usually, very few experimental points are reported), or large experimental error associated with the data, and/or issues with the formulation of the AG model itself. In these preliminary studies (Kazemi (2010)), we showed that selecting different combinations of ratios of mole fractions in the AG model (e.g., F_1/F_2 and F_1/F_3 versus F_1/F_2 and F_2/F_3) can affect the precision of the reactivity ratio estimates. This observation revealed that this model suffers from symmetry issues and thus final results depend on the arbitrary choice of different combinations of copolymer mole fractions into the parameter estimation scheme. Hence, the question becomes which

set of copolymer mole fraction ratios amongst (F_1/F_2, F_1/F_3), (F_1/F_2, F_2/F_3), and (F_1/F_3, F_2/F_3) should be used in the AG model.

6.3 A Correct Approach for Parameter Estimation

We now present a complete approach for estimating reactivity ratios in ternary systems. The first step in this regard is to resolve the issue with the instantaneous AG model stemming from its inherent derivation and the use of copolymer mole fraction ratios, by simply recasting the form of the model and isolating each of the terpolymer composition mole fractions as an individual response. The second step is about the implementation of the error-in-variables-model (EVM) parameter estimation technique, which is the most appropriate technique for the problem of reactivity ratio estimation (see Chapter 2 for more explanation). In the third step, we estimate ternary reactivity ratios using the cumulative composition model. This can potentially include medium to high conversion data for the parameter estimation procedure (analogous work for copolymerization can be found in Chapter 3).

6.3.1 Model recasting

In addition to the asymmetry problem with the AG model, it can also be easily seen that this model uses ratios of copolymer mole fractions as responses in the parameter estimation problem. This is done despite the fact that in ternary reactivity ratio estimation studies, as in other copolymerization or multicomponent polymerization studies, it is the individual copolymer mole fractions that are measured directly, say, from NMR analysis. In other words, what is measured directly is F_1 or F_2, and not F_1/F_2. This violates the well-known and practical recommendation in parameter estimation schemes that the model be written directly relating a measured response y_i with the right-hand side function, which involves the independent variables and unknown parameters. In other words, it is highly recommended that the measured F_1, and not the ratio (F_1/F_2), be related directly to a model right-hand side function, as the right hand-side appearing in equations (6.1) to (6.3).

This is recommended in order to avoid distorting the error structure of the measured responses during estimation. A certain error structure corresponds to the measured F_1, and this error structure will be distorted or transformed if a ratio like (F_1/F_2) is used instead. This distortion, when using mole

fraction ratios, can have severe effects on the reliability of the parameter estimates (reactivity ratios), even if one knows a priori which set of mole fractions to use. To find a remedy for such difficulties, we re-derived a new form of the terpolymerization equations in this work, where each one of the terpolymer composition mole fractions is formulated explicitly, as shown in equations (6.5) to (6.7). The derivation of the recast model is shown in Appendix G.

$$F_1 - \frac{f_1\left(\frac{f_1}{r_{21}r_{31}}+\frac{f_2}{r_{21}r_{32}}+\frac{f_3}{r_{31}r_{23}}\right)\left(f_1+\frac{f_2}{r_{12}}+\frac{f_3}{r_{13}}\right)}{f_1\left(\frac{f_1}{r_{21}r_{31}}+\frac{f_2}{r_{21}r_{32}}+\frac{f_3}{r_{31}r_{23}}\right)\left(f_1+\frac{f_2}{r_{12}}+\frac{f_3}{r_{13}}\right)+f_2\left(\frac{f_1}{r_{12}r_{31}}+\frac{f_2}{r_{21}r_{32}}+\frac{f_3}{r_{13}r_{32}}\right)\left(f_2+\frac{f_1}{r_{21}}+\frac{f_3}{r_{23}}\right)+f_3\left(\frac{f_1}{r_{13}r_{21}}+\frac{f_2}{r_{23}r_{12}}+\frac{f_3}{r_{13}r_{23}}\right)\left(f_3+\frac{f_1}{r_{31}}+\frac{f_2}{r_{32}}\right)} = 0 \quad (6.5)$$

$$F_2 - \frac{f_2\left(\frac{f_1}{r_{12}r_{31}}+\frac{f_2}{r_{21}r_{32}}+\frac{f_3}{r_{13}r_{32}}\right)\left(f_2+\frac{f_1}{r_{21}}+\frac{f_3}{r_{23}}\right)}{f_1\left(\frac{f_1}{r_{21}r_{31}}+\frac{f_2}{r_{21}r_{32}}+\frac{f_3}{r_{31}r_{23}}\right)\left(f_1+\frac{f_2}{r_{12}}+\frac{f_3}{r_{13}}\right)+f_2\left(\frac{f_1}{r_{12}r_{31}}+\frac{f_2}{r_{21}r_{32}}+\frac{f_3}{r_{13}r_{32}}\right)\left(f_2+\frac{f_1}{r_{21}}+\frac{f_3}{r_{23}}\right)+f_3\left(\frac{f_1}{r_{13}r_{21}}+\frac{f_2}{r_{23}r_{12}}+\frac{f_3}{r_{13}r_{23}}\right)\left(f_3+\frac{f_1}{r_{31}}+\frac{f_2}{r_{32}}\right)} = 0 \quad (6.6)$$

$$F_3 - \frac{f_3\left(\frac{f_1}{r_{13}r_{21}}+\frac{f_2}{r_{23}r_{12}}+\frac{f_3}{r_{13}r_{23}}\right)\left(f_3+\frac{f_1}{r_{31}}+\frac{f_2}{r_{32}}\right)}{f_1\left(\frac{f_1}{r_{21}r_{31}}+\frac{f_2}{r_{21}r_{32}}+\frac{f_3}{r_{31}r_{23}}\right)\left(f_1+\frac{f_2}{r_{12}}+\frac{f_3}{r_{13}}\right)+f_2\left(\frac{f_1}{r_{12}r_{31}}+\frac{f_2}{r_{21}r_{32}}+\frac{f_3}{r_{13}r_{32}}\right)\left(f_2+\frac{f_1}{r_{21}}+\frac{f_3}{r_{23}}\right)+f_3\left(\frac{f_1}{r_{13}r_{21}}+\frac{f_2}{r_{23}r_{12}}+\frac{f_3}{r_{13}r_{23}}\right)\left(f_3+\frac{f_1}{r_{31}}+\frac{f_2}{r_{32}}\right)} = 0 \quad (6.7)$$

This new formulation (equations (6.5) to (6.7)) is symmetrical and does not deal with ratios of different copolymer mole fractions (as F_i/F_j and F_i/F_k). Therefore, the model responses are direct measurements from the system and their error structures are not distorted by the use of mole fraction ratios. One only needs to select any two mole fractions out of F_1, F_2, and F_3, as responses for the parameter estimation problem, and due to the symmetrical nature of this model (unlike the original AG model), the results are consistent regardless of the selection. This approach also extends directly to usage of a cumulative model and including both composition and conversion values in the procedure of finding more reliable ternary reactivity ratios (section 6.3.3). Of course, the new formulation is in agreement with the AG model, in terms of predictions, once the six reactivity ratios are known and fixed. An example of their agreement is shown in Figure 6-1. This figure illustrates composition versus conversion trajectories calculated by the AG model (equations (6.1) to (6.3)) and the recast model (equations (6.5) to (6.7)); the trajectories are identical.

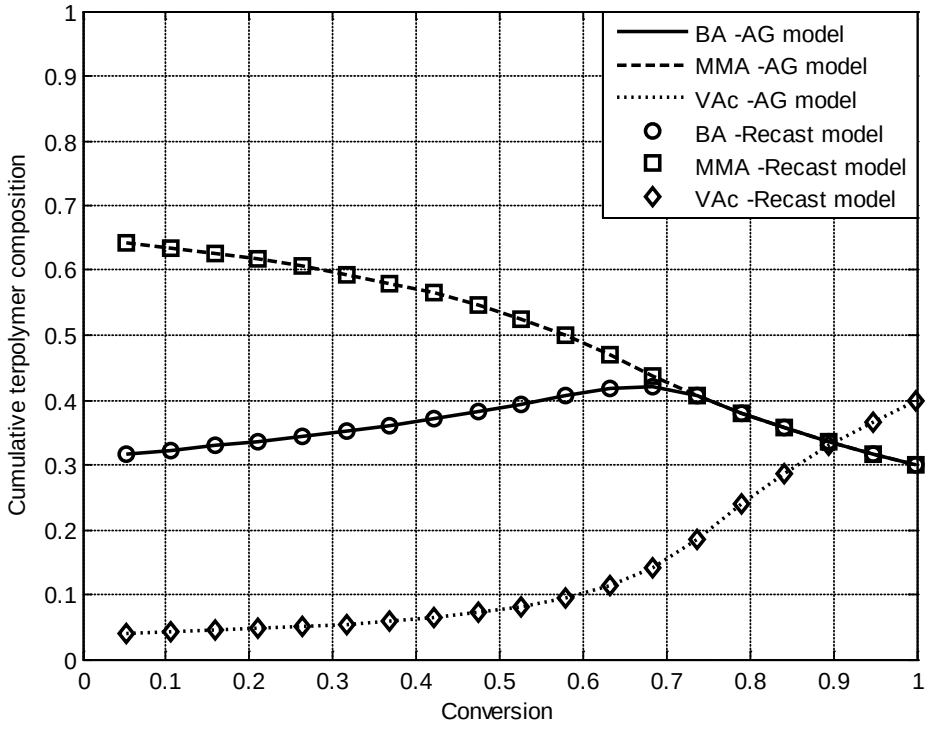

Figure 6-1. Composition versus conversion trajectory comparison between the AG model and the recast model; Butyl acrylate/Methyl methacrylate/Vinyl acetate terpolymerization; initial feed composition: 0.3/0.3/0.4; r_{12}=0.298, r_{21}=1.789, r_{13}=5.939, r_{31}=0.0262, r_{23}=24.025, and r_{32}=0.0261; Dubé and Penlidis (1995b)

6.3.2 EVM estimation

As it has been shown in the previous chapters, EVM is the perfect method for estimating reactivity ratios in multicomponent polymerizations. The preliminary attempt for showing the application of the EVM algorithm for estimating ternary reactivity ratios using the original form of the instantaneous AG model was shown in Duever et al. (1983). The performance of these works along with several other case studies was shown in Kazemi (2010). These sources point towards potential problems in the results attributed to the structure of the AG model and also the lack of adequate information in the terpolymerization literature. In this chapter, the EVM procedure has been modified in several parts based on the computational requirements of the ternary problem and the problematic nature of the original form of the AG model. In the following, the application of the EVM algorithm on the ternary

reactivity ratio estimation problem is shown in terms of the key equations (more explanations about the EVM algorithm can be found in Chapter 2, section 2.3). Extensive details about the particular ternary case are given later in the results and discussion section.

As shown in Chapter 2, equation (2.34), the first statement of EVM relates the measurement values to their true values. For composition data, this relation is assumed to be relative (multiplicative, see equation (2.38)), shown by equation (6.8) for the feed composition (for f_1, f_2, and f_3), and equation (6.9) for the terpolymer composition (F_1, F_2, and F_3). An asterisk denotes true values and ε is the error term. For the purpose of ternary reactivity ratio estimation, equations (6.10) to (6.13) represent an example of the instantaneous ternary model that the EVM program works with. Among the true values of terpolymer and feed mole fractions, there are two linear relations as shown in equations (6.12) and (6.13). Given these two relations, any two of the mole fractions along with the linear relations can represent the terpolymerization model.

$$\ln(f_i) = \ln(f_i^*) + \varepsilon_{f_i} \qquad \text{where i=1, 2, and 3} \tag{6.8}$$

$$\ln(F_i) = \ln(F_i^*) + \varepsilon_{F_i} \qquad \text{where i=1, 2, and 3} \tag{6.9}$$

$$\underline{g}_1\left(\underline{\xi}, \underline{\theta}^*\right) = {F_1}^* - \frac{{f_1}^*\left(\frac{{f_1}^*}{{r_{21}}^* {r_{31}}^*} + \frac{{f_2}^*}{{r_{21}}^* {r_{32}}^*} + \frac{{f_3}^*}{{r_{13}}^* {r_{32}}^*}\right)\left({f_1}^* + \frac{{f_2}^*}{{r_{21}}^*} + \frac{{f_3}^*}{{r_{13}}^*}\right)}{{f_1}^*\left(\frac{{f_1}^*}{{r_{12}}^* {r_{31}}^*} + \frac{{f_2}^*}{{r_{21}}^* {r_{32}}^*} + \frac{{f_3}^*}{{r_{31}}^* {r_{23}}^*}\right)\left({f_1}^* + \frac{{f_2}^*}{{r_{12}}^*} + \frac{{f_3}^*}{{r_{13}}^*}\right) + {f_2}^*\left(\frac{{f_1}^*}{{r_{12}}^* {r_{31}}^*} + \frac{{f_2}^*}{{r_{21}}^* {r_{32}}^*} + \frac{{f_3}^*}{{r_{13}}^* {r_{32}}^*}\right)\left({f_2}^* + \frac{{f_1}^*}{{r_{21}}^*} + \frac{{f_3}^*}{{r_{23}}^*}\right) + {f_3}^*\left(\frac{{f_1}^*}{{r_{13}}^* {r_{21}}^*} + \frac{{f_2}^*}{{r_{23}}^* {r_{12}}^*} + \frac{{f_3}^*}{{r_{13}}^* {r_{23}}^*}\right)\left({f_3}^* + \frac{{f_1}^*}{{r_{31}}^*} + \frac{{f_2}^*}{{r_{32}}^*}\right)} \tag{6.10}$$

$$\underline{g}_2\left(\underline{\xi}, \underline{\theta}^*\right) = {F_2}^* - \frac{{f_2}^*\left(\frac{{f_1}^*}{{r_{12}}^* {r_{31}}^*} + \frac{{f_2}^*}{{r_{21}}^* {r_{32}}^*} + \frac{{f_3}^*}{{r_{13}}^* {r_{32}}^*}\right)\left({f_2}^* + \frac{{f_1}^*}{{r_{21}}^*} + \frac{{f_3}^*}{{r_{23}}^*}\right)}{{f_1}^*\left(\frac{{f_1}^*}{{r_{12}}^* {r_{31}}^*} + \frac{{f_2}^*}{{r_{21}}^* {r_{32}}^*} + \frac{{f_3}^*}{{r_{31}}^* {r_{23}}^*}\right)\left({f_1}^* + \frac{{f_2}^*}{{r_{12}}^*} + \frac{{f_3}^*}{{r_{13}}^*}\right) + {f_2}^*\left(\frac{{f_1}^*}{{r_{12}}^* {r_{31}}^*} + \frac{{f_2}^*}{{r_{21}}^* {r_{32}}^*} + \frac{{f_3}^*}{{r_{13}}^* {r_{32}}^*}\right)\left({f_2}^* + \frac{{f_1}^*}{{r_{21}}^*} + \frac{{f_3}^*}{{r_{23}}^*}\right) + {f_3}^*\left(\frac{{f_1}^*}{{r_{13}}^* {r_{21}}^*} + \frac{{f_2}^*}{{r_{23}}^* {r_{12}}^*} + \frac{{f_3}^*}{{r_{13}}^* {r_{23}}^*}\right)\left({f_3}^* + \frac{{f_1}^*}{{r_{31}}^*} + \frac{{f_2}^*}{{r_{32}}^*}\right)} \tag{6.11}$$

$$\underline{g}_3\left(\underline{\xi}, \underline{\theta}^*\right) = {F_1}^* + {F_2}^* + {F_3}^* - 1 \tag{6.12}$$

$$\underline{g}_4\left(\underline{\xi}, \underline{\theta}^*\right) = {f_1}^* + {f_2}^* + {f_3}^* - 1 \tag{6.13}$$

The EVM model needs derivatives of the $\underline{g}_i\left(\underline{\xi}, \underline{\theta}^*\right)$ functions with respect to the parameters (r_{12}, r_{13}, r_{21}, r_{23}, r_{31}, r_{32}) for the $\underline{Z}$ matrix (Chapter 2, equation (2.54)), which is a 4×6 matrix (4 equations and 6 parameters). Also, it need the derivative of the function with respect to the variables (f_1, f_2, f_3, F_1, F_2,

F_3) for the $\underline{B}$ matrix (Chapter 2, equation (2.46)), which is in this case, a 4×6 matrix (4 equations and 6 variables).

For the estimation of ternary reactivity ratios, the EVM structure can include all variables that are subject to error for the purpose of determining values for these parameters. As shown earlier, this multi-response problem has six variables that could be involved in the parameter estimation. That is, f_1, f_2, and f_3 for the mole fractions of the feed composition, and F_1, F_2, and F_3 for the mole fractions of the terpolymer composition. For these variables, we can consider three kinds of dependencies, commonly existing among variables of multi-response problems (Box et al. (1973)).

The first kind is the linear dependencies among true (expected) values of the mole fractions in the feed and terpolymer compositions. These dependencies, as shown earlier in equations (6.12) and (6.13), are stoichiometric, stating that the sum of mole fractions in the feed or in the terpolymer is always unity. In this case, data sets in which all these six variables are measured can be used. In fact, this type of data set is the most preferred one, because it contains more information about the system. The composition model handled by the EVM program should also be selected, and for the case where all six variables are available, we can choose any two out of three terpolymer mole fractions, shown in equations (6.5) to (6.7), along with the two mole fraction relations in equations (6.12) and (6.13).

The second kind of linear dependencies is among the measurements (observed data). This happens when the experimenter forces the stoichiometric relation between the mole fractions to become true for the observed mole fractions either by normalizing the mole fraction values or by measuring only two out of three mole fractions and calculating the third one based on the summation expression. If not all six variables are directly measured from the experiments, then only two out of three variables in both feed and terpolymer compositions are random variables and hence included in the EVM structure. The EVM model should again be selected according to the measured variables.

The third and last kind of dependencies is among the errors. This relation refers to the correlation among variables, which translates into the correlation among the error components in the variance-covariance matrix of measurements ($\underline{V}$). This $\underline{V}$ matrix, as shown previously in equation (2.44), consists of variances and covariances of the variables involved. The dimensions of this matrix are also defined by the number of variables involved in the EVM structure. For the case where all six variables (i.e., all six mole fractions) are available, the $\underline{V}$ matrix can be constructed as shown in equation (6.14).

Since the feed composition mole fractions are usually obtained by gravimetery, the measurements are independent. Therefore, in the $\underline{V}$ matrix, we have $\sigma_{f_i}^2$ as the diagonal elements (i.e., variances of f_i), yet the off-diagonal elements (i.e., covariances among the measured f_i's) are all zero. On the other hand, for the mole fractions of the terpolymer composition, every two out of three terms are correlated. The reason is that all these mole fractions (F_i's) are obtained from one instrument (e.g., via NMR) and therefore, they are not independent. In this work, to describe these covariances, we use equation (6.15), which employs the correlation coefficient factor (ρ) to determine the magnitude and direction of the correlations among each two variables. In a way analogous to equation (6.14), if there are only 4 random variables in the system, i.e., for instance, if only f_1, f_2, F_1, and F_2 are measured and hence available, then the $\underline{V}$ matrix can be given by equation (6.16).

$$\underline{V} = \begin{bmatrix} \sigma_{f_1}^2 & 0 & 0 & 0 & 0 & 0 \\ 0 & \sigma_{f_2}^2 & 0 & 0 & 0 & 0 \\ 0 & 0 & \sigma_{f_3}^2 & 0 & 0 & 0 \\ 0 & 0 & 0 & \sigma_{F_1}^2 & \sigma_{F_1F_2}^2 & \sigma_{F_1F3}^2 \\ 0 & 0 & 0 & \sigma_{F_1F_2}^2 & \sigma_{F_2}^2 & \sigma_{F_2F_3}^2 \\ 0 & 0 & 0 & \sigma_{F_1F3}^2 & \sigma_{F_2F_3}^2 & \sigma_{F_3}^2 \end{bmatrix} \tag{6.14}$$

$$\sigma_{F_iF_j}^2 = \rho * \sqrt{\sigma_{F_i}^2 * \sigma_{F_j}^2} \tag{6.15}$$

$$\underline{V} = \begin{bmatrix} \sigma_{f_1}^2 & 0 & 0 & 0 \\ 0 & \sigma_{f_2}^2 & 0 & 0 \\ 0 & 0 & \sigma_{F_1}^2 & \sigma_{F_1F_2}^2 \\ 0 & 0 & \sigma_{F_1F_2}^2 & \sigma_{F_2}^2 \end{bmatrix} \tag{6.16}$$

As discussed in Chapter 2 for elements of the $\underline{V}$ matrix, as well as, in Chapter 3 regarding the error levels of composition data in copolymerizations, in order to calculate the variances of each measurement/variable, data from extensive and independently replicated experiments must be collected. In the absence of an extensive database, one can resort to "expert" opinions about the amount of expected error in certain measurements, with the recognition that the quality of information in this case is of a lower grade than in the former case. Relating now the elements of the $\underline{V}$ matrix in equation (6.14) or (6.16), the variances of these measurements ($\sigma_{f_i}^2$ and $\sigma_{F_i}^2$) can be expressed based

on the variability in the data reflected by the constant multiplier k which has common values of ±1% for feed and ±5% for terpolymer compositions (i.e., $\sigma_{f_i}^2 = \frac{k_{f_i}^2}{3}$ and $\sigma_{F_i}^2 = \frac{k_{F_i}^2}{3}$) .

The original EVM algorithm (Reilly and Patino-Leal (1981)) uses a quasi-Newton optimization algorithm that works very effectively only in the vicinity of the given initial guesses (working perfectly for the copolymerization reactivity ratio estimation problem). In the ternary problem, the size of the variable space and the number of parameters are greater than binary problem, and in turn, the magnitude of this search problem increases and several difficulties can arise in the process of locating the parameter estimates. We have modified the EVM procedure by using a global optimization algorithm, called the Shuffled Complex Evolutionary (SCE) algorithm, introduced briefly in Chapter 2, section 2.3.5.2. Moreover, for the evaluation of the parameter estimation results, a joint confidence region (JCR) should be presented that quantifies and visualizes the measure of uncertainty in the estimated parameters by presenting a contour/JCR (see Chapter 2, section 2.3.4). Values of the parameters inside or on the contour represent plausible values of the parameters at the specified confidence level, and the smaller the JCR the higher the precision of the results.

6.3.3 From low conversion to high conversion

One of the major limitations in reactivity ratio estimation studies, for both binary and ternary systems, in the literature has been about using the instantaneous composition model. In order to use the instantaneous model, the experimental data must be collected at very low conversion levels (less than 5%), based on the assumption that up to such a conversion level, the compositional drift of the system is negligible; therefore, the cumulative composition that is being measured is actually equal to its instantaneous value (F_1 instead of $\bar{F}_1$) and the initial feed compositions have remained the same (f_{10} instead of f_1). These assumptions may not hold for many cases and thus using low conversion data introduces immediately experimental error and hence becomes a source of bias in reactivity ratio estimates. In addition, the error during low conversion experimental procedures is accentuated. Chapter 3 discusses the potential problems with this approach for copolymerization systems and establishes an alternative procedure for estimation of reactivity ratios based on full conversion experimental data.

The AG ternary model (equations (6.1) to (6.3)) is originally in differential equation form, where df_i is substituted with F_i, assuming that we can collect F_i at low conversion levels. This assumption is despite the fact that most of the reactions are run up to higher conversion levels, and all this valuable information is usually discarded simply because the estimation approach/model cannot incorporate this into the analysis. Even though using higher conversion level data for estimating binary reactivity ratios has gained more attention in the literature these days, there has been no attempt at estimating ternary reactivity ratios using the cumulative ternary composition model. Therefore, a necessary extension to our approach for estimating ternary reactivity ratios is to include the full conversion trajectory into our program.

Our approach for this problem is exactly the same as the one for copolymerization systems (as shown in Chapter 3, section 3.2.3). The EVM model, in this case consists of equations that relate cumulative terpolymer composition for each monomer ($\bar{F}_i$) to the mole fraction of unreacted monomer (f_i) in the polymerizing mixture and molar conversion, X_n. This relation is the so-called Skeist equation given by equation (6.17), where f_{i0} and f_i are mole fractions of monomer i (i=1, 2, and 3 for three monomers) in the initial and remaining mixtures, and F_i and $\bar{F}_i$ are instantaneous and cumulative compositions (X_n can be related to X_w, as shown in equation (2.13)). As the reaction proceeds with time, X_n changes, and f_i is evaluated by the numerical solution of the differential copolymer composition equation, given by equation (6.18), given the initial conditions of $f_i=f_{i0}$ when $X_n=0$. The set of differential equations for all three unreacted monomer compositions f_1, f_2, and f_3 versus conversion (X_n) is being integrated over the course of conversion. The unreacted monomer mixture composition, f_i, is then used in equation (6.17) to evaluate the corresponding cumulative copolymer compositions, $\bar{F}_1$, $\bar{F}_2$, and $\bar{F}_3$. The expanded versions of these equations are given in Chapter 2, section 2.1.2.2.

$$\underline{g}\left(\underline{\xi}, \underline{\theta}^*\right) = \bar{F}_i^* - \frac{f_{i0} - f_i(1 - X_n)}{X_n} \qquad \textit{for i=1, 2, and 3} \tag{6.17}$$

$$\frac{df_i}{dX_n} = \frac{f_i - F_i}{1 - X_n} \qquad \textit{for i=1, 2, and 3} \tag{6.18}$$

The EVM variables for this model are $\overline{F}_1$, $\overline{F}_2$, and $\overline{F}_3$. The elements of the $\underline{Z}_{(3 \times 6)}$ matrix for the EVM algorithm with this model cannot be calculated explicitly. Therefore, the elements of the $\underline{Z}$ matrix are worked out using equations (6.19), in which the values of Δr_{ij} are chosen to be reasonably small. In an analogous way, the elements of the $\underline{B}_{(3 \times 3)}$ matrix are calculated as shown in equation (6.20).

$$\frac{\partial \underline{g}\left(\underline{\xi},\underline{\theta}\right)}{\partial r_{ij}} = \frac{\underline{g}\left(\underline{\xi},\, r_{ij}+\Delta r_{ij},\, r_{ik},\, r_{kj},\, r_{ki},\, r_{ji},\, r_{jk}\right)}{\Delta\, r_{ij}} \tag{6.19}$$

$$\frac{\partial \underline{g}\left(\underline{\xi},\underline{\theta}\right)}{\partial \ln(\overline{F}_i)} = \overline{F}_i \tag{6.20}$$

A similar structure, as per equation (6.14), is used for the variance-covariance matrix for this model, as well. The variance-covariance matrix is a 3×3 matrix, reflecting the error in the cumulative copolymer composition, $\overline{F}_i$. The value of *k*, as mentioned for the other two models, is usually ±5%, and in case of dealing with an unreliable data source, it can be increased to ±10% or even higher.

Using the DNI approach and medium and high conversion data points for estimating reactivity ratios can significantly improve the quality of the results by (simply) including more information in the analysis as well as avoiding (practical) limitations of collecting low conversion data (with their inherent sources of errors). This extension completes our approach for estimating ternary reactivity ratios directly based on terpolymerization experimental data. By using the EVM method, we utilize the most statistically appropriate parameter estimation technique for this problem and by implementing the DNI approach we use all the available information in the system for the determination of its parameters. Therefore, the results can be considered to be the most reliable ones in the literature to date.

6.4 Results and Discussion

6.4.1 Overview of case studies

In order to compare our work with prior information, we first looked into the literature for existing terpolymerization experimental publications with reactivity ratio estimation studies. In all these publications, almost with no exception, binary reactivity ratios were estimated (as per normal practice) with classical linear/nonlinear approaches. A condensed summary of our literature review is compiled in Table 6-1, where these reactivity ratios are shown for each system with labels of ‘binary’ (B) or ‘ternary’ (T). Additional explanations for the entries of Table 6-1 are given at the bottom of the table. In our work, these published terpolymerization systems were analyzed and ternary reactivity ratios were estimated using our approach with the instantaneous ternary model and the EVM

methodology. These reactivity ratios are presented in Table 6-1 for each system as well. For the publications where the conversion values were provided, the cumulative model was also used to determine reactivity ratios, and these values are also listed in Table 6-1.

Several important points can now be made concerning our observations, based on our estimation results, as summarized in Table 6-1.

- ✓ Our methodology does not use approximate binary reactivity ratios when ternary data are directly available.
- ✓ The methodology is not restricted to any simplifying assumptions regarding the error structure.
- ✓ The approach can apply to any terpolymer data set at any conversion level.
- ✓ Overall, the methodology provides reliable reactivity ratios, as will be shown in more detail with the case studies that follow.
- ✓ Ternary reactivity ratios differ from binary ones; differences ranging from slight to considerable have been observed, depending on the values of the reactivity ratios.
- ✓ The basic premise of our investigations, based on the case studies that follow, is that use of binary reactivity ratios may reduce the reliability of terpolymerization model predictions.

In the three subsections that follow, we concentrate on specific cases (examples and counter-examples) and offer more information about different aspects of our investigations. The first subsection evaluates the performance of our approach while pointing out differences with earlier and alternative methodologies. Also, within the context of these results, we focus on the error structure of the measurements that mimics real experimental settings. The second subsection is about using the DNI approach and higher conversion values for estimation of ternary reactivity ratios. Finally, the third and last subsections show how our results can be evaluated and provides justifications as to why binary reactivity ratios should not be used in terpolymerization system studies.

Table 6-1. Values of reactivity ratios estimated based on terpolymerization experimental data

	M_1[a]	M_2[a]	M_3[a]	Type[b]	Model[c]	Source[d]	r_{12}	r_{21}	r_{13}	r_{31}	r_{23}	r_{32}
1	Maleic anhydride	Acrylonitrile	Styrene	T	Inst.	EVM	2.40	0.40	0.07	0.05	0.14	0.58
				B	Inst.	Kressler et al. (1987)	0.001	6.00	0.001	0.04	0.04	0.41
2	Indene	Methyl methacrylate	Acrylonitrile	T	Inst.	EVM	0.001	0.40	0.001	2.87	0.24	0.99
				B	Inst.	Naguib et al. (2009)	0.03	0.40	0.02	3.82	0.15	1.20
3	Ethyl methacrylate	Phenylmaleimide	Itaconic acid	T	Inst.	EVM	0.33	0.43	3.48	0.21	0.08	1.83
				B	Inst.	Naguib et al. (2003)	0.37	0.11	2.12	0.59	0.08	1.08
4	Acrylonitrile	Styrene	Dibromopropyl acrylate	T	Inst.	EVM	0.19	0.23	0.99	1.98	0.39	0.16
				B	Inst.	Saric et al (1983)	0.16	0.3	0.87	0.75	0.41	0.22
5	DMAEM[e]	Methyl methacrylate	Dodecyl methacrylate	T	Inst.	EVM	0.80	0.75	0.80	0.80	1.09	1.20
				T	Cum.	EVM	0.80	0.75	0.80	0.80	1.09	1.20
				B	Inst.	Soljic et al. (2010)	0.85	0.86	0.79	0.75	1.12	1.19
6	DMAEM	Styrene	Dodecyl methacrylate	T	Inst.	EVM	0.45	1.50	0.78	1.06	3.07	0.55
				T	Cum.	EVM	0.43	1.50	0.77	1.06	3.07	0.55
				B	Inst.	Soljic et al. (2010)	0.43	1.79	0.79	0.75	2.19	0.45
7	Leucine-NCA[f]	β-benzyl aspartate-NCA	Valine-NCA	T	Inst.	EVM	0.45	1.65	1.03	0.72	3.12	0.41
				B	Inst.	Wamsley et al. (2004)	0.40	1.46	1.37	0.55	2.34	0.34
8	Acrylonitrile	Styrene	Methyl methacrylate	T	Inst.	EVM	0.07	0.29	0.20	1.32	0.57	0.55
				B	Inst.	Brar and Hekmatyar (1999)	0.04	0.31	0.17	1.45	0.47	0.52
9	Ethylene (P=1900,T=180)[g]	Methyl acrylate	Vinyl acetate	T	Inst.	EVM	0.05	2.29	0.90	0.82	3.34	0.35
				T	Inst.	Luft et al. (1993)	0.05	2.07	0.89	0.92	3.23	0.39
10	Ethylene (P=1100,T=180)	Methyl acrylate	Vinyl acetate	T	Inst.	EVM	0.05	3.67	0.73	0.90	3.47	0.08
				T	Inst.	Luft et al. (1993)	0.09	2.01	0.92	0.78	3.89	0.24
11	Ethylene (P=1100,T=230)	Methyl acrylate	Vinyl acetate	T	Inst.	EVM	0.09	2.44	0.95	0.64	4.00	0.12
				T	Inst.	Luft et al. (1993)	0.05	3.34	0.71	0.79	3.25	0.07
12	Methyl methacrylate	NPGMA[h]	HEMA[i]	T	Inst.	EVM	1.05	1.16	1.07	1.86	0.93	1.31
				T	Inst.	Iglesias et al. (1996)	1.03	1.55	1.00	1.19	0.88	1.25
				B	Inst.	Iglesias et al. (1996)	0.94	1.00	0.60	0.77	0.98	1.40

13	Fumaronitirle	Dodecyl vinyl ether	β-Chloroethyl acrylate	T	Inst.	EVM	0.009	0.001	0.043	7.03	0.006	0.134
				B	Inst.	Iwarsuki et al. (1967)	0.019	0.004	0.11	10.2	0.013	1.97
14	Methacylonitrile	Styrene	α-Methylstyrene	T	Inst.	EVM	0.44	0.37	0.39	0.55	1.12	0.64
				B	Inst.	Rudin et al. (1972)	0.44	0.37	0.38	0.53	1.12	0.63
15	Styrene	Acrylonitrile	Methyl methacrylate	T	Inst.	EVM	0.42	0.02	0.65	0.61	0.07	0.98
				B	Inst.	Steinfatt and Schmidt-Naake (2001)	0.41	0.04	0.64	0.55	0.16	1.24
16	Maleic anhydride	Methyl methacrylate	Styrene	T	Inst.	EVM	0.001	7.04	0.001	0.41	0.40	3.52
				B	Inst.	Kysela and Staudner (1992)	0.046	3.496	0.064	0.078	0.530	0.534

a) M_1, M_2 and M_3 denote the three monomers in each terpolymerization system.
b) Type indicates whether reactivity ratios are obtained from terpolymerization (ternary) data, denoted as "T", or from (binary) copolymerization data, denoted as "B".
c) Model refers to the terpolymerization model used for parameter estimation; "Inst." and "Cum." stand for instantaneous and cumulative models, respectively.
d) Source indicates whether the results are obtained in the current work, denoted by "EVM", or reported in the reference articles, denoted by reference.
e) DMAEM: N,N- dimethylaminoethyl methacrylate.
f) NCA: N-carboxyanhydride.
g) Operating conditions are given as degrees Celsius and atm.
h) NPGMA: 3-hydroxyneopentyl methacrylate.
i) HEMA: 2-hydroxyethyl methacrylate.

6.4.2 Old pitfalls versus the correct approach for estimating ternary reactivity ratios

As mentioned earlier, published experimental data in the literature are not usually accompanied by adequate information about measuring procedures and therefore it is not possible for such cases to decide whether six variables are indeed directly measured or only two. Based on existing information in the literature, it seems more likely that either only two out of three compositions are measured and/or the mole fraction data are normalized after the fact by imposing that the summation of all three mole fractions is unity. Therefore, our goal in this section is to illustrate the performance of EVM with a certain representative system with typically available information. For this system, we want to point out some of the problems with the original AG model and also advantages and disadvantages of having six or four independently measured variables in the ternary problem.

The terpolymerization system of N, N-dimethylaminoethyl methacrylate (DMAEM, M_1), methyl methacrylate (MMA, M_2), and dodecyl methacrylate (DDMA, M_3) was investigated by Soljic et al. (2010). Terpolymerizations were performed at isothermal conditions at low conversion levels, in toluene solution. Experimental and calculated data sets are shown in Table 6-2. The authors used binary reactivity ratios that were estimated based on copolymerization data from separate binary copolymerization trials (i.e., DMAEM/MMA, DDMA/MMA, and DMAEMA/DDMA) (Soljic et al. (2009) and (2010)). Those reactivity ratio estimates were averaged between estimates from both linear and nonlinear regression. These values are cited in Table 6-1 as binary reactivity ratios. For this system, we used the terpolymerization experimental data to estimate ternary reactivity ratios with ***(1)*** the original AG model in all possible combinations (equations (6.1) to (6.3)), ***(2)*** the recast terpolymer composition model with six variables (equations (6.10) to (6.13)), ***(3)*** the recast terpolymer composition model with four variables (only, equations (6.10) and (6.11)), and ***(4)*** different amounts of correlation between the terpolymer composition mole fractions.

The representative reactivity ratio estimates for this system, cited in the 5^{th} row of Table 6-1, were obtained from case (2).

Table 6-2. Terpolymerization data for DMAEM (M_1)/MMA (M_2)/DDMA (M_3), Soljic et al. (2010)

Feed composition			Experimental terpolymer composition			Calculated terpolymer composition, reference			Calculated terpolymer composition, current work		
M_1	M_2	M_3	M_1	M_2	M_3	M_1	M_2	M_3	M_1	M_2	M_3
0.100	0.100	0.800	0.114	0.084	0.802	0.126	0.086	0.788	0.120	0.087	0.793
0.100	0.400	0.500	0.125	0.381	0.494	0.128	0.377	0.495	0.126	0.376	0.498
0.100	0.700	0.200	0.128	0.690	0.182	0.125	0.686	0.189	0.126	0.683	0.191
0.200	0.200	0.600	0.243	0.118	0.569	0.237	0.179	0.584	0.230	0.181	0.589
0.200	0.500	0.300	0.237	0.476	0.287	0.236	0.476	0.288	0.236	0.475	0.289
0.400	0.100	0.500	0.422	0.090	0.488	0.424	0.089	0.487	0.416	0.092	0.492
0.400	0.400	0.200	0.423	0.378	0.199	0.425	0.381	0.194	0.424	0.384	0.192
0.600	0.200	0.200	0.599	0.195	0.206	0.600	0.196	0.204	0.597	0.200	0.203
0.800	0.100	0.100	0.310	0.118	0.099	0.782	0.106	0.110	0.781	0.110	0.109

In the first part of the analysis (case (1)), we used the EVM method with the three combinations of the AG model, meaning that the model was described as the ratios of (F_2/F_1 and F_3/F_1), (F_1/F_3 and F_2/F_3), and (F_1/F_2 and F_2/F_3). The results from parameter estimation for the reactivity ratio pairs of (r_{12} and r_{21}), (r_{13} and r_{31}), and (r_{23} and r_{32}) along with their corresponding joint confidence regions (JCRs) are shown in Figures 6-2 to 6-4, respectively. In these figures, the line styles ——, - - - -, and -.-.-.- refer to different combinations of (F_2/F_1 and F_3/F_1), (F_1/F_3 and F_2/F_3), and (F_1/F_2 and F_2/F_3), respectively. Also, the reported values of reactivity ratios by Soljic et al. (2010) and the EVM point estimates are shown in these figures with "o" and "x", respectively.

As can be seen in Figures 6-2 to 6-4, the EVM point estimates are always the same regardless of the AG model combinations, as all these point estimates overlap at a single point. However, the visualization of the JCRs in these figures illustrates how the choice of different combinations in the AG model (e.g., (F_2/F_1 and F_3/F_1) versus (F_1/F_2 and F_2/F_3)) affects the precision of these results. In particular for this system, it can be seen that the (F_2/F_1 and F_3/F_1) combination gives the smallest JCRs for all three pairs of reactivity ratios (see Figures 6-2 to 6-4); meanwhile, for the (r_{13}, r_{31}) and (r_{23}, r_{32}) pairs of reactivity ratios (Figures 6-3 and 6-4), the (F_1/F_3 and F_2/F_3) combination results in JCRs crossing inside the negative region. The changes in the level of uncertainty in our parameter estimation results, when one combination is taken into account versus another, are affected either by

the choice of the specific combination or by experimental error associated to the data. Hence, these observations indicate that the estimation results from the AG model are very much combination-specific and should be used with great caution.

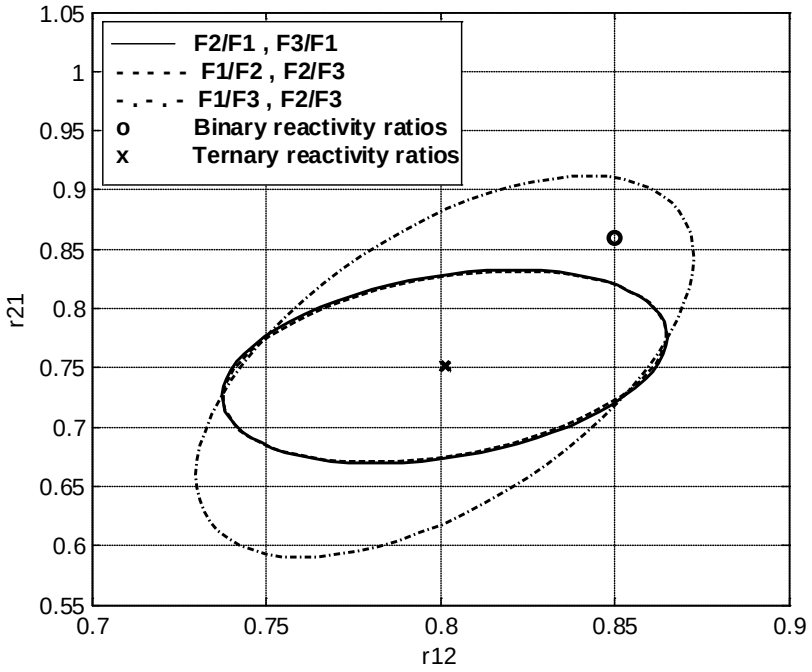

Figure 6-2. r_{12} and r_{21} estimation results for different combinations of the AG model

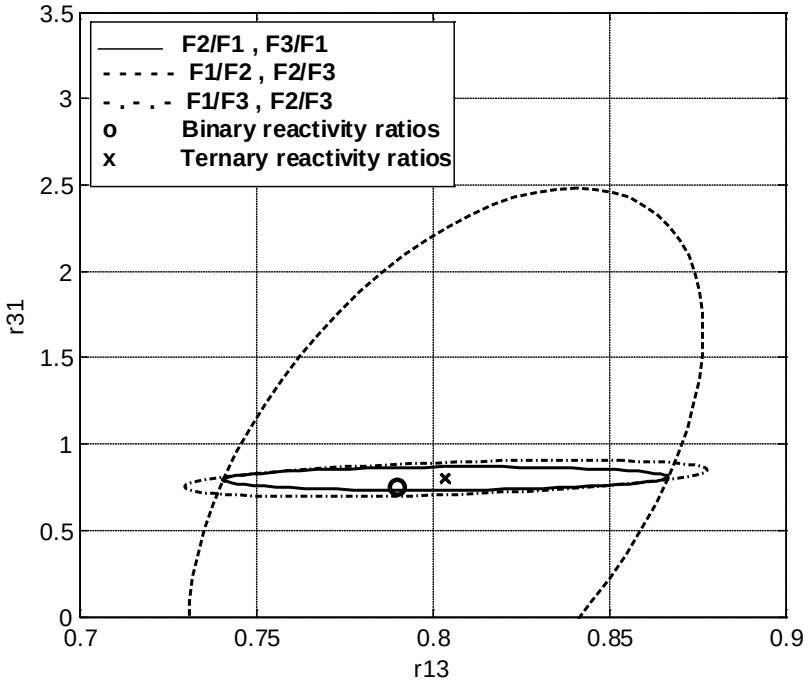

Figure 6-3. r_{13} and r_{31} estimation results for different combinations of the AG model

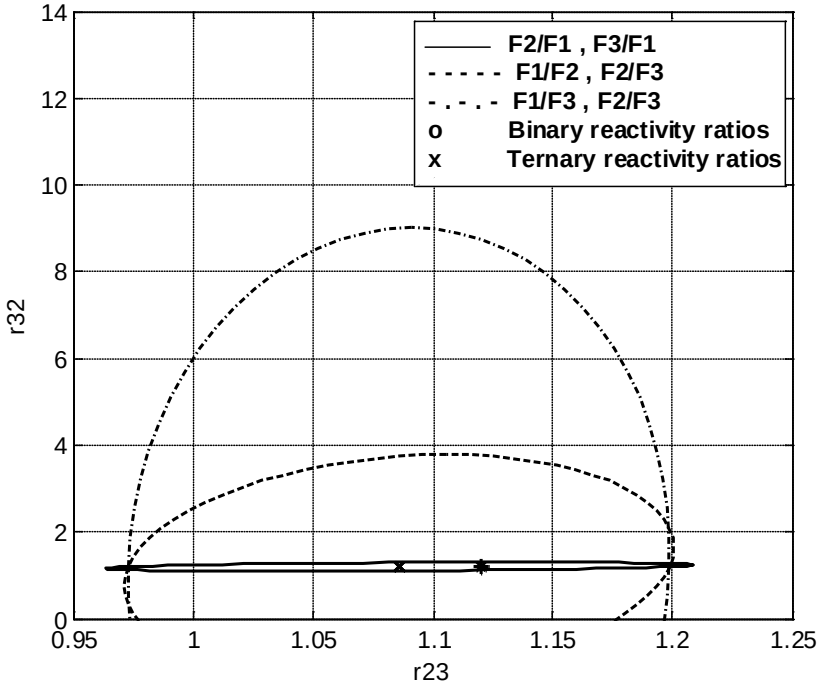

Figure 6-4. r_{23} and r_{32} estimation results for different combinations of the AG model

In the second step of the analysis, we used the recast expression of the terpolymer composition model (equations (6.10)-(6.13)) to estimate ternary reactivity ratios for this terpolymerization system based on the same data as before (see Table 6-2). For this procedure, the most general scenario is selected first, with six variables (all three composition mole fractions are considered as measured in both feed and terpolymer) and no correlation between any of the measurements. The $\underline{\underline{V}}$ matrix in this case would be similar to equation (6.14) for the diagonal elements (variances), whereas the off-diagonal elements (covariances) are all zero. The results from parameter estimation are shown in Figure 6-5, where all six reactivity ratios are shown in pairs with their JCRs. This figure shows that for all three pairs of reactivity ratios, we have reasonable JCRs indicating that these reactivity ratio estimates have acceptable level of precision.

The symmetrical nature of the recast form of the composition model allows us to choose any two responses out of three without affecting the results. The same results were obtained for all combinations of (F_1, F_2, and F_3) in pairs. The point estimates of Figure 6-5 are the ones cited in Table 6-1. Figure 6-5 also shows the reported binary reactivity ratios in the reference paper and it can be seen (almost) all of those estimates are included inside the EVM JCRs. The results from this estimation represent a “best case” scenario, since ternary reactivity ratios are in good agreement with their respected binary values. This is not necessarily the case for many other terpolymerization systems, as is evident from Table 6-1.

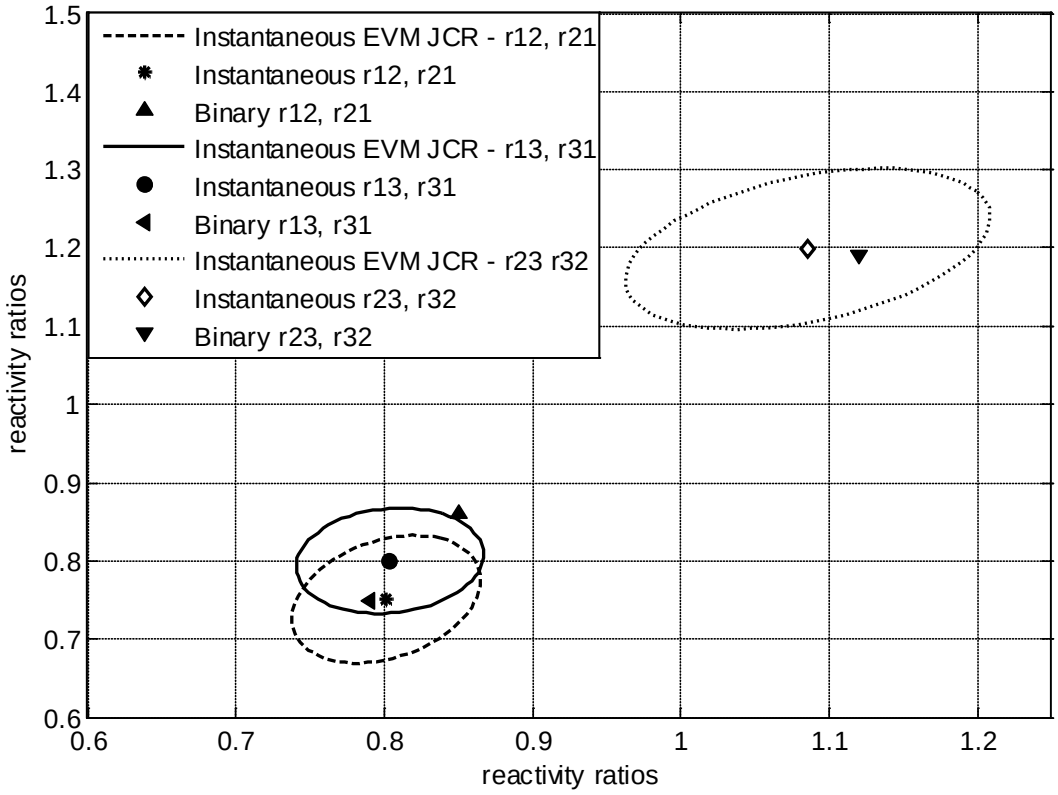

Figure 6-5. Reactivity ratio estimates and JCRs based on the recast composition model with six variables

In the third step of the analysis of DMAEM/MMA/DDMA, a different number of measured variables was chosen (four in this case) for the EVM parameter estimation problem (e.g., f_1, f_2, F_1, and F_2). Figures 6-6 to 6-8 show the results for the reactivity ratios pairs of (r_{12} and r_{21}), (r_{13} and r_{31}), and (r_{23} and r_{32}). For each pair of reactivity ratios (e.g., (r_{12} and r_{21}) in Figure 5), the line styles ——, - - - -, and -.-.-.- represent the JCRs of the cases where (F_1 and F_3), (F_2 and F_3), and (F_1 and F_2) are selected as the measured responses (and hence, as the EVM variables). Their corresponding point estimates are shown as an open circle, 'o', in the center of each JCR. In addition to these results, the reactivity ratio estimates and their JCRs from case (2) (the "best case" scenario) for (r_{12} and r_{21}), (r_{13} and r_{31}), and (r_{23} and r_{32}) are included in Figures 6-6 to 6-8, respectively. For example, in Figure 6-6, this JCR is shown with line style –x-x-x and the corresponding point estimates are indicated with an open square, '□', in the center of the JCR. This formatting is used in Figures 6-7 and 6-8 as well. The

binary reactivity ratios from the reference paper are also included in Figures 6-6 to 6-8 for each reactivity ratio pair, denoted with a filled star, '★'.

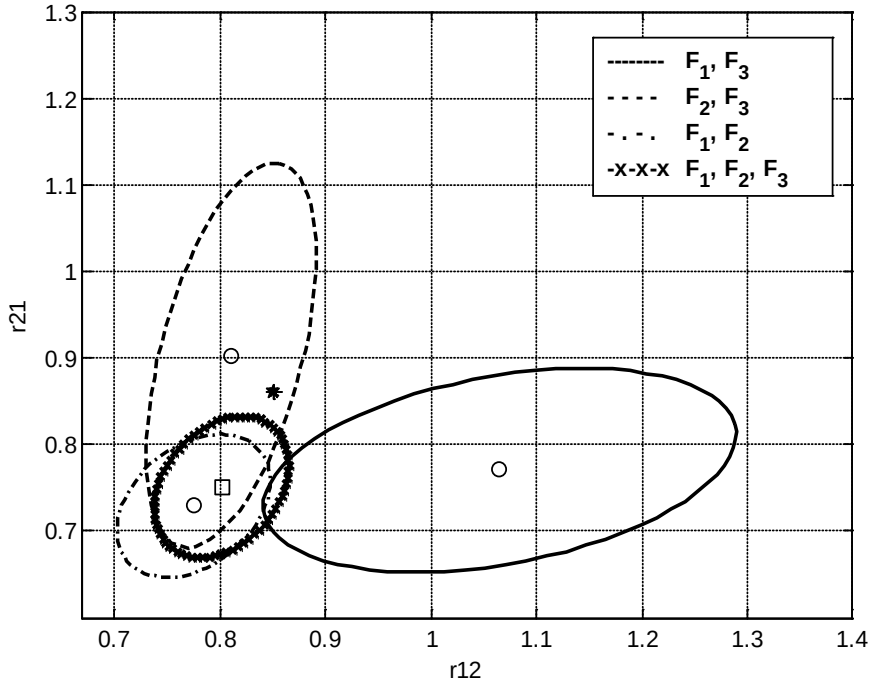

Figure 6-6. r_{12} and r_{21} estimates for the recast composition model with four variables

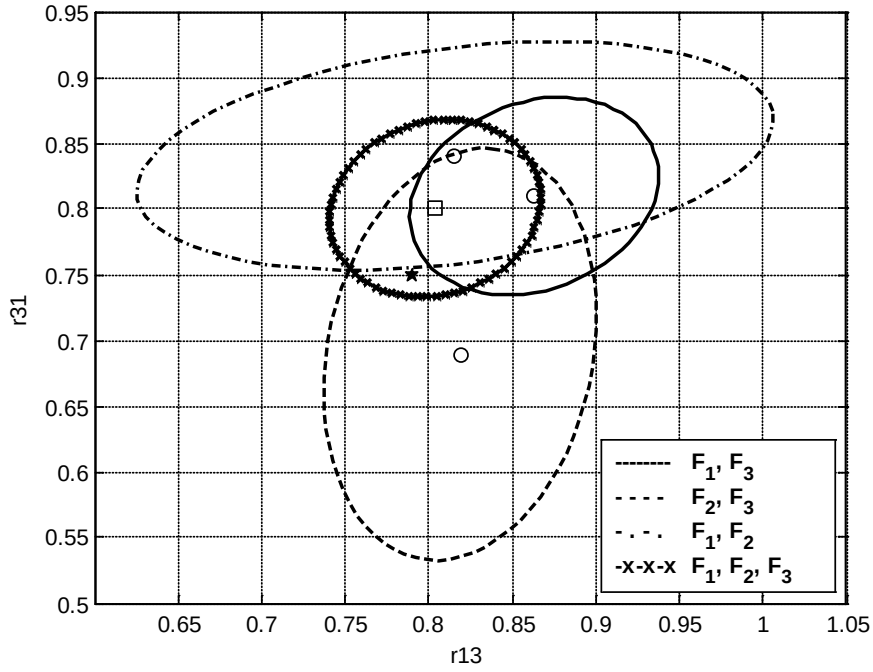

Figure 6-7. r_{13} and r_{31} estimates for the recast composition model with four variables

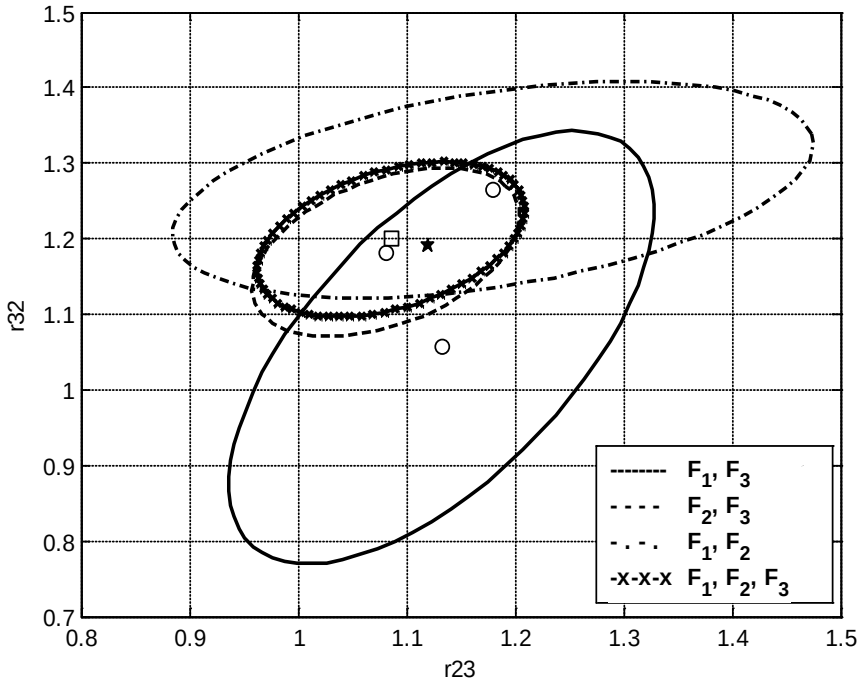

Figure 6-8. r_{23} and r_{32} estimates for the recast composition model with four variables

Figures 6-6 to 6-8 clearly show that not only can the point estimates shift with the choice of variables, but also the sizes of the obtained JCRs change considerably. Finding reliable results within this approach needs more information about the measurement procedure, indicating which one of the mole fractions in the feed and terpolymer compositions are actually measured. Those measured responses can then be chosen as the EVM variables, and the reactivity ratio estimation results mimic the real nature of the measurements and offer, in turn, an acceptable level of reliability. In the absence of such information, a pair of mole fractions in the feed and terpolymer compositions should be selected randomly and, therefore, the results may not be truly representative. For instance, since there is no such information available for the ternary system in question, any of the (F_1 and F_3), (F_2 and F_3), and (F_2 and F_3) JCRs for the (r_{12} and r_{21}) pair in Figure 6-6 can be selected at random. Obviously, this arbitrary choice may lead to a non-representative set of reactivity ratios for this ternary system. Comparing these results with the case where all six variables were involved, it can be suggested that having all six variables measured would provide much more reliable values for the reactivity ratios, since results are consistent and with an acceptable level of precision, as can be seen in Figure 6-5.

So far in the analysis, all measurements were treated as uncorrelated. The last part of the analysis is about the correct error structure, specifically the correlation between the measurements. The effect of different correlations is tested by using different correlation coefficients between the measurements coming from NMR (i.e., different values for the correlation coefficient, ρ, in equation (6.15)). The terpolymer composition mole fractions measured from NMR can be assumed to be negatively correlated, as these mole fractions sum up to one and if one of them increases, the other two mole fractions should decrease. Results from the EVM program were obtained with correlation coefficients of -0.2 and -0.4, and also with 0.2 and 0.4, to see the effect of change in the direction of the correlation. The reactivity ratio estimates for these cases are shown in Table 6-3, along with the correlation coefficient of zero (middle column), which acts as our standard case. Although the true value of the correlation is unknown, the results in Table 6-3 clearly show that by changing the amount of correlation from -0.4 to 0.4, the change in the values of the reactivity ratios for this system is very minimal and apparently the choice of the correlation coefficient does not affect the general outcome.

The most appropriate approach to find the value of the correlation coefficient is to estimate it from the analysis of residuals of a rich replicated experimental data set. Such an investigation is not possible with existing data sets in the literature due to the limited number of data points. In the absence of this information, looking into the effect of varying the correlation coefficient on the reactivity ratio

estimation results can determine whether it is necessary to run the extra step of the analysis of residuals, depending on the significance of the different correlations between the measurements on the estimation results. For this ternary system, the reactivity ratios in Table 6-3 shift insignificantly so that having a more detailed analysis of residuals may not be justified. While this is true for this case, there might be other terpolymerization systems where the analyses of their NMR data are subject to higher error levels and, in turn, their correlations could have more of a substantial effect.

Table 6-3. Effect of correlation on the reactivity ratio estimates for DMAEM (M_1)/MMA (M_2)/DDMA (M_3)

	ρ = -0.4	**ρ = -0.2**	**ρ = 0**	**ρ = 0.2**	**ρ = 0.4**
$\mathbf{r_{12}}$	0.82	0.80	0.80	0.79	0.79
$\mathbf{r_{21}}$	0.78	0.76	0.75	0.74	0.74
$\mathbf{r_{13}}$	0.79	0.80	0.80	0.80	0.80
$\mathbf{r_{31}}$	0.80	0.80	0.80	0.79	0.79
$\mathbf{r_{23}}$	1.09	1.09	1.08	1.08	1.07
$\mathbf{r_{32}}$	1.21	1.20	1.19	1.19	1.18

6.4.3 Combining conversion information with the cumulative terpolymer composition equation

As mentioned before, using the cumulative terpolymer composition model and incorporating conversion values in the parameter estimation process improves the precision of the obtained reactivity ratios, based on trends established for the DNI approach in copolymerization systems as well as theoretical explanations supporting this point (see Chapter 3 for more explanations). The key equations for the terpolymerization cumulative composition model are shown in equations (6.17) and (6.18). To show the implementation of EVM and DNI approach, we retained the same reference as previous section, Soljic et al. (2010), where two terpolymerization systems of DMAEM (M_1)/ MMA (M_2)/ DDMA (M_3) and DMAEM (M_1)/ Styrene (Sty) (M_2)/ DDMA (M_3) (as shown in the 5th and 6th rows of Table 6-1 were studied. Their experimental data including conversion values are shown in Tables 6-4 and 6-5. Although these data points were collected at low conversion levels, they can still be used to illustrate how the cumulative terpolymerization model can be incorporated into the EVM ternary reactivity ratio estimation program and how beneficial this can be. These data sets were

analyzed and the reactivity ratio estimates are shown in Figures 6-9 and 6-10 for each system. These figures also show the point estimates and JCRs from the instantaneous model (case (2)) and the binary reactivity ratios reported in the reference paper.

Table 6-4. Composition data for DMAEM (M_1)/MMA (M_2)/DDMA (M_3)

Feed composition			Conversion	Experimental terpolymer composition		
M_1	M_2	M_3	Xw %	M_1	M_2	M_3
0.100	0.100	0.800	0.70	0.114	0.084	0.802
0.100	0.400	0.500	0.96	0.125	0.381	0.494
0.100	0.700	0.200	1.32	0.128	0.690	0.182
0.200	0.200	0.600	1.69	0.243	0.118	0.569
0.200	0.500	0.300	2.11	0.237	0.476	0.287
0.400	0.100	0.500	2.97	0.422	0.090	0.488
0.400	0.400	0.200	3.82	0.423	0.378	0.199
0.600	0.200	0.200	5.05	0.599	0.195	0.206
0.800	0.100	0.100	6.85	0.783	0.118	0.099

Table 6-5. Composition data for DMAEM (M_1)/Styrene (Sty) (M_2)/DDMA (M_3)

Feed composition			Conversion	Experimental terpolymer composition		
M_1	M_2	M_3	Xw %	M_1	M_2	M_3
0.100	0.100	0.800	0.70	0.108	0.181	0.711
0.100	0.400	0.500	0.84	0.095	0.579	0.326
0.100	0.700	0.200	1.09	0.077	0.829	0.094
0.200	0.200	0.600	1.46	0.194	0.330	0.476
0.200	0.500	0.300	1.74	0.160	0.669	0.171
0.400	0.100	0.500	2.66	0.367	0.172	0.461
0.400	0.400	0.200	3.11	0.312	0.557	0.131
0.600	0.200	0.200	4.55	0.509	0.322	0.169
0.800	0.100	0.100	6.43	0.718	0.189	0.093

As can be seen in Figures 6-9 and 6-10, the point estimates and their JCRs from the cumulative model are almost identical to those from the instantaneous model. The closeness of the reactivity ratio estimates from both instantaneous and cumulative models is an indication that the cumulative model works perfectly for the ternary systems. Typically, one would expect that the cumulative model adds more information to the parameter estimation procedure and therefore provides more reliable reactivity ratio estimates. However, our results for these two systems indicate that the instantaneous data are of high quality and the assumptions of the instantaneous ternary model are met to a very good extent. It must be kept in mind, however, that this is not the case for most of the experimental work in the literature as the "so-called" low conversion data often go to higher conversion levels and therefore the error in the instantaneous data cannot be neglected. That is when using cumulative data would be more beneficial.

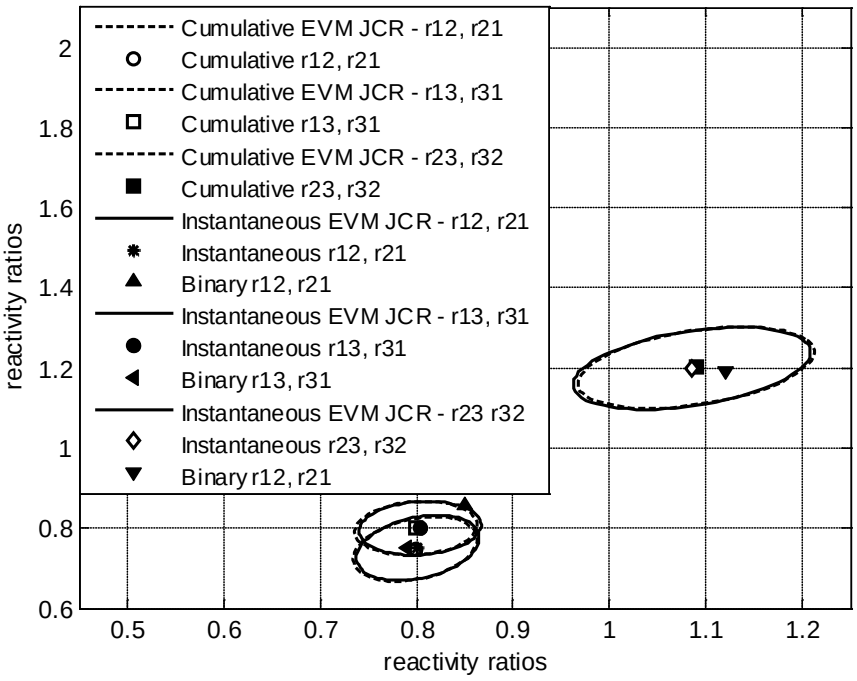

Figure 6-9. Reactivity ratio estimates from cumulative data for DMAEM (M_1)/MMA (M_2)/DDMA (M_3)

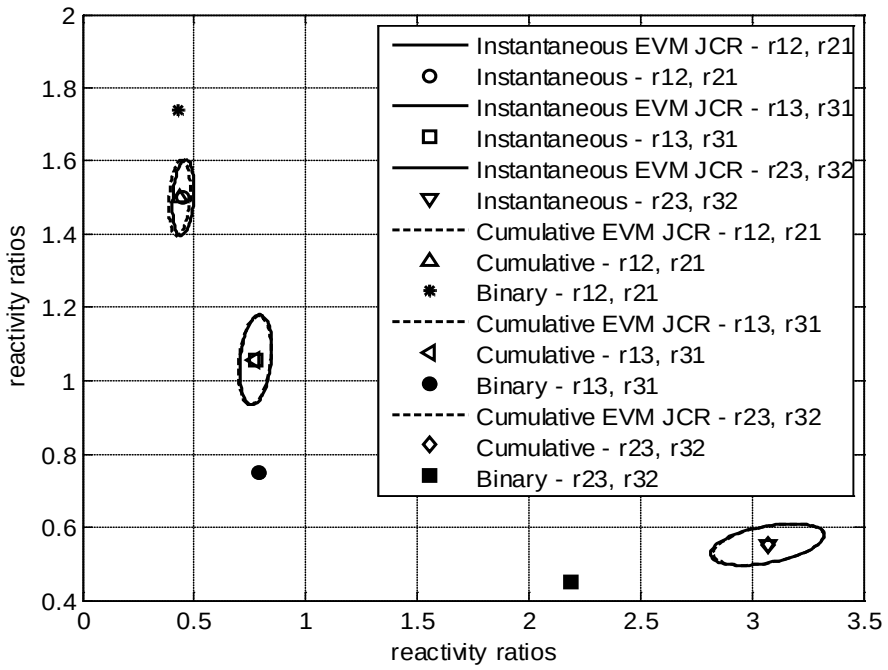

Figure 6-10. Reactivity ratio estimates from cumulative data for DMAEM (M_1)/Styrene (Sty) (M_2)/DDMA (M_3)

Having confirmed the performance of the EVM algorithm and DNI approach in Figures 6-9 and 6-10, and since the combination of the EVM method with the DNI approach is being tested here for the first time ever, the question becomes whether the EVM program can converge when using high conversion data as well. Unfortunately, the literature do not have high conversion data that can be used for this reactivity ratio estimation step, since almost all high conversion studies are done only for one initial feed composition (not sufficient for reactivity ratio estimation). In order to address this concern, computer simulations were used to generate high conversion experimental data for the ternary system of Acrylonitrile (AN)/Methyl methacrylate (MMA)/Styrene (Sty), as reported in Brar and Hekmatyar (1999). This reference reported low conversion terpolymerization data and binary reactivity ratios.

Binary reactivity ratios for this system were used to simulate ternary experiments up to high conversion (70%), and random error was added to the simulated data in order to mimic real experimental observations at high conversion. This generated data set was subsequently used for estimating reactivity ratios with the DNI approach, and results from the parameter estimation are shown in Figure 6-11, where the ternary reactivity ratio pairs of (r_{12} and r_{21}), (r_{13} and r_{31}), and (r_{23} and

r_{32}) along with their JCRs are shown. The binary reactivity ratios that were used to simulate the experimental data are also shown in this figure. The fact that using simulated high conversion experimental data resulted in ternary reactivity ratio estimates confirm that the EVM DNI approach does indeed converge also for high conversion data, a first time ever observation that points out the potentials of the EVM application for estimating ternary reactivity ratios. The binary reactivity ratios from the reference paper and our point estimates are also shown in Table 6-1.

An actual terpolymerization experimental example and further confirmation of the implementation of the DNI approach with high conversion experimental data are given in Chapter 8.

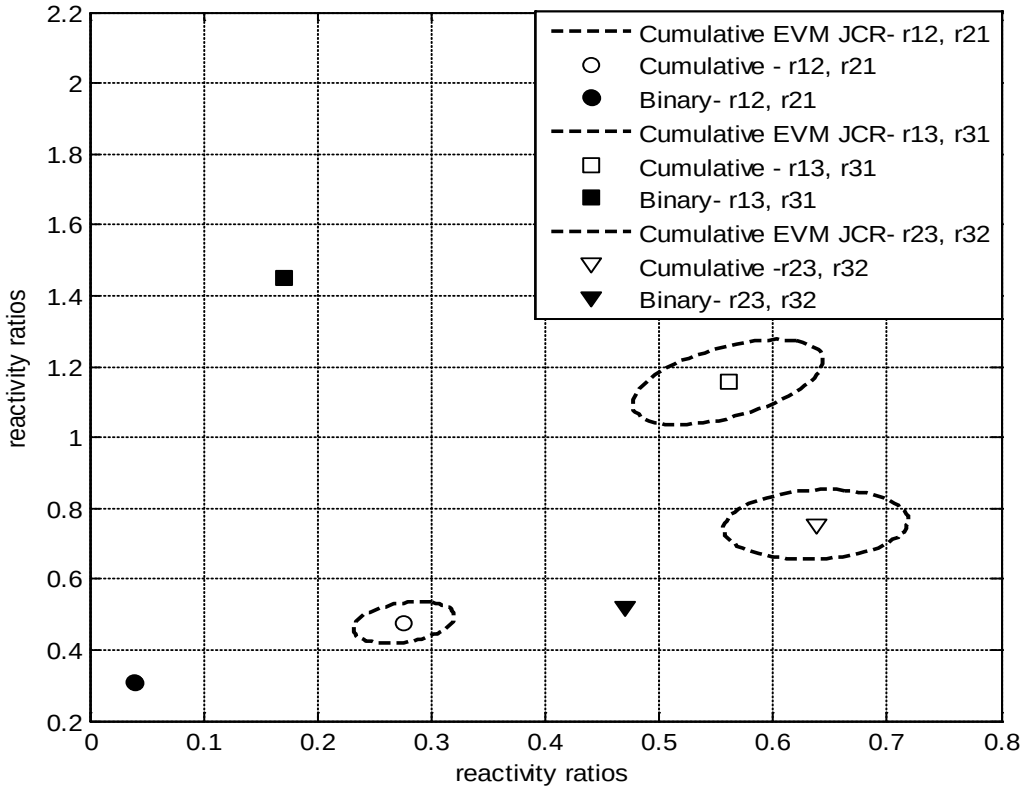

Figure 6-11. Reactivity ratio estimates from simulated cumulative data at high conversion, AN (M_1)/MMA (M_2)/Sty (M_3);
r_{12}=0.04, r_{21}=0.31, r_{13}=0.17, r_{31}=1.45, r_{23}=0.47, and r_{32}=0.52

6.4.4 Evaluation of the reliability of the reactivity ratio estimates

In order to show the evaluation process of the reactivity ratio results, an example is given in this section for the terpolymerization system of methyl methacrylate (MMA, M_1), 3-hydroxyneopentyl methacrylate (NPGMA, M_2), 2-hydroxyethyl methacrylate (HEMA, M_3). This system was investigated by Iglesias et al. (1996) where terpolymerization and copolymerizations were performed at low conversion levels and binary reactivity ratios were estimated, albeit with linear estimation techniques. The terpolymerization data were also used with a nonlinear least squares technique to estimate ternary reactivity ratios (these values are shown in the 12th row of Table 6-1). In our work, we used the experimental data (as shown in Table 6-6) and estimated ternary reactivity ratios, using the recast terpolymerization model with six variables, assuming no correlation amongst the measurements. The published binary and ternary reactivity ratios along with our point estimates are given in Table 6-1 and their JCRs are shown in Figure 6-12.

Table 6-6. Terpolymerization experimental data for the MMA (M_1)/NPGMA (M_2)/HEMA (M_3) ternary system, Iglesias et al. (1996)

Feed composition			Experimental terpolymer composition		
M_1	M_2	M_3	M_1	M_2	M_3
0.32	0.34	0.34	0.28	0.32	0.40
0.21	0.20	0.59	0.20	0.18	0.62
0.20	0.40	0.40	0.16	0.4	0.44
0.20	0.60	0.2	0.14	0.61	0.25
0.41	0.21	0.38	0.40	0.19	0.41
0.62	0.19	0.19	0.58	0.19	0.23
0.10	0.10	0.80	0.05	0.09	0.86
0.79	0.10	0.11	0.78	0.11	0.11
0.41	0.39	0.41	0.37	0.40	0.23
0.10	0.79	0.11	0.10	0.79	0.11

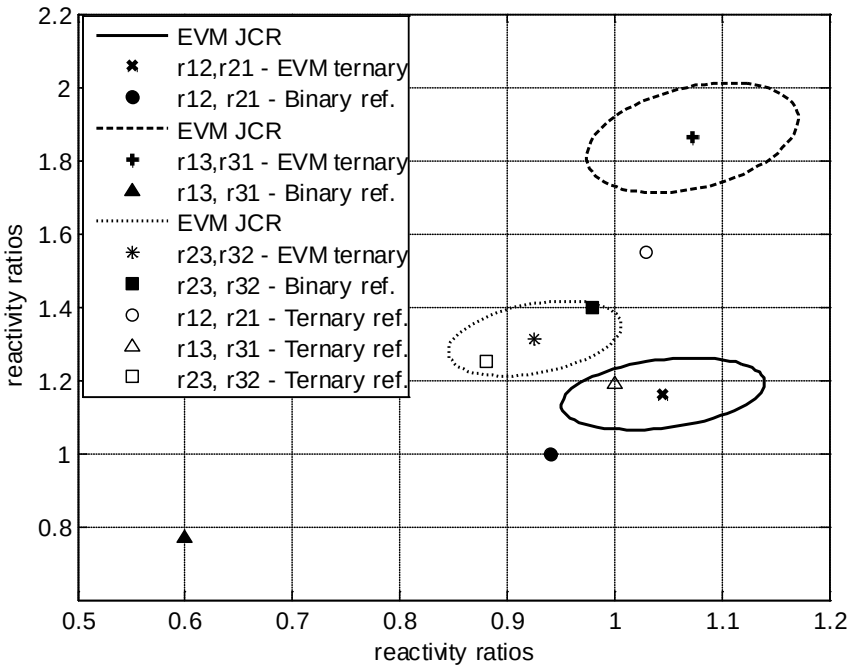

Figure 6-12. Reactivity ratio estimates for the terpolymerization system of MMA (M_1)/NPGMA (M_2)/HEMA (M_3)

As shown in Figure 6-12, the difference between binary and ternary reactivity ratios in the reference paper is very significant for two of the reactivity ratio pairs (except for r_{23} and r_{32}). With respect to our results, the estimated ternary reactivity ratios do not agree well with neither of the reported reactivity ratios, again with the exception of the pair r_{23} and r_{32}. It is also noted that for both (r_{12} and r_{21}) and (r_{13} and r_{31}) pairs, the reactivity ratio values are greater than one. While such binary systems are not feasible on their own, in this case, the reactivity ratios lie very close to unity and therefore, these results may reflect a large level of error in the experimental data that in turn introduces bias in the ternary reactivity ratio estimates.

The shifts in the values of the reactivity ratios from a binary system to a ternary one clearly illustrates that using binary reactivity ratios can be a grossly incorrect choice as they do not necessarily reflect the actual (true) reactivities of the monomers in the ternary system. The importance of the variation in reactivity ratios values can also be illustrated in terms of the prediction of the experimental data, and more specifically, by looking at the agreement between experimental and theoretical terpolymer compositions. Figure 6-13 shows a triangular plot for the terpolymer composition of this ternary system. The experimental data from the reference paper along with calculated terpolymer

compositions based on reported binary, reported ternary and our estimated ternary reactivity ratios are also shown in this figure.

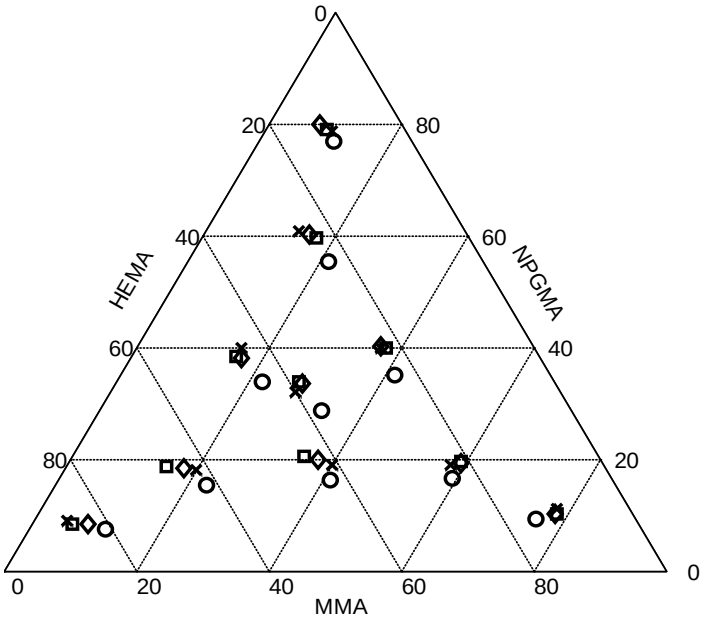

Figure 6-13. Comparison of experimental and calculated terpolymerization compositions; (x) Experimental data; (o) calculated based on binary reactivity ratios (Iglesias et al. (1966); (◊) calculated based on ternary reactivity ratios (reference); (□) calculated based on ternary reactivity ratios in current work.

Looking at different sets of predicted compositions in Figure 6-13, it can be seen that although the experimental and predicted ternary compositions are close, they are quite far from the ternary compositions calculated from binary reactivity ratios. The largest difference, and hence, disagreement, in Figure 6-13 is indeed between experimental data and calculated compositions based on binary reactivity ratios! Such results can be associated to, firstly, the EVM methodology that was used to obtain these estimated reactivity ratios and, secondly, to including the third monomer and the subsequent changes in the reaction medium in the estimation process compared to binary studies. This influence can be realized with the shifts in the values of ternary and binary reactivity ratios, but it is also noticeable through the change in the predicted composition values. Since this comparison and the importance of estimating ternary reactivity ratios based on ternary data are very crucial for the research in this area, the following section points out compelling pieces of evidence that establish the necessity of avoiding using binary reactivity ratio for ternary systems.

6.4.5 How important is it to avoid using binary reactivity ratios in terpolymerization studies?

It has been pointed out throughout this chapter that since the binary reactivity ratios from copolymerization systems (commonly used in place of ternary reactivity ratios) are not determined based on terpolymerization experimental data, they can only be considered as gross approximation to the real ternary reactivity ratios. In addition, the database of binary reactivity ratios in the literature is very inconsistent, having suffered over many years from the implementation of several incorrect reactivity ratio estimation techniques. Therefore, if such binary values are to be used in a ternary system study, the question is which pairs of reactivity ratios should be used in the terpolymerization study, amongst several incorrect (and widely differing) reactivity ratios for the same copolymerization system?!

In line with these issues, we now outline three important risks/problems in using binary reactivity ratios in terpolymerization kinetic studies.

6.4.5.1 Prediction performance of the terpolymerization composition equation

One of the main reasons for determining terpolymerization reactivity ratios is to be able to use the terpolymerization composition equation to predict terpolymer composition. An example of this practice was presented in section 6.4.4, showing that changes in the reactivity ratios values lead to changes in the predicted terpolymer compositions. However, this problem is a much more crucial issue than a simple comparison. Generally, evaluating the fit between experimental and predicted composition values has been a standard check for the credibility of the model. In this regard, we can see in many literature papers that because of using approximate binary reactivity ratios, serious deviations between predictions of terpolymerization composition and experimental data have been observed, leading researchers to question the credibility of the terpolymerization composition AG model instead of reviewing the accuracy of the parameter values used in the model!

A good example of this point is with respect to the investigation of the terpolymerization system of acrylonitrile (AN, M_1), styrene (Sty, M_2), and maleic anhydride (MA, M_3). This system was investigated by Kressler et al. (1987), where the corresponding binary reactivity ratios were obtained from the literature. In our work, we estimated the ternary reactivity ratios directly from the experimental data, and the results are shown in Table 6-1. Figure 6-14 shows two triangular

composition plots for the experimental terpolymerization data and the predicted ones using binary reactivity ratios (left side triangle) and ternary reactivity ratios (right side triangle).

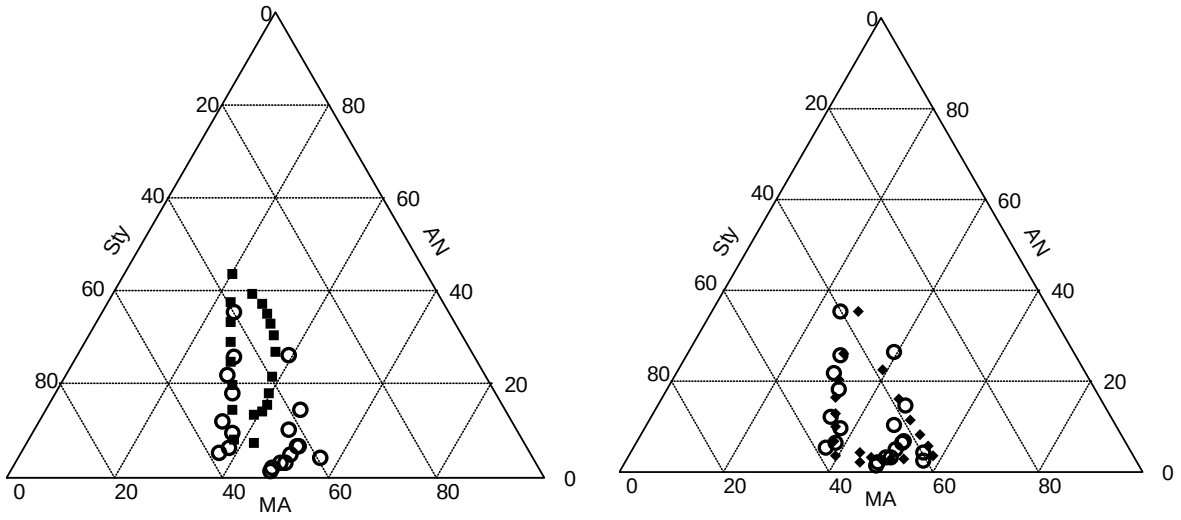

Figure 6-14. Experimental and predicted terpolymerization compositions for MA/AN/Sty; (○) experimental data, (■) binary reactivity ratios predictions, and (♦) ternary reactivity ratio predictions; see Table 6-1 for the reactivity ratio values

Comparing the two triangles in Figures 6-14, it can be clearly seen that there is a large difference, and hence, unacceptable disagreement, between experimental data and calculated compositions based on binary reactivity ratios. To the contrary, the predicted composition values with the ternary reactivity ratios lie close to the experimental points. Such results can be associated to, firstly, including the presence of the third monomer by using terpolymerization data in the estimation process compared to binary studies and, secondly, to the methodology that is used to obtain these estimated reactivity ratios. This influence appears in the values of the ternary and binary reactivity ratios, but more importantly it is noticeable through the change in the predicted composition values.

6.4.5.2 Studying important characteristics of a terpolymerization system

Reactivity ratios in a ternary system not only describe the tendency of incorporation of monomers with respect to each other, but also they can be utilized to assess important characteristics of the ternary system. One of the important characteristics of a ternary system is whether the system has an

azeotrope or not. Based on the definition of the azeotropic point, a polymer composition that remains constant throughout the polymerization and equal to the feed composition (thus resulting in a homogenous polymer product), it is of interest to identify such a composition with almost no compositional drift, at which there is a high probability of obtaining homogenous polymer product. The value of an azeotropic composition is calculated based on the values of the reactivity ratios of the system. Determining the ternary azeotropic composition seems to be controversial in the literature simply due to the fact that many terpolymerization systems exhibit the azeotropic behavior for certain compositions, however, using binary reactivity ratios for the corresponding binary pairs does not result in an azeotropic point (Kazemi et al. (2010)).

In our work, we looked at the problem of the azeotrope composition in ternary systems and found that, if the system has an azeotrope, using six "ternary" reactivity ratios can confirm that composition in all cases. An example for this observation is for the ternary system of acrylonitrile/styrene/dibromopropyl acrylate, studied by Saric et al. (1983). The binary reactivity ratios reported in the reference paper and the ternary reactivity ratios estimated in the current work are cited in Table 6-1. Saric et al. (1983) pointed out that this system does not seem to have an azeotrope based on binary reactivity ratios. However, using ternary reactivity ratios, we found an azeotropic composition which agrees with the fact that the authors reported that the system does exhibit azeotropic behavior (experimentally!) at a certain composition.

Such an observation is due to the fact that the values of the reactivity ratios from binary pairs to a ternary system do change, and these values can subsequently affect the location (or even the existence) of the azeotropic point in a terpolymerization system. Thus, studying characteristics such as azeotropic compositions that are directly linked to the values of reactivity ratios highlights the importance of not using approximate binary reactivity ratios instead of accurate and direct ternary ones.

6.4.5.3 Experimental workload

An undeniable fact is that the success of the overall reactivity ratio estimation analysis (or any other parameter estimation analysis for that matter) strongly depends on the diligent work of the practitioner in gathering experimental data that are reliable and informative. Despite the unfortunate fact that this approach is usually translated in gathering experimental data from several different

(randomly chosen) points, covering the whole range of experimentation, the correct approach, as mentioned for the copolymerization studies in Chapter 4, is to implement design of experiments techniques and collect only necessary experimental data at optimal points. When it comes to estimating binary reactivity ratios for three pairs involved in a terpolymerization, the experimental work can be very extensive (assuming one does not want to dive into the questionable and inconsistent pool of reactivity ratios in the literature). It involves investigating three different binary systems and at least performing two experiments for each pair (at least a minimum of six different experiments). This experimental workload is yet another reason why using binary reactivity ratios should be avoided. The next chapter discusses how implementing the design of experiments approach can significantly reduce this workload and also improve the results of ternary reactivity ratio estimation.

6.5 Concluding Remarks

The problem of estimating ternary reactivity ratios has been thoroughly discussed in this chapter. It has been shown that there is significant gap in the literature regarding reactivity ratios estimation for ternary system, since the terpolymerization studies are very scarce in the literature and binary reactivity ratios have been commonly and misleadingly used in ternary studies. The terpolymerization composition models were discussed to be used with low and high conversion terpolymerization experimental data, along with the implementation of the EVM algorithm. The following points have been made, and justified by our analysis, related to the estimation of ternary reactivity ratios:

(a) The recast terpolymerization model, which uses terpolymer composition mole fractions explicitly (and not in ratios), avoids the estimation pitfalls with the original AG model.

(b) Estimating ternary reactivity ratios based on terpolymerization data directly protects against unnecessary propagation of errors from badly estimated binary reactivity ratios, at the same time without essentially ignoring the presence of the third comonomer.

(c) EVM is the methodology to employ, especially with terpolymerization systems which contain inherently more error (than copolymerizations) in all variables.

(d) Several examples and counter-examples with literature ternary experimental data showed how one can go towards consistent and reliable ternary reactivity ratios, when the correct information content is taken into account (with respect to (i) the choice of measurements, (ii) their error structure, and (iii) the correlation between measurements).

(e) An extensive review table of several systems is presented where the binary reactivity ratios from the reference papers and our results from the EVM approach are cited. The same trends and observations were also confirmed for these systems.

(f) Careful attention has been paid to the comparison between using binary versus ternary reactivity ratios in terpolymerization studies and concrete reasons are provided discouraging the use of binary values and establishing the correct method as outlined in this chapter.

Chapter 7

Reactivity Ratios in Terpolymerization Systems: Design of Experiments

Following Chapter 6, where the method of estimating reactivity ratios for terpolymerization systems directly from terpolymerization data was extensively studied and the correct method was established, this chapter looks at the model-based design of experiments approach for the problem of reactivity ratio estimation in terpolymerization systems, for the first time in the literature. The optimal terpolymerization feed compositions are calculated using the EVM design criterion. The results show that there are three optimal feed compositions and their locations depend on the values of the reactivity ratios, and in most cases they are located close to the borders of the feasible region, which are the corners of the terpolymerization composition triangular plot. The structure of this design criterion and its implementation are explained in detail, validating the effectiveness and reliability of this procedure. In addition, the impact of the reactivity ratio values and their differences on the location of the optimal points is explored and "practical heuristics" are presented that determine optimal feed compositions for terpolymerization experiments for reliable reactivity ratio estimation.

7.1 Introduction and Literature Review

As mentioned in Chapter 6, there is a significant gap in the literature regarding the estimation and investigation of ternary (terpolymerization) reactivity ratios. This is mainly related to the established common practice of using binary reactivity ratios in terpolymerization studies, despite the fact that these reactivity ratios are obtained for binary pairs from separate copolymerization systems and in most cases provide poor approximation for ternary reactivity ratios. The correct approach for determining ternary reactivity ratios would be to use experimental data directly from terpolymerization experiments and estimate reactivity ratios. As shown in Chapter 6, the EVM parameter estimation technique is the most appropriate method in this regard and reliable reactivity ratios for terpolymerization systems can be obtained that are not affected by the approximation and restriction of using binary reactivity ratios.

As mentioned in Chapters 4 and 5, the question of estimating reactivity ratios for multicomponent polymerizations needs to be combined with the design of experiments step that aims at improving the results of parameter estimation. Implementing design of experiments also minimizes the resource-intensive task of collecting experimental data, and has the potential to improve the quality of parameter estimates until they achieve satisfactory levels of precision.

The basic idea behind the optimal design of experiments is to select experimental trials which minimize variability in the parameter estimates, which is related to the variance-covariance matrix of the parameter estimates. A geometrical interpretation of such a design strategy is extensively discussed in Chapters 2 and 4, and different design criteria that can be used for the purpose of improving parameter estimation results are mentioned. The D-optimal criterion, perhaps the most common criterion used in the literature for obtaining improved parameter estimates, aims at minimization of the determinant of the variance-covariance matrix of the parameters ($|V_\theta|$) (see, for instance, Box and Lucas (1959), Box and Draper (1965), Draper and Hunter (1966), Draper and Hunter (1967), Atkinson and Hunter (1968), and Box (1970)).

Moreover, Chapter 4 introduces the EVM design criterion to be used instead of the D-optimal design criterion where the traditional nonlinear regression assumptions do not hold (that is, when independent variables are exactly known and the model can be expressed in an explicit form). Problems arise when the variables are related to each other with single or multiple equations in an implicit form and/or the variables cannot be distinguished as dependent or independent anymore. The idea of design of experiments was implemented in Chapter 4 on the reactivity ratio estimation problem in copolymerization systems (first proposed by Tidwell and Mortimer (1965)). Chapter 4 presented the most recent and appropriate approach for this problem, where the EVM design criterion was used to locate optimal experiments for copolymerizations.

For terpolymerization systems, on the other hand, research for determining ternary reactivity ratios is in a much earlier stage than for copolymerizations. As discussed previously, the assumptions involved in the development of the terpolymerization model are similar to those used for describing copolymerization systems. Therefore, studies about the ternary composition equations were initially based on the reactivity ratios extracted from binary systems. Based on this analogy, a ternary system is treated as three separate binary copolymerizations, and the effect of the interactions between all three monomers on their reactivity towards each other is overlooked. This approach, even though

established as common practice, is very approximate at best, and is not at all reliable for predicting ternary compositions. In fact, there are several cases in the literature of reporting issues with the Alfrey-Goldfinger model (see Chapter 6, equations (6.1) to (6.3)) prediction results that are simply due to the usage of binary reactivity ratios instead of reactivity ratios based directly on terpolymerization experimental data (e.g., see Chapter 6, section 6.4.4, the example by Kressler et al. (1987)).

The Alfrey and Goldfinger (1944) model for the instantaneous terpolymerization composition has been a source of discrepancies in terpolymerization studies, and as shown in Chapter 6, we can use a recast form of the Alfrey-Golfinger model, shown in equations (6.5) to (6.7), which considers the mole fractions of the monomers in the terpolymer (F_1, F_2, and F_3) as individual responses. Overall, it can be concluded that there has barely been any work for parameter estimation for ternary systems, and with this perspective, as expected, absolutely no work has been reported in the literature considering the design of experiments strategy for estimating ternary reactivity ratios (to the best of our knowledge).

Our goal in this chapter is to implement the EVM design criterion on terpolymerizations and calculate optimal feed compositions that can lead to the most reliable reactivity ratios. This work considers several details of the design problem structure, such as statistical issues for choosing the EVM method, the specific design criterion, and its implementation on different terpolymerization systems. Also, based on the results of the optimal feed compositions, practical heuristics are presented which will quickly suggest optimal points without the need for complex mathematical computations. We believe that this practical guide for the optimal ternary points not only leads to reliable reactivity ratio estimates but also promotes the usage of this practical design strategy, which will in turn contribute to a more reliable database for ternary reactivity ratios in the literature.

7.2 Design of Experiments for Terpolymerization Reactivity Ratio Estimation

7.2.1 The EVM design criterion formulation

Detailed explanations about the EVM algorithm have already been given in Chapters 2 and 3, and the design of experiments for parameter estimation in the EVM context has also been explained and implemented in Chapters 4 and 5 for the copolymerization reactivity ratio estimation study. Herein, certain key equations from the EVM algorithm are included again but details are eliminated for the sake of brievity. The EVM design criterion aims at maximizing the determinant of the information matrix, which is the inverse of the variance-covariance matrix of the parameters, given by matrix $\underline{G}$, in equation (7.1). $\underline{Z}$ is the vector of partial derivatives of the (model) function with respect to the parameters, and $\underline{B}$ is the vector of partial derivatives of the function with respect to the variables (see Chapter 2, section 2.3.3).

$$\underline{G} = \sum_{i=1}^{n} r_i \underline{Z}_i' (\underline{B}_i \underline{V} \underline{B}_i')^{-1} \underline{Z}_i \tag{7.1}$$

The most common approach for model-based design of experiments is the so-called initial design (Keeler (1989)). The initial design refers to the problem where no prior information is available and the objective is to design initial trials in order to collect the first data set and commence the parameter estimation process. The design criterion for minimization is given by equation (7.2):

$$Max_{\underline{\xi}^d} \left| \sum_{i=1}^{n} \underline{Z}_i' \left(\underline{B}_i \underline{V} \underline{B}_i' \right)^{-1} \underline{Z}_i \right| \quad \text{subject to} \begin{cases} \underline{g}(\underline{\xi}_i, \underline{\theta}) = 0 \\ L \leq \underline{\xi}_i^{\,d} \leq U \\ c\left(\underline{\xi}_i^{\,d} \right) \leq 0 \\ ceq\left(\underline{\xi}_i^{\,d} \right) = 0 \end{cases} \tag{7.2}$$

where $\underline{\xi}_i^{\,d}$ denotes the design variables, L and U represent lower and upper bounds, and c and ceq represent inequality and equality constraints for the design variables. The choice of which variables are the subjects of the design problem is related to the nature of the system under study. In general, the design variables involved in the optimization are those that determine the experimental conditions. Nonetheless, the model expression, $\underline{g}(\underline{\xi}_i, \underline{\theta}) = 0$, must hold between all the variables in

the problem, which means that the maximization/minimization procedures are all subject to a constraint given by $\underline{g}(\underline{\xi}_i, \underline{\theta}) = 0$ This constraint ensures that the variables chosen for the designed experiments fall on the function's surface (i.e., they satisfy the model).

The formulation of the EVM design criterion depends on the model chosen to represent the system (which is the terpolymerization model, as shown in equations (7.3) to (7.5)), and the design variables that are the subject of the design. In the ternary reactivity ratio estimation and design of experiments problems, the EVM structure can include all variables that are subject to error. The total number of variables that could be involved in the parameter estimation procedure is six. That is, f_1, f_2, and f_3 for the mole fractions of the feed composition, and F_1, F_2, and F_3 for the mole fractions of the terpolymer composition. However, for the design, we are only concerned with two of the mole fractions in the feed (e.g., f_1 and f_2), as the third one can be obtained from the relation of $\sum_{i=1}^{3} f_i = 1$

$$F_1 - \frac{f_1\left(\frac{f_1}{r_{21}r_{31}}+\frac{f_2}{r_{21}r_{32}}+\frac{f_3}{r_{31}r_{23}}\right)\left(f_1+\frac{f_2}{r_{12}}+\frac{f_3}{r_{13}}\right)}{f_1\left(\frac{f_1}{r_{21}r_{31}}+\frac{f_2}{r_{21}r_{32}}+\frac{f_3}{r_{31}r_{23}}\right)\left(f_1+\frac{f_2}{r_{12}}+\frac{f_3}{r_{13}}\right)+f_2\left(\frac{f_1}{r_{12}r_{31}}+\frac{f_2}{r_{21}r_{32}}+\frac{f_3}{r_{13}r_{32}}\right)\left(f_2+\frac{f_1}{r_{21}}+\frac{f_3}{r_{23}}\right)+f_3\left(\frac{f_1}{r_{13}r_{21}}+\frac{f_2}{r_{23}r_{12}}+\frac{f_3}{r_{13}r_{23}}\right)\left(f_3+\frac{f_1}{r_{31}}+\frac{f_2}{r_{32}}\right)} = 0 \quad (7.3)$$

$$F_2 - \frac{f_2\left(\frac{f_1}{r_{12}r_{31}}+\frac{f_2}{r_{21}r_{32}}+\frac{f_3}{r_{13}r_{32}}\right)\left(f_2+\frac{f_1}{r_{21}}+\frac{f_3}{r_{23}}\right)}{f_1\left(\frac{f_1}{r_{21}r_{31}}+\frac{f_2}{r_{21}r_{32}}+\frac{f_3}{r_{31}r_{23}}\right)\left(f_1+\frac{f_2}{r_{12}}+\frac{f_3}{r_{13}}\right)+f_2\left(\frac{f_1}{r_{12}r_{31}}+\frac{f_2}{r_{21}r_{32}}+\frac{f_3}{r_{13}r_{32}}\right)\left(f_2+\frac{f_1}{r_{21}}+\frac{f_3}{r_{23}}\right)+f_3\left(\frac{f_1}{r_{13}r_{21}}+\frac{f_2}{r_{23}r_{12}}+\frac{f_3}{r_{13}r_{23}}\right)\left(f_3+\frac{f_1}{r_{31}}+\frac{f_2}{r_{32}}\right)} = 0 \quad (7.4)$$

$$F_3 - \frac{f_3\left(\frac{f_1}{r_{13}r_{21}}+\frac{f_2}{r_{23}r_{12}}+\frac{f_3}{r_{13}r_{23}}\right)\left(f_3+\frac{f_1}{r_{31}}+\frac{f_2}{r_{32}}\right)}{f_1\left(\frac{f_1}{r_{21}r_{31}}+\frac{f_2}{r_{21}r_{32}}+\frac{f_3}{r_{31}r_{23}}\right)\left(f_1+\frac{f_2}{r_{12}}+\frac{f_3}{r_{13}}\right)+f_2\left(\frac{f_1}{r_{12}r_{31}}+\frac{f_2}{r_{21}r_{32}}+\frac{f_3}{r_{13}r_{32}}\right)\left(f_2+\frac{f_1}{r_{21}}+\frac{f_3}{r_{23}}\right)+f_3\left(\frac{f_1}{r_{13}r_{21}}+\frac{f_2}{r_{23}r_{12}}+\frac{f_3}{r_{13}r_{23}}\right)\left(f_3+\frac{f_1}{r_{31}}+\frac{f_2}{r_{32}}\right)} = 0 \quad (7.5)$$

Based on the choice of the design variables of f_1 and f_2, the terpolymerization model, $\underline{g}(\underline{\xi}_i, \underline{\theta})$ is given by equations (7.3) to (7.5), and f_3 is replaced as a function of f_1 and f_2 in all of the equations. Hence, the number of variables in the problem is reduced to five, and the $\underline{V}$ matrix can be given by equation (7.6), where the diagonal elements are the variances of the measurements and the off-diagonal elements are the correlations between measurements (for more information about the V matrix derivation, see Chapter 2, section 2.3.2 and Chapter 6, section 6.3.2).

$$\underline{V} = \begin{bmatrix} \sigma_{f_1}^2 & 0 & 0 & 0 & 0 \\ 0 & \sigma_{f_2}^2 & 0 & 0 & 0 \\ 0 & 0 & \sigma_{F_1}^2 & \sigma_{F_1F_2}^2 & \sigma_{F_1F3}^2 \\ 0 & 0 & \sigma_{F_1F_2}^2 & \sigma_{F_2}^2 & \sigma_{F_2F_3}^2 \\ 0 & 0 & \sigma_{F_1F3}^2 & \sigma_{F_2F_3}^2 & \sigma_{F_3}^2 \end{bmatrix}$$

(7.6)

Considering f_1 and f_2 as the design variables in our example affects other constraints, and thus the EVM design criterion and its constraints are given in equation (7.7). The first constraint, as mentioned earlier, is the terpolymerization model that must hold. The second constraint defines the feasible region for f_1 and f_2 between 0.1 and 0.9. The third constraint in equation (7.7) ensures that the summation of f_1 and f_2 does not exceed 0.9. The last two constraints ensure that we have all three components with optimal feed compositions, with f_3 having at least 10% of the optimal feed composition. The existence of this constraint is absolutely necessary in order to obtain practically feasible results.

$$Max_{\underline{\xi}^d} \left| \sum_{i=1}^{n} \underline{Z}_i' \left(\underline{B}_i \underline{V} \underline{B}_i' \right)^{-1} \underline{Z}_i \right| \quad \text{subject to} \begin{cases} \underline{g}(\underline{\xi}_i, \underline{\theta}) = 0 \\ 0.1 \le \underline{\xi}_i^{\,d} \le 0.9 \\ \sum \underline{\xi}_i^{\,d} \le 0.9 \end{cases} \tag{7.7}$$

Alternatively, the design criterion can be formulated considering all three feed mole fractions, f_1, f_2, and f_3, as the design variables. In this case, the terpolymerization model should be given as equations (7.3) to (7.5), along with the stoichiometric relation between mole fractions of the three monomers in the monomer mixture, as $f_1+f_2+f_3=1$. Meanwhile, the constraints of the design criterion reduce to $\underline{g}\left(\underline{\xi}_i, \underline{\theta}\right) = 0$ and the lower and upper bound constraints. Using this approach has the advantage of less complicated constraints but the disadvantage of more design variables, which means more dimensions for search in the optimization procedure. In our experience, considering three variables resulted in a much more complicated path to obtain the optima of the optimization problem, and so this alternative approach is not used in our work.

7.2.1.1 Number of optimal points

An important issue in the design of experiment problem is the number of optimal points that becomes the number of optimal experiments to run. As shown in Chapter 4, the rule of thumb for parameter estimation problems states that the number of optimal experiments, n, should be equal to the number of parameters, p (i.e., $n=p$). If one wants to run $n>p$ experiments, n should be a multiple of p and so optimal experiments must be replicated to achieve higher information content (for more information see, for example, Atkinson and Hunter (1968) and Box (1969)). This statement is only true for single response problems. When working with a multi-response problem, with m as the number of responses, we need $(m\times n)$ experiments in order to estimate p parameters. Therefore, the number of optimal experiments should be $n=p/m$ (see Bard (1974)).

In the EVM context, the number of responses translates into the number of independent EVM variables. The number of independent EVM variables is introduced as the mathematical degrees of freedom, which is basically the number of total EVM variables minus the number of equations included in the EVM model (Duever et al. (1987)). For the design criterion for the terpolymerization problem, the EVM model consists of three equations (equation (7.3) to (7.5)) and we have five variables, thus there are two independent variables and six parameters (i.e., $m=2$ and $p=6$). As a result of the relation $n=p/m$, there should be three optimal experiments for estimating terpolymerization reactivity ratios. This is a very important remark, as it states that only three optimal terpolymerization experiments would provide sufficient information for reliable reactivity ratio estimation.

7.2.1.2 Error structure

The error structure of the variables in EVM has been discussed in Chapter 2 for parameter estimation and in Chapter 4 with respect to the design of experiments. As mentioned in Chapter 2, there are two possible options: error being either additive (equation (7.8)) or multiplicative (equations (7.9) or (7.10)), where x^* is the true value of the measured quantity x, k is a constant, and ε is a random variable, which, in the simplest case, has a uniform distribution in the interval from -1 to 1.

$$x = x^* + k\varepsilon \tag{7.8}$$

$$x = x^*(1 + k\varepsilon) \tag{7.9}$$

$$\ln(x) = \ln(x^*) + k\varepsilon \tag{7.10}$$

The discussion regarding the choice of the error structure can be found in Chapter 2 and 4 and will not be repeated herein. The very important conclusion is that this selection has no effect on the results of parameter estimation in the EVM context, but it changes the design of experiments results. Here, we show comparisons between results from choosing each error type, while our choice for composition data in polymerizations, based on previous publications and experts' opinions is the multiplicative error.

7.2.1.3 Optimization procedure

The minimization procedure for the EVM design criterion, as shown in equation (7.7), should be able to handle nonlinear problems subject to nonlinear equality, inequality, lower, and upper bound constraints. Also, since the search dimension of this problem is relatively large, the optimization method should be able to find the global optima. Based on these criteria, we chose the Generalized Pattern Search (GPS) method implemented by a built-in function in Matlab, for minimizing this design criterion (more information about the GPS method is provided in Chapter 2, section 2.3.5.4).

7.2.2 Improved design of experiments

Model-based design of experiments techniques aim at improving the precision of the parameter estimates. The basic assumption is that if the information content of the data increases, the precision of the parameter estimates also increases. However, design of experiments techniques for nonlinear models always start with a set of values for the parameters, and thus the quality of these initial estimates affects the effectiveness of the design procedure. Therefore, in some cases, in order to improve the information content for parameter estimation, a sequential design scheme should be used, where the existing data/information are used in the EVM design criterion (Keeler (1989)). Such design procedures consist of a series of alternating steps between designing experiments, using the experimental data for parameter estimation and designing further experiments, a process that continues until the parameter estimates achieve satisfactory levels of precision.

In addition, the precision of the parameter estimates is not given just by their individual variability and so maximizing only the determinant of the information matrix may not lead to the most reliable parameter estimates. One important factor in parameter estimation is the correlation between the parameters. Large correlation among parameters decreases the reliability of the parameter estimates and creates problem with convergence for the parameter estimation procedure. Hence, it might also be desirable to add an anti-correlation term to the design of experiments technique in order to reduce the correlation problem.

7.2.2.1 Sequential design criterion

In the sequential design of experiments, and after having conducted a set of *n* initial experiments, it is desired to find the optimal location of the next experiment(s) which can increase the precision of the results. The objective function is given by equation (7.11) and the constraints are similar to those discussed for equation (7.7). In equation (7.11), the hat sign (ˆ) denotes that the converged parameter estimates from the first set of *n* experiments are being used. The first term in equation (7.11) is generated by the EVM algorithm upon convergence of the parameter estimates. Therefore, the only term that is not known in equation (7.11) is the second term, involving $\underline{\xi}_{n+1}{}^{d}$. A search is then performed to find the maximum of this equation. An example of the implementation of this design criterion is shown in section 7.3.1, Figures 7-3 and 7-4.

$$Max_{\underline{\xi}_{n+1}{}^{d}} \left| \left[\sum_{i=1}^{n} \underline{\hat{Z}}_i' \left(\underline{\hat{B}}_i \underline{V} \underline{\hat{B}}_i' \right)^{-1} \underline{\hat{Z}}_i \right] + \underline{\hat{Z}}_{n+1}' \left(\underline{\hat{B}}_{n+1} \underline{V} \underline{\hat{B}}_{n+1}' \right)^{-1} \underline{\hat{Z}}_{n+1} \right| \qquad (7.11)$$

$$\text{subject to} \begin{cases} \underline{g}(\underline{\xi}_{n+1}, \underline{\theta}) = 0 \\ L \leq \underline{\xi}_{n+1}{}^{d} \leq U \end{cases}$$

7.2.2.2 Anti-correlation design criterion

The initial and sequential design criteria have the objective to maximize the information content of the experiments, maximizing the determinant of the information matrix of the analysis. The determinant of the information matrix for a two-parameter problem considers the correlation between two parameters, as the correlation term is also involved in the determinant expression. However, for cases with more than two parameters, similar to the ternary reactivity ratio estimation problem in this

work, the determinant of the information matrix cannot effectively address the correlation problem between the parameters, if the correlation magnitude is of an issue.

One way to quantify the correlation among parameters is by determining the correlation matrix, $\underline{C}$, which is based on the correlation coefficients of the parameters, given by equation (7.12). According to Draper and Smith (1998), the size of the determinant of the correlation matrix $\underline{C}$, which lies between 0 and 1, is a guide for the extent of the overall collinearity of the problem. When this determinant is zero ($|C|=0$), there is an exact dependence between the columns of the matrix, and when it is one ($|C|=1$), all correlations are zero.

$$\underline{C} = \begin{bmatrix} \rho_{1i} & \cdots & \rho_{1p} \\ \vdots & \ddots & \vdots \\ \rho_{p1} & \cdots & \rho_{pp} \end{bmatrix} \quad where \quad \rho_{ij} = \frac{\sigma^2_{p_i p_j}}{\sqrt{\sigma^2_{p_i} * \sigma^2_{p_j}}} \tag{7.12}$$

According to the definition of this matrix and its determinant, maximizing the determinant of $\underline{C}$ matrix (with the maximum of 1) minimizes the correlations amongst the parameters. Therefore, the anti-correlation criterion can be defined as maximization of the determinant of the C matrix. For estimation problems where the correlation of "specific" parameters should be reduced, Franceschini and Macchietto (2008) proposed an anti-correlation design criterion in which the design seeks to find a trade-off between reducing parameter correlation and increasing the information content. Using their approach, the EVM design criterion can be given as shown in equation (7.7), only with an additional constraint, regarding the correlation coefficients between certain parameters. To implement this approach, correlation coefficients can be constrained within an acceptable range (usually below ~0.5).

7.3 Results and Discussion

This section presents results and discusses the important aspects in implementing the EVM design criterion for several terpolymerization systems. Firstly, an ideal terpolymerization system where all reactivity ratios are equal to one is discussed in order to explain the effect of using different error structures and design schemes on a standard system that is easier to visualize. Secondly, a case study

from the literature is investigated where the results from the implementation of the EVM design criterion allows us to understand the effect of using different data sets with different types of information on the ternary reactivity ratio estimates. Subsequently, the relation between ternary reactivity ratio values and the location of the optimal feed compositions based on the EVM design criterion is comprehensively studied and conclusions are drawn as to how optimal feed compositions can be affected in this regard. The results of this section lead to practical heuristics that can guide experimenters and researchers to the location of optimal feed compositions without having to implement the whole complex design procedure every time, in other words, obtaining reliable ternary reactivity ratios with the least effort.

7.3.1 Ideal terpolymerization systems

A terpolymerization system for which all the reactivity ratios are equal to one is an "ideal" terpolymerization system. We first look at this system in order to be able to evaluate the results of the EVM design criterion for a system with equal reactivity ratios and easy to visualize behavior. Our goal is to look at the effect of using additive versus multiplicative error structures on the designed experiments, as well as considering the sequential and anti-correlation design schemes. First, the EVM design criterion as shown in equation (7.7) was used for calculating optimal compositions with the two types of error structure. These results are shown in Table 7-1 and Figure 7-1.

Table 7-1.Optimal feed compositions for ideal terpolymerization, additive versus multiplicative error

Additive error	f_1	f_2	f_3	***Multiplicative error***	f_1	f_2	f_3
expt. 1	0.17	0.18	0.65	**expt. 1**	0.10	0.10	0.80
expt. 2	0.65	0.18	0.17	**expt. 2**	0.80	0.10	0.10
expt. 3	0.18	0.65	0.17	**expt. 3**	0.10	0.80	0.10

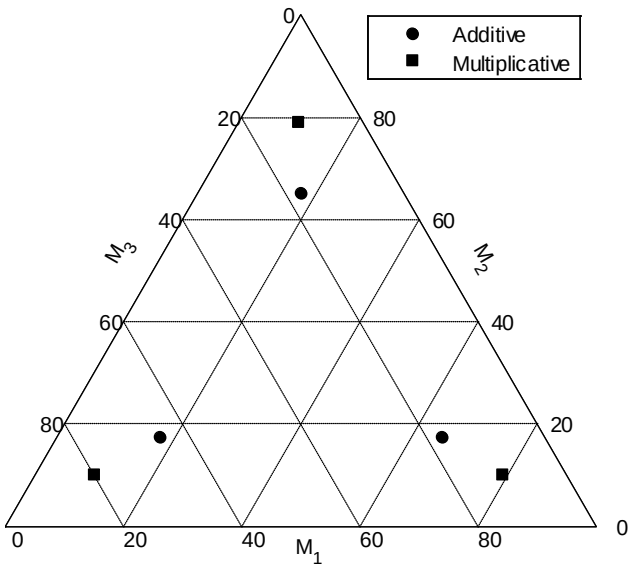

Figure 7-1. Optimal feed compositions (ideal terpolymerization system, r_{ij}=1); error structure effect

The optimal feed compositions for the ideal terpolymerization system, as shown in Table 7-1 and Figure 7-1, point to a very interesting observation. That is, each of the three optimal feed compositions is rich in one of the monomers and the other two monomers have equal amounts in the composition. The additive optimal compositions are more inclined towards the center of the triangle, whereas the multiplicative optimal points exhibit a tendency towards the corners of the triangular plot. This difference can be explained based on the fact that the multiplicative error structure, as explained in Chapter 4, has a *ln* (f_i) transformation and thus in the vicinity of $f_i=0$, *ln* (f_i) goes to negative infinity, which maximizes the EVM design criterion. The fact that the optimal points fall on the boundary of the feasible region is a phenomenon that is frequently observed in the design of experiments problems. Due to this fact, it is highly important to adjust the feasible region based on practical considerations. In our case, as explained for equation (7.7), the lower and upper bounds of the feasible region for the mole fractions of monomers in the feed are 0.1 and 0.9, respectively.

Next, the sequential design criterion, as shown in equation (7.11), was implemented for this terpolymerization system, and similar to the initial design implementation, the two types of error structure were checked again. The results obtained from the sequential design criterion are shown in Figure 7-2, with one triangular plot showing the sequential optimal experiments for the additive error

structure (left-side triangle), and a second showing the results for the multiplicative error structure (right-side triangle). As discussed earlier, the goal of the sequential design scheme is to find the optimal feed composition for the "next" experiment. However, as can be seen in Figure 7-2, there are more than one option for the sequential optimal experiments. For the additive error, we can have six suggestions for the next optimal experiments, as indicated by "o" in the left triangle. These points are very close to the initial optimal points, symmetrical in terms of mole fraction values for the three monomers, and have the same amount of information. For the multiplicative error, we can have three suggestions, indicated by "o" in the right triangle. These points also have the same amount of information as they exactly match the initial design optimal points.

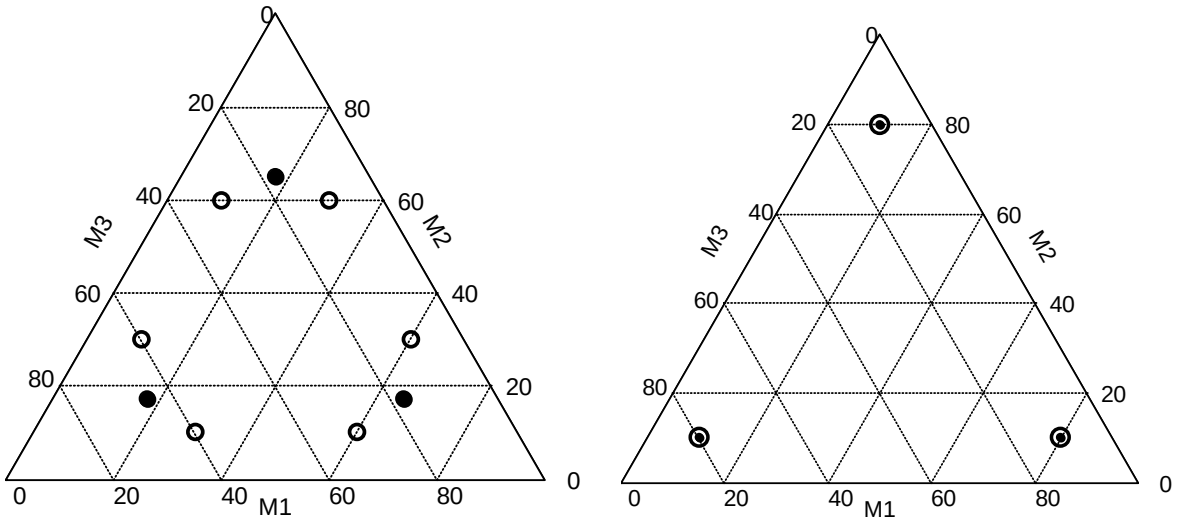

Figure 7-2. Sequential optimal feed compositions for: (left triangle) additive error, and (right) multiplicative error, with "•" as the initial and "o" as the sequential design points

In order to explore these findings further, the surface of the objective function for the sequential design criterion (i.e., the determinant of the inverse of $\underline{G}$ of equation (7.11)) can be plotted, which is a function of f_1 and f_2. The minima (or minimum) of this surface represent the optimal points of the sequential design criterion. Figures 7-3 and 7-4 show the surface of the sequential design objective function along with the optima, indicated by "•", for multiplicative and additive error types, respectively. As can be seen in Figure 7-3, for the multiplicative error, the surface has a "parachute" shape and the corners are the minima of the surface (the optimal points shown in Figure 7-2). For the additive error, as shown in Figure 7-4, the design criterion surface has six minima with the same

amount of information, which are shown with "•" in the figure (also plotted in Figure 7-2). The results in Figures 7-2 to7-4 clearly show that the sequential design scheme for ternary experiments leads to very similar points as the initial design. It is, therefore, reasonable to suggest that carrying out experiments at these feed compositions or replicating the initial optimal points can lead to the same level of improvement in the precision of the ternary reactivity ratios.

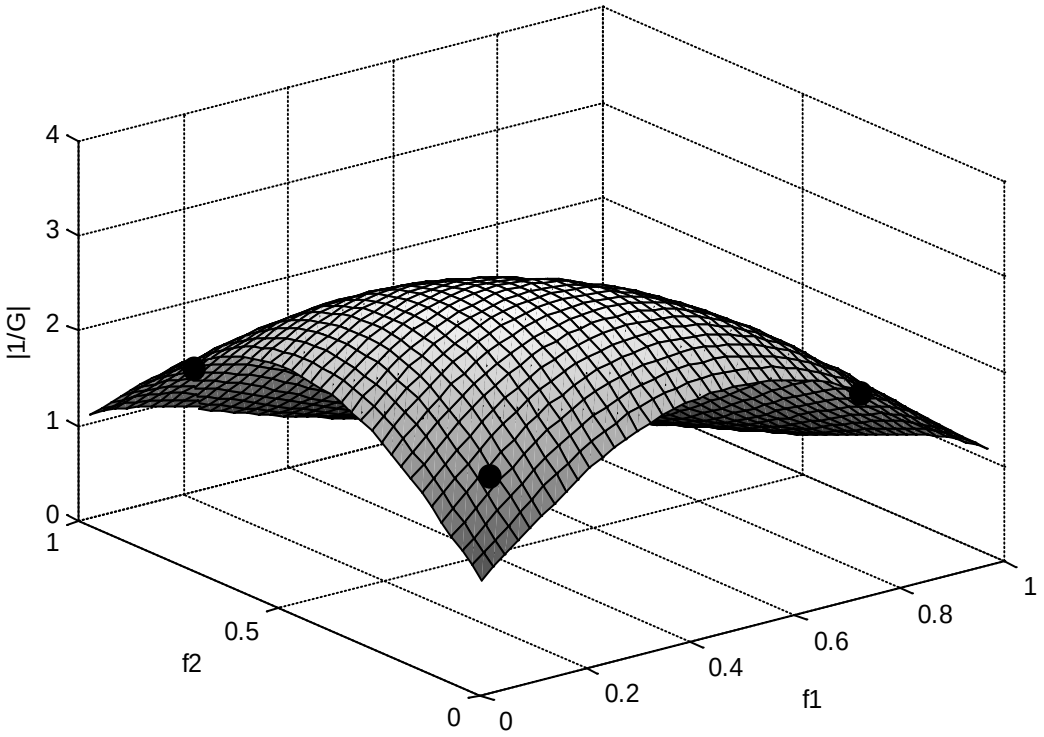

Figure 7-3. The objective function surface for the sequential design criterion with multiplicative error (ideal terpolymerization system, with "•" as the optima)

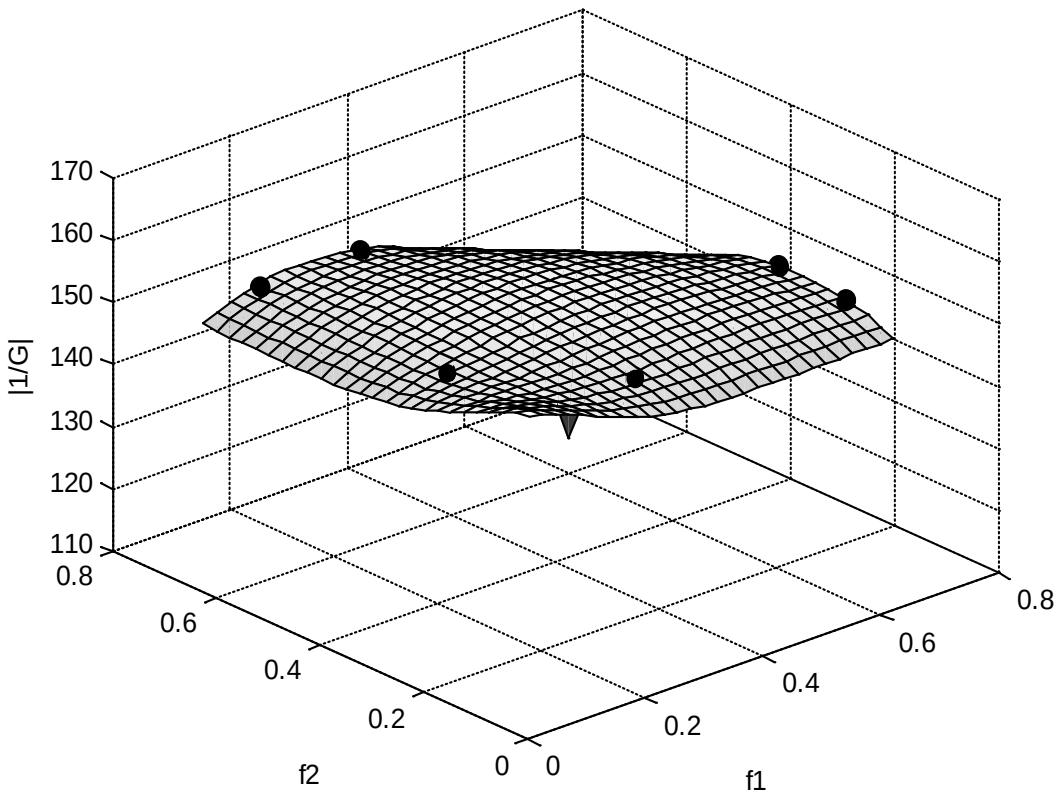

Figure 7-4. The objective function surface for the sequential design criterion with additive error (ideal terpolymerization system, with "•" as the optima)

The final point in the investigation of the optimal feed compositions in an ideal terpolymerization system concerns the anti-correlation criterion. This criterion, which is based on the maximization of the determinant of the correlation matrix $\underline{C}$, as shown in equation (7.12), was implemented for both types of errors and the results are shown in Figure 7-5. The left-side triangle presents results for the additive error, while the right-side triangle presents those for the multiplicative error structure, with circles "o" denoting the anti-correlation optimal points and squares "□" the maximum information optimal points (for the initial design, as shown in Figure 7-1). As can be seen in Figure 7-5, for the additive error, the optimal points shift towards the corners of the feasible region when the reduction of the correlation is the objective of the design, while for the multiplicative error the optimal points remain at the same locations.

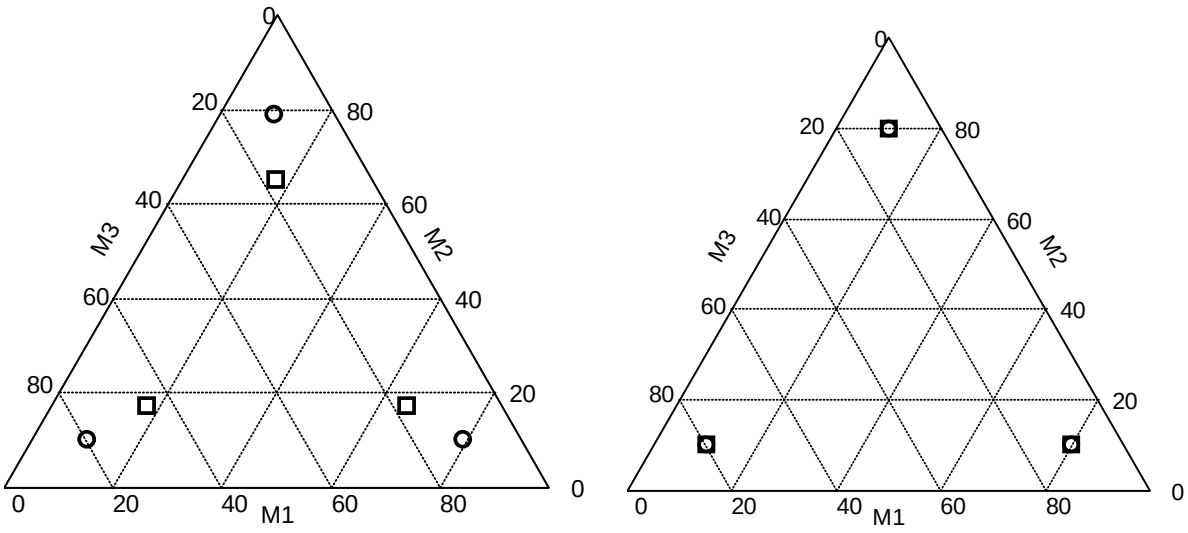

Figure 7-5. Anti-correlation optimal feed compositions for: (left) additive error, and (right) multiplicative error, with "□" as the maximum information and "o" as the anti-correlation design

These results suggest two important points. Firstly, that by moving towards the corners of the triangle and enriching the feed composition with one of the three monomers, the effect of the presence of one monomer is dominant and therefore the interaction between the monomers is such that the correlations between the reactivity ratios of the monomers are reduced. Secondly, the maximum information designed experiments do fulfill the requirement for least correlation as well, and therefore implementation of this criterion may not be necessary in most cases (in order to simplify the numerical problem). It must be noted, however, that the anti-correlation criterion presents a very useful solution and offers valuable guidance when dealing with highly correlated situations.

7.3.2 Illustrative case study

The terpolymerization system of N,N-dimethylaminoethyl methacrylate (DMAEM, M_1), methyl methacrylate (MMA, M_2), and dodecyl methacrylate (DDMA, M_3) (Soljic et al. (2010)) was investigated for ternary reactivity ratio estimation in Chapter 6. Soljic et al. (2009,2010) reported the binary reactivity ratios that were estimated based on copolymerization data from separate binary copolymerization trials (i.e., DMAEM/MMA, DDMA/MMA, and DMAEMA/DDMA). These values

are cited in Table 7-3 as “binary” reactivity ratios. Table 7-3 also includes reactivity ratios that were estimated directly from terpolymerization data (see, Chapter 6, Table 6-1). Our goal in this case study is to illustrate the application of the EVM design criterion for estimating ternary reactivity ratios, and to investigate the following questions in order to shed more light on the significance of this approach in improving the precision of ternary reactivity ratios. The questions considered in the following subsections are:

(1) What are the optimal feed compositions for this system?

(2) What is the effect of using the experimental feed versus the optimal feed compositions?

(3) What is the effect of using ***only*** the experimental data close to the optimal points?

7.3.2.1 What are the optimal feed compositions for this system?

Optimal feed compositions for the ternary system of DMAEM/MMA/DDMA were determined by implementing the design criterion as given in equation (7.7) with the multiplicative error structure. The optimal compositions are shown in Table 7-2 and also illustrated in the triangular composition plot of Figure 7-6. This figure also includes the actual experimental feed compositions used, as cited in Table 7-2. As can be seen from this triangular plot, the optimal points for this system are very close to the corners of the triangle. Also, comparing these optimal points with the results from the ideal system of section 7.3.1, shown in Figure 7-1, we can see that the optimal points are almost identical in both cases. This observation is mainly due to the fact that the “binary” reactivity ratios for this system, as shown in Table 7-3, are not very different from each other.

Table 7-2. Terpolymerization data for DMAEM (M_1)/MMA (M_2)/DDMA (M_3); experimental data from Soljic et al. (2010); optimal feeds from this work

	Feed composition			Experimental terpolymer composition		
	M_1	M_2	M_3	M_1	M_2	M_3
Experimental compositions	0.100	0.100	0.800	0.114	0.084	0.802
	0.800	0.100	0.100	0.310	0.118	0.099
	0.100	0.700	0.200	0.128	0.690	0.182
	0.100	0.400	0.500	0.125	0.381	0.494
	0.200	0.200	0.600	0.243	0.118	0.569
	0.200	0.500	0.300	0.237	0.476	0.287
	0.400	0.100	0.500	0.422	0.090	0.488
	0.400	0.400	0.200	0.423	0.378	0.199
	0.600	0.200	0.200	0.599	0.195	0.206
	0.560	0.410	0.030	0.563	0.404	0.033
Optimal feed compositions	0.100	0.790	0.110			
	0.790	0.110	0.100			
	0.100	0.100	0.800			

Table 7-3. Reactivity ratio estimates from various data sets

	r_{12}	r_{21}	r_{13}	r_{31}	r_{23}	r_{32}
Binary experiments (Soljic et al. (2010))	0.85	0.86	0.79	0.75	1.12	1.19
Ternary experiments (Chapter 6, Table 6-1)	0.8	0.75	0.80	0.80	1.09	1.20
Simulated optimal experiments	0.85	0.86	0.78	0.76	1.15	1.19
Informative experiments	0.74	0.73	0.91	0.89	1.18	1.36
Non-Informative experiments	0.86	0.78	0.77	0.69	1.03	1.02

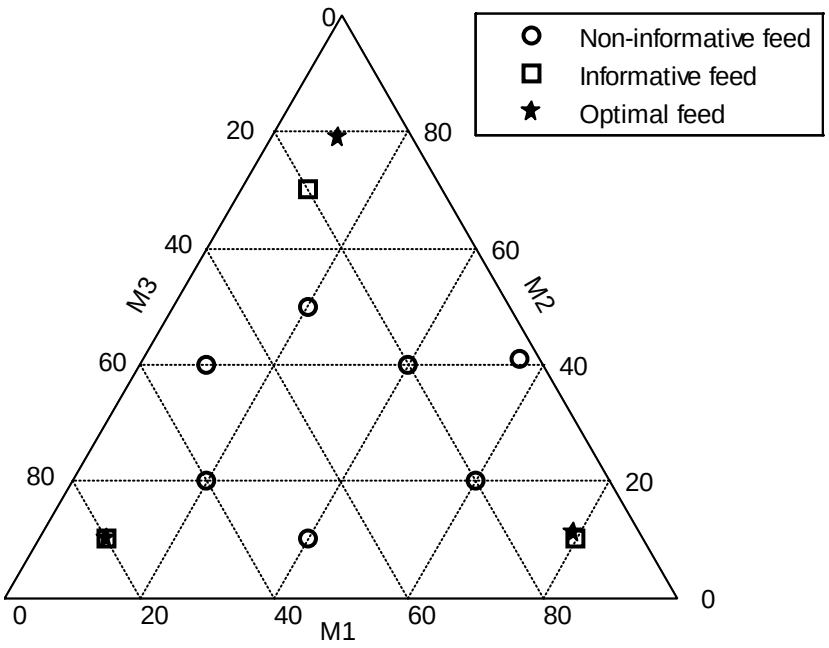

Figure 7-6. Terpolymerization composition triangular plot with experimental and optimal data

7.3.2.2 What is the effect of using the experimental feed versus the optimal feed compositions?

In order to study the effect of using optimal points versus the actual experimental feed points (usually arrived at randomly), the optimal feed compositions (of subsection 7.3.2.1), as shown in the last three rows of Table 7-2, were used to simulate terpolymerization experiments with the instantaneous composition equations (equations (7.3-7.5)). The binary reactivity ratios were used for simulating these experiments and random errors (1% for feed composition and 5% for terpolymer composition) were added to the simulated data set. Subsequently, the data set (with the added error) was used for reactivity ratio estimation. The point estimates are shown in the "simulated optimal experiments" row of Table 7-3.

To evaluate the amount of information from these two data sets, the joint confidence regions (JCR) for the reactivity ratio estimates are calculated in Figure 7-7. The JCRs are shown for reactivity ratios pairs of (r_{12}, r_{21}), (r_{13}, r_{31}), and (r_{23}, r_{32}). The JCRs with dashed lines represent the results from the original experimental data set, while the JCRs with solid lines represent the results from the simulated

optimal data set. Based on these results, it can be seen that the reactivity ratio estimates from the simulated data points are close to the binary reactivity ratios, as they were simulated using these binary values. However, Figure 7-7 shows clearly that the JCRs for reactivity ratios from the optimal data set are all considerably smaller than the JCRs for reactivity ratios from the original experimental data set. These results confirm that only three optimal experiments could provide an adequate amount of information for estimating ternary reactivity ratios for this system with even higher precision than the original data set that employed (unnecessarily) ten different feed compositions.

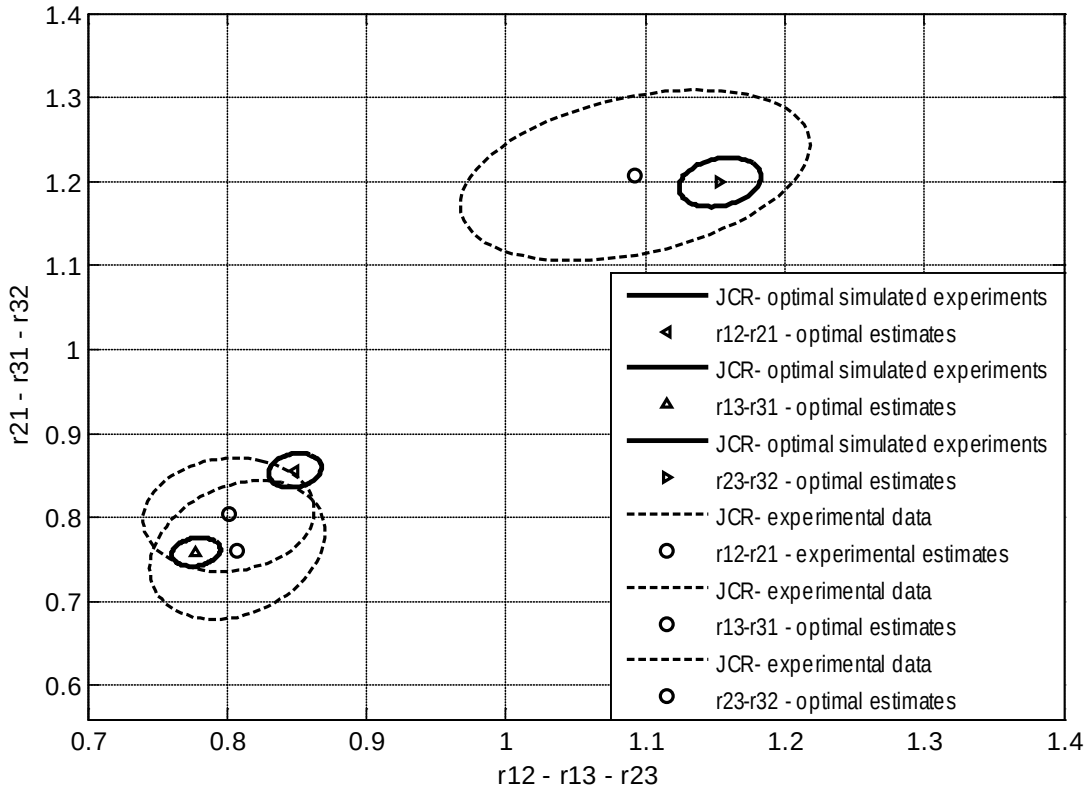

Figure 7-7. Optimal versus experimental data sets: reactivity ratio estimation results

7.3.2.3 What is the effect of using only the experimental data close to the optimal points?

The previous analysis points to the fact that only three experiments at optimal locations can provide enough information for all six reactivity ratios to be estimated. While the use of simulated optimal experiments confirmed this point, it would be much more interesting to see if the real experimental

points, cited in Table 7-2, support this observation as well. To perform this check, we divided the experimental feeds into two groups, namely those of “informative” and “non-informative” feed data sets. These two data sets are shown in Figure 7-6. The informative feed compositions, denoted by squares in this figure, are located close or exactly over the optimal feed composition, and thus these experiments are expected to contain more information than the rest of the data points. Subsequently, the remaining data points that are mainly located towards the center of the triangular plot of Figure 7-6, denoted by circles, were considered as the non-informative feed compositions, carrying less information.

Next, in order to see the effect of using the informative feed compositions compared to the non-informative ones, these two data sets were used for estimating reactivity ratios separately. The point estimates are reported in Table 7-3, at the “informative” and “non-informative” rows, respectively, and the JCRs from both data sets are shown in Figure 7-8, for the three reactivity ratios pairs. The results in Figure 7-8 clearly show that for each pair of reactivity ratios, the point estimates using the informative data set are slightly different from those from the non-informative data. However, the JCRs for the informative data set are all considerably smaller, even though the informative data set has less than half of the sample size of the non-informative data set (3 points versus 7 points). This is a very important observation, confirming that the large amount of information in the informative feeds, compared to the rest of the experiments, results in estimated reactivity ratios of higher precision. This also confirms that the feeds that are far from the optimal ones (the seven points, designated by circles in Figure 7-6 and concentrated at the center of the triangle) carry less information to the extent that even having more than twice as much feed points could not compensate for the non-informative nature of these data points.

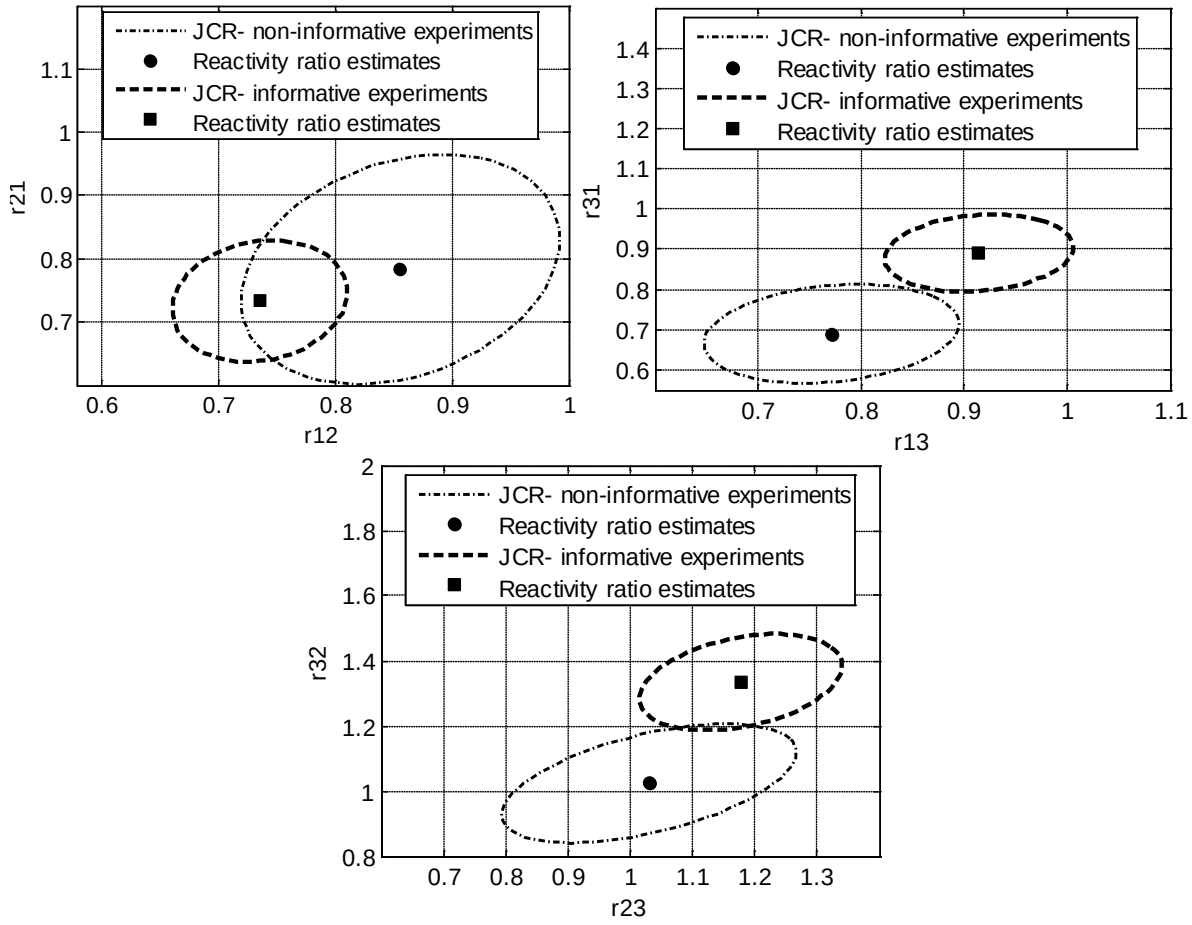

Figure 7-8. Informative versus non-informative reactivity ratio estimation results; see also Figure 7-6

7.3.3 Relation between reactivity ratio values and optimal feed compositions

So far, our observations and results of determining optimal feed compositions for several ternary systems point to very important conclusions: optimal terpolymerization feed compositions for estimating ternary reactivity ratios can be calculated by implementing the EVM design criterion; there are three optimal feed points and their locations depend on the values of the reactivity ratios; these optimal points are located close to the border of the feasible region, i.e., close to the corners of the triangular plot. These conclusions, while confirming the significance of using the EVM design criterion, can also lead to a very useful *rule of thumb*. That is, the regions at the corners of the

triangular terpolymerization plot are “suboptimal” regions from which optimal experiments can be selected without having to deal with the EVM design criterion directly.

However, in order to support such a statement, an in-depth investigation about the relation between the values of the reactivity ratios and the location of the optimal feed points is necessary, especially to identify systems where this general rule of thumb might not apply. That is, we can either use the rule of thumb and select experiments from the “suboptimal” regions, or we can establish relations between the values of the reactivity ratios and the location of optimal feed points, and subsequently, arrive at practical heuristics that can suggest optimal points for a specific system without having resort to numerically complex calculations each time.

To explore the possibilities when dealing with systems with different reactivity ratios, we defined 8 hypothetical terpolymerization systems, namely systems A to H, with different values of reactivity ratios. The selection of these systems was based on the ratios of their reactivity ratio values, that is (r_{12}/r_{21}), (r_{13}/r_{31}), and (r_{23}/r_{32}). The different ratios were obtained by assigning either 0.5, 1.5, and 5 to the reactivity ratio values, in a way that these ratios can be 0.1, 0.3, 1, 3, and 10. For instance, system A represents a terpolymerization system where M_1 is more reactive that M_2 (r_{12}/r_{21}=3) and M_2 is more reactive than M_3 (r_{23}/r_{32}=3), and so by comparison, M_1 is much more reactive than M_3 (r_{13}/r_{31}=10). This situation can be in the reverse order as well, which is the case for system D. These systems with the corresponding reactivity ratio values and the ratios of their reactivity ratio values are shown in Table 7-4.

Next, for each of the systems in Table 7-4, optimal feed compositions were determined, using the EVM design criterion (equation (7.7)) with the additive and multiplicative error types. These optimal feed compositions are reported in Tables 7-5 and 7-6, respectively. Table 7-5 shows that for additive error, ternary systems with considerably different reactivity ratio ratios have different optimal feed compositions. On the other hand, Table 7-6 shows that for multiplicative error, the optimal feed compositions are always the same as with the ideal system of section 7.3.1. Moreover, in order to have a better visual idea about the relation between the reactivity ratios of each system and the location of the optimal feed points, Table 7-7 presents these results for each system in the form of a radar chart, where the magnitudes of the ratios of reactivity ratio values are plotted, along with the corresponding triangular plot with the optimal feed points presented for additive and multiplicative error structures.

Table 7-4. Hypothetical terpolymerization systems

	A	*B*	*C*	*D*	*E*	*F*	*G*	*H*
r_{12}	1.5	0.5	1.5	0.5	0.5	5.0	5.0	0.5
r_{21}	0.5	1.5	0.5	1.5	5.0	0.5	0.5	0.5
r_{13}	5.0	1.5	0.5	0.5	0.5	1.5	5.0	5.0
r_{31}	0.5	0.5	1.5	5.0	1.5	0.5	0.5	0.5
r_{23}	1.5	5.0	0.5	0.5	1.5	0.5	0.5	5.0
r_{32}	0.5	0.5	5	1.5	0.5	1.5	0.5	0.5
r_{12}/r_{21}	3.0	0.3	3.0	0.3	0.1	10	10	1.0
r_{13}/r_{31}	10	3.0	0.3	0.1	0.3	3.0	10	10
r_{23}/r_{32}	3.0	10	0.1	0.3	3.0	0.3	1.0	10

Table 7-5. Optimal feed compositions for systems A to H of Table 7-4; additive error

A	f_1	f_2	f_3	*B*	f_1	f_2	f_3
expt. 1	0.10	0.11	0.79	**expt. 1**	0.60	0.10	0.30
expt. 2	0.44	0.16	0.40	**expt. 2**	0.11	0.10	0.79
expt. 3	0.10	0.60	0.30	**expt. 3**	0.16	0.44	0.40
C	f_1	f_2	f_3	*D*	f_1	f_2	f_3
expt. 1	0.11	0.79	0.10	**expt. 1**	0.30	0.60	0.10
expt. 2	0.60	0.30	0.10	**expt. 2**	0.79	0.11	0.10
expt. 3	0.16	0.40	0.44	**expt. 3**	0.40	0.16	0.44
E	f_1	f_2	f_3	*F*	f_1	f_2	f_3
expt. 1	0.79	0.10	0.11	**expt. 1**	0.44	0.40	0.16
expt. 2	0.40	0.44	0.16	**expt. 2**	0.10	0.30	0.60
expt. 3	0.30	0.10	0.60	**expt. 3**	0.11	0.79	0.10
G	f_1	f_2	f_3	*H*	f_1	f_2	f_3
expt. 1	0.10	0.10	0.80	**expt. 1**	0.54	0.10	0.36
expt. 2	0.10	0.80	0.10	**expt. 2**	0.10	0.54	0.36
expt. 3	0.50	0.25	0.25	**expt. 3**	0.10	0.10	0.80

Table 7-6. Optimal feed compositions for systems A to H of Table 7-4; multiplicative error

A-H	f_1	f_2	f_3
expt. 1	0.10	0.10	0.80
expt. 2	0.80	0.10	0.10
expt. 3	0.10	0.80	0.10

Table 7-7. Ratio radar charts and optimal feed composition triangular plots for systems A to H; additive "o" and multiplicative "□" error

A	B
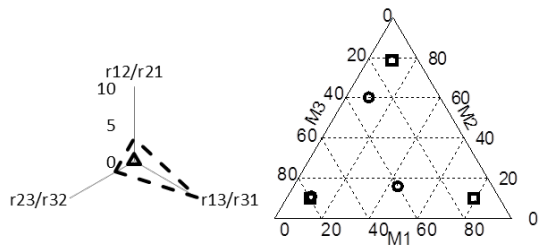	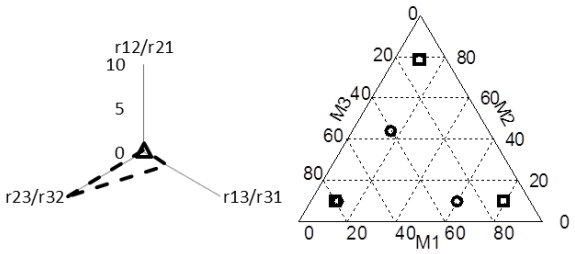
C	D
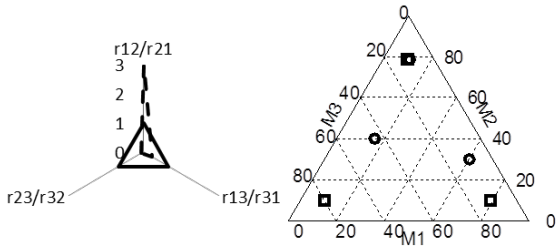	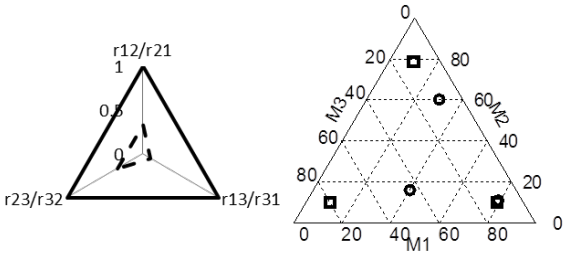
E	F
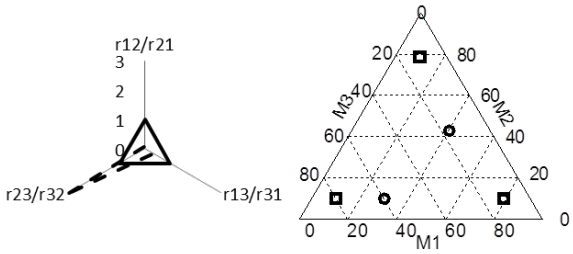	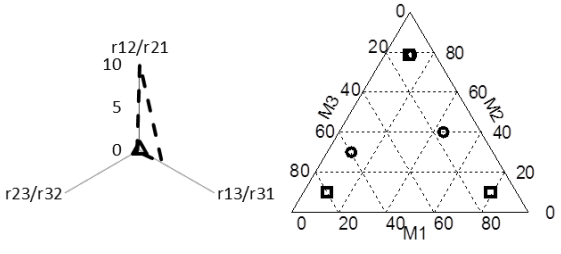
G	H
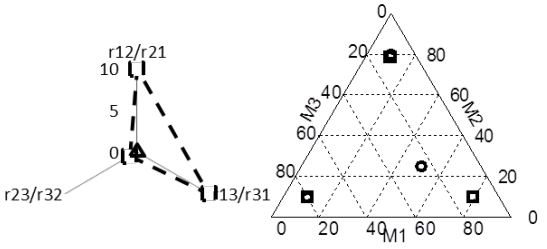	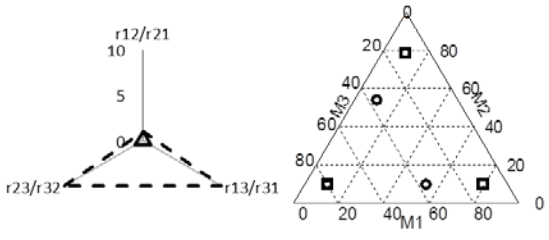

According to the results presented in Tables 7-5 to 7-7, we can highlight the following points:

(1) The optimal feed compositions for all systems, A-H, with multiplicative error, are in exact agreement with the locations of the optimal points of the ideal system.

(2) For systems A to F, with additive error, the reactivities of the three monomers decreases consecutively and the ratios of the reactivity ratios are considerably different from 1, and thus, not all three optimal feed compositions are located close to the corners of the triangle. Instead, two of them are located away from the corner so that the most reactive monomer has less of a presence in the feed mixture (and hence, in the polymerization).

(3) For systems G and H, with additive error, where two monomers have equivalent reactivities and are much more reactive or less reactive than the third monomer, the optimal feed points are located such that the two equally reactive monomers have the same mole fraction in the feed compositions.

An overall look at all the results with the additive error structure shows how the design can moderate its extreme optimal feed compositions when one or two monomers show higher reactivities than others. The optimal feed composition moves away from the corners to favor the less reactive monomers, depending on the extent of the difference between reactivity ratios. Nonetheless, for the multiplicative error, the tendency towards the extremes of the feasible region overcomes the effect of the variation of the reactivity ratios and the optimal feed compositions are consistently at the same location.

7.3.4 Practical heuristics for determining optimal feed compositions

Our findings in the previous sections point towards a very practical solution that can be used for this design problem in order to, firstly, reduce the computational load of executing the design procedure numerically, and secondly, promote the application of this design procedure for estimating ternary reactivity ratios among practitioners, since this is a rather new research area with a substantial research potential.

Such a practical heuristic is a result of calculating optimal feed compositions for a large number of ternary systems. This heuristic is depicted in Figure 7-9, indicating the “suboptimal” regions (as the

shaded areas), which contain the optimal feed compositions (provided, of course, that these regions do not violate any other process constraints). The ideal optimal feed compositions are also contained within these regions. With paying careful attention to the feasible region for experimentation, three experiments chosen from the shaded areas can provide the optimal feed compositions for estimating reliable reactivity ratios in ternary systems. As these points move toward the corners of the triangular plot, the information content of the final optimal data set would be higher.

It must be pointed out that our heuristic is based on our results with the multiplicative error structure, as it has been repeatedly mentioned throughout this thesis that the error associated with experimental data in our field is usually in the form of a certain percentage of the measured observation; hence, most of the practitioners "believe" that the error is multiplicative in nature.

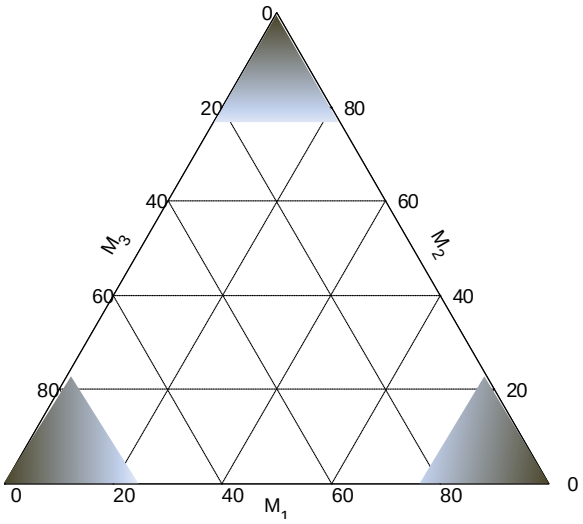

Figure 7-9. Terpolymerization composition triangle with optimal feed compositions as shaded areas

7.4 Concluding Remarks

This chapter focuses on the model-based design of experiments for the purpose of estimating terpolymerization reactivity ratios. This optimal design strategy is part of our approach to the problem

of estimating ternary reactivity ratios, as described for copolymerization systems in Chapter 4. The design of experiments for the problem of estimating ternary reactivity ratios is considered for the first time in the literature.

The design of experiments is presented within the EVM statistical context, and the structure of the EVM design criterion is studied in detail by looking at the formulation of the objective function, the definition of the feasible regions, the number of optimal points, and the error structure of the data. Paying attention to these details ensures that the design criterion matches the characteristics of the problem and the results are reliable and accurate.

The results of implementation of the EVM design criterion for this problem are presented in three parts. Firstly, the different aspects of implementing this design criterion are discussed for the ideal terpolymerization system where all the reactivity ratio values are equal to unity, for easier visualization of the results. Secondly, an illustrative case study with terpolymerization data from Soljic et al. (2010) is presented, where the effect of using optimal feed compositions versus preliminary (non-optimal) experiments on the quality of the reactivity ratios is investigated. Finally, the overall trends and observations from studying several ternary systems point towards a distinct pattern for locating optimal feed compositions in a terpolymerization system without having to carry out each time the full mathematical calculations. Practical heuristics follow for easily locating optimal feed compositions.

Overall, the contributions of this work are very important for resolving the issue of ternary reactivity ratio estimation. The common perception of “more experiments, better estimates” is seriously challenged in this chapter, showing that only three experiments, arrived at in an optimal or suboptimal fashion, each one rich in one of the monomers, are adequate in providing sufficient information for estimating six reactivity ratios for ternary systems. The mathematical derivations for the design criterion and the details of the implementation of the approach are useful not only for research in the area of reactivity ratio estimation but also for problems dealing with the more general multi-response design of experiments. Moreover, the simple heuristics for locating optimal feed compositions can greatly promote the idea of using designed experiments in such studies for the practitioners.

Chapter 8

Experimental Verification of the EVM Framework for Terpolymerization Reactivity Ratio Estimation

Experimental verification is an important step in the development and use of mathematical models and statistical analysis. The experimental information and data allow us to assess the reliability of developed theoretical concepts and, in turn, reinforce the ability and potential of the mathematical approach under study. The problem of estimating ternary reactivity ratios, which is a rather new research area with very little related studies in the literature, has been extensively studied in Chapter 6 using experimental data from several terpolymerization systems from the literature. Subsequently, Chapter 7 examined, for the first time, the problem of the design of experiments for the purpose of estimating ternary reactivity ratios. Since our main objective is to verify the EVM framework for this largely unstudied problem, this chapter explains the steps in the EVM framework for estimating ternary reactivity ratios and presents the results of an experimental verification project for the implementation of this framework.

The terpolymerization system chosen in this chapter is rather new; the kinetics of the terpolymerization and the monomer reactivity ratios have never been studied before. Firstly, the experimental procedure and the techniques for collecting data are explained. Next, the parameter estimation and the implementation of the design of experiments strategy are discussed. Finally, the reactivity ratio estimates obtained from the experimental data along with the interpretation of their precision and accuracy are discussed in detail.

8.1 Introduction and literature review

As discussed throughout this thesis, the relative reactivities of monomers (towards their radicals) present in the reaction medium govern monomer reactivity ratios, which are crucial to the study of the kinetics of multicomponent polymerization systems. Terpolymerization systems are frequently utilized in industry and they possess valuable information for academic research as well, yet there is a considerable lack of reactivity ratio estimation studies for such systems. We looked at the problem of

reactivity ratio estimation and the design of experiments for the purpose of estimating reliable reactivity ratios earlier. However, as mentioned in Chapter 5, it is important that we put together these techniques along with explanations and comments based on our experience within the structure of a recommended framework that clearly guides practitioners towards determining ternary reactivity ratios for any given system. In addition, experimental verification of such a framework is a very important step. It gives us the chance to explore the potentials of the EVM framework with real experimental data and evaluate the efficiency and performance of our approach for arriving at reliable reactivity ratio estimates.

The terpolymerization system that we selected for the experimental verification step is a water-soluble polymer that has been broadly utilized in industry. Water-soluble polymers, as polymers that are highly hydrophilic and therefore soluble in water, find applications in a wide variety of areas such as Enhanced Oil Recovery (EOR), dewatering, superabsorbent hydrogels (cosmetics and bio-medical applications), mineral processing, flocculants, and etc. Most applications of these materials arise from their role in modifying the rheology of an aqueous medium and/or adsorbtion onto particles (Stahl and Shulz (1986)). Generally, the objectives for using these polymeric materials are (i) rheological control, where these polymers can control the viscosity of the solution, (ii) adsorption, stabilization, and flocculation, where adsorption of these polymers onto the surface of a dispersed particle may affect at stabilization or flocculation characteristics, and (iii) gels, where cross-linked polymers can swell in water and create hydrogels (Finch (1996)).

Among the synthetic water-soluble polymers, polyacrylamide (PAAm) is widely used in many applications. Since it is often difficult for one single polymer to meet all of the requirements of an application, copolymers and terpolymers (i.e., acrylamide (AAm) with one or two other monomers) are usually employed in order to deliver specific properties. AAm shows favorable reactivity ratios with many monomers, which allows for a large number of co- and ter- polymers to be made (most or all are compatible with the human body or skin). One of the most important copolymers of acrylamide is with acrylic acid (AAc). The AAm/AAc copolymer can be used in many of the above-mentioned applications, such as the EOR application that has gained more attention recently (Wei et al. (2013)).

Some of the requirements of the AAm/AAc copolymer for EOR applications are thermal and shear stability for the harsh environment of the oil field. However, it has been reported that the AAm/AAc

copolymer shows signs of degradation under such conditions, and therefore, the addition of a third monomer with higher thermal and shear stability has been suggested to overcome this problem. One of the monomers in particular that can enhance AAm/AAc copolymer stability in harsh environments is 2-Acrylamido-2-methyl-1-propanesulfonic acid (AMPS). AMPS is a larger monomer molecule compared to AAm and AAc that results in better thermal and shear stability of the final polymer and, in turn, makes the polymer more suitable for EOR application (Zaitoun et al. (2012)).

The copolymerization of AMPS/AAm has received considerable attention in the literature. Examples of the applications of this copolymer can be found for EOR (McCormick and Chen (1982) and Qi et al. (2013)) and superabsorbent hydrogels (Durmaz and Okay (2000), Rosa et al. (2002), Zhang et al. (2003), and Liu et al. (2004)). For the copolymerization of AMPS/AAc, on the other hand, there are fewer studies available with respect to various applications. This copolymer has been mainly studied for superabsorbent hydrogels in waste water treatment and drug delivery applications (see, for example, Pourjavadi (2007), Yu et al. (2012), Wang et al. (2013), and Zhu et al. (2014)). For both copolymerization systems, the studies are around the properties of the polymers, while their kinetics have been studied only in a few papers (mentioned later in section 8.3).

The AMPS/AAm/AAc terpolymer is a novel and largely unstudied system that has appeared in the literature within the past five years or so. Some of the applications for this terpolymer have been reported in oil-field drilling (Peng et al. (2010)), superabsorbent hydrogels (Bao et al. (2011)), EOR (Zaitoun et al. (2012)), sludge dewatering (Ma et al. (2013)), and controlled drug-delivery systems (Anirudhan and Rejeena (2014)). In these few studies, final properties of this terpolymer, such as the swelling behavior and resistance to temperature and shear stress, have been discussed, but there has been no work on the kinetics of this terpolymerization reaction reported. Since the characteristics of this terpolymer are directly related to its microstructure, it is essential to have a clear understanding of the terpolymerization kinetics. Therefore, the first step in this regard is to determine reliable reactivity ratios for this terpolymerization system.

In this chapter, we start by explaining the EVM framework for estimating ternary reactivity ratios in the form of a flowchart. Then the polymerization procedure for AMPS/AAm/AAc system is explained. Next, reactivity ratio estimates for the AMPS/AAm/AAc terpolymer are determined and discussed in detail, along with a comparison between using optimal designed experiments versus

preliminary experiments, and the effect of utilizing low and high conversion level data on reactivity ratio estimation results.

8.2 Reactivity Ratio Estimation Steps: The EVM Framework

In this section the complete procedure for estimating reliable ternary reactivity ratios for terpolymerizations is explained. This procedure is mainly based on the general approach of the EVM framework that was discussed in Chapter 5 for copolymerizations (Figure 5-1), but adjusted to meet the requirements of the terpolymerization problem. The implementation of this overall procedure is also experimentally demonstrated and verified with data from the AMPS/AAm/AAc terpolymerization system. A summary of the recommended approach is presented in the following steps and the flowchart of Figure 8-1.

1. Start with the given terpolymerization system.
2. Use the literature and the prior knowledge of this terpolymerization system to find reasonable preliminary reactivity ratios for this system and determine whether there are any constraints on the feed compositions.
   2.1. In the absence of any preliminary information, run preliminary experiments, with compositions rich in each of the three monomers (e.g., 80% or higher), and note any limitations in the feasible experimental region (constraints). Estimate preliminary ternary reactivity ratios.
3. The selection of optimal feed compositions is based on our prescriptions in Chapter 7, section 7.3.4. According to those prescriptions, choose three optimal feed compositions, each 80% in one monomer and equal amount of the other two (that is, f_i /f_j /f_k : (0.8/0.1/0.1), (0.1/0.8/0.1), and (0.1/0.1/0.8)). If the 80% content is not possible according to possible feed composition constraints, choose lower percentages than 80%.
4. Experiments should be performed at low conversion (≤ 5-10%) and up to medium-high conversion levels (50-70%). Collect data for terpolymer composition and corresponding conversion values.
5. Use the EVM parameter estimation methodology for estimating reactivity ratios. Refer to Chapter 6 for a detailed implementation of this method

5.1. For low conversion data, use the recast terpolymerization model (equations (6.10) to (6.13)).

5.2. For full conversion data, use the integrated DNI approach for the terpolymerization model (equations (6.17)).

6. Construct joint confidence regions for reactivity ratios. If satisfied with the precision of the results, move to the next step. If not satisfied, perform independent replicates of the optimal experiments and re-estimate reactivity ratios (replicating the optimal feed compositions is equivalent of including the sequentially optimal experiments, as described in section 7.2.2.1).
7. Present reactivity ratio estimates and their joint confidence regions.

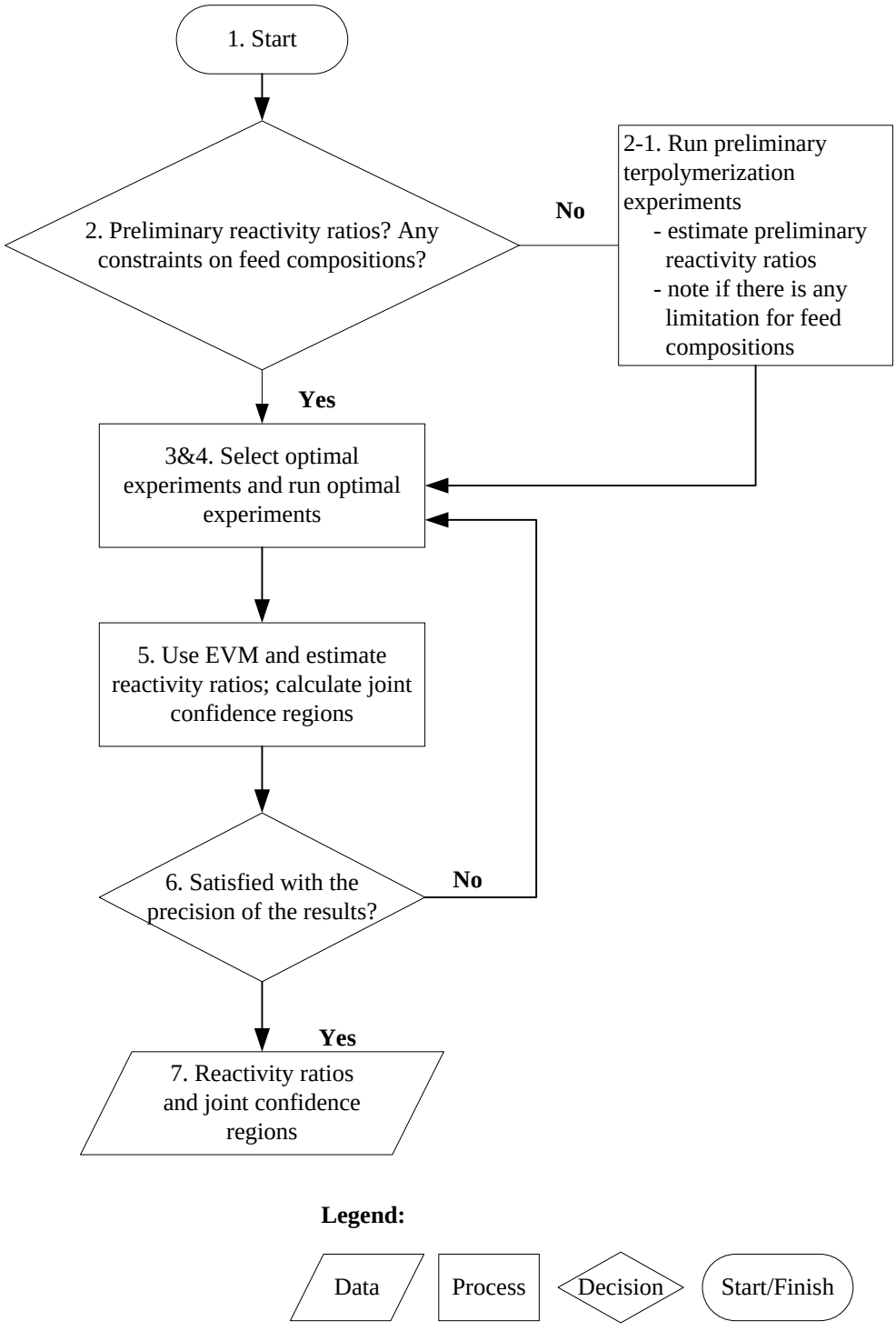

Figure 8-1. Flowchart of EVM framework for ternary reactivity ratio estimation

8.3 Experimental

8.3.1 Materials

The monomers 2-acrylamido-2-methyl-1-propanesulfonic acid (AMPS, 99%), acrylamide (AAm, 99%), acrylic acid (AAc, 99%), as well as the initiator (4,4′-azo-bis-(4-cyano valeric acid)), inhibitor (hydroquinone), sodium hydroxide, and sodium chloride were purchased from Sigma-Aldrich. Water was Millipore quality (18 MΩ cm^{-1}) and acetone and methanol were ACS grade from VWR. Nitrogen gas from Praxair (4.8 grade) was used for degassing of solutions.

8.3.2 Polymerization

AAc was purified by vacuum distillation at 30 °C. Primary monomer stock solutions with a total monomer concentration of 2 M were prepared with the chosen monomer fractions (see Table 8-3). In order to conduct all experimental runs at the same experimental conditions for important polymerization environment factors like pH and ionic strength (IS), various amounts of sodium hydroxide base and sodium chloride salt were added to the reaction mixture to control the pH and IS levels, respectively. A pH of 7 was chosen in order to make sure that there are only ionized AAc and AMPS in the system. After adding the initiator to the solution, the solution was further diluted with high purity water to achieve a total monomer concentration of 1 M. The chosen polymerization conditions are summarized in Table 8-1.

Table 8-1. Polymerization conditions

Monomer concentration (mol/ L)	Initiator concentration (mol/L)	pH	T (^{o}C)
1	0.004	7	40

The solution was purged with nitrogen gas for 120 minutes with a gas flow rate of 200 mL/min, while being kept in ice and away from light to make sure the polymerization reaction was not initiated before the desired time. Then, 20 mL of solution were transferred to a vial (fitted with crimped rubber seals) using the cannula transfer method (Riahinezhad et al. (2013)). For the polymerization, the vials were put in a temperature-controlled water shaker-bath (Grant, OLS200) at 40 °C and 100 rpm. They were removed at specific time intervals and chilled in an ice bath. A few drops of inhibitor solution were quickly syringed into the vials to stop any further polymerization.

8.3.3 Characterization

To determine monomer conversion, precipitation and gravimetry methods were used. After polymerization, polymer products were precipitated using a 10-fold excess of acetone and methanol. Then, the polymer products were filtered (paper filter grade number 41, Whatman) and put in a vacuum oven at 50 °C until they reached constant weight (7 days). Monomer conversions were determined as polymer mass over initial monomer mass.

Elemental analysis (CHNS, Vario Micro Cube, Elementar) was used to measure the C, H, N, and S contents of the samples. The terpolymer composition was subsequently calculated based on the percentages of the S, N and C elements only (in order to remove the effect of residual water in the samples, which causes variability in the percentage of H). Appendix H shows sample calculation for conversions and terpolymer composition.

8.4 Results and Discussion

This section illustrates the complete procedure for estimating ternary reactivity ratios using the EVM framework for the AMPS/AAm/AAc terpolymerization system. The first subsection presents preliminary reactivity ratios for the three binary copolymerization systems. Since there has been no prior kinetic study for this terpolymerization in the literature, the binary values are chosen as preliminary reactivity ratios. Next, the preliminary experimental results are reported that are used in order to determine the constraints on the feasible region for feed compositions. Subsequently, the optimal feed compositions along with the experimental data set used for the reactivity ratio estimation are presented. Finally, the terpolymer composition trajectory as a function of conversion is calculated based on the optimal reactivity ratio estimates, and the agreement between predicted and experimental data is examined.

8.4.1 Preliminary reactivity ratios (Step 2, Figure 8-1)

As mentioned earlier, the preliminary values of the binary reactivity ratios for AAm/AAc, AMPS/AAm, and AMPS/AAc copolymerizations were obtained from the literature. Table 8-2 presents a list of these reactivity ratio values.

For AAm/AAc copolymerization, Riahinezhad et al. (2013) conducted a thorough investigation for the reactivity ratios of this copolymerization system at exactly the same polymerization conditions that are used in this work, and thus, these reactivity ratios are chosen, confidently, as the binary reactivity ratios for the AAm/AAc pair.

For AMPS/AAm copolymerization, as shown in Table 8-2, there are four sets of reactivity ratios for these monomers in the literature. The variation in the values of reactivity ratios emphasizes our point about the inconsistencies in the binary reactivity ratios pairs in the literature, and that random selection from these values as ternary reactivity ratios may have serious consequences. In our work, due to the importance of pH, we selected the reactivity ratios from McCormick and Chen (1982), since the pH was similar to our experimental conditions and other literature sources did not even report the employed pH level.

For AMPS/AAc copolymerization, there are only two publications in the literature where the reactivity ratios were estimated for this system. Again, for the same reasons as above for the AMPS/AAm system, the estimated reactivity ratios from Stahl and Shulz (1986) were chosen.

Table 8-2. Binary reactivity ratios from the literature for AAm/AAc, AMPS/AAm, and AMPS/AAc copolymerizations

Source	T(°C)	pH	r_{AAm}	r_{AAc}	r_{AMPS}	r_{AAm}	r_{AMPS}	r_{AAc}
Riahinezhad et al. (2013)	40	7	1.33	0.23				
McCormick and Chen (1982)	30	7.4			0.50	1.02		
Aggour (1994)	x	x			0.62	1.21		
Abdel-Azim et al. (1998)	55	x			0.13	1.53		
Travas-Sejdic and Easteal (1999)	60	x			0.42	1.05		
Stahl and Shulz (1986)	x	7					0.19	0.74
Abdel-Azim et al. (1998)	55	x					0.15	0.98

"x" indicates missing information

8.4.2 Experimental data (Step 3, Figure 8-1)

As the first step in collecting experimental data for this system, six different feed compositions were selected for the preliminary dataset. These feed compositions are shown in Table 8-3 as well as in the ternary plot in Figure 8-2. These feed compositions were selected in a way that three points are located close to the corners of the triangular plot (i.e., rich in each of the three monomers), and three others are located in the middle section of the triangular plot. The preliminary experiments were run up to medium-high conversion levels.

Table 8-3. Feed compositions for AMPS/AAm/AAc preliminary experiments

Run #	$f_{0,\ AMPS}$	$f_{0,\ AAm}$	$f_{0,\ AAc}$
1	0.800	0.100	0.100
2	0.100	0.800	0.100
3	0.100	0.200	0.700
4	0.200	0.400	0.400
5	0.300	0.500	0.200
6	0.500	0.100	0.400

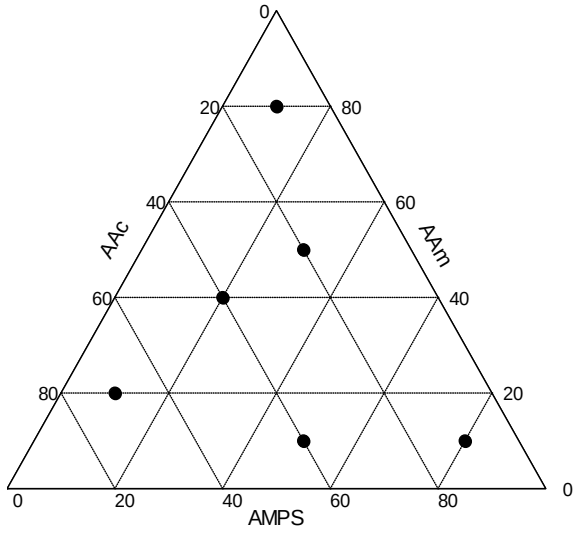

Figure 8-2. Triangular plot for chosen feed compositions for the AMPS/AAm/AAc terpolymerization experiments; see also Table 8-3

8.4.3 Design of experiments (Step 4, Figure 8-1)

Chapter 7 of this thesis is dedicated to establishing a procedure for locating optimal feed compositions for estimating reliable reactivity ratios for terpolymerizations. Based on the extensive discussions in that chapter, it is concluded that optimal feed compositions for ternary reactivity ratios estimation are located at the corners of the triangular composition plot for terpolymerizations. To visualize the location of the optimal feed compositions for this system, Figure 8-3 combines the "suboptimal" regions (see Chapter 7, Figure 7-9) as well as the three optimal points located close or inside these regions from Figure 8-2.

To confirm the feasible region for the optimal experiments with 80% of each monomer, we should find out whether runs with 80% of each monomer are successful. Runs #1 and #2 with 80% AMPS and AAm, respectively, showed no problems and the produced polymer was successfully precipitated for characterization. While run #3 with 70% AAc was also successfully performed and the polymer was successfully isolated, it is mentioned in the literature that achieving the exact optimal feed composition with 80% AAc could be problematic for isolating the polymer, and subsequently, filtering/precipitation due to phase separation (Stahl and Schulz (1988)). We did experience such types of difficulties in some preliminary tests that we performed, and thus, we decided that 70% would be the highest content allowable for AAc in the terpolymerization experiments in this study. So, it can be concluded that the optimal experiments have already been covered in the preliminary runs. Therefore, in the remainder of this chapter, feed compositions for runs #1, #2, and #3 will be referred to as the optimal data set, as opposed to the full data set as shown in Table 8-3. The influence of using these different data sets is studied in the following subsections.

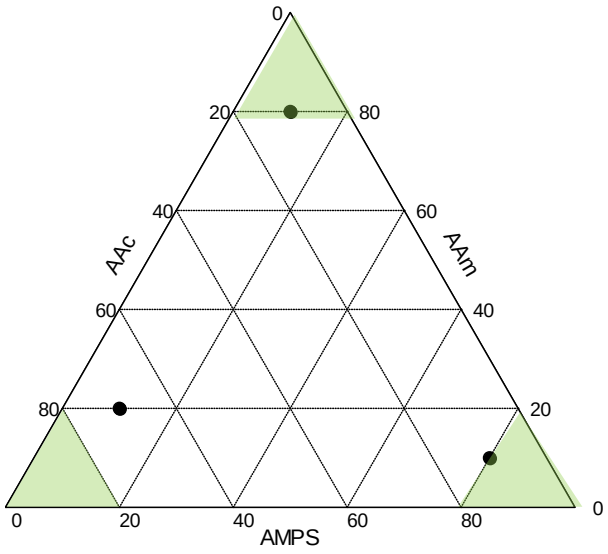

Figure 8-3. Optimal regions and 'optimal' feed compositions for AMPS/AAm/AAc terpolymerization

8.4.4 Parameter estimation results (Step 6, Figure 8-1)

8.4.4.1 Using low conversion experiments

The first attempt at estimating the reactivity ratios of the AMPS/AAm/AAc terpolymerization was done by analyzing low conversion data, similar to the conventional approaches for estimating reactivity ratios of copolymerizations and terpolymerizations (see Chapters 3 and 6 for more information). The preliminary low conversion experimental data (i.e., the full dataset) for the AMPS/AAm/AAc terpolymerization are reported in Table 8-4. The experimental data are limited to low conversion (below 10%), and they are given in terms of conversion (X_w), initial feed compositions (f_o), and the cumulative terpolymer compositions ($\overline{F}$). Also, these data points are categorized based on the run number, cited in Table 8-3. For analyzing low conversion data for estimation of reactivity ratios, the instantaneous terpolymer composition model and the EVM parameter estimation technique (see Chapter 6, section 6.3.2) were implemented. Using the instantaneous terpolymer composition for such data sets is only possible when the conversion level is low, as it can be assumed that the compositional drift in the reaction is negligible.

As mentioned in previous chapters (e.g., Chapter 3, section 3.2.1), the variability in our measurements is commonly specified as a percentage of the measured value, which can be interpreted as a uniformly distributed error within the range of ±*k%* of the measured value. For this terpolymerization system, the feed composition data were measured with typical approaches and thus, the value of *k* for the feed composition variable can be assumed to be the typical 1%. On the other hand, considering the associated difficulties in characterizing the experimental polymer properties for this water-soluble terpolymerization system, the *k* value for the terpolymer composition data can be assumed to be 10%, which is the largest typical error associated to composition values.

In this section, we used two experimental data sets. One contains the experimental results at low conversion (below 10%) for all six feed compositions, whereas the other has only three optimal feed compositions (i.e., runs # 1, #2, and #3). It is our intention to compare the reactivity ratio estimation results between these two data sets in order to highlight the potential of using optimally designed experiments (as discussed in section 8.4.3) for estimating reliable ternary reactivity ratios. The results of the reactivity ratio estimation from the low conversion data are reported in Table 8-5. In this table, the ternary reactivity ratio estimates from the low conversion-optimal and low conversion-full data sets are reported, along with binary reactivity ratios for the copolymerization systems of AMPS/AAm, AMPS/AAc, and AAm/AAc as mentioned in section 8.4.1. Table 8-5 also shows the ternary reactivity ratio estimates from medium-high conversion-optimal experiments, which will be discussed in section 8.4.4.2.

Table 8-4. Experimental data for AMPS/AAm/AAc terpolymerization; low conversion

Run	X_w	f_{AMPS}	f_{AAm}	f_{AAc}	$\overline{F}_{AMPS}$	$\overline{F}_{AAm}$	$\overline{F}_{AAc}$
#1	0.047	0.800	0.100	0.100	0.664	0.161	0.175
	0.057	0.800	0.100	0.100	0.693	0.187	0.120
	0.085	0.800	0.100	0.100	0.775	0.152	0.073
#2	0.025	0.100	0.800	0.100	0.101	0.826	0.073
	0.046	0.100	0.800	0.100	0.099	0.824	0.077
	0.078	0.100	0.800	0.100	0.103	0.827	0.070
	0.085	0.100	0.800	0.100	0.106	0.813	0.081
	0.098	0.100	0.800	0.100	0.081	0.754	0.165
#3	0.029	0.100	0.200	0.700	0.052	0.400	0.548
	0.035	0.100	0.200	0.700	0.037	0.402	0.561
	0.042	0.100	0.200	0.700	0.066	0.420	0.514
	0.055	0.100	0.200	0.700	0.084	0.364	0.552
	0.077	0.100	0.200	0.700	0.180	0.342	0.478
	0.081	0.100	0.200	0.700	0.119	0.380	0.501
	0.048	0.100	0.200	0.700	0.079	0.363	0.558
	0.089	0.100	0.200	0.700	0.103	0.330	0.565
#4	0.057	0.200	0.400	0.400	0.312	0.471	0.217
	0.100	0.200	0.400	0.400	0.241	0.499	0.260
#5	0.037	0.300	0.500	0.200	0.224	0.592	0.184
	0.059	0.300	0.500	0.200	0.245	0.518	0.237
	0.067	0.300	0.500	0.200	0.226	0.568	0.206
	0.070	0.300	0.500	0.200	0.245	0.546	0.209
#6	0.013	0.500	0.100	0.400	0.470	0.191	0.339
	0.026	0.500	0.100	0.400	0.498	0.165	0.337
	0.059	0.500	0.100	0.400	0.389	0.241	0.370
	0.036	0.500	0.100	0.400	0.470	0.188	0.342
	0.040	0.500	0.100	0.400	0.415	0.243	0.342
	0.078	0.500	0.100	0.400	0.468	0.195	0.337

Table 8-5. Reactivity ratio estimates for AMPS (M_1)/AAm (M_2)/AAc (M_3) terpolymerization

Experimental data	Conversion	Type	r_{12}	r_{21}	r_{13}	r_{31}	r_{23}	r_{32}
Full preliminary data	Low (<10%)	Ternary	0.58	0.89	0.73	0.80	0.99	0.21
Optimal data	Low (<10%)	Ternary	0.56	0.90	0.70	1.00	1.05	0.23
Optimal data	Medium-high	Ternary	0.46	0.93	0.57	0.92	1.08	0.24
Literature [a]	Low (<10%)	Binary	0.50	1.02	0.19	0.74	1.33	0.23

a: AMPS/AAc and AMPS/AAm from Aziz et al. (1998); AAm/AAc from Reihaninezhad et al. (2014)

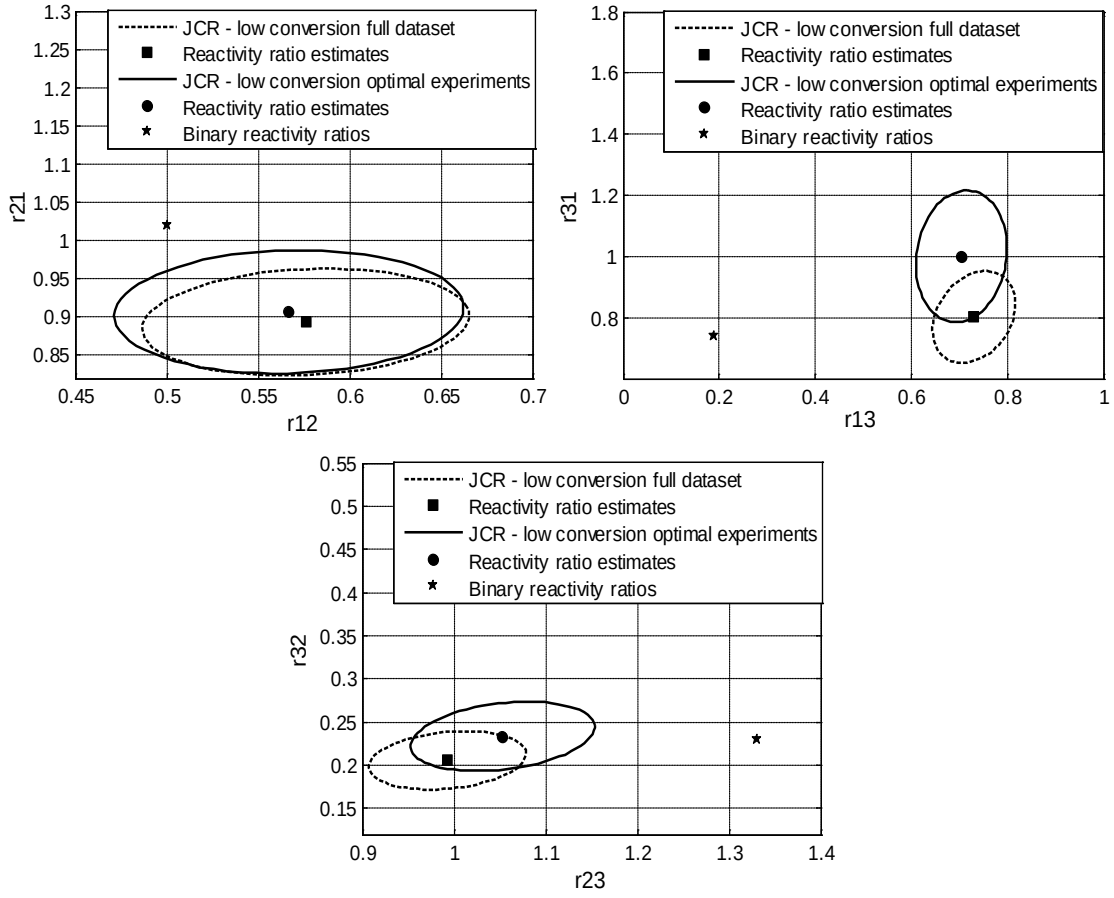

Figure 8-4. Optimal versus preliminary reactivity ratio estimation results for AMPS (M_1)/AAm (M_2)/AAc (M_3) terpolymerization; low conversion

In addition to the point estimates, the JCRs for the monomer pairs are shown in Figure 8-4, where the results from the optimal data are shown with solid line JCRs and the results from the full dataset are shown with dashed line JCRs. The results in Table 8-5 and Figure 8-4 show that the ternary reactivity ratios from AMPS/AAm/AAc can be estimated (satisfactorily) from low conversion experiments, either based on the full data set or only the optimal feed compositions. The point estimates obtained from the full data set compared to those of the optimal data set are not significantly different, confirming that both data sets lead to similar results. More importantly, it can be seen in Figure 8-4 that the JCRs for the reactivity ratio estimates from the optimal and the full data sets are all of almost equal size despite the fact that the optimal data set is composed of three feed compositions and the full data set contains six feed compositions!

These very interesting results, once again, support our points, mentioned in Chapter 7 and here, that the optimal feed compositions for terpolymerization systems contain sufficient amount of information for reliable estimation of the reactivity ratios. Also, they clearly show that the other three feed compositions (at the center of the triangle in Figure 8-2) have little information, and therefore, a very small contribution to the results of reactivity ratio estimation for this system (for more similar results, see Chapter 7, section 7.3.2.3).

As mentioned in the introduction, using binary reactivity ratios in place of ternary reactivity ratios is a common practice in the literature. In Chapter 6, we discussed in detail the potential problems with such a poor approximation, and the literature reviews for the reactivity ratios of AMPS/AAm and AMPS/AAc have shown, yet another, explicit example of the inconsistencies of binary reactivity ratios in the literature. Nonetheless, comparison between the ternary reactivity ratios from the current work and the binary reactivity ratios reported in the literature can be informative in a sense that the difference between these two sets of reactivity ratio may explain certain points about the behavior of the three monomers when they come in contact with each other compared to the binary combinations.

Therefore, we compare the values of the reactivity ratios from binary systems in Table 8-5, as reported in the literature, with the ternary reactivity ratio estimates in the current work. It can be seen that for AMPS/AAm and AAm/AAc, we have the same trend in both binary or ternary reactivity ratios, indicating that AAm is more reactive than AMPS and AAc in both binary and ternary media. However, for the AMPS/AAc, the difference between the ternary reactivity ratios of this pair is not as significant as the difference between the corresponding binary reactivity ratios. Generally speaking,

AMPS is a stronger acid with (sterically) larger chemical groups than AAc; in a binary mixture of these monomers, steric effects dominate in favor of AAc, and therefore, the reactivity ratio of AAc is larger than AMPS (Stahl and Shulz (1986)). On the other hand, in a ternary mixture, AMPS and AAc seem to have similar levels of reactivity in the medium, which can be associated to the presence of the third monomer in the system (non-ionized AAm), and in turn, less direct interaction between the two ionized acid groups.

8.4.4.2 Using medium-high conversion experiments

The next step in estimating reactivity ratios for the AMPS/AAm/AAc terpolymerization in this work is by using medium-high conversion data and the optimal feed compositions. The reasons behind utilizing experimental data at higher conversion levels and the cumulative composition models were discussed extensively throughout this thesis, specifically in Chapter 3. For copolymerizations, it has been shown that the reactivity ratios estimated from high conversion data using the cumulative copolymer composition model (the so-called DNI approach) are superior to those obtained from the conventional methods in terms of precision. This observation is mainly related to the fact that the DNI method includes all available information from the system in the parameter estimation procedure and also does not suffer from the assumptions of the low conversion data, as mentioned in section 8.4.4.1.

In Chapter 6, the extension of the DNI method was described for the ternary reactivity ratio estimation problem (see Chapter 6, section 6.3.3). The implementation of the EVM methodology was shown for experimental data at lower conversion levels as well as simulated high conversion (see Chapter 6, section 6.4.3). For this terpolymerization system, we now have the opportunity to show the implementation of the EVM procedure on the cumulative terpolymer composition, using the optimal feed composition experiments, up to medium-high conversion levels. These data points are reported in Table 8-6, for runs #1, #2, and #3 (i.e., the optimal experiments). Regarding the error in the cumulative terpolymer composition data, to reflect that the variability in the terpolymer composition is considerable, the k value is 10% for the terpolymer composition variable. The estimated reactivity ratios are reported in Table 8-5, third row, and Figure 8-7 shows their corresponding JCRs for all three pairs.

Table 8-6. Optimal experiments for AMPS/AAm/AAc terpolymerization; medium to high conversion

Run	X_w	f_{AMPS}	f_{AAm}	f_{AAc}	$\overline{F}_{AMPS}$	$\overline{F}_{AAm}$	$\overline{F}_{AAc}$
#1	0.047	0.800	0.100	0.100	0.664	0.161	0.175
	0.057	0.800	0.100	0.100	0.693	0.187	0.120
	0.085	0.800	0.100	0.100	0.775	0.152	0.073
	0.101	0.800	0.100	0.100	0.620	0.205	0.175
	0.232	0.800	0.100	0.100	0.623	0.192	0.185
	0.254	0.800	0.100	0.100	0.667	0.227	0.106
	0.576	0.800	0.100	0.100	0.782	0.079	0.139
	0.628	0.800	0.100	0.100	0.772	0.107	0.121
#2	0.025	0.100	0.800	0.100	0.101	0.826	0.073
	0.046	0.100	0.800	0.100	0.099	0.824	0.077
	0.078	0.100	0.800	0.100	0.103	0.827	0.070
	0.085	0.100	0.800	0.100	0.106	0.813	0.081
	0.098	0.100	0.800	0.100	0.081	0.754	0.165
	0.124	0.100	0.800	0.100	0.104	0.839	0.057
	0.151	0.100	0.800	0.100	0.102	0.836	0.062
	0.201	0.100	0.800	0.100	0.081	0.781	0.138
	0.206	0.100	0.800	0.100	0.080	0.779	0.141
	0.247	0.100	0.800	0.100	0.096	0.832	0.072
	0.392	0.100	0.800	0.100	0.104	0.817	0.079
	0.411	0.100	0.800	0.100	0.087	0.782	0.131
	0.542	0.100	0.800	0.100	0.112	0.801	0.087
	0.574	0.100	0.800	0.100	0.097	0.824	0.077
	0.594	0.100	0.800	0.100	0.106	0.809	0.085
#3	0.029	0.100	0.200	0.700	0.052	0.400	0.548
	0.035	0.100	0.200	0.700	0.037	0.402	0.561
	0.042	0.100	0.200	0.700	0.066	0.420	0.514
	0.048	0.100	0.200	0.700	0.079	0.363	0.558
	0.055	0.100	0.200	0.700	0.084	0.364	0.552
	0.077	0.100	0.200	0.700	0.180	0.342	0.478
	0.081	0.100	0.200	0.700	0.119	0.380	0.501
	0.089	0.100	0.200	0.700	0.104	0.330	0.566
	0.122	0.100	0.200	0.700	0.060	0.270	0.670
	0.175	0.100	0.200	0.700	0.074	0.335	0.591
	0.194	0.100	0.200	0.700	0.079	0.382	0.539
	0.210	0.100	0.200	0.700	0.098	0.342	0.560
	0.268	0.100	0.200	0.700	0.117	0.334	0.553
	0.363	0.100	0.200	0.700	0.126	0.340	0.534

Figure 8-5 shows the JCRs for the reactivity ratios from low and medium-high conversion data, along with binary reactivity ratios, as reported in Table 8-5. It can be seen in this figure that the JCRs for all three pairs of monomers from high conversion data have acceptable and smaller size than the JCRs for reactivity ratios from low conversion data. These results are expected as utilizing all the information available in the experimental data can improve the precision of the point estimates. This, for the first time ever, confirms that the EVM method can successfully be used for real experimental data at high conversion levels. Also, once more, it clearly shows that only three optimal compositions studied over a conversion range do have sufficient information for acceptable reactivity ratio estimation for this terpolymerization system.

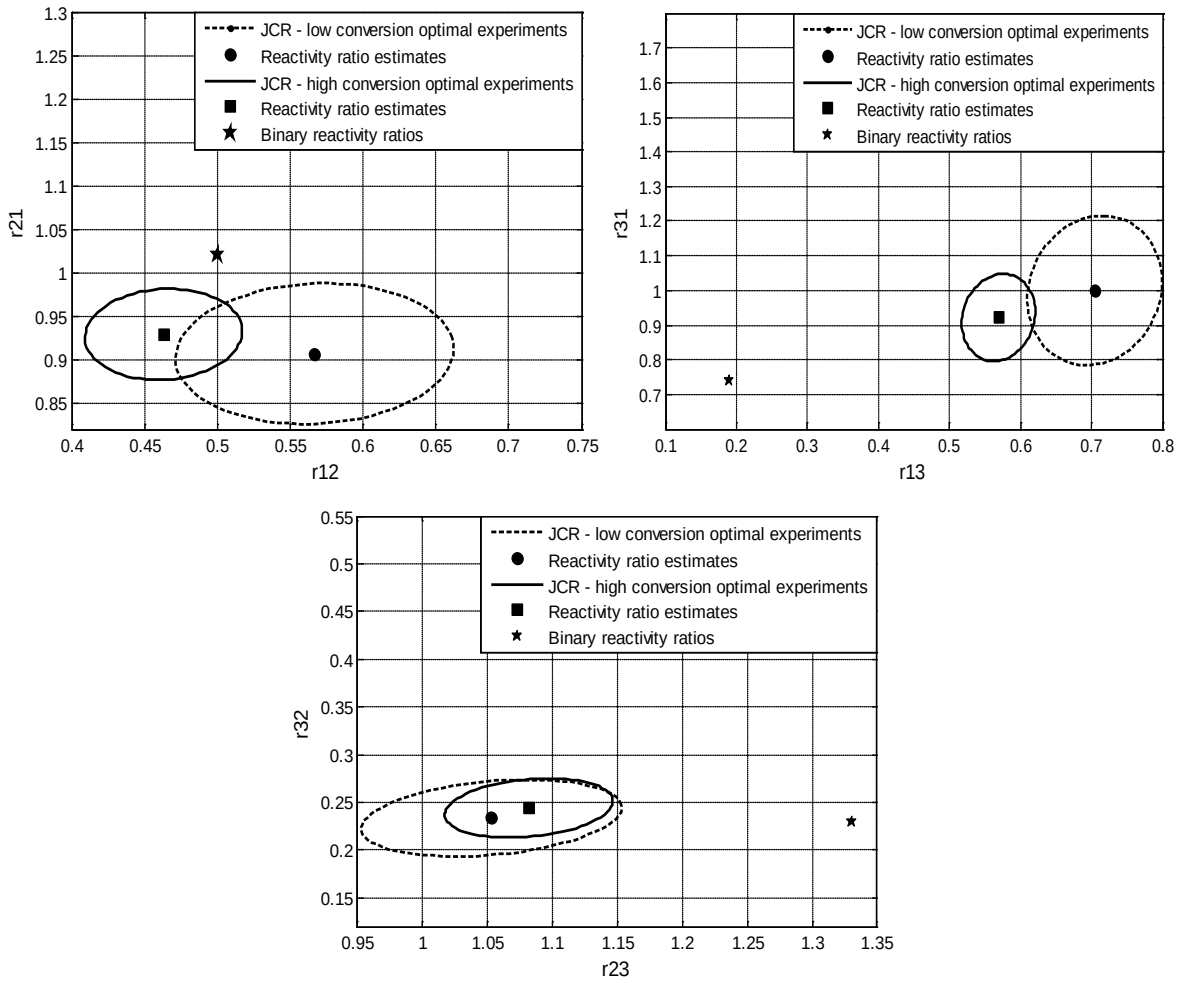

Figure 8-5. Optimal reactivity ratio estimation results from optimal feed compositions for AMPS (M_1)/AAm (M_2)/AAc (M_3) terpolymerization; low and medium to high conversions

8.4.4.3 Diagnostic checks

The estimated reactivity ratios for the AMPS/AAm/AAc terpolymerization system in the previous section confirm that our EVM parameter estimation method for ternary systems works very well with actual experimental data and returns reasonable and reliable results. However, we can still investigate the accuracy of these reactivity ratios by running certain diagnostic checks. The most common type of diagnostic check is evaluating the performance of the estimated reactivity ratios in predicting the behavior of the system over the polymerization trajectory. An acceptable agreement between predicted and experimental results reflects the reliability and accuracy of the reactivity ratios for this terpolymerization system.

To explore this, we used the integrated terpolymer composition equation (as shown in Chapter 2, section 2.1.2.2) to calculate terpolymer compositions using the reactivity ratio estimates from the optimal feeds at medium-high conversion levels (as cited in the third row of Table 8-4). These predictions were performed for the optimal feed compositions with f_{AMPS} /f_{AAm} /f_{AAc}: 0.8/0.1/0.1, 0.1/0.8/0.1, and 0.1/0.2/0.7. Figures 8-6 to 8-8 show the predicted cumulative terpolymer composition trajectories versus conversion, as well as the experimental points obtained for each of these optimal feeds, respectively. It should be mentioned that in these plots, each terpolymer composition is represented with three mole fractions.

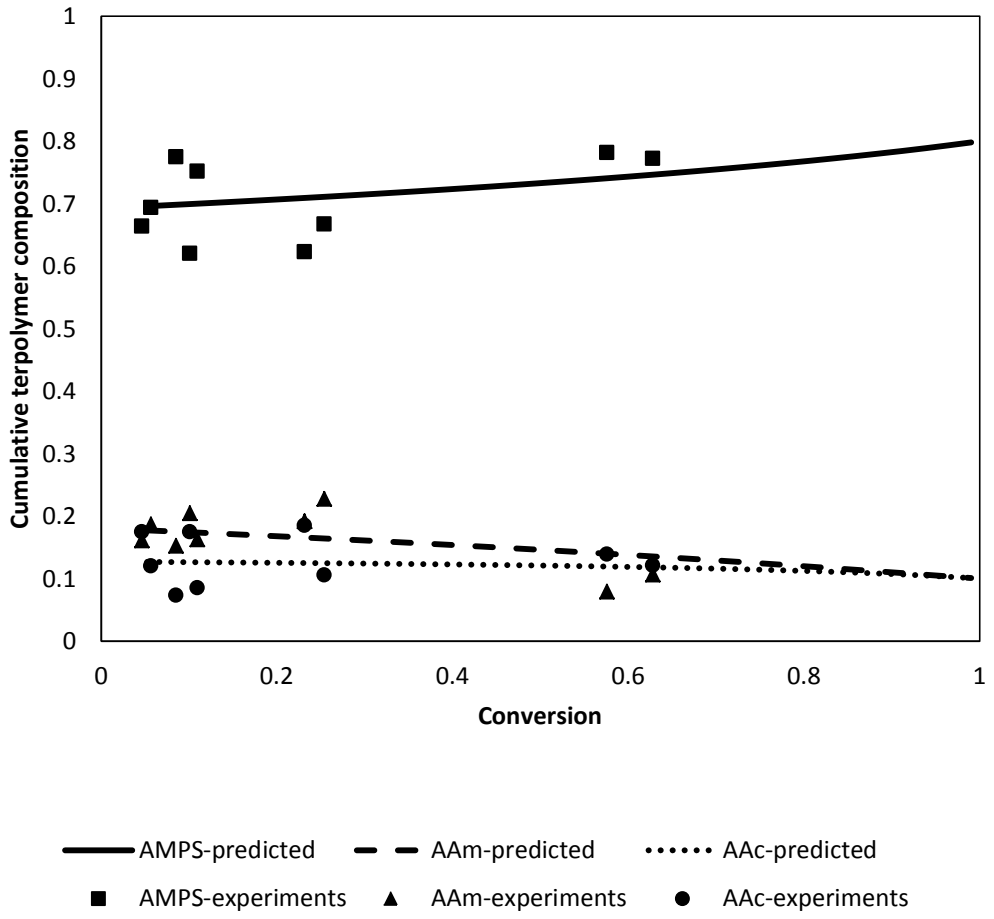

Figure 8-6. Cumulative terpolymer composition versus conversion for AMPS/AAm/AAc terpolymerization; initial composition $f_{o,AMPS}/f_{o,AAm}/f_{o,AAc}$: 0.8/0.1/0.1; experimental and predicted cumulative composition

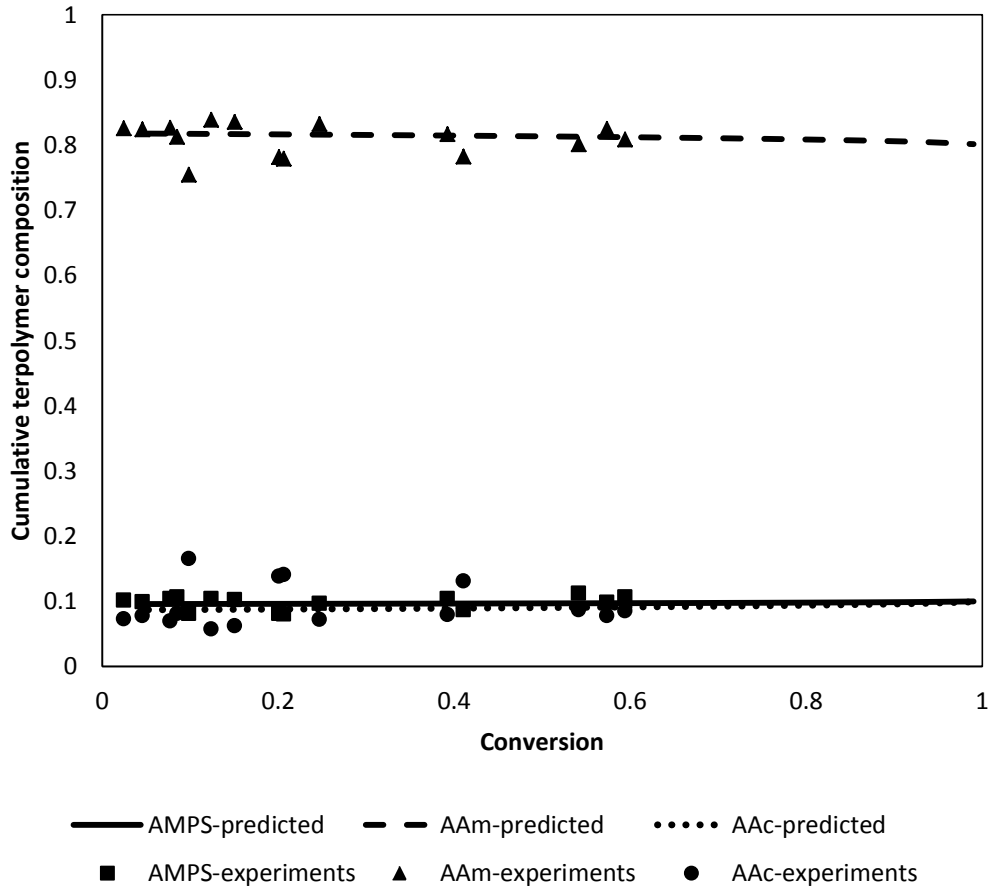

Figure 8-7. Cumulative terpolymer composition versus conversion for AMPS/AAm/AAc terpolymerization; initial composition $f_{o,AMPS}/f_{o,AAm}/f_{o,AAc}$: 0.1/0.8/0.1; experimental and predicted cumulative composition

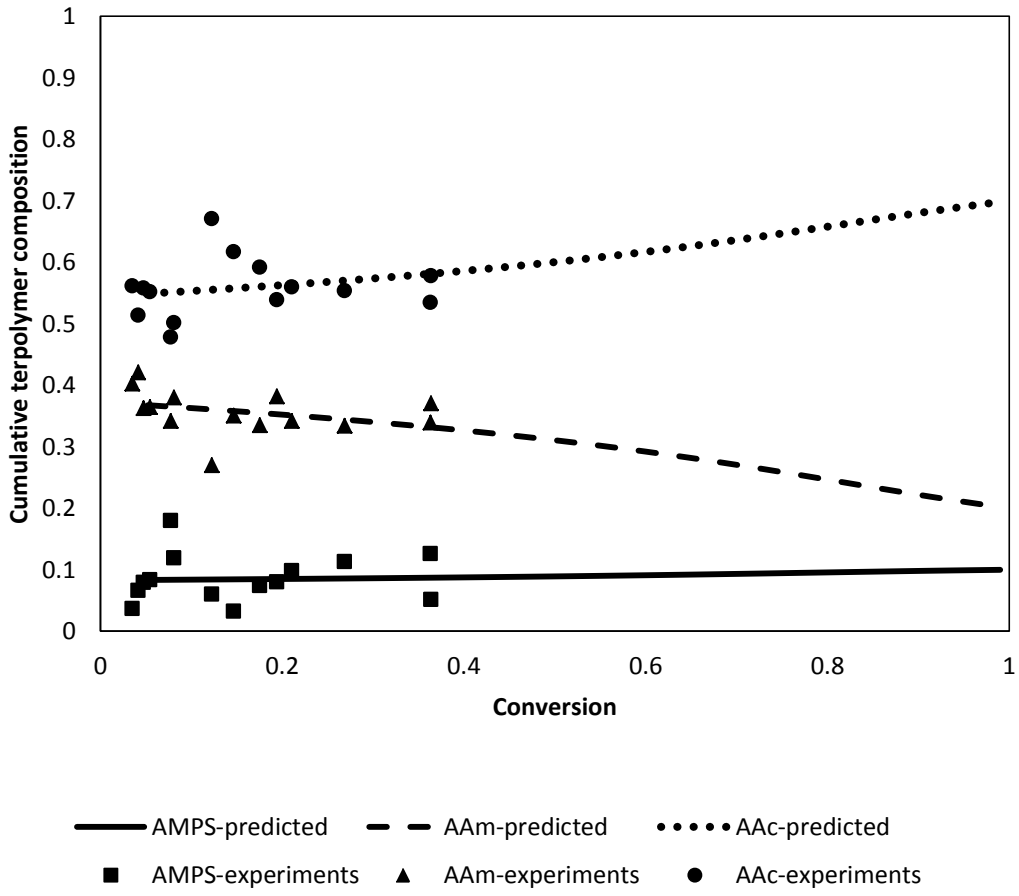

Figure 8-8. Cumulative terpolymer composition versus conversion for AMPS/AAm/AAc terpolymerization; initial composition $f_{o,AMPS}/f_{o,AAm}/f_{o,AAc}$: 0.1/0.2/0.7; experimental and predicted cumulative composition

Figures 8-6 to 8-8 show that the predicted terpolymer composition trajectories based on the ternary reactivity ratios capture the experimental behavior, confirming that the cumulative terpolymer composition model and the estimated reactivity ratios actually do predict the behavior of the system well up to high conversion levels. This is a very important diagnostic check, for this system and, in general, for terpolymerization studies, as it indicates that employing the terpolymerization composition model and the EVM framework implementation efficiently lead to precise and reliable reactivity ratios for the system.

8.5 Concluding Remarks

The experimental verification project, as a crucial part of our studies, was performed to determine whether or not the theoretical and simulation studies shown in previous chapters were in fact a realistic reflection of laboratory experiments.

The EVM framework, consisting of the parameter estimation and the design of experiments methodologies that were explained in Chapters 6 and 7, respectively, was implemented for the problem of estimating reactivity ratios for the terpolymerization of AMPS/AAm/AAc. Preliminary experiments along with optimal data points were collected, and the reactivity ratios were estimated based on low and medium-high conversion data. The results of the medium-high conversion data were used for predicting the terpolymer composition trajectory over the course of conversion, showing a very good agreement between experimental and predicted data.

The analysis of this chapter not only shows the verification of the EVM framework, it provides the reliable reactivity ratios for the terpolymerization of AMPS/AAm/AAc system. This ternary system is a water-soluble polymer with wide variety of applications that has been proposed in the literature less than a decade ago. Therefore, kinetic studies for this system have outmost importance for the future investigations in this area.

Chapter 9

Overall Thesis Conclusions, Main Thesis Contributions, and Recommendations

9.1 Overall Thesis Conclusions

The problem of estimating reactivity ratios for multicomponent polymerization (copolymerizations and terpolymerizations) is extensively studied in this thesis. The error-in-variables-model (EVM) framework is a statistical approach that is further developed and refined in this work, with the intention of providing a precise, powerful, and complete procedure that guarantees optimal reactivity ratio estimates from an efficient experimental workload. The EVM algorithm is explained in great detail in Chapter 2. Subsequent chapters deal with different aspects of estimating reliable reactivity ratios and provide detailed concluding remarks for different aspects at the end of each corresponding chapter. In this section, the main conclusions are summarized.

For the problem of estimating reactivity ratios for copolymerization systems, we implemented the EVM parameter estimation method for the numerically integrated form of the cumulative composition model. Subsequently, this method was implemented on several high conversion data sets. It was found out that:

- The direct numerical integration (DNI) approach is the most general and appropriate approach for reactivity ratio estimation, in that it does not suffer from any limiting assumptions and it can successfully handle experimental data at any conversion level for estimating reactivity ratios.
- The reactivity ratio estimation approach based on the DNI method and high conversion data is superior to the conventional approach based on the Mayo-Lewis model and low conversion data due to the fact that DNI uses all available information in the system for estimating reactivity ratios, and the data at higher conversion have less error and therefore more accurate information for reactivity ratio estimation.

Following the establishment of the estimation procedure, we looked at the effect of using optimally designed experiments, thus studying different aspects of the EVM design criterion. It was observed that:

- Since the main assumptions of D-optimality are violated for the problem of reactivity ratio estimation, the EVM design criterion should be used for locating optimal feed compositions. The differences between the results from these two design criteria become more considerable as the error in the independent variables become more significant.
- The relatively newly developed EVM design criterion performance was studied with respect to efficiency, error structure of the data, the effect of constraints on feed compositions, and the optimization procedure of the criterion.

Our ultimate goal in solving the problem of estimating reactivity ratios for copolymerization systems was to establish a framework that presents a recommended procedure, resulting in reliable reactivity ratios.

- All the considerations from the studies in all chapters were summarized in the EVM framework, to ensure that optimal reactivity ratios can be estimated from efficient and effective experimental work.
- The application of this framework was demonstrated and verified with the novel system of 9-(4-vinylbenzyl)-9H-carbazole (VBK) and methyl methacrylate (MMA) copolymerization, showing that using the EVM framework, the reliability of the results for this system are greatly improved; a perfect experimental verification for the findings in Chapters 3 to 5.

Next, we tackled the problem of estimating ternary reactivity ratios for terpolymerization systems. Since the research in this area is at a much earlier stage than for copolymerizations and also the binary reactivity ratios are commonly used in place of ternary reactivity ratios, we set out to look at all existing approaches in this field. We offer the following remarks:

- Using binary reactivity ratios is an over simplified assumption that results in bias in investigations of ternary systems. So, the terpolymerization reactivity ratios must be estimated directly based on terpolymerization data.

- The Alfrey-Goldfinger model, which is the most widely used model in this area, can be a source of bias in the results of reactivity ratio estimation, and thus, a recast form of the instantaneous terpolymerization composition model was proposed and used in this work.
- The EVM parameter estimation technique was implemented successfully on low conversion data and the recast ternary model for several cases from the literature.
- The EVM approach was also implemented on high conversion data and the cumulative ternary model, for the first time in the literature. This extension allows us to utilize ternary data at any conversion level for estimating reactivity ratios.
- Overall, the ternary reactivity ratio estimates were consistently reliable and precise, and diagnostic checks such as comparing the agreement between experimental and predicted data showed that they were accurate as well.

In order to further establish the EVM framework for the problem of estimating ternary reactivity ratios, the design of experiments within the EVM context was studied, for the first time in the literature, for terpolymerization experiments. Our observations indicated that:

- The EVM design criterion implementation results in three optimal experiments. Each one of these feed compositions is rich in one of the three monomers (based on the feasible region for the feed compositions). These results seem to be independent of the values of reactivity ratios.
- By looking at the results of optimal experiments versus the values of reactivity ratios, a practical heuristic was derived, arriving at the optimal locations without the implementation of complex mathematics.
- Three optimal experiments provide sufficient information for ternary reactivity ratio estimation, only if they are selected from the optimal regions.
- Feed compositions with similar amounts of all three monomers cannot provide enough information for reliable estimation of reactivity ratios.

After establishing the procedures for ternary reactivity ratio estimation and design of experiments for the EVM framework, we have verified experimentally the implementation of this framework on a novel terpolymerization system.

- The reactivity ratios for the terpolymerization system of 2-Acrylamido-2-methyl-1-propanesulfonic acid (AMPS)/Acrylamide (AAm)/Acrylic acid (AAc) were estimated based on low and high conversion experimental data, collected in the current work.
- Implementation of different stages of the EVM framework on this terpolymerization system confirmed that the optimal experiments carry more information for parameter estimation, and the EVM algorithm works for estimating ternary reactivity ratios from ternary data at any conversion level.

9.2 Main Thesis Contributions

The research in this thesis has made the following original contributions:

1. A significant contribution of this work for the copolymerization reactivity ratios is a concrete, superior approach after almost 70 years of different attempts in this area. The utilization of high conversion data for estimating reactivity ratios using the DNI approach (not limited by any assumptions) is a step further from all previous approaches in the literature (Chapter 3). This work has been published in Kazemi et al. (2011).

2. Even though the EVM algorithm for parameter estimation has been given in Reilly and Patino-Leal (1981) and Reilly et al. (1993), through work in this thesis (Chapters 2 and 3), a step by step guide for executing the EVM algorithm is presented and its practical/numerical aspects are investigated in detail. This work has been published in Kazemi et al. (2013a).

3. The EVM design criterion has had a few earlier implementations (e.g., Keeler and Reilly (1992) and Rossignolli and Duever (1995)). With the focus on the specific application of estimating copolymerization reactivity ratios, the integral aspects of the EVM design criterion are investigated, and qualitative/quantitative comparisons between the performances of this design criterion with other criteria along with guidelines for its implementation are presented in our work (Chapter 4). This work has been published in Kazemi et al. (2013b).

4. The EVM framework is introduced in our work as a combination of the design of experiments and parameter estimation steps within the EVM context with a sequential scheme that can continue to improve the reactivity ratio estimates (Chapters 3, 4, and 5). Such a solution, never implemented in

the literature for this problem, has been experimentally verified in our work (Chapter 5) and published in Kazemi et al. (2014a). In this sense, the contribution of our EVM framework can also be found in collaborative work with other projects, where the EVM framework has been implemented to estimate the reactivity ratios of Acrylamide (AAm)/Acrylic acid (AAc) copolymerization (Riahinezhad et al. (2013), (2014)).

5. The problem of estimating reactivity ratios for terpolymerizations (ternary reactivity ratios) is investigated thoroughly and the best approach for this problem is established for the first time in the literature (Chapter 6). Also since the practice of implementing design of experiments for estimating ternary reactivity ratios is sorely missing in the literature, we have shown the implementation of the EVM design criterion for this problem and also provided practical heuristics that support the application of our approach in this field (Chapter 7). Our parameter estimation work for ternary reactivity ratios has been published in Kazemi et al. (2014b).

6. The contributions of our EVM framework are examined with our experimental project for the 2-Acrylamido-2-methyl-1-propanesulfonic acid (AMPS)/Acrylamide (AAm)/Acrylic acid (AAc) terpolymerization system. This water-soluble terpolymer has several applications that depend closely on the composition of the terpolymer. Therefore, this work not only presents the application of the EVM framework for ternary reactivity ratio studies, but it can also be considered a pioneering work in studying the reactivity ratios of this terpolymerization system (Chapter 8). Another collaborative work for the EVM framework implementation for ternary systems was for the reactivity ratios of the terpolymerization of N-vinyl pyrrolidone/maleic anhydride/styrene system, which were estimated using the EVM parameter estimation method (Ajithkumar et al. (2014)). These examples showcase the potential of the EVM framework implementation in ternary studies, and its place in the research in this field will only unveil in time.

9.3 Recommendations

9.3.1 Short-term future steps

1. Joint confidence regions (JCRs) shown throughout this work are all approximate shape/approximate probability. The alternative approaches are exact shape/approximate probability

and exact shape/exact probability. The former alternative can be derived using equation (2.59). This approach has been tried for copolymerization in previous works in our group (for example, see, Hauch (2005)) and the exact shapes versus approximate JCRs are not different considerably, while the effort to obtain the exact shape is rather significant. The exact shape/exact probability JCR for copolymerization has also been calculated using the Markov Chain Monte Carlo (MCMC) approach (Mathew (2013)), where it is shown that for the DNI approach, the difference is not considerable. We expect the situation not to be very different for terpolymerizations, and that is the reason we used the approximate JCR throughout this thesis. Nonetheless, the above-mentioned resources can be tried to plot the JCRs with exact shape and approximate or exact probabilities.

2. The problem of the error structure in terms of the relation of the error and the true value of the variables has remained an open question in this work. Whether this relation is additive or multiplicative can be answered based on an extensive replicated experimental project. For example, if the error is assumed to be additive, the residual analysis based on extensively replicated data can show whether the residuals have a random pattern and the error structure is in fact additive, or they have a pattern/trend that suggests they are related multiplicatively.

3. For the terpolymerization reactivity ratio estimation procedure, the amount of correlation between the mole fractions of the three components in the terpolymer composition was studied in Chapter 6 in order to examine the significance of the correlation amount. An estimate of the actual value for this correlation is not available from the current literature. Even though it was observed that the amount of correlation does not change the reactivity ratios estimation results, it is recommended that the amount of this correlation be calculated for composition measurements (from common standard devices such as NMR and elemental analysis), in order to have a better idea about the scale of this relation and the consequences of including or excluding it from the analysis.

4. For the experimental project of AMPS/AAm/AAc terpolymerization, the estimated ternary reactivity ratios were compared to the binary reactivity ratios for the three pairs from the literature. One pair (AAm/AAc) was studied within the same experimental setting and with the EVM framework, and so the results for that pair are completely acceptable in our work. It is recommended that the reactivity ratios for the other two pairs be estimated optimally within the same experimental setting as well.

5. In Chapter 3, the implementation of the EVM algorithm for the DNI approach involves the derivative of the cumulative composition equation with respect to the variables, which is in this case the cumulative polymer composition. The conversion value that is used in this model is the molar conversion that is calculated based on the raw measurement of experimental mass conversion. As shown in Appendix I, another term for dX/dF can be added to this derivative to account for the fact that calculating molar conversion from mass conversion involves the cumulative polymer composition as well.

6. In this work, for the optimization problem, we used the Newton method where the problem was very well-behaved with one global minimum. We then used the SCE method to ensure that we can find the global optima when there were only lower and upper bound constraints for the optimization variables in the problem. And finally, we used the Generalized Pattern Search method to make sure we found the global optima when we had equality, inequality, and nonlinear constraints in the problem. Ideally, all these optimization problems can be handled with the GPS technique or some other optimization routine with all the above capabilities.

9.3.2 Long-term future steps

9.3.2.1 Copolymerization in a Continuous Stirred Tank Reactor (CSTR)

While the majority of the copolymerization reactions are carried out in batch reactors, one alternative approach could be using continuous copolymerization to estimate reactivity ratios. Theoretical and experimental pieces of work on copolymerization in a CSTR appear in a limited number of papers (e.g., Duerksen and Hamielec (1968) and O'Driscoll and Knorr (1968))). Moreover, based on the possibility of creating a more homogenous environment in a CSTR, a few papers have been published regarding running copolymerizations in CSTRs to estimate rate parameters that are of higher precision (Balaraman et al. (1982), Kulkanrni et al. (1986), and Wolf et al. (2002)).

Hence, a recommended extension of our work is determining the reactivity ratios by using CSTR copolymerization data, using the EVM framework. The mathematical model equations (i.e., mass balances, copolymer composition, etc.) used to describe a CSTR at steady state are given in Appendix J. This work should find applications in reactivity ratio estimation studies for industrial

copolymerizations in CSTRs, since it is in direct contrast with the commonly employed estimation based on batch copolymerization data only! After a CSTR reaches steady state, the composition of the product remains the same. This point may be beneficial from the point of view of collecting data at the same composition (no composition drift), whereas at the same time one may have better control over conversion levels (as opposed to typically used batch operation, i.e., the low conversion experimentation limitation is no longer required for collecting data points).

In principle, the first step would be to design an experiment, which can be done by using the EVM design criterion. Having found the optimal initial points for the feed ratio of the monomers to a CSTR, the concentration of the product stream should be monitored to obtain the data. The data can then be analyzed by the EVM method to estimate reactivity ratios.

9.3.2.2 Reactivity Ratio Estimation from Continuously Sampled Data

As another alternative, it is proposed to use a sequential sampling technique for collecting experimental data, which potentially leads to more experimental data (hopefully, enhanced experimental information). Essentially, the procedure of obtaining experimental data from multicomponent polymerizations consists of measuring the polymer composition obtained from low conversion experiments by spectroscopic methods such as NMR, while monomer composition is simply determined by the initial amount of the monomer in the mixture. Each experiment only gives one point and, for instance, for a copolymerization, one needs to perform at least two experiments to estimate reactivity ratios. As one can see from the literature on reactivity ratio estimation, typical practice is to use at best 4-8 copolymer composition data points, usually at low conversions, collected off-line in the batch mode. If data points are used at higher conversions, again 20-30 (at best) off-line copolymer compositions may be used over several feed mole fractions. In contrast with this technique, online techniques are very suitable for this type of experimentation, since one single copolymerization reaction can provide numerous data point.

This could be done using sequential sampling or continuously by an on-line method such as the automatic, continuous on-line monitoring of a polymerization (ACOMP) (Catalgil et al. (2002)), or the experiment performed *in situ* (e.g., Giz et al. (2000), Hua and Dubé (2002), Shaikh et al. (2004), and Sunbul et al. (2004)). On-line and in situ continuous monitoring methods yield hundreds, even thousands, of data points from each experiment; thus they enable the greatest possible amount of

information to be extracted. However they require an expensive and specialized setup that is available in only few laboratories with access to the specific instruments, detectors, pumping facilities, and so forth, required for these methods. Sequential sampling methods (SSM) (German and Heikens (1971)), on the other hand, yield several data points from each experiment. Although these techniques are not as powerful as the on-line methods, they do not require specialized equipment and can be implemented in any laboratory. The SSM technique has been practiced by Paril et al. (2004) rather recently. A detailed overview of on-line and in-line techniques for the monitoring of polymerization reactors has recently been given by Fonseca et al. (2009). These methods allow multiple data points to be obtained from each experiment.

A large number of data points is indeed advantageous from a statistical analysis viewpoint, because in principle it can increase the information content obtained from the experiment. Subsequently, it depends on the application of the most appropriate parameter estimation technique to exploit/make use of this enhanced information content. This is exactly the point where the implementation of the EVM framework can be advantageous. To implement this approach, we need to adjust and implement the direct numerical integration (DNI) approach to estimate reactivity ratios, since the variables are the unreacted monomer feed composition and conversion measurements.

9.3.2.3 Modeling of terpolymerizations considering the penultimate model

While the terminal model for the propagation step in binary and ternary polymerization reactions can yield analogous results, it should be acknowledged that for terpolymerization reactions, there is a third component involved in the propagation step. Ignoring the presence of the third monomer may be an assumption that can affect the predictions from the terpolymer composition equation. The penultimate model (an alternative mechanistic model) involves the two last monomer units in the propagating radical chain, and thus may be able to include better the presence of the third monomer in the modeling of the propagation step. Undoubtedly, considering the penultimate unit effect is more complicated because of 27 propagating reactions compared with only 9 in the terminal model (and hence, many more parameters to be estimated). Yet, the question whether this modeling scheme can provide more accurate predictions for experimental data in terpolymerizations requires more investigations and effort.

References

1. Abdel-Azim, A.A.A., Farahat, M.S., Atta, A.M. and Abdel-Fattah, A.A., “Preparation and properties of two-component hydrogels based on 2-acrylamido-2-methylpropane sulphonic acid”, Polymers for Advanced Technologies, 9, 282-289 (1998).
2. Aggour, Y.A., “Thermal degradation of copolymers of 2-acrylamido-2-methylpropane sulphonic acid with acrylamide”, Polymer Degradation and Stability, 44, 1, 71-73 (1994).
3. Ajithkumar, M.P., Yashoda, M.P., and Prasannakumar, S. “Synthesis, characterization, microstructure determination and thermal studies of poly (N-vinyl-2-pyrrolidone–maleic anhydride–styrene) terpolymer”, Iranian Polymer Journal, 23, 2, 93-101 (2014).
4. Alfrey, T. and Goldfinger, A., “Copolymerization of systems containing three components”, Journal of Chemical Physics, 12, 7, 322-322 (1944).
5. Anirudhan, T.S. and Rejeena, S.R., “Poly(acrylic acid- co -acrylamide- co -2-acrylamido-2-methyl-1-propanesulfonic acid)-grafted nanocellulose/poly(vinyl alcohol) composite for the in vitro gastrointestinal release of amoxicillin”, Journal of Applied Polymer Science (2014).
6. Atkinson, C. and Hunter, W.G., “The design of experiments for parameter estimation”, Technometrics, 10, 2, 271-289 (1968).
7. Atkinson, A.C. and Donev, A., Optimum Experiment Designs. Oxford University press, Oxford (1992).
8. Atkinson, A. and Bogacka, B., “Compound D-and Ds-optimum designs for determining the order of a chemical reaction”, Technometrics, 39, 4, 347-356 (1997).
9. Balaraman, K., Kulkarni, B., and Mashelkar, R., “An alternate approach to the determination of rate parameters in copolymerization”, Journal of Applied Polymer Science, 27, 2815-2825 (1982).
10. Bao, Y., Ma, J., and Li, N., “Synthesis and swelling behaviors of sodium carboxymethyl cellulose-g-poly(AA-co-AM-co-AMPS)/MMT superabsorbent hydrogel”, Carbohydrate Polymers, 84, 76-82 (2011).
11. Bard, Y., Nonlinear Parameter Estimation. Academic Press, New York (1974).
12. Bates, D.M. and Watts, D.G., Nonlinear Regression Analysis and its Applications. New York: Wiley (1988).
13. Behnken, D.W., “Estimation of copolymer reactivity ratios: an example of nonlinear estimation”, Journal of Polymer Science Part A: General Papers, 2, 2, 645-668 (1964).

14. Benbayer, C., Saidi-Besbes, S., De Givenchy, E.T., Amigoni, S., Guittard, F., and Derdour, A., “Copolymerization of novel reactive fluorinated acrylic monomers with styrene: reactivity ratio determination”, Colloid and Polymer Science, 1-7 (2014).
15. Biglari, M., Nicholson, R.V., Reilly, P.M., and Scharer, J.M., “Model development and parameter estimation for the oxidation of pyrrhotite-containing rock surfaces”, The Canadian Journal of Chemical Engineering, 84, 1, 116-124 (2006).
16. Bourdais, J., “Reactivity of acrylic acid in copolymerization" Bulletin De La Societe Chimique De France, 485-489 (1955).
17. Box, G.E.P. and Lucas, H.L., “Design of experiments in non-linear situations”, Biometrika, 46, 1, 77-90 (1959).
18. Box, G.E.P. and Draper, N.R., “The Bayesian estimation of common parameters from several responses”, Biometrika, 52, 3-4, 355-365 (1965).
19. Box, M.J., “Planning experiments to test the adequacy of non-linear models”, Applied Statistics, 18, 3, 241 (1969).
20. Box, M.J. “Some Experiences with a Nonlinear Experimental Design Criterion”, Technometrics, 12, 569 (1970).
21. Box, G.E.P., Hunter, W.G., MacGregor, J.F, and Erjavec, J., “Some problems associated with the analysis of multiresponse data”, Technometrics, 15, 1, 33-51 (1973).
22. Brar, A.S. and Hekmatyar, S.K., “Investigation of microstructure of the acrylonitrile-styrene copolymers by 2-D NMR spectroscopy”, Journal of Polymer Science Part A: Polymer Chemistry, 37, 6, 721-727 (1999).
23. Britt, H. and Luecke, R., “The estimation of parameters in nonlinear, implicit models”, Technometrics, 15, 2, 233-247 (1973).
24. Burke, A.L., Duever, T.A, and Penlidis, A. “Revisiting the design of experiments for copolymer reactivity ratio estimation”, Journal of Polymer Science Part A: Polymer Chemistry, 31, 3065-3072 (1993).
25. Burke, A.L., Duever, T.A., and Penlidis, A., “Model discrimination via designed experiments: Discriminating between the terminal and penultimate models on the basis of composition data”, Macromolecules, 27, 2, 386-399 (1994).
26. Çatalgil-Giz, H., Giz, A., Alb, A.M., Öncül Koç, A., and Reed, W.F., “Online monitoring of composition, sequence length, and molecular weight distributions during free radical

copolymerization, and subsequent determination of reactivity ratios", Macromolecules, 35, 17, 6557-6571 (2002).

27. Deming, W. E., Statistical adjustment of data, New York (1944).
28. Donckels, B Shuffled Complex Evolution in Matlab, "http://biomath.ugent.be/~brecht/downloads.html" (2012).
29. Dovi, V.G., Reverberi, A.P., and Maga, L., "Optimal design of sequential experiments for error-in-variable models", 17, 1, 111-115 (1993).
30. Draper, N.R. and Hunter, W.G., "Design of experiments for parameter estimation in multiresponse situations", Biometrika, 53, 3-4, 525-533 (1966).
31. Draper, N.R. and Hunter, W.G., "The use of prior distributions in the design of experiments for parameter estimation in non-linear situations", Biometrika, 54, 1, 147-153 (1967).
32. Draper, N.R. and Smith, H., "Applied Regression Analysis", 3rd Edition (1998).
33. Duan, Q., Gupta, V., and Sorooshian, S., "Shuffled complex evolution approach for effective and efficient global minimization", Optimization, 76, 3, 501-521 (1993).
34. Dubé, M., Sanayei, R.A., Penlidis, A., O'Driscoll, K.F., and Reilly, P.M., "A microcomputer program for estimation of copolymerization reactivity ratios", Journal of Polymer Science Part A: Polymer Chemistry, 29, 703-708 (1991).
35. Dubé, M.A, and Penlidis, A., "A systematic approach to the study of multicomponent polymerization kinetics--the butyl acrylate/methyl methacrylate/vinyl acetate example: 1. Bulk copolymerization", Polymer, 36, 3, 587-598 (1995a).
36. Dubé, M.A, and Penlidis, A., "A systematic approach to the study of multicomponent polymerization kinetics: butyl acrylate/methyl methacrylate/vinyl acetate, 2 a) Bulk (ans solution) terpolymerization", Macromolecular Chemistry and Science, 196, 1101-1112 (1995b).
37. Dubé, M.A, and Penlidis, A., "Hierarchical data analysis of a replicate experiment in emulsion terpolymerization", AIChE journal, 42, 7, 1985-1994 (1996).
38. Duerksen, J.H. and Hamielec, A.E., "Polymer reactors and molecular weight distribution. IV. Free-radical polymerization in a steady-state stirred-tank reactor train", Journal of Polymer Science Part C: Polymer Symposia, 25, 155-166 (1968).
39. Duever, T.A., O'Driscoll, K.F., and Reilly, P.M., "The use of the error-in-variables model in terpolymerization", Journal of Polymer Science: Polymer Chemistry Edition, 21, 7, 2003-2010 (1983).

40. Duever, T.A., Keeler, S.E., Reilly, P.M., Vera, J.H., and Williams, P.A., “An application of the Error-in-Variables Model-parameter estimation from Van Ness-type vapour-liquid equilibrium experiments”, Chemical engineering science, 42, 3, 403-412 (1987).
41. Durmaz, S. and Okay, O., “Acrylamide/2-acrylamido-2-methylpropane sulfonic acid sodium salt-based hydrogels: synthesis and characterization”, Polymer, 41, 3693-3704 (2000).
42. Erbil, C., Terlan, B., Akdemir, Ö., and Gökçeören, A.T., “Monomer reactivity ratios of< i> N</i>-isopropylacrylamide–itaconic acid copolymers at low and high conversions”, European Polymer Journal, 45, 6, 1728-1737 (2009).
43. Fernandez-Garcia, M., Canamero, P.F., and Fuente, J.L., “Synthesis and characterization of functional gradient copolymers of glycidyl methacrylate and butyl acrylate”, Reactive & Functional Polymers, 68, 1384-1391 (2008).
44. Finch, C.A. Industrial Water Soluble Polymers, Royal Society of Chemistry (1996).
45. Finemann, M. and Ross, S., “Linear method for determining monomer reactivity ratios in copolymerization”, Journal of Polymer Science, 5, 259-262 (1950).
46. Fletcher, R., Practical Methods of Optimization, Wiley-Interscience, New York (1987).
47. Fonseca, G.E., Dubé, M.A., and Penlidis, A., “A Critical overview of sensors for monitoring polymerizations”, Macromolecular Reaction Engineering, 3, 327-373 (2009).
48. Fordyce, R. and Ham, G., “Copolymerization. VIII. Reactivity of fumaronitrile in vinyl copolymerization”, Journal of the American Chemical Society, 1538, 1, 1186-1189 (1951).
49. Franceschini, G. and Macchietto, S., “Novel anticorrelation criteria for model-based experiment design: Theory and formulations”, AIChE Journal, 54, 4, 1009-1024 (2008).
50. Gao, J. and A. Penlidis. “A comprehensive simulator/database package for reviewing free-radical copolymerizations, 651-780 (1998).
51. German, A.L. and Heikens, D., “Copolymerization of ethylene and vinyl acetate at low pressure: Determination of the kinetics by sequential sampling”, Journal of Polymer Science Part A-1: Polymer Chemistry, 9, 2225-2232 (1971).
52. Giz, A., Çatalgil-Giz, H., Alb, A., Brousseau, J.L., and Reed, W.F., “Kinetics and mechanisms of acrylamide polymerization from absolute, online monitoring of polymerization reaction”, Macromolecules, 34, 1180-1191 (2001).
53. Hooke, R. and Jeeves, T.A., “Direct search solution of numerical and statistical problems”, Journal of the ACM, 8, 2, 212-229 (1961).

54. Ham, G., “Penultimate unit effects in terpolymerization”, Journal of Polymer Science Part A: General Papers, 2, 4191-4200 (1964).
55. Ham, G.E., and Lipman, R.D.A., “Computation of monomer feeds and probability products for given terpolymer systems”, Journal of Macromolecular Science-Chemistry, 1, 6, 1005-1010 (1967).
56. Hagiopol, C., Frangu, O., and Dumitru, L., “A nonlinear method for the estimation of reactivity ratios in copolymerization processes”, Journal of Macromolecular Science-Chemistry, 26, 10, 1363-1379 (1989).
57. Hagiopol, C., Copolymerization, Towards Systematic Approach. New York: Kluwer Academic/Plenum (1999).
58. Hua, H. and Dubé, M, “In-Line monitoring of emulsion homo- and copolymerizations using atr-ftir spectrometry”. Polymer Reaction Engineering, 10, 1&2, 21-39 (2002).
59. Hauch, E.K.D., “Parameter estimation in multiresponse problems for the modelling of multicomponent polymerization reactions”, MASc thesis, Department of Chemical Engineering, University of Waterloo (2005).
60. Hautus, F.L.M., German, A.L., and Linssen, H.N., “On numerical problems when reactivity ratios are computed using the integrated copolymer equation”, Journal of Polymer Science: Polymer Letters Edition, 23, 311-315 (1985).
61. Hocking, M.B. and Klimchuk, K.A. “A refinement of the terpolymer equation and its simple extension to two- and four-component systems”, Journal of Polymer Science Part A: Polymer Chemistry, 34, 12, 2481-2497 (1996).
62. Iglesias, M., Guzmán, J., and Riande, E., “Copolymerization and terpolymerization of methacrylic ester monomers containing hydroxyl groups in their structure”, Polymer, 37, 8, 1443-1452 (1996).
63. Iwatsuki, S., Shin, M., and Yamashita, Y., “Radical terpolymerization of dodecyl vinyl ether, fumaronitrile and Chloroethyl acrylate”, Die Makromolekulare Chemie, 102, 2197, 232-244 (1967).
64. Jitjareonchai, J.J., Reilly, P.M., Duever, T.A., and Chambers, D.B., “Parameter estimation in the error-in-variables models using the Gibbs sampler”, The Canadian Journal of Chemical Engineering, 84, 1, 125-138 (2006).
65. Kahn, D.J. and Horowitz, H.H., “Evaluation of the terpolymer composition equation”, Journal of Polymer Science, 54, 160, 363–374 (1961).

66. Kazantsev, O.A., Kamorin, D.M., Sivokhin, A.P., Samodurova, S.I., Orekhov, D.V., and Korotkova, T.V., "Copolymerization of amine-containing monomers and dodecyl (meth) acrylate in toluene: controlling compositional heterogeneity", Journal of Polymer Research, 21, 2, 1-6 (2014).

67. Kazemi, N., "Reactivity ratio estimation aspects in multicomponent polymerizations at low and high conversion levels", MASc thesis, Department of Chemical Engineering, University of Waterloo (2010).

68. Kazemi, N., Duever, T.A., and Penlidis, A. "Investigations on azeotropy in multicomponent polymerizations", Chemical Engineering & Technology, 33, 11, 1841-1849 (2010).

69. Kazemi, N., Duever, T.A., and Penlidis, A., "Reactivity ratio estimation from cumulative copolymer composition data", Macromolecular Reaction Engineering, 5, 385-403 (2011).

70. Kazemi, N., Duever, T.A., and Penlidis, A., "A powerful estimation scheme with the error-in-variables-model for nonlinear cases: reactivity ratio estimation examples", Computer and Chemical Engineering, 48, 200-208 (2013a).

71. Kazemi, N., Duever, T.A., and Penlidis, A., "Design of experiments for reactivity ratio estimation in multicomponent polymerizations using the error-in-variables-model approach", Macromolecular Theory and Simulation, 22, 5, 261-272 (2013b).

72. Kazemi, N., Lessard, B.H., Marić, M., Duever, T.A., and Penlidis, A., "Reactivity ratio estimation in radical copolymerization: from preliminary estimates to optimal design of experiments", Industrial & Engineering Chemistry Research, 53, 7305-7312 (2014a).

73. Kazemi, N., Duever, T. A., and Penlidis, A., "Demystifying the estimation of reactivity ratios for terpolymerization systems", AIChE Journal, 60, 5, 1752-1766 (2014b).

74. Keeler, S.E., "The error-in-variables model applied to parameter estimation when the error covariance matrix is unknown and to the design of experiments", PhD thesis, Department of Chemical Engineering, University of Waterloo (1989).

75. Keeler, S.E. and Reilly, P.M. "The error-in-variables model applied to parameter estimation when the error covariance matrix is unknown", The Canadian Journal of Chemical Engineering, 69, 27-34 (1991).

76. Keeler, S.E. and Reilly, P.M., "The design of experiments when there are errors in all the variables", The Canadian Journal of Chemical Engineering, 70, 774-779 (1992).

77. Kelen, T. and Tudos, F., “Analysis of linear methods for determining copolymerization reactivity ratios .1. New improved linear graphic method”, Journal of Macromolecular Science-Chemistry, A9, 1-27 (1975).

78. Kim, I.W., Liebman, M.J., and Edgar, T.F., “Robust error-in-variables estimation using nonlinear programming techniques”, AIChE Journal, 36, 7, 985-993 (1990).

79. Kressler, J., Bieger, W., Horvath, B., and Schmidt-Naake, G., “Experimental investigation of ternary azeotropy in the copolymerization of acrylonitrile, styrene, and maleic anhydride”, Journal of Macromolecular Science, Part A, 24, 6, 681-687 (1987).

80. Kulkarni, B.D., Balaraman, K.S., and Mashelkar, R.A., “Reactivity ratio estimation in copolymerization: a new analysis of unresolved conflicts”, Chemical Engineering Communications, 46, 29-42 (1986).

81. Kyselá, G. and Štaudner, E., “Terpolymerization of maleic anhydride, methyl methacrylate and styrene”, Die Makromolekulare Chemie, 264, 261–264 (1992).

82. Lessard, B.H., Ling, E.J.Y., Morin, M.S., and Marić, M., “Nitroxide-mediated radical copolymerization of Methyl Methacrylate controlled with a minimal amount of 9-(4-Vinylbenzyl)-9H-Carbazole”, Journal of Polymer Science, Part A: Polymer Chemisty, 49, 4, 1033-1045 (2011).

83. Lessard, B.H., Ling, E.J.Y., and Marić, M., “Fluorescent, thermoresponsive oligo (ethylene glycol) Methacrylate/9-(4-Vinylbenzyl)-9 H-carbazole copolymers designed with multiple LCSTs via nitroxide mediated controlled radical polymerization”, Macromolecules, 45, 1879-1891 (2012a).

84. Lessard, B.H., Savelyeva, X., and Marić, M. “Smart morpholine-functional statistical copolymers synthesized by nitroxide mediated polymerization”, Polymer, 53, 5649-5656 (2012b).

85. Lessard, B.H., and Marić, M., “Water-soluble/dispersible Carbazole-containing random and block copolymers by nitroxide-mediated radical polymerization”, Canadian Journal of Chemical Engineering, 91, 618-629 (2013a).

86. Lessard, B.H., Guillaneuf, Y., Mathew, M., Liang, K., Clement, J.L., Gigmes, D., Hutchinson, R.A., and Marić, M., “Understanding the controlled polymerization of Methyl Methacrylate with low concentrations of 9-(4-Vinylbenzyl)-9 H-carbazole comonomer by nitroxide-mediated polymerization: The pivotal role of reactivity ratios”, Macromolecules, 46, 805-813 (2013b).

87. Liu, Y., Xie, J., Zhu, M., and Zhang, X., “A study of the synthesis and properties of AM/AMPS copolymer as superabsorbent”, Macromolecular Materials and Engineering, 289, 1074-1078 (2004).

88. Luft, G., Stein F., and Dorn M., “The free-radical terpolymerisation of ethylene, methyl acrylate and vinyl acetate at high pressure”, Die Angewandte Makromolekulare Chemie., 211, 3677, 131-140 (1993).

89. Ma, J., Zheng, H., Tan, M., Liu, L., Chen, W., Guan, Q., and Zheng, X., “Synthesis, characterization, and flocculation performance of anionic polyacrylamide P (AM-AA-AMPS)”, Journal of Applied Polymer Science, 129, 1984-1991 (2013).

90. Mathew, M., “The application of markov chain monte carlo techniques in non-linear parameter estimation for chemical engineering models”, MASc thesis, Department of Chemical Engineering, University of Waterloo (2013).

91. Mayo, F.R., and Lewis, F.M., “Copolymerization. I. A basis for comparing the behavior of monomers in copolymerization; the copolymerization of styrene and methyl methacrylate”, Journal of the American Chemical Society, 66, 1594-1601 (1944).

92. McCormick, C.L. and Chen, G.S., “Water-soluble copolymers. IV. random copolymers of acrylamide with sulfonated comonomers”, Journal of Polymer Science: Polymer Chemistry Edition, 20, 817-838 (1982).

93. McFarlane, R.C., Reilly, P.M., and O’Driscoll, K.F., “Comparison of the precision of estimation of copolymerization reactivity ratios by current methods”, Journal of Polymer Science: Polymer Chemistry Edition, 18, 251-257 (1980).

94. McManus, N.T. and Penlidis, A., “A kinetic investigation of styrene/ethyl acrylate copolymerization”, Journal of Polymer Science Part A: Polymer Chemistry 34, 237-248 (1996).

95. Meyer, V.E. and Lowry, G.G., “Integral and differential binary copolymerization equations”, Journal of Polymer Science Part A: General Papers *3*, 2843-2851 (1965).

96. Mielańczyk, A., Biela, T., and Neugebauer, D., “Synthesis and self-assembly behavior of amphiphilic methyl α-D-glucopyranoside-centered copolymers”, Journal of Polymer Research, 21, 5, 1-13 (2014).

97. Naguib, H.F., Mokhtar, S.M., Ali, R.O., and Elsabee, M.Z., “Terpolymerization of ethyl methacrylate, N-phenylmaleimide, and itaconic acid”, Journal of Polymer Science Part A: Polymer Chemistry, 41, 3180-3187 (2003).

98. Naguib, H.F., Mokhtar, S.M., Khalil, N.Z., and Elsabee, M.Z., “Polymerization kinetics of indene, methyl methacrylate and acrylonitrile and characterization of their terpolymer”, Journal of Polymer Research, 16, 6, 693-702 (2009).
99. O’Driscoll, K.F. and Knorr, R., “Multicomponent polymerization. I. integration of the rate equations”, Macromolecules, 1, 367-371 (1968).
100. O’Driscoll, K.F., Kale, L.T., Rubio, L.H.G., and Reilly, P.M. “Applicability of the Mayo–Lewis equation to high conversion copolymerization of styrene and methylmethacrylate”, Journal of Polymer Science: Polymer Chemistry Edition, 22, 2777-2788 (1984).
101. O’Driscoll, K.F. and Reilly, P.M., “Determination of reactivity ratios in copolymerization”, Makromolekulare Chemie. Macromolecular Symposia, 10-11, 1, 355-374 (1987).
102. O’Driscoll, K.F., and Huang, J., “The rate of copolymerization of styrene and methyl methacrylate-II. The gel effect in copolymerization”, European polymer journal, 26, 6, 643-647 (1990).
103. Odian, G. G. Principles of Polymerization, Wiley- Interscience, (2004).
104. Paril, A., Giz, A., and Catalgil-Giz, H., “Copolymerization reactivity ratios analysis of sequentially sampled data by error in variables method”, Journal of Applied Polymer Science 95, 393-399 (2004).
105. Patino-Leal, H., Reilly, P.M. and O’Driscoll, K.F., “On the estimation of reactivity ratios”, Journal of Polymer Science: Polymer Letters Edition, 18, 219-227 (1980).
106. Peng, B., Peng, S., and Long, B., “Properties of high-temperature-resistant drilling fluids incorporating acrylamide/(acrylic acid)/(2-acrylamido-2-methyl-1-propane sulfonic acid) terpolymer and aluminum citrate”, Journal of Vinyl and Additive Technology, 6, 84-89 (2010).
107. Plaumann, H.P. and Branston, R.E., “On estimating reactivity ratios using the integrated mayo–lewis equation”, Journal of Polymer Science Part A: Polymer Chemistry, 27, 8, 2819-2822 (1989).
108. Polic, L., Duever, T.A., Penlidis, A., “Case studies and literature review on the estimation of copolymerization reactivity ratios”, Journal of Polymer Science, Part A: Polymer Chemistry, 36, 813-822 (1998).
109. Pourjavadi, A., Barzegar, S., and Zeidabadi, F., “Synthesis and properties of biodegradable hydrogels of κ-carrageenan grafted acrylic acid-co-2-acrylamido-2-methylpropanesulfonic

acid as candidates for drug delivery systems", Reactive and Functional Polymers, 67, 644-654 (2007).

110. Preusser, C. and Hutchinson, R.A., "An in-Situ NMR study of radical copolymerization kinetics of acrylamide and non-Ionized acrylic acid in aqueous solution", In Macromolecular Symposia, 333, 1, 122-137 (2013).

111. Qi, L., Wanfen, P., Yabo, W., and Tianhong, Z., "Synthesis and assessment of a novel AM-co-AMPS polymer for enhanced oil recovery (EOR)", International Conference on Computational and Information Sciences, 997-1000 (2013).

112. Reilly, P.M. and Patino-Leal, H., "A Bayesian study of the error-in-variables model", Technometrics, 23, 221-231 (1981).

113. Reilly, P.M., Reilly, H.V., and Keeler, S.E., "Parameter estimation in the error-in-variables model", Applied statistics, 42, 693-709 (1993).

114. Riahinezhad, M., Kazemi, N., McManus, N., and Penlidis, A., "Optimal estimation of reactivity ratios for acrylamide/acrylic acid copolymerization", Journal of Polymer Science Part A: Polymer Chemistry, 51, 4819-4827 (2013).

115. Riahinezhad, M., Kazemi, N., McManus, N., and Penlidis, A., "Effect of ionic strength on the reactivity ratios of acrylamide/acrylic acid (sodium acrylate) copolymerization", Journal of Applied Polymer Science (2014).

116. Rosa, F., Bordado, J., and Casquilho, M., "Kinetics of water absorbency in AA/AMPS copolymers: applications of a diffusion–relaxation model", Polymer, 43, 63-70 (2002).

117. Rossignolli, P.J. and Duever, T.A., "The Estimation of copolymer reactivity ratios: A review and case studies using the error-in-variables mode and nonlinear least squares", Polymer Reaction Engineering, 3, 4, 361-395 (1995).

118. Rudin, A., Chiang, S.S.M., Johnston, H.K., and Paulin, P.D., "Terpolymerization of Methacrylonitrile, Styrene, and α-Methylstyrene", Canadian Journal of Chemistry, 50, 11, 1757-1766 (1972).

119. Saric, K. and Janovic, Z., "Terpolymerization of acrylonitrile, styrene, and 2,3-dibromopropyl acrylate", Journal of Polymer Science: Polymer Chemistry Eddition, 21, 1913-1928 (1983).

120. Seber, J.A.F. and Wild, C.J., Nonlinear Regression. Wiley (1989).

121. Shaikh, S., Puskas, J.E., and Kaszas, G., "A new high-throughput approach to measure copolymerization reactivity ratios using real-time FTIR monitoring", Journal of Polymer Science, Part A: Polymer Chemistry, 42, 4084-4100 (2004).

122. Shawki, S.M. and Hamielec, A.E., “Estimation of the reactivity ratios in the copolymerization of acrylic acid and acrylamide from composition-conversion measurements by an improved nonlinear least-squares method”, Journal of Applied Polymer Science, 23, 3155-3166 (1979).
123. Siołek, M. and Matlengiewicz, M., “Reactivity ratios of butyl acrylates in radical copolymerization with methacrylates”, International Journal of Polymer Analysis and Characterization, 19, 3, 222-233 (2014).
124. Skeist, I., “Copolymerization: the composition distribution curve”, Journal of the American Chemical Society, 68, 1781-1784 (1946).
125. Slocombe, R., “Multicomponent polymers. I. Three-component systems”, Journal of Polymer Science, 26, 112, 9-22 (1957).
126. Šoljić, I., Jukić, A., and Janović, Z., “Free radical copolymerization of N,N-dimethylaminoethyl methacrylate with styrene and methyl methacrylate: monomer reactivity ratios and glass transition temperatures”, Polymer International, 58, 9, 1014-1022 (2009).
127. Šoljić, I., Jukić, A., and Janović, Z., “Terpolymerization kinetics of N,N-dimethylaminoethyl Methacrylate/Alkyl Methacrylate/Styrene systems”, Polymer Engineering & Science, 50, 3, 577-584 (2010).
128. Stahl, G.A. and Schulz, D.N., Water-Soluble Polymers for Petroleum Recovery, Springer (1986).
129. Steinfatt, I. and Schmidt-Naake, G., “Free radical co-and terpolymerization reactions of Methyl Methacrylate, Acrylonitrile, 4-Vinylpyridine, and Styrene in microemulsion”, Macromolecular Chemistry and Physics, 202, 3198-3204 (2001).
130. Sünbül, D., Çatalgil-Giz, H., Reed, W., and Giz, A. “An error-in-variables method for determining reactivity ratios by on-line monitoring of copolymerization reactions”, Macromolecular theory and simulations, 13, 2, 162-168 (2004).
131. Sutton, T.L. and MacGregor J.F., “The analysis and design of binary vapour-liquid equilibrium experiments”, The Canadian Journal of Chemical Engineering, 55, 609-613 (1977).
132. Tidwell, P.W. and Mortimer, G.A., “An improved method of calculating copolymerization reactivity ratios”, Journal of Polymer Science Part A: General Papers, 3, 369-387 (1965).
133. Touchal, S., Jonquieres, A., Clément, R., and Lochon, P., “Copolymerization of 1-vinylpyrrolidone with N-substituted methacrylamides: monomer reactivity ratios and copolymer sequence distribution”, Polymer, 45, 25, 8311-8322 (2004).

134. Travas-Sejdic, J. and Easteal, A., “Study of free-radical copolymerization of acrylamide with 2-acrylamido-2-methyl-1-propane sulfonic acid”, Journal of Applied Polymer Science, 75, 619-628 (2000).

135. Valvassori, A. and Sartori, G., “Present status of the multicomponent copolymerization theory”, Advance in Polymer Science, 5, 28-58 (1967).

136. Van Den Brink, M., Van Herk, A.M., and German, A.L., “Nonlinear regression by visualization of the sum of residual space applied to the integrated copolymerization equation with errors in all variables. I. Introduction of the model, simulations and design of experiments”, Journal of Polymer Science Part A: Polymer Chemistry, 37, 3793-3803 (1999).

137. Van Der Meer, R., Linssen, H.N., and German, A.L., “Improved methods of estimating monomer reactivity ratios in copolymerization by considering experimental errors in both variables”, Journal of Polymer Science: Polymer Chemistry Edition, 16, 2915-2930 (1978).

138. Van Herk, A. M. and Dröge, T., “Nonlinear least squares fitting applied to copolymerization modeling”, Macromolecular Theory and Simulations, 6, 1263-1276 (1997).

139. Vila, J.P. and Gauchi, J.P. “Optimal designs based on exact confidence regions for parameter estimation of a nonlinear regression model”, Journal of statistical planning and inference, 137, 9, 2935-2953 (2007).

140. Walling, C. and Briggs, E.R., “Copolymerization. III. Systems containing more than two monomers”, Journal of the American Chemical Society, 67, 1774-1778 (1945).

141. Wamsley, A., Jasti, B., Phiasivongsa, P., and Li, X., “Synthesis of random terpolymers and determination of reactivity ratios of N-carboxyanhydrides of leucine, β-benzyl aspartate, and valine”, Journal of Polymer Science Part A-1: Polymer Chemistry, 42, 317-325 (2004).

142. Wang, W. and Hutchinson, R.A., “PLP/SEC/NMR study of free radical copolymerization of styrene and glycidyl methacrylate”, Macromolecules, 41, 23, 9011-9018 (2008).

143. Wang, Y., Shi, X., Wang, W., and Wang, A., “Synthesis, characterization, and swelling behaviors of a pH-responsive CMC-g -poly (AA-co-AMPS) superabsorbent hydrogel”, Turkish Journal of Chemistry, 37, 149-159 (2013).

144. Wei, B., Romero-Zerón, L., and Rodrigue, D., “Oil displacement mechanisms of viscoelastic polymers in enhanced oil recovery (EOR): a review”, Journal of Petroleum Exploration and Production Technology, 1-9 (2013).

145. Wittmer, F., “Uber das vorkommen von azeotropen bei copolymerisationen mit mehr als zwei comonomeren”, Makromolekulare Chemie 104, 101-119 (1967).

146. Wolf, A., Bandermann, F., and Schwede, C., “Batch and Continuous Thermal Free-Radical Copolymerization of Styrene with Glycidyl Methacrylate at High Reaction Temperatures”, Macromolecular Chemistry and Physics, 203, 2, 393-400 (2002).
147. Yilmaz, E. and Küçükyavuz, Z., “Monomer reactivity ratios of styrene-4-vinylpyridine copolymers at low and high conversions”, Polymer, 34, 1, 145-149 (1993).
148. Yu, X.L., Tan, Z.D., and Wang, X.Y., “Prediction of monomer reactivity parameters using quantum chemical descriptors”, Journal of Structural Chemistry, 53, 443-448 (2012).
149. Zaitoun, A., Makakou, P., Blin, N., Al-Maamari, R., Al-Hashmi, A.A., and Abdel-Goad, M., “Shear Stability of EOR Polymers”, SPE Journal, 17, 335-339 (2012).
150. Zelzer, M. and Heise, A., “Terpolymerization kinetics of amino acid N-carboxy anhydrides”, Journal of Polymer Science, Part A: Polymer Chemistry, 52, 1228–1236 (2014)
151. Zhang, C. and Easteal, A.J., “Study of poly (acrylamide-co-2-acrylamido-2-methylpropane sulfonic acid) hydrogels made using gamma radiation initiation”, Journal of Applied Polymer Science, 89, 1322-1330 (2003).
152. Zhu, L., Zhang, L., Tang, Y., Ma, D., and Yang, J., “Synthesis of kaolin/sodium alginate-grafted poly(acrylic acid-co-2-acrylamido-2-methyl-1-propane sulfonic acid) hydrogel composite and its sorption of lead, cadmium, and zinc ions”, Journal of Elastomers and Plastics (2014).
153. Zwanzig, S., “On the criteria for experimental design in nonlinear error-in-variables model”, p. 153-165, in Balakrishnan, N., Melas, V.B., Ermakov, S.M. (eds.), Advances in Stochastic Simulation Methods. Birkhäuser (2000).

Appendix A: Derivation of the Mayo-Lewis Model

This appendix shows the derivation of the Mayo-lewis model, as given in Chapter 2, equation (2.1), section 2.1.1.1.

The copolymerization propagation reactions happen between four type of species, M_1, M_2, M_1^*, and M_2^*, as shown in equation (A.1). k_{ij} is the rate constant for each one of these reaction (i refers to radical type and j refers to monomer type). Based on these reaction, the rate of disappearance of the two monomers can be written as in equations (A.2) and (A.3), for monomers 1 and 2, respectively.

$$\begin{cases} M_1^* + M_1 \xrightarrow{k_{11}} M_1^*, & M_2^* + M_1 \xrightarrow{k_{21}} M_1^* \\ M_1^* + M_2 \xrightarrow{k_{12}} M_2^*, & M_2^* + M_2 \xrightarrow{k_{22}} M_2^* \end{cases} \tag{A.1}$$

$$\frac{d[M_1]}{d\mathrm{t}} = k_{11}[M_1][M_1^*] + k_{12}[M_2][M_1^*] \tag{A.2}$$

$$\frac{d[M_2]}{d\mathrm{t}} = k_{21}[M_1][M_2^*] + k_{22}[M_2][M_2^*] \tag{A.3}$$

Equation (A.4) can then be obtained by dividing the rate of disappearance of the two monomers. This equation then can be written as equation (A.7), considering the assumption of long chain approximation as shown in equation (A.5), and also substituting r_1 and r_2 in place of ratios of the rate constants as shown in equation (A.6).

$$\frac{d[M_1]}{d[M_2]} = \frac{k_{11}[M_1][M_1^*]+k_{12}[M_2][M_1^*]}{k_{21}[M_1][M_2^*]+k_{22}[M_2][M_2^*]} \tag{A.4}$$

$$k_{12}[M_2][M_1^*] = k_{21}[M_1][M_2^*] \tag{A.5}$$

$$r_1 = \frac{k_{11}}{k_{12}}\ , \quad r_2 = \frac{k_{22}}{k_{21}} \tag{A.6}$$

$$\frac{d[M_1]}{d[M_2]} = \frac{[M_1](r_1[M_1]+[M_2])}{[M_2]([M_1]+r_2[M_2])} \tag{A.7}$$

Equation (A.7) can be re-arranged by substituting F_1 and f_1 using equation (A.8). The resulting equation (A.9) is the instantaneous copolymer composition equation, or the Mayo-Lewis model.

$$F_1 = \frac{d[M_1]}{d[M_1]+d[M_2]} \quad , \quad f_1 = \frac{[M_1]}{[M_1]+[M_2]} \tag{A.8}$$

$$F_1 = \frac{r_1 f_1^2 + f_1(1-f_1)}{r_1 f_1^2 + 2f_1(1-f_1) + r_2(1-f_1)^2} \tag{A.9}$$

Appendix B: Derivation of the Skeist Equation

This appendix shows the derivation of the Skeist equation, as given in Chapter 2, equation (2.6), section 2.1.1.2.

To derive the Skeist equation, we can write the material balance for monomer 1, showing that the moles of M_1 copolymerized ($F_1 dM$) should be equal to the difference in the moles of M_1 in the feed before and after the reaction. This mole balance is given in equation (B.1) that can also be re-arranged as in equation (B.3). At the same time, conversion of the reaction can be defined by equation (B.2), which can also be written in a differential form as in equation (B.4). Now, since the left-sides of equations (B.3) and (B.4) are the same, we can obtain equation (B.5) that gives the differential equation for f_1 versus conversion. F_1 in these equations can be found by the Mayo-Lewis model, or equation (A.9).

$$Mf_1 - (M - dM)(f_1 - df_1) = F_1 dM \tag{B.1}$$

$$X_n = 1 - \frac{M}{M_0} \tag{B.2}$$

$$\frac{dM}{M} = \frac{df_1}{F_1 - f_1} \tag{B.3}$$

$$\frac{dM}{M} = \frac{dX_n}{X_n - 1} \tag{B.4}$$

$$\frac{df_1}{dX_n} = \frac{f_1 - F_1}{1 - X_n} \tag{B.5}$$

Now, similar to the mole balance of equation (B.1) for the time interval of *dt*, we can write the mole balance for the extent of the reaction, at time *t*. This mole balance is given in equation (B.6), where the copolymer composition is defined by equation (B.7) and the initial feed composition is given by equation (B.8). The mole balance of equation (B.6) can finally be re-written in the form of equation (B.9), which is the so-called Skeist equation.

$$[M_0]\, f_{10} - f_1[M_0]\,(1 - X_n) = \bar{F_1}[M_0]\, X_n \tag{B.6}$$

$$\bar{F_1} = \frac{[M_{10}] - [M_1]}{[M_{10}] + [M_{20}] - [M_1] + [M_2]} \tag{B.7}$$

$$f_{10} = \frac{[M_{10}]}{[M_{10}]+[M_{20}]} \quad \text{(B.8)}$$

$$\overline{F_1} = \frac{f_{10}-f_1(1-X_n)}{X_n} \quad \text{(B.9)}$$

Appendix C: Derivation of the Alfrey-Goldfinger Model

This appendix shows the derivation of the Alfrey-Goldfinger model, as given in Chapter 2, equations (2.14)-(2.16), section 2.1.2.1.

Similar to the derivation of the Mayo-Lewis model, as shown in Appendix A, for a terpolymerization reaction, the propagation step has 9 reactions that are shown in equation (C.1). The rates of all these reactions are included in equation (C.1). These rates are later used in equations (C.2) to (C.4) to write the rate of disappearance of three monomers in the system.

$$\begin{cases} M_1^* + M_1 \xrightarrow{k_{11}} M_1^*, & R_{11} = k_{11}[M_1][M_1^*] \\ M_1^* + M_2 \xrightarrow{k_{12}} M_2^*, & R_{12} = k_{12}[M_2][M_1^*] \\ M_1^* + M_3 \xrightarrow{k_{13}} M_3^*, & R_{13} = k_{13}[M_3][M_1^*] \\ M_2^* + M_1 \xrightarrow{k_{21}} M_1^*, & R_{21} = k_{21}[M_1][M_2^*] \\ M_2^* + M_2 \xrightarrow{k_{22}} M_2^*, & R_{22} = k_{22}[M_2][M_2^*] \\ M_2^* + M_3 \xrightarrow{k_{23}} M_3^*, & R_{23} = k_{23}[M_3][M_2^*] \\ M_3^* + M_1 \xrightarrow{k_{31}} M_1^*, & R_{31} = k_{31}[M_1][M_3^*] \\ M_3^* + M_2 \xrightarrow{k_{32}} M_2^*, & R_{32} = k_{32}[M_2][M_3^*] \\ M_3^* + M_3 \xrightarrow{k_{33}} M_3^*, & R_{33} = k_{33}[M_3][M_3^*] \end{cases} \tag{C.1}$$

$$\frac{d[M_1]}{d\mathrm{t}} = R_{11} + R_{21} + R_{31} \tag{C.2}$$

$$\frac{d[M_2]}{d\mathrm{t}} = R_{12} + R_{22} + R_{32} \tag{C.3}$$

$$\frac{d[M_3]}{d\mathrm{t}} = R_{13} + R_{23} + R_{33} \tag{C.4}$$

Using equations (C.2) to (C.4) and considering again the long chain approximation assumption for the radicals (equations (C.5) to (C.7)), and involving in parallel the definition of equation (C.8), we can obtain equation (C.9) as the instantaneous terpolymer composition model, also known as the Alfrey-Goldfinger equation.

$$R_{12} + R_{13} = R_{21} + R_{31} \tag{C.5}$$

$$R_{21} + R_{23} = R_{12} + R_{32} \tag{C.6}$$

$$R_{31} + R_{32} = R_{13} + R_{23} \tag{C.7}$$

$$r_{12} = \frac{k_{11}}{k_{12}},\ \ r_{13} = \frac{k_{11}}{k_{13}},\ \ r_{21} = \frac{k_{22}}{k_{21}},\ \ r_{23} = \frac{k_{22}}{k_{23}},\ \ r_{31} = \frac{k_{33}}{k_{31}},\ \ r_{32} = \frac{k_{33}}{k_{32}} \tag{C.8}$$

$$d[M_1]: d[M_2]: d[M_3] =$$

$$[M_1]\left(\frac{[M_1]}{r_{21}r_{31}} + \frac{[M_2]}{r_{21}r_{32}} + \frac{[M_3]}{r_{31}r_{23}}\right)\left([M_1] + \frac{[M_2]}{r_{12}} + \frac{[M_3]}{r_{13}}\right)$$

$$: [M_2]\left(\frac{[M_1]}{r_{12}r_{31}} + \frac{[M_2]}{r_{21}r_{32}} + \frac{[M_3]}{r_{13}r_{32}}\right)\left([M_2] + \frac{[M_1]}{r_{21}} + \frac{[M_3]}{r_{23}}\right) \tag{C.9}$$

$$: [M_3]\left(\frac{[M_1]}{r_{13}r_{21}} + \frac{[M_2]}{r_{23}r_{12}} + \frac{[M_3]}{r_{13}r_{23}}\right)([M_3] + \frac{[M_1]}{r_{31}} + \frac{[M_2]}{r_{32}})$$

Appendix D: Derivation of the EVM Objective Function

This appendix presents supplementary equations for material presented in Chapter 2, section 2.3.1, and specifically for the derivation of the EVM objective function given in equation (2.36).

Based on equations (2.34) and (2.35), and the assumption regarding the error distribution, the likelihood function is given by equation (D.1), where $\underline{\overline{x}}_i$ is given by equation (D.2) and $\underline{\hat{\xi}}_i$ is obtained from the iterative equation (D.3) at the function surface. The terms of equations (D.1) to (D.3) are described in Chapter 2, sections 2.3.1 and 2.3.3.

$$\text{Likelihood} \propto \exp\left\{-\frac{1}{2}\sum_{i=1}^{n} r_i \left(\underline{\overline{x}}_i - \underline{\hat{\xi}}_i\right)' \underline{V}^{-1} \left(\underline{\overline{x}}_i - \underline{\hat{\xi}}_i\right)\right\} \tag{D.1}$$

$$\underline{\overline{x}}_i = \frac{1}{r_i} \sum_{j=1}^{r_j} \underline{x}_{ij} \tag{D.2}$$

$$\underline{\xi}_i^{(k+1)} = \underline{\bar{x}}_i - \underline{VB_i'}\left(\underline{B_i V B_i'}\right)^{-1}\left[\underline{g}\left(\underline{\xi}^{(k)}, \underline{\theta}\right) + \underline{B_i}\left(\underline{\bar{x}}_i - \underline{\xi}^{(k)}\right)\right] \tag{D.3}$$

Using Bayesian design and a locally uniform prior proportional to the inverse of the variance-covariance matrix of the measurements (i.e., $\propto \left|\underline{V}\right|^{-\frac{1}{2}}$), the posterior distribution function is derived as equation (D.4). Maximizing this posterior distribution function is equivalent to minimizing the exponential expression, which yields us the EVM objective function, equation (D.5) to be minimized.

$$Df\ (\theta|X) \propto \exp\left\{-\frac{1}{2}\sum_{i=1}^{n} r_i \left(\underline{\overline{x}}_i - \underline{\hat{\xi}}_i\right)' \underline{V}^{-1} \left(\underline{\overline{x}}_i - \underline{\hat{\xi}}_i\right)\right\} \tag{D.4}$$

$$\phi = \frac{1}{2}\sum_{i=1}^{n} r_i \left(\underline{\overline{x}}_i - \underline{\hat{\xi}}_i\right)' \underline{V}^{-1} \left(\underline{\overline{x}}_i - \underline{\hat{\xi}}_i\right) \tag{D.5}$$

Appendix E: Calculation of Joint Confidence Regions

This appendix shows the derivation of the equations used for calculating joint confidence regions (JCRs) in the EVM algorithm, as explained in Chapter 2, section 2.3.4.

A joint confidence region for the EVM parameter estimation results is obtained using equation (E.1).

$$\phi(\underline{\theta}) \leq \phi(\underline{\hat{\theta}}) + 0.5 \times \chi^2{}_{(p,1-\alpha)} \tag{E.1}$$

To derive this equation, we use the expression for the posterior density function for estimating parameters in the EVM algorithm (see Appendix D) given by equation (E.2). Based on the normal distribution assumption for the variables, we can write equation (E.3), where χ^2 represents the value of the chi-squared distribution, *n* represents degrees of freedom, and (*1-α*) is the chosen confidence level. Using equation (E.3) inside equation (E.2), we can derive equation (E.4).

$$Df\ (\theta|X) \propto \exp\left\{-\frac{1}{2}\sum_{i=1}^{n} r_i \left(\underline{\overline{x}}_i - \underline{\hat{\xi}}_i\right)' \underline{V}^{-1} \left(\underline{\overline{x}}_i - \underline{\hat{\xi}}_i\right)\right\} \tag{E.2}$$

$$\sum_{i=1}^{n} r_i \left(\underline{\overline{x}}_i - \underline{\hat{\xi}}_i\right)' \underline{V}^{-1} \left(\underline{\overline{x}}_i - \underline{\hat{\xi}}_i\right) : \chi^2{}_{(n,1-\alpha)} \tag{E.3}$$

$$\phi(\underline{\theta}) : -\ln(Df\ (\theta|X)) : 0.5 \times \chi^2{}_{(n,1-\alpha)} \tag{E.4}$$

Similar to equation (E.2), we can have the posterior density function at the converged values of the parameters ,$Df\ (\hat{\theta}|X)$, with *n-p* degrees of freedom that is related to $\chi^2{}_{(n-p,1-\alpha)}$, as shown in equation (E.5).Using equations (E.4) and (E.5), we have the relation of equation (E.6), which gives us the equation for the exact shape joint confidence region with approximate probability in the EVM context.

$$\phi(\underline{\hat{\theta}}) : -\ln\left(Df\ (\hat{\theta}|X)\right) : 0.5 \times \chi^2{}_{(n-p,1-\alpha)} \tag{E.5}$$

$$\phi(\underline{\theta}) - \phi(\underline{\hat{\theta}}) : \ln\left(Df\ (\hat{\theta}|X)\right) - \ln(Df\ (\theta|X)) : 0.5 \times \chi^2{}_{(p,1-\alpha)} \tag{E.6}$$

Appendix F: Design Efficiency Analysis

In Chapter 4, section 4.3.2., we presented a summary table based on the analysis of 153 hypothetical systems, shown in Table F-1 with reactivity ratios values ranging from $0.01 \leq r_1 \leq 1.5$ and $0.01 \leq r_2 \leq 20$. Since model-based design of experiments for the problem of reactivity ratio estimation depends on the values of reactivity ratios of copolymerization systems, it is reasonable to wonder whether the performance of the mentioned design criteria in Chapter 4 would show similar trends when applied on different systems with various reactivity ratio values. Herein, we present our analysis for these 153 hypothetical systems, based on comparisons between the performances of (1) D-optimal design, the initial EVM design, and the sequential EVM design criteria, (2) different error levels of design variables, (3) different feasible regions chosen for design variables, and (4) different optimization procedures.

Table F-1. Simulated systems for different copolymer reactivity ratio pairs

r_2 \ r_1	**0.01**	**0.05**	**0.1**	**0.2**	**0.3**	**0.4**	**0.5**	**0.6**	**0.7**	**0.8**	**0.9**	**1**	**1.5**
0.01	1												
0.1	2	16	30										
0.3	3	17	31	44	57								
0.5	4	18	32	45	58	70	82						
0.7	5	19	33	46	59	71	83	94	105				
0.9	6	20	34	47	60	72	84	95	106	116	126		
1.1	7	21	35	48	61	73	85	96	107	117	127	136	145
1.5	8	22	36	49	62	74	86	97	108	118	128	137	146
2	9	23	37	50	63	75	87	98	109	119	129	138	147
3	10	24	38	51	64	76	88	99	110	120	130	139	148
4	11	25	39	52	65	77	89	100	111	121	131	140	149
5	12	26	40	53	66	78	90	101	112	122	132	141	150
10	13	27	41	54	67	79	91	102	113	123	133	142	151
15	14	28	42	55	68	80	92	103	114	124	134	143	152
20	15	29	43	56	69	81	93	104	115	125	135	144	153

As discussed in Chapter 4, section 4.3.2, for the Sty/MMA case study, the performances of different design criteria can be compared with each other based on the ratios of the volumes of their corresponding parameters' confidence regions. A smaller volume/size reflects less uncertainty in the results and thus more efficient design criteria. Therefore, looking at the volume ratios of different designs, a smaller volume ratio than one indicates a more efficient (better) design with respect to the base design. In this appendix, we present the averages values, obtained from the complete analysis of all the hypothetical systems, for the four mentioned aspects. This information supplements the materials presented in Table 4-2, Chapter 4. Hence, the related interpretations are not repeated herein.

The first comparison is made between the performance of D-optimal design, the initial EVM design criterion, and the sequential EVM design for both additive and multiplicative error models. Table F-2 shows the average values of the volume ratios of these different design criteria. The volume of the confidence region obtained from the EVM initial design criterion is chosen as the basis, hence the other ratios are the ratios of a certain volume to this basis.

Table F-2. Average performance of different design criteria

	Average of volume ratio to initial EVM design	
	Additive error	Multiplicative error
D-optimal	0.85	5.85
EVM-initial	1	1
EVM-sequential	0.033	0.1659

The second comparison is between the effect of different error levels on the performance of the EVM design criterion itself and in comparison with D-optimal design. As shown in Table F-3, the initial EVM design criterion was implemented with three different error levels for the feed composition. The smallest error (f_1 error: 1%) is our basis and two medium and large levels are selected to see the effect of increasing error.

Table F-3. Average performance of design criteria at different error levels-Additive error model

	Average volume ratio		
% k error in measurements	$f_1 \rightarrow 5\%$ $F_1 \rightarrow 5\%$	$f_1 \rightarrow 2.5\%$ $F_1 \rightarrow 5\%$	$f_1 \rightarrow 1\%$ $F_1 \rightarrow 5\%$
EVM	2.77	1.51	1
D-optimal/EVM	0.37	0.62	0.85

The third comparison is between the performances of the EVM design criterion with different feasible ranges for the design variables. In this case, the design variable (i.e., initial feed composition) can have values from 0 to 1. Since running a homo-polymerization experiments (at $f_1=0$) is not practical (since we are dealing with copolymerizations), a small value of f_1 is selected as the lowest bound of the feasible region, and the optimizer chooses this point as the first optimal points in all cases. As shown in section 4.3.2, our usual lower bound is $f_1= 0.1$. Although ignoring $f_1=0$ as the first initial point sounds more practical from a chemist's point of view, it reduces the precision of the parameter estimation based on such a design. To investigate this effect, we changed the lower bound of f_1 to a smaller value, 0.05, and a larger one, 0.3, and repeated the analysis for all the hypothetical systems. The averages of the ratios of the volumes of parameters inference in the parameter space are given in Table F-4.

Table F-4. Average performance of EVM design criterion with different feasible regions-Multiplicative error model

	Average volume ratio		
Feasible f_1 composition range	$0.05 \leq f_1 \leq 0.99$	$0.1 \leq f_1 \leq 0.99$	$0.3 \leq f_1 \leq 0.99$
EVM	0.61	1	7.01

The final comparison is between the performances of different optimization procedures for the implementation of the different design criteria. Being able to implement a DOE technique with reliable and efficient optimization technique facilitates the usage of that technique. On the contrary, numerically intensive, inefficient, and unreliable optimization techniques may often have such a dramatic influence on the end-result (and hence, the end-user!) that a good DOE technique can never compensate for. Amongst the most common optimization techniques, we introduced the SCE and SQP algorithms in Chapter 2. For the sake of determining which one of these algorithms have a better performance for our case, we looked at their performance for the 153 hypothetical copolymerization systems in terms of their number of function evaluations and number of iterations. The results are summarized in Table F-5.

Table F-5. Average of computational performance of SQP and SCE optimization algorithms

Optimization algorithm	Algorithm output	Additive error	Multiplicative error
SQP	No. of function evaluations	97.78	141.36
	No. of iterations	15.98	23.47
SCE	No. of function evaluations	881.43	1622.82
	No. of iterations	2.66	3.98

Appendix G: Derivation of the Recast Terpolymerization Composition Model

This appendix shows the derivation of the recast terpolymerization composition model, as given in Chapter 6, equations (6.5)-(6.7), section 6.3.1.

To derive the recast form of the terpolymerization composition model, we can start from the Alfrey-Goldfinger equations (Appendix C), and given here in equations (G.1) to (G.3) in terms of the ratios of the mole fractions of monomers, f_1, f_2, and f_3. The right-hand sides of these equations are summarized as shown in equation (G.4) for the sake of brevity of the subsequent calculations.

$$\frac{df_1}{df_2} = \frac{F_1}{F_2} = \frac{f_1\left(\frac{f_1}{r_{21}r_{31}} + \frac{f_2}{r_{21}r_{32}} + \frac{f_3}{r_{31}r_{23}}\right)\left(f_1 + \frac{f_2}{r_{12}} + \frac{f_3}{r_{13}}\right)}{f_2\left(\frac{f_1}{r_{12}r_{31}} + \frac{f_2}{r_{21}r_{32}} + \frac{f_3}{r_{13}r_{32}}\right)\left(f_2 + \frac{f_1}{r_{21}} + \frac{f_3}{r_{23}}\right)} \tag{G.1}$$

$$\frac{df_1}{df_3} = \frac{F_1}{F_3} = \frac{f_1\left(\frac{f_1}{r_{21}r_{31}} + \frac{f_2}{r_{21}r_{32}} + \frac{f_3}{r_{31}r_{23}}\right)\left(f_1 + \frac{f_2}{r_{12}} + \frac{f_3}{r_{13}}\right)}{f_3\left(\frac{f_1}{r_{13}r_{21}} + \frac{f_2}{r_{23}r_{12}} + \frac{f_3}{r_{13}r_{23}}\right)\left(f_3 + \frac{f_1}{r_{31}} + \frac{f_2}{r_{32}}\right)} \tag{G.2}$$

$$\frac{df_2}{df_3} = \frac{F_2}{F_3} = \frac{f_2\left(\frac{f_1}{r_{12}r_{31}} + \frac{f_2}{r_{21}r_{32}} + \frac{f_3}{r_{13}r_{32}}\right)\left(f_2 + \frac{f_1}{r_{21}} + \frac{f_3}{r_{23}}\right)}{f_3\left(\frac{f_1}{r_{13}r_{21}} + \frac{f_2}{r_{23}r_{12}} + \frac{f_3}{r_{13}r_{23}}\right)\left(f_3 + \frac{f_1}{r_{31}} + \frac{f_2}{r_{32}}\right)} \tag{G.3}$$

$$\frac{F_1}{F_2} = \frac{g_1}{g_2}, \quad \frac{F_1}{F_3} = \frac{g_1}{g_3}, \quad \frac{F_2}{F_3} = \frac{g_2}{g_3} \tag{G.4}$$

The stoichiometry constraints on the mole fractions of terpolymer composition is given by equation (G.5), in which we can make substitutions based on the relations shown in equation (G.4), as shown in equation (G.6). By further simplification, we have equation (G.7) for F_1 mole fraction, and F_2 and F_3 can be similarly derived. The final recast model, in terms of F_1, F_2, and F_3 is shown in equations (G.8) to (G.10).

$$F_1 + F_2 + F_3 = 1 \tag{G.5}$$

$$F_1 + \frac{g_2}{g_1}F_1 + \frac{g_3}{g_1}F_1 = 1 \tag{G.6}$$

$$F_1 = \frac{g_1}{g_1 + g_2 + g_3} \tag{G.7}$$

$$F_1 - \frac{f_1\left(\frac{f_1}{r_{21}r_{31}}+\frac{f_2}{r_{21}r_{32}}+\frac{f_3}{r_{31}r_{23}}\right)\left(f_1+\frac{f_2}{r_{12}}+\frac{f_3}{r_{13}}\right)}{f_1\left(\frac{f_1}{r_{21}r_{31}}+\frac{f_2}{r_{21}r_{32}}+\frac{f_3}{r_{31}r_{23}}\right)\left(f_1+\frac{f_2}{r_{12}}+\frac{f_3}{r_{13}}\right)+f_2\left(\frac{f_1}{r_{12}r_{31}}+\frac{f_2}{r_{21}r_{32}}+\frac{f_3}{r_{13}r_{32}}\right)\left(f_2+\frac{f_1}{r_{21}}+\frac{f_3}{r_{23}}\right)+f_3\left(\frac{f_1}{r_{13}r_{21}}+\frac{f_2}{r_{23}r_{12}}+\frac{f_3}{r_{13}r_{23}}\right)\left(f_3+\frac{f_1}{r_{31}}+\frac{f_2}{r_{32}}\right)} = 0 \quad \text{(G.8)}$$

$$F_2 - \frac{f_2\left(\frac{f_1}{r_{12}r_{31}}+\frac{f_2}{r_{21}r_{32}}+\frac{f_3}{r_{13}r_{32}}\right)\left(f_2+\frac{f_1}{r_{21}}+\frac{f_3}{r_{23}}\right)}{f_1\left(\frac{f_1}{r_{21}r_{31}}+\frac{f_2}{r_{21}r_{32}}+\frac{f_3}{r_{31}r_{23}}\right)\left(f_1+\frac{f_2}{r_{12}}+\frac{f_3}{r_{13}}\right)+f_2\left(\frac{f_1}{r_{12}r_{31}}+\frac{f_2}{r_{21}r_{32}}+\frac{f_3}{r_{13}r_{32}}\right)\left(f_2+\frac{f_1}{r_{21}}+\frac{f_3}{r_{23}}\right)+f_3\left(\frac{f_1}{r_{13}r_{21}}+\frac{f_2}{r_{23}r_{12}}+\frac{f_3}{r_{13}r_{23}}\right)\left(f_3+\frac{f_1}{r_{31}}+\frac{f_2}{r_{32}}\right)} = 0 \quad \text{(G.9)}$$

$$F_3 - \frac{f_3\left(\frac{f_1}{r_{13}r_{21}}+\frac{f_2}{r_{23}r_{12}}+\frac{f_3}{r_{13}r_{23}}\right)\left(f_3+\frac{f_1}{r_{31}}+\frac{f_2}{r_{32}}\right)}{f_1\left(\frac{f_1}{r_{21}r_{31}}+\frac{f_2}{r_{21}r_{32}}+\frac{f_3}{r_{31}r_{23}}\right)\left(f_1+\frac{f_2}{r_{12}}+\frac{f_3}{r_{13}}\right)+f_2\left(\frac{f_1}{r_{12}r_{31}}+\frac{f_2}{r_{21}r_{32}}+\frac{f_3}{r_{13}r_{32}}\right)\left(f_2+\frac{f_1}{r_{21}}+\frac{f_3}{r_{23}}\right)+f_3\left(\frac{f_1}{r_{13}r_{21}}+\frac{f_2}{r_{23}r_{12}}+\frac{f_3}{r_{13}r_{23}}\right)\left(f_3+\frac{f_1}{r_{31}}+\frac{f_2}{r_{32}}\right)} = 0 \quad \text{(G.10)}$$

Appendix H: Elemental Analysis Sample Calculations

To calculate the terpolymer composition for the terpolymerization of AMPS/AAm/AAc system, as discussed in Chapter 8, section 8.3.3, elemental analysis data are used as shown in this appendix. Herein, we present an illustrative example of the calculations involved.

Considering three monomers in the terpolymerization, each monomer has a certain amount of moles, as shown by "a", "b", and "c" for AMPS, AAm, and AAc in equation (H.1), respectively. Based on the structure of each monomer (as shown in equation (H.1) as well), we can write the number of moles for each element of C, N, and S, as shown in equations (H.2) to (H.4).

$$\begin{cases} AMPS: C_7H_{13}NO_4S \rightarrow \text{“}a\text{” } moles \\ \text{AAm: } C_3H_5NO \rightarrow \text{“b” moles} \\ \text{AAc: } C_3H_4O_2 \rightarrow \text{“c” moles} \end{cases} \quad \text{(H.1)}$$

$$C = 7a+3b+3c \quad \text{(H.2)}$$

$$N = a+b \quad \text{(H.3)}$$

$$S = a \quad \text{(H.4)}$$

The outcome of the elemental analysis is percentage values of C, N, and S in the sample, as shown in Table H-1 for one of our samples. For analyzing the elemental analysis data, we need to select an element as the basis. This element should only be present in one of our three monomers, so that we can calculate how much of other monomers we have according to this basis. Sulfur is our basis here since only AMPS has it. So, if we divide the moles of all of the elements by the moles of sulfur, we have:

$$S=1 \rightarrow \begin{cases} a = 1 \\ b = (\text{molar ratio for N}) - a \\ c = \big((\text{molar ratio for C}) - 7 \times a - 3 \times b\big)/3 \end{cases} \quad \text{(H.5)}$$

By calculating a, b, and c from equation (H.5), we can calculate the mole fractions of the three monomers as shown in equations (H.6) to (H.8).

$$F_{AMPS} = \frac{a}{a+b+c} \quad \text{(H.6)}$$

$$F_{AAm} = \frac{b}{a+b+c} \quad \text{(H.7)}$$

$$F_{AAc} = \frac{c}{a+b+c} \quad \text{(H.8)}$$

Table H-1 shows a complete example for our calculations. The weights of the elements are measured, as shown in the second column. These values are divided by the molecular weight of each element, and the moles in the third column are calculated. Then these moles are divided by the moles of sulfur to calculate the mole ratios in the fourth column. Then, a, b, and c are calculated using equation (H.5), and finally, the mole fractions are obtained using equations (H.6) to (H.8).

Table H-1. Sample results for calculating terpolymer composition from elemental analysis data

Element	Weight	Mole	Mole ratio	a	b	c	F_{AMPS}	F_{AAm}	F_{AAc}
C	36.520	3.041	32.894	1	8.083	0.549	0.104	0.839	0.057
H	5.607	5.563	60.176						
N	11.760	0.840	9.083						
S	2.964	0.092	1.000						

Appendix I: Extension of the DNI Approach

Chapter 3 shows the derivatives of the cumulative composition model with respect to the variables, used in the EVM algorithm, in equations (3.19). In Chapter 9, section 9.3.1-point 5, we suggest an extension of this derivative approach, where the relation between molar conversion, X_n, and mass conversion, X_w, is used to update the derivative in equation (3.19). This extension is sketched in this appendix.

In our original program, the EVM model in the DNI approach is given by equation (I.1), and the derivative of this model with respect to the variable of the problem, $\bar{F}_1$, is given by equation (I.2). Now, in this extension, the relation between X_n and X_w, as shown in equation (I.3), is used to update equation (I.2), as shown in equation (I.4), where $\frac{\partial X_n}{\partial \bar{F}_1}$ is given by equation (I.5). As can be seen in equation (I.5), the magnitude of this derivative depends on the difference between the molecular weights of monomer 1, M_{w1}, and monomer 2, M_{w2}. For almost all of our cases, we have very similar molecular weights between the monomers, and even for those cases where the difference seems considerable, the derivative is still a very small value, and thus has little or no effect on the outcome of the reactivity ratio estimation.

$$\bar{F}_1 = \frac{f_{10} - f_1(1 - X_n)}{X_n} \tag{I.1}$$

$$\frac{\partial \underline{g}(\underline{\xi}, \underline{\theta})}{\partial \bar{F}_1} = 1 \tag{I.2}$$

$$X_n = X_w \frac{Mw_1 f_{10} + (1 - f_{10}) Mw_2}{Mw_1 \bar{F}_1 + (1 - \bar{F}_1) Mw_2} \tag{I.3}$$

$$\frac{\partial \underline{g}(\underline{\xi}, \underline{\theta})}{\partial \bar{F}_1} = 1 + \left(\frac{f_{10} - f_1}{{X_n}^2}\right) \times \frac{\partial X_n}{\partial \bar{F}_1} \tag{I.4}$$

$$\frac{\partial X_n}{\partial \bar{F}_1} = \frac{(Mw_2 - Mw_1) \times X_w \times (Mw_1 f_{10} + (1 - f_{10}) Mw_2)}{Mw_1 \bar{F}_1 + (1 - \bar{F}_1) Mw_2} \tag{I.5}$$

Appendix J: Copolymer Composition Calculations in a CSTR

Chapter 9 (section 9.3.2.1) presents a long-tern future step regarding utilization of data from a CSTR for the purpose of estimating copolymerization reactivity ratios. This appendix provides the mathematical basis/models that should be used in this approach for obtaining composition data from a steady-state CSTR.

A continuous stirred tank reactor (CSTR), as the name implies, is a reactor in which input materials are continuously fed to the reactor and the reactor mixture is stirred. Therefore, the contents of a CSTR are often considered to be well-mixed and uniform in composition throughout. The exit stream from this reactor has the same composition as the fluid within the reactor. A schematic of this reactor is shown in Figure J-1. In a well-mixed CSTR at steady state, the monomer composition is the same throughout the tank and time invariant, resulting in a uniform copolymer product. The feed is assumed to be blended instantly and the effluent composition and temperature are the same as the reactor contents. Problems with heat removal are alleviated to a great extent because of the beneficial effect of the colder monomer feed and the removal of the reaction heat with the effluent.

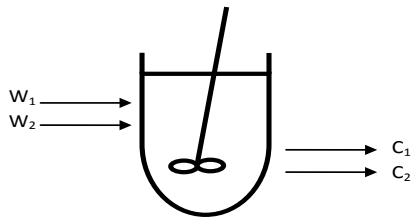

Figure J-1: CSTR schematic; W_i is monomer inlet flow rate (gr/sec); C_i is unreacted monomer concentration in the outlet (mol/lit)

The basic calculations for the analysis and operation of a steady state CSTR for copolymerization are presented in what follows. The notations used match the CSTR schematic in Figure J-1. The copolymer equation is written as in the Mayo-Lewis model, given by equation (J.1). Also, the unreacted monomer mixture composition and the copolymer composition are defined as in equations (J.2) and (J.3).

$$F_1 = \frac{r_1 f_1^2 + f_1(1-f_1)}{(r_1+r_2-2)f_1^2 + 2(1-r_2)f_1 + r_2} \quad \text{(J.1)}$$

$$f_1 = \frac{c_1}{c_1+c_2} \quad \text{(J.2)}$$

$$F_1 = \frac{P_1}{P_1+P_2} \quad \text{(J.3)}$$

where c_i is the molar concentration of monomer *i*, unbound in the residual monomer mixture, and P_i denotes monomer units of monomer *i* (M_i) bound in the copolymer (product) per second, which can be obtained by equations (J.4) and (J.5). In these equations, Mw_1 and Mw_2 are the molecular weights of monomer 1 and 2, and *v* is the volumetric outflow from the reactor, given by equation (J.6). Here, ρ_1, ρ_2, and ρ_p are the densities of monomer 1 and 2 and the copolymer, respectively. All densities are evaluated at the reactor conditions. Of course, the overall situation can be simplified assuming $\rho_1 \sim \rho_2 \sim \rho_p$.

$$P_1 = \frac{w_1}{M_{w_1}} - c_1 v \quad \text{(J.4)}$$

$$P_2 = \frac{w_2}{M_{w_2}} - c_2 v \quad \text{(J.5)}$$

$$v = \left(\frac{w_1}{\rho_1} + \frac{w_2}{\rho_2}\right) - P_1 Mw_1 \left(\frac{1}{\rho_1} - \frac{1}{\rho_p}\right) - P_2 Mw_2 \left(\frac{1}{\rho_2} - \frac{1}{\rho_p}\right) \quad \text{(J.6)}$$

Substituting equation (J.6) into equations (J.4) and (J.5), we re-express P_1 and P_2 as in equations (J.7) and (J.8). Solving these two equations for P_1 and P_2, using matrix notation, provides copolymer and monomer compositions for a steady state CSTR.

$$P_1 = \frac{w_1}{M_{w_1}} - c_1\left(\frac{w_1}{\rho_1} + \frac{w_2}{\rho_2}\right) - c_1 P_1 Mw_1 \left(\frac{1}{\rho_1} - \frac{1}{\rho_p}\right) - c_1 P_2 Mw_2 \left(\frac{1}{\rho_2} - \frac{1}{\rho_p}\right) \quad \text{(J.7)}$$

$$P_2 = \frac{w_2}{M_{w_2}} - c_2\left(\frac{w_1}{\rho_1} + \frac{w_2}{\rho_2}\right) - c_2 P_1 Mw_1 \left(\frac{1}{\rho_1} - \frac{1}{\rho_p}\right) - c_2 P_2 Mw_2 \left(\frac{1}{\rho_2} - \frac{1}{\rho_p}\right) \quad \text{(J.8)}$$

In matrix notation, we then have equation (J.9) which is solved as $\begin{bmatrix} P_1 \\ P_2 \end{bmatrix} = A^{-1} B$, where A and B are the matrices in equation (J.10).

$$\begin{bmatrix} 1 + c_1 Mw_1 \left(\frac{1}{\rho_1} - \frac{1}{\rho_p}\right) & c_1 Mw_1 \left(\frac{1}{\rho_2} - \frac{1}{\rho_p}\right) \\ c_2 Mw_2 \left(\frac{1}{\rho_1} - \frac{1}{\rho_p}\right) & 1 + c_2 Mw_2 \left(\frac{1}{\rho_2} - \frac{1}{\rho_p}\right) \end{bmatrix} \times \begin{bmatrix} P_1 \\ P_2 \end{bmatrix} = \begin{bmatrix} \frac{w_1}{M_{w_1}} - c_1 \left(\frac{w_1}{\rho_1} + \frac{w_2}{\rho_2}\right) \\ \frac{w_2}{M_{w_2}} - c_2 \left(\frac{w_1}{\rho_1} + \frac{w_2}{\rho_2}\right) \end{bmatrix} \quad \text{(J.9)}$$

$$A = \begin{bmatrix} 1 + c_1 Mw_1 \left(\frac{1}{\rho_1} - \frac{1}{\rho_p}\right) & c_1 Mw_1 \left(\frac{1}{\rho_2} - \frac{1}{\rho_p}\right) \\ c_2 Mw_2 \left(\frac{1}{\rho_1} - \frac{1}{\rho_p}\right) & 1 + c_2 Mw_2 \left(\frac{1}{\rho_2} - \frac{1}{\rho_p}\right) \end{bmatrix}, \quad B = \begin{bmatrix} \frac{w_1}{M_{w_1}} - c_1 \left(\frac{w_1}{\rho_1} + \frac{w_2}{\rho_2}\right) \\ \frac{w_2}{M_{w_2}} - c_2 \left(\frac{w_1}{\rho_1} + \frac{w_2}{\rho_2}\right) \end{bmatrix} \quad \text{(J.10)}$$